Nanoengineered and Biomimetic Protein-derived Adhesives with Improved Adhesion Strength and Water Resistance

by

Nandika Priyantha Bandara

A thesis submitted in partial fulfillment of the requirements for the degree of

Doctor of Philosophy

in
Food Science and Technology

Department of Agricultural, Food and Nutritional Science
University of Alberta

ABSTRACT

The oilseed industry generates a great deal of meal after oil extraction. Soy meal has a number of value added applications while canola meal is used mainly as a low-value animal feed. There is a growing interest on value addition of meal beyond feed uses. Canola and soy meal contain ~ 33-37% and 43-47% (w/w on DM basis) of protein, respectively. As protein-rich biomass, there is a potential to develop protein-based adhesives as an alternative to petrochemical based adhesives. However, protein based adhesives suffer from weak water resistance and adhesion that limit their widespread commercial applications.

Nanomaterials are widely used in composite research to improve flexural strength, elasticity, and thermal stability, while biomimetics are used in biomedical field to develop improved materials by mimicking natural materials as a model. Therefore, the overall objective of this research was to develop protein based adhesive with improved adhesion and water resistance using oilseed proteins via nanotechnological and biomimetic approaches. Two hypotheses were tested in this research: (1) exfoliating nanomaterials in canola protein and preparing hybrid adhesives with chemically modified canola protein will improve adhesion and water resistance; (2) biomimetic modification of soy protein to impart 3,4-dyhydroxyphenylalanine groups will improve adhesion and water resistance.

In the first study, exfoliating nanomaterials in canola protein at 1% (w/w) increased the dry, wet and soaked adhesion strengths from 6.38 ± 0.84, 1.98 ± 0.22, and 5.65 ± 0.46 MPa (control sample) to 10.37 ± 1.63, 3.57 ± 0.57, and 7.66 ± 1.37 MPa (nanocrystalline cellulose - NCC) and 8.14 ± 0.45, 3.25 ± 0.36, and 7.76 ± 0.53 MPa (graphite oxide - GO) respectively. Nanomaterial induced increase in thermal stability, exposed hydrophobic groups due to secondary structural changes, and nanomaterial induced cohesion were responsible for the

improved adhesion. In the second study, effect of different oxidation levels of GO on adhesion was studied. Increasing oxidation time decreased C/O ratio while relative proportion of C-OH, and C=O groups initially increased up to 2 h of oxidation, but reduced upon further oxidation. Canola protein-GO hybrid adhesive (CPA-GO – with 1% GO (w/w) addition) prepared with 2 h oxidized GO increased ($p < 0.05$) dry, wet and soaked strength to 11.67 ± 1.00, 4.85 ± 0.61, and 10.73 ± 0.45 MPa respectively. Improved exfoliation of GO, improved adhesive and cohesive interactions, increased hydrogen and hydrophobic interactions and improved thermal stability of CPA-GO contributed towards the improved adhesion.

In the third study chemically modified canola protein-nanomaterial (CMCP-NM) hybrid wood adhesives were developed. Modifying canola protein with ammonium persulphate (1% w/w APS/protein) significantly improved ($p < 0.05$) adhesion to 10.47 ± 1.35, 4.12 ± 0.64 and 9.39 ± 1.20 MPa for dry, wet and soaked strength respectively. Exfoliating 1% NCC into CMCP further improved adhesion to 12.50 ± 0.71, 4.79 ± 0.40, and 10.92 ± 0.75 MPa while 1% GO increased the adhesion to 11.82 ± 1.15, 4.99 ± 0.28, and 10.74 ± 0.72 MPa for dry, wet and soaked strength respectively. In the fourth study randomly oriented strand boards (ROSB) were produced using nanoengineered canola protein adhesive (CPA) at pilot scale. The mechanical performances, bond durability and water resistance were not affected by CPA addition up to a level of 40%, compared to commercial LPF adhesives. Mechanical performance of all ROSB panels exceeded the acceptable minimum standards specified by CSA O437.0-93 standards; therefore it can be used in commercial ROSB production, either as 100% resin for interior application or up to 40% replacement of LPF for exterior applications.

In the fifth study, mussel inspired biomimetic soy protein adhesive was developed by converting inherent amino acids tyrosine into 3,4-dihydroxyphenylalanine (DOPA) by reacting

with tyrosinase followed by adding NaOH and $FeCl_3$. Adhesion was significantly increased from 4.97 ± 0.94, 1.79 ± 0.52, and 5.62 ± 0.65 MPa to 13.21 ± 1.58, 3.93 ± 0.21, and 12.10 ± 0.46 MPa for dry, wet and soaked strength respectively, mainly due to DOPA mediated polymerization and crosslinking, increased cohesive interactions, and hydrophobic interactions with wood surface. In addition, prepared adhesive showed acceptable adhesion to mica, glass and polystyrene surfaces as well.

The findings of this thesis provide evidence on the potential of nanotechnological and biomimetic methods to develop protein based adhesives with improved adhesion and water resistance.

PREFACE

This thesis contains original research work done by Nandika Priyantha Bandara and has been written according to the guidelines for a paper format thesis of the Faculty of Graduate Studies and Research at the University of Alberta. The concept of the thesis was originated from my PhD supervisor Dr. Jianping Wu and the research was funded by grants received from Alberta Innovates Biosolutions (ALBIO) and Alberta Livestock and Meat Agency (ALMA) to Dr. Jianping Wu; and scholarship funds received from Alberta Innovates Technology Futures (AITF) doctoral scholarship, Queen Elizabeth II (QE II) doctoral scholarship, Mitacs Accelerate Internship, and Agricultural Institute of Canada Foundation (AICF) Karl Iverson Award to myself.

The thesis consists of eight chapters. Chapter 1 provides a general introduction and the objectives of the thesis. Chapter 2 provides a detailed literature review regarding the agricultural and oilseed industry byproducts, oilseed industry byproduct value addition, wood adhesion, wood adhesive and current innovations in biobased wood adhesives. Chapter 3 has been published as "Exfoliating nanomaterials in canola protein derived adhesive improves strength and water resistance" in *RSC Advances* [2017, ***7(11)***, 6743-6752], chapter 4 entitled as "Graphite oxide improves adhesion and water resistance of canola protein–graphite oxide hybrid wood adhesive" has been submitted for consideration to *Scientific Reports*. Chapter 5 entitled as "Chemically Modified Canola Protein-Nanomaterial Hybrid Wood Adhesive Shows Improved Adhesion and Water Resistance" in ready for the submission for publication. Chapter 6 entitled as "Randomly Oriented Strand Board Composites from Nanoengineered Protein Based Wood Adhesive" has been submitted for consideration to *Composite Part A – Applied Science and*

Manufacturing and chapter 7 entitled as "Biomimetic soyprotein adhesive inspired by mussel adhesion" is ready for submission. Chapter 8 provides an overall conclusions and future recommendations to the thesis. A patent application was filed under the United States Provisional Patent Application Serial No. 62/380,043 – "Improved Protein Based Adhesives" covering all the research findings presented in this thesis from chapter 3 to chapter 7.

I was responsible for the literature search relevant to all the chapters above, designing and performing laboratory experiments, data analysis and writing first draft of manuscript, and manuscript revision while Dr. Jianping Wu contributed to experimental design, data interpretation, preparation and submission of manuscripts. Dr. Hongbo Zeng contributed to experimental design, and data interpretation of chapter 7. Mr. Yussef Ezparza contributed to the FTIR and XPS data analysis and interpretation of chapters 4 and 5. Mr. Jiancheng Qi from Agri-Food Discovery Place of University of Alberta contributed in pilot scale canola protein extraction. Dr. Siguo Chen, Mr. Grant Reekie, Mr. David Bilyk, and Mr. Steve Lee from Alberta Innovates Technology Futures contributed in performing pilot scale trails in Chapter 6.

DEDICATION

This thesis is dedicated

To my beloved parents A.M. Heenbanda and W.M. Somawasala, who guided me throughout my life, and encouraged me; to my wife Chamila, my lovely kids Chathuli and Navindu….

ACKNOWLEDGEMENTS

There are countless people who have encouraged and supported me throughout my graduate studies and who I am forever grateful to. First and foremost, I would like to express my heartiest gratitude to my supervisor Dr. Jianping Wu for providing the opportunity to pursue my graduate studies and for his enormous support, encouragement and guidance given throughout the program. I am also very thankful to Dr. Hongbo Zeng and Dr. Lingyun Chen, for their guidance, help and support throughout the graduate program as my PhD supervisory committee members. Their contribution towards designing and executing my research program provided me with a valuable experience in my PhD studies. I would like to express my sincere thanks to Dr. Ning Yan for accepting to be the external examiner for my PhD defense and to Dr. David Bressler for serving as the arm's length examiner.

I would also like to thank Alberta Innovates Biosolutions (ALBIO), and Alberta Livestock and Meat Agency (ALMA) for the financial support provided throughout my doctoral program. In addition, I would like to acknowledge the financial support I received through Alberta Innovates Technology Futures (AITF) doctoral scholarship, Queen Elizabeth II (QE II) doctoral scholarship, Mitacs Accelerate Internship, Karl Iverson Agricultural Scholarship of Agricultural Institute of Canada Foundation (AICF).

I am deeply grateful for all the support given by the Graduate Program support staff of the Department of Agricultural Food and Nutritional Science (AFNS), Jody Forslund, Nicole Dube, and Holly Horvath. In addition, the technical support provided by Garry Sedgwick from Chromatography lab, the access and training provided by Jane Batcheller on mechanical characterization facility of Department of Human Ecology are greatly acknowledged.

I would like to express my sincere thanks to my fellow graduate students and colleagues, both past and present, from Dr. Wu's laboratory: Dr. Shengwen Shen, Dr. Sunjong you, Dr. Jiapei Wang, Dr. Morshedur Rahman, Dr. Chanchan Wang, Dr. Aman Ullah, April Milne, Maria Offengenden, Alexandra Acero, Dr. Kaustav Majumder, Li Sen, Dr. Sahar Navidghasemizad, Mejo Remanan, Jiandong Ren, Dr. Wenlin Yu, Dr. Yuchen Gu, Justina Zhang, Qiyi Li, Yussef Esparza, Xiahong Sun, Ali Akbari, Forough Jahandideh, Nan Shang, Liao Wang, Shreyak Chaplot, Selene Gonzales, Dr. Meram Chalamaiah, Dr. Qingbiao Xu, Dr. Hui Hong, Dr. Myoungjin Son, Qiufang Liang, Liang Chen, and Hongbin Fan. I am thankful for their numerous support and company that made my memories of good times we shared together.

I am blessed to have a group of wonderful friends who I consider as my family in Edmonton. Nimesh & Dhanuja, Chamila & Nilu, Prasanna & Sumali, Wijaya & Thushani, Dinuka & Kethmi, Chandana & Lalani, Chandila & Anusha, Dilhara & Dilini, Viraj & Sureka, Sumal & Gayashani, Ravindra & Shakila and Brasathe will always be remembered for their love and support.

I would not have come so far without the support of my family. I am so grateful for my loving parents, and my brother Tharaka Bandara for their endless love, caring and for always been helping throughout my life. I would also like to thank my loving parents-in law and brother and sister in-laws Madara, Kalpana & Dharshin, Madhavi & Isuru for their love and support. Words cannot express my gratitude towards my loving wife Chamila Nimalaratne and my loving kids Chathuli Bandara and Navindu Bandara for their unconditional love, care, and understanding and for always being by my side.

TABLE OF CONTENTS

LIST OF TABLES

LIST OF FIGURES

LIST OF ABBREVIATIONS

APS – Ammonium persulphate

Bento - Bentonite

CMCP – Chemically modified canola protein

CMCP-GO - Chemically modified canola protein adhesive with 1% graphite oxide

CMCP-NCC - Chemically modified canola protein adhesive with 1% nanocrystalline cellulose

CPA – Canola protein adhesives

CPA GO – Canola Protein-Graphite Oxide Hybrid Wood Adhesive

DOPA – 3,4-dihydroxyphenylalanine

DSC – Differential scanning calorimetry

EWP - Engineered wood product

FTIR – Fourier transformed infrared spectroscopy

GO – Graphite oxide

IB – Internal bond strength

LPF – Liquid phenol formaldehyde

MC – Moisture content

MOE – Modulus of elasticity

MOR – Modulus of rupture

NCC – Nanocrystalline cellulose

OSB – Oriented strand board

pMDI – polymeric diphenyl methane diisocyanate

PVA – Polyvinyl acetate

ROSB – Randomly oriented strand board

SM-MMT – Surface modified montmorillonite

SPI – soy protein isolate

SPI-NaOH/Fe^{3+} - soy protein adhesive with 30 μL/mL 6 M NaOH and 30 μL/mL 0.2 M $FeCl_3$

TEM – Transmission electron microscopy

TS – Thickness swell

TSPI – tyrosinase modified soy protein isolate

TSPI-NaOH/Fe^{3+} - tyrosinase modified soy protein adhesive with 30 μL/mL 6 M NaOH and 30 μL/mL 0.2 M $FeCl_3$

WA – Water absorption

XPS – X-ray photoelectron spectroscopy

XRD – X-ray diffraction

CHAPTER 1 – General Introduction and Thesis Objectives

Alberta's economy relies heavily on the fossil resource, but is vulnerable to changes in global policies and politics. There is a growing interest in many part of the world, particularly in Alberta, to develop value-added bioproducts from low-value agriculture/forestry biomass to develop a diversified bioeconomy (AlBIO, 2013; Qi, 2013; Staffas et al., 2013). Agricultural and food industries are among the major contributors to the Canadian economy (Staffas et al., 2013). These industries generate a great deal of byproducts and waste materials, which are generally low value or sometimes are a liability to the industry due to cost associated with disposal, but are vital to the development of bioproducts due to their abundance, renewability, and low cost (Arshad et al., 2016; Wang & Wu, 2012).

The world oilseed industry has experienced continuous growth in the past decades, with an annual production of over 319.7 million metric tonnes of soybean and 68.7 million metric tonnes of canola in 2015 (OECD & FAO, 2016). Canada produced 18.4 million metric tonnes of Canola in 2015 (Canola Council of Canada, 2016), and over 6.2 million metric tonnes of soybean (COPA, 2016). In 2015, oilseed processing industry alone contributed around $1.3 billion towards Canadian economy (Canola Council of Canada, 2016; COPA, 2016), while generating 4.7 million metric tonnes of canola meal and 1.5 million metric tonnes of soybean meal as the major byproduct (COPA, 2016). The main similarity between both byproducts is the high protein content where soy meal has an approximate protein content of ~ 43-47 % (w/w on dry matter basis) (Kumar et al., 2002), while canola meal contains 33-37% protein (w/w on dry matter basis).

Irrespective to high protein content, canola meal has a limited number of value added applications, where most of the previous research has been focused on low value animal feed

industry (Khajali & Slominski, 2012). In comparison, there are a number of value-added applications of soy meal, while the industry is continuously expanding its novel uses including bioadhesives (Damodaran & Zhu, 2016).

The adhesive industry is one of the fastest growing industries in the world where 20.2 million metric tonnes of adhesives at a value of $ 64 billion were produced in 2015 (Freedonia Group, 2016). Global adhesive production is projected to have an 4.5% steady annual growth until 2019 (Freedonia Group, 2016). Among many industries, the wood product industry accounts for 65% of total adhesive usage (Pizzi, 2016). Synthetic adhesives such as urea formaldehyde (UF), phenol formaldehyde (PF), melamine formaldehyde (MF), melamine urea formaldehyde (MUF), and aqueous polymer isocyanates (API) made with petrochemical refinery byproducts are considered as the leading wood adhesives (Frihart, 2016; Pizzi, 2016). Despite their low cost, excellent functional properties and easy application, synthetic adhesives are facing increased criticism due to their non-renewability, emission of formaldehyde/other volatile organic compounds, and adverse effects on human health (Frihart, 2013; Gandini, 2008; Pizzi, 2016). Therefore, there is a great interest in developing wood adhesives from renewable polymers such as proteins (Frihart, 2016; Imam et al., 2013; Raquez et al., 2010). This shows an excellent synchronization with the Canadian agenda of developing biobased economy via value addition to agriculture/forestry biomass (AlBIO, 2013; Staffas et al., 2013).

Early studies on protein based adhesives were mainly focused on soy protein (Damodaran & Zhu, 2016; Qi et al., 2016) and wheat gluten (Khosravi et al., 2014; Nordqvist et al., 2012) for adhesive applications. Attempts were made to use canola protein (Li et al., 2011, 2012; Wang et al., 2014), cotton seed protein (Cheng et al., 2013; He et al., 2014), spent hen protein (Wang & Wu, 2012), jatropha seed protein (Hamarneh et al., 2010) and triticale protein (Bandara et al.,

2013) for adhesive preparation. However, poor water resistance and adhesion strength of protein based adhesives remains as a major challenge associated with developing protein based adhesive.

Nanotechnology and biomimetics are two novel areas of wood adhesive research (Qi et al., 2016; Song et al., 2016). Exfoliation of nanomaterials have been used as an effective method in improving flexural, thermal and electrical properties of composites and plastics (Bandara et al., 2017; Kaboorani et al., 2012). A limited number of studies were conducted on the application of nanomaterials in polymer based adhesives such as poly vinyl acetate; however, the reported application of protein based adhesives are extremely limited (Bandara et al., 2017; Qi et al., 2016). Amorphous polymer such as proteins generally have a limited mechanical strength (Khan et al., 2013); therefore exfoliating nanomaterials have the potential to increase adhesion and water resistance properties of protein based adhesives via "physical filling effect" (Li et al., 2016), cohesive interactions and nanomaterial induced crosslinking of protein network (Li et al., 2016; Qi et al., 2016). Appropriate exfoliation of nanomaterial has a direct impact on improving polymer properties (Qi et al., 2016); therefore developing methods to exfoliate nanomaterials in protein matrix is essential.

On the other hand, mother nature has set several examples to learn from, on adhesives with excellent water resistance (Bandara et al., 2013). Mussels (*Mytilus edulis*) are an organism that lives in sea water and has extremely strong protein based adhesive. The adhesion of mussel protein is a result of the presence of 3,4-dihydroxyphenylalanine (DOPA) that can oxidized into DOPA quinone followed by polymerization and crosslinking with the aid of metal ions (Bandara et al., 2013; Lee et al., 2006). However, most of the natural proteins do not have DOPA groups in their structure. Therefore, modification of proteins via biomimetics approach to mimic mussel adhesion mechanism will have a great potential in protein based adhesives.

Therefore, the overall objective of this research is to develop biobased wood adhesives with improved adhesion and water resistance properties from renewable proteins extracted from agricultural/food industry byproducts via nanotechnological and biomimetic approaches. Two hypotheses were proposed in this research: (1) Exfoliating nanomaterials in protein matrix, and preparing hybrid wood adhesives with chemically modified canola protein will improve the adhesion and water resistance of canola protein based adhesive, (2) Biomimetic modification of soy protein to impart DOPA functional groups will improve adhesion and water resistance of soy protein based adhesives.

In order to investigate the above hypotheses, following specific objectives were addressed in this research.

1. To study the effects of exfoliating different nanomaterials at various levels on adhesion properties
2. To develop and characterize nanomaterial reinforced canola protein adhesive with improved adhesion and water resistance, and to understand the mechanism of adhesion improvement.
3. To develop chemically modified (with ammonium persulphate - APS) canola protein-nanomaterial hybrid adhesive by exfoliating GO or nanocrystalline cellulose (NCC).
4. To apply chemically modified canola protein-nanomaterial hybrid adhesive in producing randomly oriented strand board composites at pilot-scale facility.
5. To develop biomimetically modified soy protein adhesive with improved adhesion and water resistance.

1.1 References:

AlBIO-Alberta Innovates Biosolutions. (**2013**). Recommendations to build Alberta's bioeconomy. Available at: http://bio.albertainnovates.ca/media/57924/bioe_final_report_web_may2013.pdf [2016/12/30]

Arshad, M., Kaur, M., & Ullah, A. (**2016**). Green biocomposites from nanoengineered hybrid natural fiber and biopolymer. *ACS Sustainable Chemistry & Engineering*, ***4***(***3***), 1785–1793.

Bandara, N., Chen, L., & Wu, J. (**2013**). Adhesive properties of modified triticale distillers grain proteins. *International Journal of Adhesion and Adhesives*, ***44***, 122–129.

Bandara, N., Esparza, Y., & Wu, J. (**2017**). Exfoliating nanomaterials in canola protein derived adhesive improves strength and water resistance. *RSC Advances*, ***7(11)***, 6743-6752.

Bandara, N., Zeng, H., & Wu, J. (**2013**). Marine mussel adhesion: biochemistry, mechanisms, and biomimetics. *Journal of Adhesion Science and Technology*, ***27***(***18***–***19***), 2139–2162.

Canola Council of Canada. (**2016**). Canadian canola production 2016. Available at: http://www.canolacouncil.org/markets-stats/statistics/tonnes/ [2016/12/28]

Cheng, H. N., Dowd, M. K., & He, Z. (**2013**). Investigation of modified cottonseed protein adhesives for wood composites. *Industrial Crops and Products*, ***46***, 399–403.

COPA-Canadian Oilseed Processors Association. (**2016**). Canadian oilseed processing industry. Available at: http://copacanada.com/crush-oil-meal-production/ [2016/12/25]

Damodaran, S., & Zhu, D. (**2016**). A formaldehyde-free water-resistant soy flour-based adhesive for plywood. *Journal of the American Oil Chemists' Society*, ***93***(***9***), 1311–1318.

Freedonia Group. (**2016**). World adhesives and sealents - Industry study with forcast for 2019 & 2024. Available at: http://www.freedoniagroup.com/industry-study/world-adhesives-sealants-3377.htm [2016/12/27]

Frihart, C. (**2013**). Wood adhesion and adhesives. In R. M. Rowell (Ed.), *Handbook of Wood Chemistry and Wood Composites* (2nd Ed, pp. 255–319). Boca Raton, FL: CRC.

Frihart, C. (**2016**). Potential for biobased adhesives in wood bonding. In *International Convention of Society of Wood Science and Technology* (pp. 84–91). Curitiba, Brazil: Society of Wood Science and Technology.

Gandini, A. (**2008**). Polymers from renewable resources: a challenge for the future of macromolecular materials. *Macromolecules*, ***41***(***24***), 9491–9504.

Hamarneh, A. I., Heeres, H. J., Broekhuis, A. A., & Picchioni, F. (**2010**). Extraction of *Jatropha curcas* proteins and application in polyketone-based wood adhesives. *International Journal of Adhesion and Adhesives*, ***30***(***7***), 615–625.

He, Z., Chapital, D. C., Cheng, H. N., & Dowd, M. K. (**2014**). Comparison of adhesive properties of water- and phosphate buffer-washed cottonseed meals with cottonseed protein isolate on maple and poplar veneers. *International Journal of Adhesion and Adhesives*, ***50***, 102–106.

Imam, S. H., Bilbao-Sainz, C., Chiou, B.S., Glenn, G. M., & Orts, W. J. (**2013**). Biobased adhesives, gums, emulsions, and binders: current trends and future prospects. *Journal of Adhesion Science and Technology*, ***27***(***18–19***), 1972–1997.

Kaboorani, A., Riedl, B., Blanchet, P., Fellin, M., Hosseinaei, O., & Wang, S. (**2012**).

Nanocrystalline cellulose (NCC): A renewable nano-material for polyvinyl acetate (PVA) adhesive. *European Polymer Journal*, ***48***(***11***), 1829–1837.

Khajali, F., & Slominski, B. A. (**2012**). Factors that affect the nutritive value of canola meal for poultry. *Poultry science*, ***91***(***10***), 2564–2575.

Khan, U., May, P., Porwal, H., Nawaz, K., & Coleman, J. N. (**2013**). Improved adhesive strength and toughness of polyvinyl acetate glue on addition of small quantities of graphene. *ACS Applied Materials & Interfaces*, ***5***(***4***), 1423–1428.

Khosravi, S., Khabbaz, F., Nordqvist, P., & Johansson, M. (**2014**). Wheat gluten based adhesives for particle boards: effect of crosslinking agents. *Macromolecular Materials and Engineering*, ***299***(***1***), 116–124.

Lee, H., Scherer, N. F., & Messersmith, P. B. (**2006**). Single-molecule mechanics of mussel adhesion. *Proceedings of the National Academy of Sciences of the United States of America*, ***103***(***35***), 12999–13003.

Li, N., Qi, G., Sun, X. S., Stamm, M. J., & Wang, D. (**2011**). Physicochemical properties and adhesion performance of canola protein modified with sodium bisulfite. *Journal of the American Oil Chemists' Society*, ***89***(***5***), 897–908.

Li, N., Qi, G., Sun, X. S., & Wang, D. (**2012**). Effects of sodium bisulfite on the physicochemical and adhesion properties of canola protein fractions. *Journal of Polymers and the Environment*, ***20***(***4***), 905–915.

Li, X., Luo, J., Gao, Q., & Li, J. (**2016**). A sepiolite-based united cross-linked network in a soybean meal-based wood adhesive and its performance. *RSC Advances*, ***6***(***51***), 45158–

45165.

Nordqvist, P., Thedjil, D., Khosravi, S., Lawther, M., Malmström, E., & Khabbaz, F. (**2012**). Wheat gluten fractions as wood adhesives-glutenins versus gliadins. *Journal of Applied Polymer Science*, ***123***(***3***), 1530–1538.

OECD, & FAO. (**2016a**). OECD-FAO Agricultural outlook 2016-2025. Available at: http://www.oecd-ilibrary.org/agriculture-and-food/oecd-fao-agricultural-outlook-2016_agr_outlook-2016-en [2016/12/25].

Pizzi, A. (**2016**). Wood products and green chemistry. *Annals of Forest Science*, ***73***(***1***), 185–203.

Qi, G., Li, N., Wang, D., & Sun, X. S. (**2016**). Development of high-strength soy protein adhesives modified with sodium montmorillonite clay. *Journal of the American Oil Chemists' Society*, ***93***(***11***), 1509–1517.

Qi, H. (**2013**). Growing bioeconomy-Alberta activities and aapacities. In M. Bruins & T. Boxtel (Ed.), *Biorefinery for Food, Fuel and Materials* (pp. 103). Wageningen, The Netherlands: Proceedings of Symposium Biorefinery for food fuel and materials.

Raquez, J. M., Deleglise, M., Lacrampe, M. F., & Krawczak, P. (**2010**). Thermosetting (bio) materials derived from renewable resources: a critical review. *Progress in Polymer Science*, ***35***(***4***), 487–509.

Song, Y., Seo, J., Choi, Y., Kim, D., & Choi, B. (**2016**). Mussel adhesive protein as an environmentally-friendly harmless wood furniture adhesive. *International Journal of Adhesion and Adhesives*, ***70***, 260–264.

Staffas, L., Gustavsson, M., & McCormick, K. (**2013**). Strategies and policies for the

bioeconomy and bio-based economy: an analysis of official national approaches. *Sustainability*, ***5***(***6***), 2751–2769.

Wang, C., & Wu, J. (**2012**). Preparation and characterization of adhesive from spent hen proteins. *International Journal of Adhesion and Adhesives*, ***36***, 8–14.

Wang, C., Wu, J., & Bernard, G. M. (**2014**). Preparation and characterization of canola protein isolate–poly(glycidyl methacrylate) conjugates: a bio-based adhesive. *Industrial Crops and Products*, ***57***, 124–131.

CHAPTER 2 – Literature Review

2.1 Agricultural Byproducts

Agriculture and food industries are among the leading segments in Canadian economy that contribute towards growth and development of the country (Staffas et al., 2013). The processing operations of these industries generate a great deal of waste and byproducts each year. Considerable amounts of research were carried out in the past few decades on byproduct value addition; however, further efforts are required to explore the full potential of agri/food industry byproduct value addition (FAO, 2016). Among several agricultural and food processing industries available in Canada, the oilseed industry has a specific place due to its increasing contribution towards Canadian economy (COPA, 2016). The Canadian oilseed crushing and refining industries alone contribute around $1.3 billion in annual economic impacts towards the Canadian economy (Canola Council of Canada, 2012; COPA, 2016). Therefore, exploring potential avenues for oilseed industry byproduct values addition remains a top priority.

2.1.1 Oilseed Industry

The world oilseed industry showed continuous growth during past decade except for the 2015/16 crop year, where a marginal reduction was observed due to unfavorable weather conditions (OECD & FAO, 2016a). The world production of major oilseed crops is shown in Table 2.1. Global soybean production in 2015 continued to increase, while production of other oilseeds such as rapeseed (canola), sunflower seed, and groundnuts declined relative to 2014 production volumes (OECD & FAO, 2016a, 2016b). The demand for protein meals showed continuous growth in the past decade, which contributed towards expanding oilseed production in recent years. Among the major oilseed crops, soy bean and rapeseed have an estimated annual

production of 313.9 and 68.0 million metric tonnes in 2016 (OECD & FAO, 2016a) making them the most important oilseed crops in the world.

Table 2.1 – World Production of major oilseed crops. Adopted from (FAO, 2016)

Oilseed crop	**2013/14**	**2014/15 estimated**	**2015/16 forecast**
	Million metric tonnes		
Soybeans	283.3	319.7	313.9
Rapeseed (Canola)	71.9	71.3	68.0
Cottonseed	44.9	45.4	39.8
Groundnuts	38.6	37.7	38.1
Sunflower seed	42.3	40.9	40.8
Palm kernels	14.7	15.4	15.0
Copra	5.6	5.6	5.4
Total	501.6	535.9	523.0

Notes: The split years bring together northern hemisphere annual crops harvested in the latter part of the first year shown, with southern hemisphere annual crops harvested in the early part of second year shown. For the tree crops, which are produced throughout the year, calendar year production for the second year shown is used.

Soybean (*Glycine max*) is a legume crop that cultivated throughout the world, primarily for oil production. In 2015, United States produced the highest volume of soy bean (106.9 million metric tonnes), followed by Brazil and Argentina (100 and 58.5 million metric tonnes respectively) (ASA, 2015). Despite having a low oil content of ~ 18-20% (w/w dry matter basis) compared with other oilseeds such as canola (~ 40-45 % w/w dry matter basis), 52% of the world vegetable oil production is coming from soybean (Kumar et al., 2002). Canada has an annual soybean production (in 2014) of 6.2 million metric tonnes at a value of $ 2.4 billion. The majority of the soybean produced in Canada was exported (3.4 million metric tonnes), while rest

(1.59 million metric tonnes) was domestically processed. Over the past ten years, soybean processing in Canada has increased by 27% (SoyCanada, 2016).

Rapeseed (*Brassica spp.*) is the second largest oilseed crop grown in the world with an expected annual production volume of 68 million metric tonnes in 2015/16 growing season (FAO, 2016). Canola (*Brassica napus* L.) is the major rapeseed variety used in today's agriculture, which was developed by reducing erusic acid content (Aider & Barbana, 2011; S. Tan et al., 2011). The name canola derived by contracting Canada and "ola" (meaning oil), but need to meet specific standards on erusic acid content to use the name canola for rapeseed (Aider & Barbana, 2011; Canola Council of Canada, 2016). Canola have a seed oil content of 40-45% (w/w dry matter basis) and protein content of 17-26% (w/w dry matter basis) depending on the canola variety (Aider & Barbana, 2011). Canada remains as the world leading producer in Canola/rapeseed with annual production of 18.4 million metric tonnes followed by China and India with a production of 13.5, and 6.8 million metric tonnes respectively in 2015 (Canola Council of Canada, 2016). In contrast to soybean, canola is considered Canada's most valuable crop. A study released in 2013 showed an overall contribution of $19.3 billion into Canadian economy while creating more than 249,000 jobs in the canola industry (Canola Council of Canada, 2016). Over the past 10 years, canola processing in Canada has increased by 132%; however, only 45% of Canadian canola production was processed domestically, where rest is exported as raw seeds (COPA, 2016).

2.1.2 Oilseed Processing

Harvested soybean seeds are first transported into crushing facilities. At the time of seed processing, soybean seeds contain 9-14% moisture, 18-22% oil, 33-39% proteins, 15-25% carbohydrates, <7% fiber and <6% ash content (w/w on dry matter basis) (van Doosselaere,

2013). Soybean seeds are cleaned and conditioned according to the required standards. Clean soybeans are cracked into pieces using cracking mills equipped with corrugated rollers, and cooked at 60-70 ºC using steam cookers to condition soybean grits (Woerfel, 1995). Following cooking, conditioned grits are sent to flaking mills, to process grits into soybean flakes that are used for the oil extraction. In some extraction plants, a bulking of soybean flakes is carried out using extrusion processing. Hexane is widely used to extract soybean oil (van Doosselaere, 2013). Following extraction, hexane is removed using steam distillation, while soybean oil is sent for refining. Soybean cake is desolventized and toasted to remove hexane, followed by drying to prepare soy meal. Crude soybean oil is refined by using degumming, neutralization, bleaching, and deodorization steps (van Doosselaere, 2013; Woerfel, 1995).

Processing of canola oil shows similarities to soybean oil production. At the time of receiving canola seeds for processing they contain 7-10% moisture, 35-45% oil, 19-23% protein, 10-15% fiber and 3-4% ash and carbohydrates (van Doosselaere, 2013). Canola seeds are cleaned according to the specification for maximum moisture content, seed damage and chlorophyll content as set by Canadian grain commission (Newkirk, 2015). Canola seeds are preconditioned by heating up to ~35 ºC (in some plants even up to 60 ºC), flaking through roller mills, and cooked by increasing temperature up to 80-90 ºC using steam cookers to increase oil yield and to deactivate myrosinase enzyme (Newkirk, 2015; van Doosselaere, 2013). Unlike soybean oil extraction, cooked canola flakes are first sent through a pressing step using a series of screw presses and expellers, removing almost 50-60% of seed oil content. The resulting pressed meal is extracted using hexane to obtain remaining oil. Extracted oil is refined similar to soybean oil processing (van Doosselaere, 2013). Canola oil cake is desolventized and toasted to remove hexane, followed by drying to prepare canola meal (Newkirk, 2015).

2.1.3 Composition and Applications of Oilseed Meals

Oilseed meal is the major byproduct generated in oilseed processing industry. Therefore continuous efforts are being devoted to developing value added applications into oilseed meals. Table 2.2 shows the changes in composition of soy meal and canola meal after oil extraction.

Table 2.2 – Nutrient composition of soybean meal and canola meal. Adopted from Newkirk, (2015) and Bonnardeaux, (2007)

Component	**Soybean meal**	**Canola meal***
Moisture	12	10
Crude protein % (N×6.25)	47	35
Oil %	3.0	3.5
Linoleic acid %	0.6	0.6
Ash%	6.2	6.1
Sugar %	9.17	8.0
Starch %	5.46	5.2
Cellulose %	-	4.6
Oligosaccharide %	-	2.3
Non-starch polysaccharides %	-	16.1
Crude fiber %	5.40	12.0
Acid detergent fiber %	7.05	17.2
Neutral detergent fiber %	11.79	21.2
Tannins %	-	1.5
Phytic acid %	1.55	4.0
Glucosinolates (μ mol/g)	-	16.0

** canola meal after extracting oil by pressing and solvent extraction. Expeller press meal have higher oil content.*

In 2015, Canada produced 4.7 million metric tonnes of canola meal and 1.5 million metric tonnes of soybean meal (COPA, 2016). Soy meal has an approximate protein content of ~ 43-47% (w/w on dry matter basis) (Kumar et al., 2002), whereas canola meal contains 33-37% protein (w/w on dry matter basis). Both oilseed meals have comparatively similar oil, linoleic acid, ash, sugar, and starch contents; however, canola meal contain significantly higher amounts of fiber, phenolic acids and glucosinolates compared to soy meal (Newkirk, 2015). Soybean meal is a key ingredient in feed formulations that prepared for both fish, broilers an layer hens, pigs and cows (Kinsella, 1979; Kumar et al., 2002), and used to extract soy protein isolate and soy protein concentrate. Recently, soybean meal was used in non-food applications such as composites and adhesives as well (Luo et al., 2015; Yuan et al., 2016). In comparison to soy meal, canola meal has limited value added applications, where most of the research has been focused on animal feed trials (Khajali & Slominski, 2012). However, the use of canola meal on monogastric animal feeds is limited due to the presence of high fiber content (Bonnardeaux, 2007; Newkirk, 2015); therefore most of the feeding trials were focused on ruminant animals (Heendeniya et al., 2012). Also, presence of glucosinolates, phenolic acids and other anti-nutritional factors limit the feed applications in ruminants as well (Heendeniya et al., 2012; Khajali & Slominski, 2012). Human food applications of canola meal are yet to be explored (Aider & Barbana, 2011).

2.1.4 Properties and Extraction of Soy and Canola Proteins

Soy protein and canola protein have unique structural and functional properties that are different from each other. Therefore a proper understanding of protein structure and functionality is required to develop optimum extraction, modification and value added applications for each oilseed protein.

2.1.4.1 Soy Protein

Protein in soybean seeds are mainly composed of four subgroups; storage proteins, enzyme/enzyme inhibitors, structural proteins and membrane proteins (Krishnan, 2001). Four major globulin storage proteins were identified based on the sedimentation rate at 2S, 7S, 11S and 15S with approximate molecular mass of 25, 160, 350 and 600 KDa respectively (Liu, 2012). More than 85% soybean storage globulins are associated with 7S and 11S globulins commonly known as β-conglycinin and glycinin respectively. β-conglycinin and glycinin accounts for the 40% and 25% total seed protein content (Mojica et al., 2015). Glycinin is a hexamer that are made with six acidic and six basic polypeptides and have a molecular weight of 300-380 KDa (Liu, 2012; Mojica et al., 2015). The isoelectric point (pI) of acidic subunits are ranged between 4.5 to 5.5 (Staswick et al., 1981) whereas, pI of basic subunits are in the range of 6.5 to 8.5 (Staswick et al., 1984b). Each subunit of glycinin consist with one acidic and one basic polypeptide chain linked via a disulfide bond (Staswick et al., 1984a). At pH 7.6, all six subunits formed into a hexamer with molecular weight of 360 KDa, while at pH 3.8 they converted into two trimeric units with molecular weight of 180 KDa (Mojica et al., 2015).

β-conglycinin is a soybean storage protein with a molecular weight of 150-200 KDa (Wang et al., 2008). It is a trimeric glycoprotein which consist of α, α′, and β subunits with a molecular weights of 68, 72, and 52 KDa respectively (Thanh & Shibasaki, 1977). β-conglycinin subunits are connected with each other via strong hydrophobic interactions and hydrogen bonding (Mojica et al., 2015). The ionic strength of the solution directly affects the structure of β-conglycinin via association and dissociation phenomena. At neutral pH and ionic strength above 0.5 β-conglycinin shows 7S globulin form where reducing ionic strength to 0.2 changed the β-conglycinin into aggregated 9S globulin (Thanh & Shibasaki, 1979).

The unique pI values of glycinin and β-conglycinin has been used in extraction of soy protein by several researchers. Thanh and Shibasaki, (1976) extracted soy protein from defatted soy flour using Tris buffer with β-mercaptoethanol at pH 8.00. β-mercaptoethanol will disrupt disulfide bonds and improve protein solubility, while pH 8.00 will ensure optimum solubility for both glycinin and β-conglycinin as their pI is around 4.85 and 6.40 respectively (Thanh & Shibasaki, 1976). Further separation of glycinin and β-conglycinin can be achieved by precipitating solubilized proteins at their respective pI values (Thanh & Shibasaki, 1976). Nagano et al., (1992) extracted soy protein using an aqueous medium consist of sodium bisulfite as a reducing agent and 0.25 M NaCl to improve protein solubility. Increasing centrifugation speed of same extraction method showed an improvement in extraction yield and purity (Wu et al., 1999). In another study, using divalent cations such as Ca^{2+} and Mg^{2+} instead of Na^{+} for improving protein solubility has increased the protein yield and purity (Deak et al., 2006). Commercial soy protein extraction and purification are carried out using scaled up methods of previous laboratory technologies such as ultrafiltration, reverse osmosis, and chromatographic methods (Mojica et al., 2015).

2.1.4.2 Canola Protein

Two predominant types of canola storage proteins and another minor oil body protein have been identified from canola seeds (Wanasundara, 2011). Canola storage proteins mainly consist of cruciferin (legumin type 12S globulin protein), napin (napin-type 2S albumin protein) and oleosin with approximate compositions of ~60%, ~20% and ~8% respectively (Li et al., 2011; Wanasundara, 2011). Cruciferin belongs to the “cupin (small barrel)” protein superfamily; therefore, similar to other cupin family protein, it shows well organized hierarchical protein structure (Aachary et al., 2015). The primary structure of cruciferin consists of a polypeptide

chain that made with 465 to 509 amino acid residues (Tan et al., 2011). Cruciferin is a large neutral protein with a isoelectric point (pI) of 7.2 and molecular weight of ~ 300-310 KDa (Aider & Barbana, 2011). Cruciferin polypeptide chain consists of six sub-units that have an approximate molecular weight of ~ 50 KDa each (Tan et al., 2011; Wanasundara, 2011). Each cruciferin subunit is made with two polypeptide chains; a heavy acidic α-chain (~30 KDa, 254-296 amino acid residue) and light basic β-chain (~20 KDa, 189-191 amino acid residues) that link via a single disulfide bond between amino acid side chains (Aider & Barbana, 2011; Tandang-Silvas et al., 2010; Wanasundara, 2011). Napin is a 2S protein that consists of highly amidated amino acid residues with a strong basic pI at ~11.0. The molecular weight of napin is around ~ 12.5-14.5 KDa (Aider & Barbana, 2011; Nietzel et al., 2013). It consists of two polypeptide chains, a ~4.5 KDa polypeptide with ~40 amino acid residues and 9.5 KDa polypeptide with ~90 amino acid residues which are stabilized by two inter-chain and two intra-chain disulfide bonds (Aider & Barbana, 2011; Wanasundara, 2011). Several attempts were made in the recent past in order to extract canola protein for different applications. Tzeng et al., (1990) developed a canola protein extraction method using alkaline extraction (pH 10.5-12.5), followed by acid precipitation (pH 3.5) and membrane processing to improve extraction yield. Klockeman et al., (1997) modified the alkaline extraction process where, canola meal was first mixed with 0.4% (w/v) NaOH to solubilize protein, followed by precipitating protein at pH 3.5 using glacial acetic acid. Similar to soy protein extraction, solubilization of canola protein at higher pH using NaOH (away from pI) and subsequent precipitation at isoelectric point using HCl has been tested in both laboratory and commercial scale trials (Manamperi et al., 2010).

2.1.5 Value Addition to Oilseed Industry Byproducts

CHAPTER 2

Protein rich agricultural byproducts such as canola meal and soy meal are abundant resources in Canada and around the world. Value addition to these byproducts will increase the profitability of farmers and processing industries (Wang et al., 2014). Byproduct value addition will have an excellent synchronization with the Canadian attempts towards creating a diversified bio-economy, in order to reduce the dependency on non-renewable resources (Qi, 2013; Staffas et al., 2013). In comparison of two major oilseed byproduct proteins, soy protein have well established feed and food applications in areas such as monogastric feed rations (Denbow et al., 1995), ruminant feed rations (Van Nhiem et al., 2013), food additive to improve emulsion (Kasran et al., 2013), gelling (Li et al., 2007), and foaming (Suppavorasatit et al., 2011), and as food ingredient in meat (Herrero et al., 2008) and bakery products (Mojica et al., 2015) etc. In addition, soy protein have shown excellent properties in preparing biofilms (Mojica et al., 2015), plastics (Kumar et al., 2002) and adhesives (Damodaran & Zhu, 2016; Kumar et al., 2002). However, in order to keep up with the growing supply of soybean meal, further exploration of value added applications are essential.

On the other hand, canola protein do not have well established valued added applications, except in animal feed industry, where it has limited usage in ruminant feed formulations (Newkirk, 2015). The presence of anti-nutritional factors limit the potential applications in monogastric feed formulations (Bonnardeaux, 2007; Newkirk, 2015). Up to date, canola protein is not used as food ingredient in human diets, mainly due to the presence of anti-nutritional factors and poor functional properties compared to soy protein (Aachary et al., 2015). Limited number of research was carried out on non-food application of canola protein, mainly in preparing plastics (Manamperi et al., 2010) and adhesives (Li et al., 2011; Wang et al., 2014). Therefore, exploring potential value added applications is essential in order to improve

sustainability and profitability of canola industry. In this context, focusing on non-food applications such as developing biobased adhesives will have special impact on the oilseed industry. Protein have been used as an adhesive from ancient civilizations; however, the growth of synthetic adhesives and limitations in protein based adhesive functionality has retarded the protein adhesive market (Frihart, 2016). Therefore it would be an ideal scenario to utilize byproduct proteins from oilseed industry towards developing/reinventing biobased adhesive via novel technologies.

2.2. Adhesion

Adhesion is a complex phenomenon that has its roots in several scientific and technological areas such as macromolecular science, physical chemistry, surface and interfacial science, material science, and rheology (Schultz & Nardin, 2003). A fundamental understanding on adhesion mechanism is essential in developing high performance engineered wood products. Even though, adhesives were used several thousand years ago, the theoretical studies on adhesion was started around 60 years ago (Schultz & Nardin, 2003; Stoeckel et al., 2013).

2.2.1 Adhesion Mechanisms

Several adhesion theories/mechanisms have been proposed in the past to explain adhesion between surface (adherent) and adhesive. Among them, mechanical interlocking theory, electronic theory, theory of boundary layers and interfaces, adsorption theory, diffusion theory and chemical bonding theory are considered to be the leading theories.

Mechanical interlocking theory was proposed by McBain and Hopkins in 1924, and considered as the first major theory on adhesion (McBain & Hopkins, 1924). According to mechanical interlocking theory, adhesive will penetrate into the pores, cavities, and surface

irregularities of adhered surface displacing trapped air, followed by binding of substrate during subsequent adhesive curing (McBain & Hopkins, 1924; Baldan, 2012; Schultz & Nardin, 2003). Mechanical interlocking theory does not explain methods on adhesion improvement at molecular level, instead it explains the technical means to increase adsorption of the adhesive on the substrate via surface treatment to increase roughness, porosity, and irregularities of the surface (Baldan, 2012). In addition, wetting of the surface considered as critical in mechanical interlocking theory, where adhesive needs to penetrate into wood. Therefore rheology of the adhesive also plays an important role in mechanical interlocking (Maeva et al., 2004).

Adsorption theory of adhesion was first introduced by Sharpe and Schonhorn (Sharpe & Schonhorn, 1964), and considered as most acceptable theory of adhesion. It's also known as thermodynamic theory or acid base theory as well. This theory suggests that the materials will adhere due to interatomic and intermolecular forces that occurred between the atoms and molecules in the adhesive and substrate upon their contact (Sharpe & Schonhorn, 1964; Baldan, 2012; Gardner, 2006). According to adsorption theory, secondary interactions such as van der Waals forces, hydrogen bonds; primary interactions such as covalent, ionic, and metallic bonds; and donor acceptor interactions are the primary contributing forces in adhesion (Schultz & Nardin, 2003). Adsorption theory also suggests the importance of surface and wetting of adhesion surface as critical factors in adhesion; therefore, it led the industry to develop materials with lower surface tension than the adherend surface tension (Sharpe & Schonhorn, 1964; Baldan, 2012; Schultz & Nardin, 2003). First introduced by Voyutski in 1963, diffusion/interdiffusion theory suggests that adhesion occurs as a result of interdiffusion of macromolecules from two polymeric materials at the adhesion interface (Voyutski, 1963; Grundmeier & Stratmann, 2005). Therefore, both adhesive and adherend are supposed to be

polymeric material that are mutually miscible and compatible (Baldan, 2012; Grundmeier & Stratmann, 2005). Nature of the materials such as chain length and molecular movements play a vital role in interdiffusion theory, where two polymers are required to move around in the adhesion interface in order to have stable adhesion (Schultz & Nardin, 2003).

Electrostatic attraction theory (electrical adhesion mechanism) suggests that adhesion mechanism is based on the two materials joined at interface by mutual sharing of electrons (Kinloch, 1980, 1982). The difference in electronic band structures in adhesive and adherend at interface layer will trigger electron transfer between two materials, creating double layer of electrical charge that improves adhesion between two surface (Hale, 2013). Therefore, according to this theory, one surface should have positively charges while the other negatively charges in order to achieve adhesion (Baldan, 2012). Model of weak boundary layer explains the role of weak boundary layer that formed in adhesion interface (Schultz & Nardin, 2003). They suggest that interface between adhesive and adherend would not fail usually, but the failure was mainly caused by the formation of a week boundary layer in adhesion interface. Therefore, to improve adhesion of a substrate, they suggest to minimize the potential of forming a weak boundary layer (Baldan, 2012; Kinloch, 1980; Schultz & Nardin, 2003). For example, adhesion of metal surface would deteriorate due to the formation of metal oxide layer (a weak boundary layer), and removing surface oxide layer will improve the adhesion.

Chemical/molecular bonding theory suggests that chemical bonds formed between adhesive and adherend at the interface are the key factor in adhesion of two materials. Intermolecular interactions such as dipole-dipole interactions, van der Walls forces and primary chemical bonds (ionic, covalent and metallic bonds) are considered to be the primary means of adhesion (Kendall, 1994; Baldan, 2012; Gardner, 2006; Schultz & Nardin, 2003). Compatible

chemical functional groups present in adhesive and adherend surface will create interactions; thus adhesion will depend on the number and type of bonds formed in the adhesion interface (Kendall, 1994; Gardner, 2006). All the above adhesion theories can be broadly categorized into two groups; 1) Theories that rely on interlocking and entanglement (mechanical, diffusion), 2) Theories that rely on charge interactions (electrostatic, adsorption/acid base, weak boundary layer, chemical bonding) (Gardner, 2006). The practical length scale required for each interaction is shown in Table 2.3. The adhesion mechanisms that rely on interlocking and entanglement of molecules can have the interactions over larger rage of length scale where charge type interactions usually require molecular level or nano level length scale to have interactions with the exception for electrostatic interactions that can operate in wider range of length scale (Baldan, 2012; Gardner, 2006).

Table 2.3 – Comparison of length scale required for adhesive interactions according to each adhesion mechanism. Reproduced with the permission from Gardner (2006)

Category of adhesion mechanism	**Type of interaction**	**Length scale**
Mechanical	Interlocking or entanglement	0.01 – 1000 μm
Diffusion	Interlocking or entanglement	10 nm – 2 mm
Electrostatic	Charge	0.1 – 1.0 μm
Covalent bonding	Charge	0.1 – 0.2 nm
Acid-base interaction	Charge	0.1 – 0.4 nm
Van der Waals	Charge	0.5 – 1.0 nm

2.2.1.1 Wood Adhesion

Wood adhesion is a complex phenomenon, mainly due to the diverse nature of wood surface and the adhesives used in the process. To produce high quality wood composites, a

fundamental understanding on wood surface, and properties of other involved materials are essential (Stoeckel et al., 2013). Fig 2.1 shows the macroscopic images of wood surface (2.1 - A), enlarge image at adhesion interface (2.1 - B), and microscopic image of wood adhesion surface (2.1 - C) (Stoeckel et al., 2013). Exact form of wood adhesion is varied from one wood type to another, mainly due to nonhomogeneous nature of each wood material due to porosity, anisotropy, dimensional instability and surface properties (Gardner, 2006). Being a cellular material itself, different wood species show unique porosity; hygroscopic nature of wood dictates swelling and shrinking of wood creating dimensional instability (Frihart, 2013; Frihart & Hunt, 2010). Physical and mechanical properties of wood are dictated by the orientation of wood element (anisotropic nature) (Gardner, 2006). Wood surface properties such as chemical heterogeneity, surface inactivation, weak boundary layers and processing conditions of the wood will directly impact on the adhesion (Frihart, 2013; Gardner, 2006).

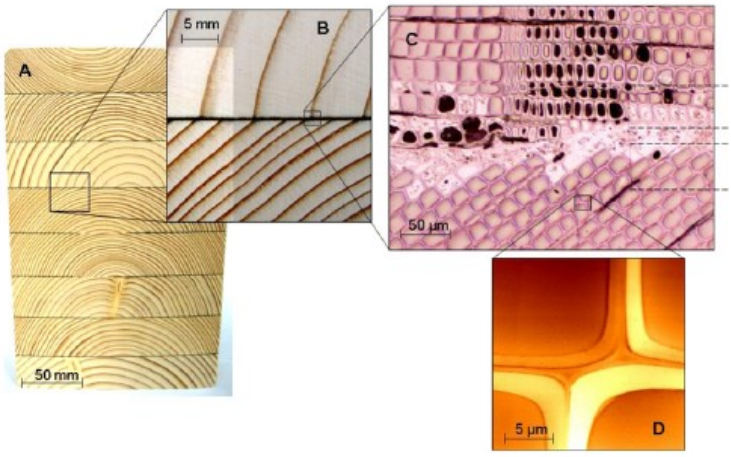

Fig 2.1 – Scales in adhesive bonds of solid wood (A) and (B) macroscopic scale, (C) microscopic scale with indicated bond regions and (D) atomic force microscopic image of wood cell walls. Reproduced with the permission from Stoeckel *et al* (2013).

The first step involving in wood adhesion is the wetting of wood surface, after adhesive application into wood surface. Wetting includes the flowing of adhesive over wood surface and penetration into the pores and cavities on wood surface (Frihart & Hunt, 2010). To achieve best adhesion, adhesive molecules should come into direct contact with wood molecules, thereby increasing mechanical interlocking and intermolecular attraction/bonding of adhesive and wood surface (Frihart, 2013). Therefore, viscosity of the adhesive plays a vital role in wood adhesion. Following wetting step, adhesion interface will consist of pure wood adhesive molecules, pure adherend (wood) molecules and mixture of adhesive and adherend molecules (Fig 2.1 C) (Frihart, 2013; Marra, 1992).

Adhesive solidification is a critical step, mainly due to the intermolecular bond formation that occurs during conversion of liquid adhesive into solid material. However, the full adhesion strength will require few hours, and in some cases few days to develop after adhesive solidification step (Frihart, 2013; Frihart & Hunt, 2010; Hale, 2013). Adhesive solidification can occur either due to loss of solvent via evaporation or diffusion into wood surface, by cooling of molten adhesive, or by chemical polymerization into crosslinked network (Frihart, 2013; Frihart & Hunt, 2010). Chemical polymerization and crosslinking can be triggered/activated using heat, catalyst, change in pH, radiation or by adding second adhesive component. In the engineered wood product industry, heat induced polymerization is the common method used in adhesive curing (Frihart & Hunt, 2010).

2.2.2 Adhesive Failure

In general, adhesion strength is measured by applying a tensile load perpendicular to adhesion interface, and recording the maximum tensile strength required to break the bond (Baier et al., 1968). Several possibilities exist in terms of bond failure at adhesion interface. Fig 2.2

shows a schematic representation of adhesive failure modes. If, adhesion failure occurred between adhesive, and one of the adherend surface, it refers as “adhesive failure” (Ebnesajjad, 2008). If the bond failure occurred in a manner that both adherend surfaces remain covered with an adhesive layer, while bond failure occurred between adhesive molecules, it refers as the “cohesive failure in adhesive layers” (Ebnesajjad, 2008; Schultz & Nardin, 2003). In certain cases, adhesive layer will have excellent strength exceeding the strength of adherend layers, thereby results in a bond failure at adherend. These type of bond failure is referred as “cohesive failure in the adherend” (Ebnesajjad, 2008). However, in a practical situation, bond failure occurs due a combination of failure modes; therefore bond failure is usually reported as a percentage of adhesive and cohesive failure (Baldan, 2012; Ebnesajjad, 2008).

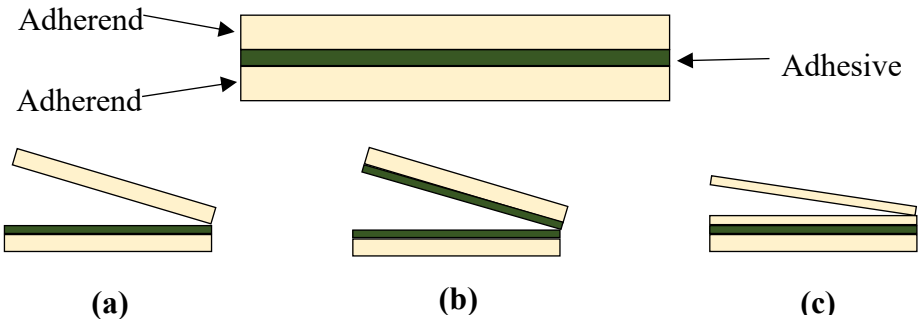

Fig 2.2 – Schematic representation of adhesive failure modes. (a) adhesive failure, (b) cohesive failure in the adhesive layer, (c) cohesive failure in the adherend

2.3 Wood Adhesives

Adhesives are defined as the non-metallic substances, usually polymers that can bind two surfaces through adhesive and cohesive interactions (Rajasekar et al., 2016). Adhesive industry is one of the fastest growing industries in the world with an estimated annual usage of 20.2 million metric tons at a value of $ 64 billion. The projected global demand for adhesives and sealants are expected to rise at steady 4.5% until 2019 (Freedonia Group, 2016). Adhesives are

widely used in several industrial segments such as construction, packaging, food and agriculture, aerospace, automotive, electronics, paints and lubricant, pharmaceuticals, furniture and engineered wood products (Imam et al., 2013). Wood industry is the largest user of adhesive industry, accounting for 65% world total adhesive usage (Pizzi, 2016), mainly in the processing of engineered wood products (Kaboorani et al., 2012). Present wood industry is saturated with petrochemical byproduct based adhesives resins due to unique advantages such as low cost and excellent mechanical strength (Pizzi, 2013).

2.3.1 History of Wood Adhesives

Even though, present adhesive industry predominantly depend on synthetic adhesives which came to the market after the second world war, utilization of adhesives are dated back to 6000 B.C (Frihart et al., 2014). Neanderthals used animal glues to create waterproof painting on cave walls around 6000 B.C, Egyptians used protein based adhesives for their crafts and paintings around 2000 B.C, and archeologist have found broken pottery, which was repaired with tree sap glue in burial sites that dated back to 1000-1500 B.C (Frihart et al., 2014; Nicholson et al., 1991). The first written evidence on adhesive usage was appeared around 200 B.C, where they showed a simple procedure of making and using animal glue (Nicholson et al., 1991). Uses of animal blood, collagen, fish glue and casein based glues were reported in early 1800s, while the first soy based glue was reported in early 1900s (Frihart et al., 2014; Hale, 2013; Nicholson et al., 1991). However, the use of biobased adhesives were quickly replaced by the rise of synthetic adhesives derived from petrochemical refinery byproducts. Urea formaldehyde was first introduced in 1930, while phenolic resins and poly (vinyl acetate) adhesives were introduced in 1935 and 1939 respectively (Keimel, 2003). Since then, synthetic adhesives kept on growing at a rapid rate, until the interest on biobased adhesives re-emerged on 1990s (Pizzi, 2013).

2.3.2 Synthetic Wood Adhesives

In present context, synthetic adhesives dominates the commercial adhesive applications in engineered wood product industry (Pizzi, 2016). Widespread applications of synthetic adhesive is a result of easiness in application, low cost, and superior adhesion properties (Frihart, 2013; Pizzi, 1994). There is a vast array of synthetic adhesives; however, they can be broadly classified into four major groups; formaldehyde based, isocyanate based, epoxy based and polyvinyl acetate based adhesives (Frihart, 2013).

2.3.2.1 Formaldehyde Based Adhesives

Formaldehyde based adhesive are among the most common synthetic wood adhesives, that are commonly made with reacting another polymer such as urea, phenol, resorcinol, or melamine (Frihart, 2013). Fig 2.3 shows the schematic representation of common formaldehyde adhesives and their addition reaction. Urea formaldehydes (UF) were first synthesized in 1844, and developed as an adhesive in 1929 (Zhao et al., 2011). UF resins are produced by reacting formaldehyde with urea either in an acidic or basic medium (Updegraff, 1990). UF resins are considered to be extremely low cost, non-flammable material with rapid curing rate (Keimel, 2003; Zhao et al., 2011). However, UF resins exhibit poor water resistance and higher degree of bondline failure in accelerated aging test, which limit UF for indoor applications. Formaldehyde emission over the time remains as another major issue related to UF resin (Keimel, 2003; Zhao et al., 2011). Phenol formaldehyde (PF) resins are the oldest synthetic resin that was developed in early 20th century (Detlefsen, 2002). Unlike UF resin, PF resins are used in both wood lamination and engineered wood products due to their outstanding durability, higher adhesion strength, and stability of the resin (Frihart, 2013).

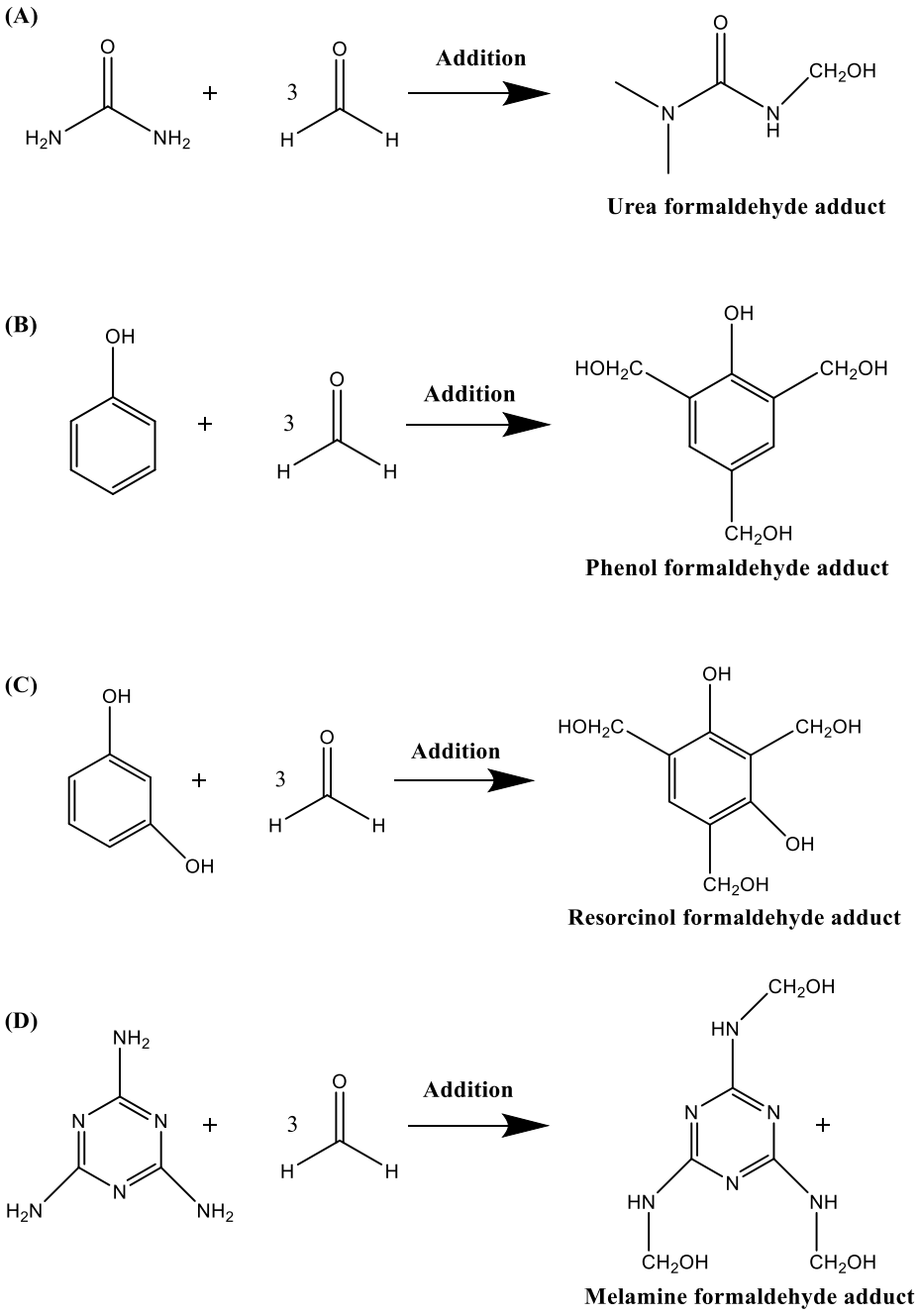

Fig 2.3 – Schematic representation of preparing major formaldehyde based adhesives (A) urea formaldehyde, (B) phenol formaldehyde, (C) resorcinol formaldehyde, (D) melamine formaldehyde adhesive

PF resins are produced by reacting formaldehyde or formaldehyde precursor with phenol either at acidic or basic pH. Two major types of PF resins are made by changing reaction pH and phenol to formaldehyde ratio. “Novolak” resins are produced by reacting formaldehyde to phenol ratios of 0.5 or 0.8 at pH 4 or 7 while “Resol” PF resins are produced by reacting formaldehyde to phenol ratios of 1.0 or 3.0 in the presence of alkali hydroxide (pH 7 to 13) (Frihart, 2013).

Resorcinol formaldehyde (RF) has unique advantage over PF resin, mainly due to its ability of curing at room temperature without external heat application. Higher reactivity of RF resin is derived from the combined effect of two hydroxyl groups on the aromatic ring that activates 2-, 4-, and -6 positions to react with formaldehyde during addition reaction (Pizzi, 2003c). Similar to PF resin, RF resins are used in applications where they need high strength and durable adhesion (Pizzi, 2003c; Zhao et al., 2011). Melamine formaldehyde (MF) adhesives are produced by reacting formaldehyde with melamine at a ratios of 1:2 or 1:3 (formaldehyde:melamine). MF resins have acceptable water resistance, and lighter in color than PF and RF resins; thus suitable for exterior and semi-exterior plywood and particle board applications (Pizzi, 2003a). However high cost of melamine limits the applications of MF resin; but a new class of adhesive named melamine urea formaldehyde (MUF) was developed by adding urea into reaction mixture, mainly to reduce cost (Frihart, 2013; Pizzi, 2003a, 2013).

2.3.2.2 Isocyanate Based Adhesives

Isocyanate’s based adhesives are widely used in the adhesive industry, mainly due to their high reactivity. It can react with any functional group that contain reactive hydrogens such as amine or hydroxyl groups at room temperature (Frihart, 2013; Zhao et al., 2011). However, high reactivity of isocyanate’s may become a limiting factor in adhesive applications as well. Water

molecules present in wood will compete with isocyanate, thereby reducing isocyanate reactivity towards –OH and –COOH groups of cellulose and lignin present in wood (Frihart, 2013; Johns, 1982). In addition, it reacts with many compounds present in human body, potentially causing detrimental health effects (Dhimiter et al., 2007; Mekonnen et al., 2014). Several types of isocyanate based adhesives are used in the adhesive industry. Self-curing isocyanate are most common type that used in composite production and wood lamination. Polymerization of self-curing adhesives will initiate upon the contact with water present in wood products (Johns, 1982). The polymeric dyphenylmethane diisocyanate (pMDI) is another isocyanate based adhesive that are primarily used in producing core layer of oriented strand boards (OSB), mainly due to its rapid polymerization under low temperature conditions (Mekonnen et al., 2014). Emulsion polymer isocyanate is two component adhesive system mainly used in OSB and other engineered wood products (Frihart, 2013). Polyurethanes are another class of isocyanate based adhesives, which are mainly being used in specialty adhesive applications (Desai et al., 2003).

2.3.2.3 Epoxy Adhesives

Epoxy adhesives are mainly used in plastic, concrete, ceramic and metal products; however, have limited applications in wood adhesion mainly due to higher cost (Frihart, 2013; Raftery et al., 2009). However, potential of curing at ambient temperatures, excellent gap filling ability and bond strength of epoxy adhesives have encouraged researchers to look into wood adhesive applications (El-Thaher et al., 2014; Pizzi, 1994a). Diglycidly ether of bisphenol A (DGEBA) is the most common epoxy type adhesive used in wood adhesion which is produced by reacting epichlorhydrin with bisphenol A. Poor adhesive performance under wet condition is one of the major obstacle in using epoxy based adhesives in wood product industry (Frihart, 2013; Pizzi, 1994; Raftery et al., 2009).

2.3.2.4 Polyvinyl Acetate Adhesives

Polyvinyl acetate (PVA) is a waterborne adhesive system, that are mainly used in assembling wood and paper products into finished goods (Kaboorani & Riedl, 2011; Khan et al., 2013). PVA adhesives are made by self-polymerization of vinyl acetate monomers under free radical initiation (Frihart, 2013). Applications of PVA in engineered wood products are limited, mainly due to the lack of water resistance and creep resistance (Kaboorani et al., 2012; Kaboorani & Riedl, 2011). Crosslinking PVA with other resins such as glyoxal, formaldehyde or isocyanate will improve the water resistance and creep resistance; however, these additives need to be added just before adhesive application to avoid premature crosslinking (Frihart, 2013).

2.3.3 Synthetic versus Biobased Adhesives

Both synthetic and biobased wood adhesives have their unique advantages and disadvantages. A selection of a suitable adhesive is mainly depend on the type of wood product and the intended usage of the product (Pizzi, 2013). Even though most of synthetic adhesives have acceptable adhesion and low cost, biobased adhesives present a major advantages in terms of environmental and human health properties (Mathias et al., 2016). Synthetic adhesives are mainly derived from petrochemical byproduct resins, therefore sustainability and renewability of synthetic adhesives has become a point of concern in last few decades (Pizzi, 2006, 2016). In addition, emission of formaldehyde and other volatile organic compounds (VOCs) becomes a human health concern. Several states in USA and Canada has made strict legislation on formaldehyde emission from wood products (Imam et al., 2013; Mathias et al., 2016). At the same time, general public awareness on synthetic adhesives, concern on potential health hazard/environmental impact of synthetic adhesives, and desire for green biobased materials are

putting pressure on adhesive industry to move towards biobased adhesives (Frihart, 2016; Imam et al., 2013; Mathias et al., 2016). Therefore, adhesive industries and academia have shown interest on biobased adhesives and extensive research efforts were made recently on utilizing biobased polymers for adhesive applications. However, success of biobased adhesive in engineered wood product industry will rely on developing bioadhesives with suitable mechanical and chemical properties at competitive price range (Mathias et al., 2016).

2.3.4 Biobased Wood Adhesives

Chemicals and materials derived from plants, microbial and animal sources have been used as adhesive over several centuries (Nicholson et al., 1991). However, the full potential of biobased adhesives has not been explored until recently (Imam et al., 2013). Global market share of biobased adhesives are keep growing in the world as specialty material where biobased adhesive and sealant industry is expected to grow up to a record $1.24 billion in 2017 (Mathias et al., 2016). Tannins, lignin's, starch and carbohydrates, unsaturated oils and proteins are the main biobased polymer sources used in adhesive applications (Imam et al., 2013).

2.3.4.1 Tannin Adhesives

Tannins are polyhydroxypolyphenolic compounds that are extracted from plant materials, but only a limited number of plant species contain tannin in commercially extractable quantities (Efhamisisi et al., 2016; Frihart, 2013). Similarity of tannin towards PF resin is one of the main reasons of interest on tannin for adhesive applications. Tannins are generally extracted from plant materials using organic, ionic or water based solvents, purified and spray dried prior to adhesive application (Pizzi, 2003b). Extracted tannin isolate has similar characteristics to resorcinol, such as high reactivity and water resistant bonds after copolymerizing with

formaldehyde (Frihart, 2013). High viscosity, limited availability, inconsistency of source and their reactivity remain as the key issues in developing commercially viable tannin adhesive (Frihart, 2013). Researchers are looking into utilize different tannin sources such as pine (Cui et al., 2015), maritime pine (Chupin et al., 2013), mimosa (Moubarik et al., 2013), and even waste forest biomass like beetle infested lodgepole pine (Zhao et al., 2013a, 2013b) in order to find commercially viable tannin source. Several research was carried out recently on effect of different crosslinking systems (Böhm et al., 2016), addition of cellulose nanofibers (Cui et al., 2015), effect of other additives such as boric acid (Efhamisisi et al., 2016) in order to improve tannin based adhesives.

2.3.4.2 Lignin Adhesives

Among many natural polymers studied, lignin can be considered as the most extensively studied polymer for adhesive preparation (Pizzi, 2016). Lignin's are abundantly available throughout the world, at a low cost, but shows extremely low reactivity towards formaldehyde or wood (Pizzi, 2016). Lignin also has a phenolic structure, but has completely different structural and functional properties than tannin, mainly due to heavy crosslinking of aromatic rings, presence of few phenolic rings, and unavailability of polyhydroxy phenyl rings (Frihart, 2013; Imam et al., 2013; Pizzi, 2016). Pulp and paper industry generate several commercially available lignin byproducts such as Kraft lignin, lignosulfonate, soda anthraquinone, and organosolv lignin's (Mansouri et al., 2007). Kraft lignin did not showed promising results in adhesive applications mainly due to higher cost of extraction and inconsistency of resulting lignin (Frihart, 2013). However, lignosulfonates and organosolv lignin found to be more useful in developing lignin based adhesives due to their higher reactivity compared to Kraft lignin (Imam et al., 2013). Several approaches were used in developing lignin based wood adhesives. These methods

include polycondensation of methylolated lignin (Kishi et al., 2006; Mansouri et al., 2007), preparing epoxy adhesives using a lignin derivatives such as 2-pyrone-4,6-dicarboxylic acid (Hasegawa et al., 2009), enzymatic modification of wood surface lignin for self-adhesion (Hüttermann et al., 2001; Widsten & Kandelbauer, 2008), preparing adhesive mixtures that contain lignin, furan and furfural adhesives (Popa et al., 2007), developing epoxy resins derived from lignophenol (Kadota et al., 2004), and enzymatic modification of lignin to produce phenol formaldehyde adhesives (Qiao et al., 2015). Lignin based adhesives have been used in developing engineered wood products such as OSB and particle boards; however, slow reaction time and curing rate remains as a challenge in effective utilization of lignin adhesives (Frihart, 2013; Imam et al., 2013; Pizzi, 2013, 2016).

2.3.4.3 Carbohydrate Adhesives

Polysaccharides, gums, oligomeric and monomeric sugars have been used as wood adhesives from several centuries (Pizzi, 2016). In most cases carbohydrates are used in adhesive applications either as modifiers for existing UF and PF resin, by producing degradation compounds that can be used as adhesive monomers, or directly as an adhesive (Frihart, 2016; Pizzi, 2016). Among other carbohydrates, starch has been explored extensively in adhesive preparation. Grafting vinyl acetate on starch granules via two stage polymerization has increased the adhesion strength and storage stability of the adhesive (Wang et al., 2015). Graft copolymerization of vinyl monomer has increased the dry and wet adhesion of starch based adhesive by 59.4% and 32.1% respectively (Wang et al., 2012). Another starch based adhesive developed by copolymerization of oxidized starch using silane coupling agent, and butyl and/or vinyl acetate monomer showed improved adhesion, water resistance and thermal stability compared to unmodified starch (Zhang et al., 2015). Starch based adhesive prepared with

blocked isocyanate at a ratio of 100:25 (stach:isocyanate) showed improved bonding and water resistance in plywood products (Tan et al., 2011). In addition to above modifications, urea (Wang et al., 2013) and silica nanoparticles (Wang et al., 2011) have been successfully used in developing improved starch based adhesives.

2.3.4.4 Lipid Based Adhesives

Lipids/oil for industrial applications are mainly extracted from soybean, maize, sunflower, canola, palm, castor, and jojoba seeds (Rajasekar et al., 2016). Functionalization of vegetable oils was performed by transesterification, epoxidation, hydro formylation and ozonolysation to improve functional properties (Rajasekar et al., 2016). Castor oil (Somani et al., 2003) and soy oil (Xia & Larock, 2010) was previously used in preparing polyols to be used in polyurethane adhesive. In a recent study, canola oil polyols were prepared by ozonolysation, and canola oil based polyurethane adhesive was prepared by reacting pMDI resin with the canola polyols. Prepared canola polyol based polyurethane adhesive showed acceptable adhesion to wood (Kong et al., 2011). Addition of nanomaterials as a filler (TiO_2) into natural castor oil based polyurethane adhesives showed improved adhesion and water resistance compared to castor polyurethane (Malik & Kaur, 2016).

2.3.4.5 Protein Based Adhesives

Protein based adhesives once dominated the adhesive applications prior to the rise of synthetic adhesives (Frihart, 2013). Proteins have unique structural and functional properties that provide wide range of modification potential to be used in adhesive preparations (Imam et al., 2013). Sensitivity of proteins to pH, ionic strength, temperature and processing conditions facilitate protein modifications to improve their functionality (Rajasekar et al., 2016). Proteins

have an hierarchical structure that dictates its specific functions (Ustunol, 2015). Amino acids bind together via amide bonds to make a polypeptide chain which is considered as the primary structure of protein. Interchain and intrachain interactions such as hydrogen bonds, disulfide linkages, or coordination bonds will facilitate protein folding that creates secondary and tertiary structure of the protein (Frihart, 2013; Ustunol, 2015). Quaternary structure of the protein consists of three dimensional arrangement of several polypeptides (Ustunol, 2015). Specific functional groups such as hydrophilic and hydrophobic groups rearrange during protein folding in order to make hydrophilic surface and hydrophobic core (Ustunol, 2015). Therefore, protein modification and denaturation is required to increase molecular interactions of protein adhesives with wood surface (Bandara et al., 2013; Mo et al., 2004; Qi et al., 2016).

2.3.5 Major Protein Sources in Adhesive Preparation

Animal blood, milk proteins, and fish skin extracts have been used as glue from early civilization. Some proteins such as bovine serum albumin is still using as a component in wood adhesives (Lambuth, 1994, 2001). Casein and collagen have been used in early adhesive preparations (Guo &Wang, 2016); however, the food value of animal proteins have encourage researchers to look into alternate protein sources from agriculture and food industry byproducts (Bandara et al., 2013; Bandara et al., 2017; Wang et al., 2014). There are several protein sources such as soybean meal, canola meal, brewers spent grain, and distillers grain that are generated from agricultural and processing industry byproducts which contain high amount of proteins (Anderson & Lamsal, 2011; Bandara et al., 2011; Kolster et al., 1997; Kumar et al., 2002; Lambuth, 1994, 2001). Among them, soy protein (Frihart et al., 2014) and wheat gluten (Khosravi et al., 2014) have been extensively explored in adhesive applications, while other

proteins such as canola (Wang et al., 2014), triticale (Bandara et al., 2013), corn (Anderson & Lamsal, 2011), cotton seed (He et al., 2014) were briefly studied.

2.3.5.1 Soy Protein Adhesive

Soy flour adhesives were first developed in early 20th century mainly for uses in the interior plywood industry (Frihart et al., 2014). Although soy adhesives were used for long time in interior type plywood production, UF resin replaced the soy based adhesives due to its low cost, easy use and enhanced water resistance properties (Frihart et al., 2014). Denaturation, chemical modification, cross linking and enzymatic modifications were used to modify soy protein for adhesive applications. In the early studies of soy adhesives, protein denaturation by alkaline agents such as NaOH (Hettiarachchy et al., 1995; Kalapathy et al., 1995, 1996, 1997, Khosravi et al., 2010, 2011), urea (Huang & Sun, 2000b; Sun & Bian, 1999), guanidine hydrochloride (Huang & Sun, 2000b), sodium dodecyl sulphate (Huang & Sun, 2000a), sodium dodecyl benzene sulfonate (Huang & Sun, 2000a), and enzymes (Kalapathy et al., 1995, 1996) were used for adhesive preparation. Alkali modification improved adhesion strength and water resistance at higher pH ranges at ~8-12, with the highest strength recorded around pH 12.0. Alkaline modification increased the dry strength from 0.75 MPa to 1.97 MPa (Hettiarachchy et al., 1995) while up to 6.5 MPa (Sun & Bian, 1999), and 5.7 MPa (Mo et al., 1999) dry strength was reported in two other studies on alkaline modification. In a another recent study by Nordqvist *et al.*, (2010), alkali modifications of wheat gluten and soy protein was increased up to the level of the European standard EN 204 for wood adhesives (10, 8, 2 MPa for dry, soaked and wet adhesion strength, respectively). Strong denaturation agents such as urea improved dry adhesion from 4.2 MPa to 5.9 MPa (Huang & Sun, 2000b) or from 3.7 MPa to 5.5 MPa (Mo et al., 2004). The wet and soaked adhesion of urea modified proteins were increased to 2.5 MPa

and 4.9 MPa compared to 0.4 MPa and 2.1 MPa in unmodified soy protein (Huang & Sun, 2000a).

Crosslinking was also used as a method of protein modification for adhesive development. Glutaraldehyde aided cross-linking of soy proteins, increased the adhesion strength up to 6.81 MPa, 3.04 MPa, and 6.27 MPa for dry, wet and soaked strength respectively (Wang et al., 2007). Another recent study used epoxy resin (EPR) and melamine formaldehyde (MF) to crosslink soy meal in order to improve adhesion and water resistance (Lei et al., 2014). Dry adhesion of soy meal was increased from 1.02 MPa to 1.32 MPa with 14% MF addition, but decreased the dry adhesion at any EPR addition level. However, wet adhesion increased up to 0.48 MPa and 0.94 MPa at 12% EPR and 14% MF addition level respectively. Authors attributed the improvement in water resistance to crosslinked soybean meal protein network with EPR and MF resin (Lei et al., 2014).

Chemical modification of soy protein and soy meal were also used in developing soy based adhesives (Liu et al., 2015; Liu & Li, 2002, 2004; Luo et al., 2016; Wang et al., 2006; Zhu & Damodaran, 2014). Esterification of soy protein for 10 h increased the adhesion strength up to 5.73, 2.16, and 5.67 MPa for dry, wet and soaked strength respectively (Wang et al., 2006). Grafting of dopamine into soy protein isolate via chemical route has improved the water resistance of soy protein up to ~3.5 MPa at 8.5% dopamine content (Liu & Li, 2002). Grafting cysteamine into soy protein via amide linkages increased the dry adhesion of soy protein up to ~5 MPa in three cycle water soaking and drying test. The increase in adhesion was attributed to the increased –SH groups in modified protein (Liu & Li, 2004). Reacting soy protein with 2-octen-1-ylsuccinic anhydride showed an improvement in dry and wet adhesion from 5.6 MPa and 1.8 MPa (unmodified soy protein), to 5.8 MPa and 3.1 MPa (dry and wet strength

respectively) at 3.5% addition level (Qi et al., 2013). Chemical modification of soy protein with undecylenic acid also improved the dry adhesion from 5.9 MPa to 6.6 MPa and wet strength from 2.1 MPa to 3.2 MPa (Liu et al., 2015). Recent studies on soy based adhesives were focused on using soy meal instead of soy protein isolate as a means of reducing cost of adhesive preparation (Damodaran & Zhu, 2016; Li et al., 2016; Yuan et al., 2016; Zhu & Damodaran, 2014). Chemical phosphorylation of soy flour followed by addition of 1.8% $Ca(NO_2)_2$ (w/w), and 10% (w/w) ethylene carbonate has increased the dry and wet adhesion of unmodified soy flour (5.91 MPa & 0.15 MPa respectively) up to 8.52 MPa and 1.86 MPa for dry and wet adhesion respectively (Damodaran & Zhu, 2016; Zhu & Damodaran, 2014). Chemical modification of soy meal with 6% (w/w) melamine/epichlorohydrin pre-polymer has increased the wet adhesion from 0.37 MPa to 1.4 MPa. Even though most modifications improved adhesion and water resistance of soy based adhesives, further modifications were required to increase water resistance and adhesion.

2.3.5.2 Wheat Gluten Based Adhesives

Wheat is the second largest cereal crop in the world behind corn based on the production volume (FAOSTAT, 2010). Wheat gluten (WG) is a byproduct of starch processing and bioethanol processing industries (Khosravi et al., 2011). It is an unique protein among the others, due to its composition, viscoelastic and cohesive properties which enable dough formation and material applications such as films, foams and adhesives (Khosravi et al., 2014; Lagrain et al., 2010). Monomeric gliadins (MW ~ 30 – 60 KDa) and polymeric glutenin (~ 80 KDa - 250 KDa, can be increased up to 1000 KDa) are the two main components of gluten proteins (Lagrain et al., 2010; Veraverbeke & Delcour, 2002).

WG have been used as an adhesive to produce particle boards in several studies (Khosravi et al., 2010, 2011; Khosravi et al., 2014; Nordqvist et al., 2012). Unmodified 20% (w/w) WG dispersions and 20% (w/w) alkali modified WG dispersion (0.1 M NaOH) were used in particleboard preparation. Alkali modified WG showed an improved internal bond strength and tensile strength in particle boards at low curing temperatures (Khosravi et al., 2010). In addition to curing temperature, method of adhesive application affected the quality of finished particle board (Khosravi et al., 2011). Modification of hydrolyzed WG using formaldehyde and glyoxal resins improved the adhesion strength up to required standard specifications for particle board production (Lei et al., 2010). Wheat flour adhesive with a protein content of ~12 % (w/w) showed 5.8 MPa dry adhesion strength at 105 ^{o}C curing temperature (Amico et al., 2013). Crosslinking of WG with polyamidoamine-epichlorohydrin resin showed improved internal bond strength and tensile strength compared to unmodified WG (Khosravi et al., 2014). One of the main issues observed with WG in adhesive preparation is their low water resistance properties compared to soy based adhesives. Therefore further research is required to improve adhesive functionalities of WG based adhesives.

2.3.5.3 Canola Protein Adhesive

In comparison to soy protein and WG, application of canola protein in adhesive development is novel area of interest (Bandara et al., 2017). Even though both soy protein and WG showed promising results on adhesive development, well established food uses will compete with adhesive applications (Bandara et al., 2017; Wang et al., 2014). The interest on finding alternate protein source with limited value added applications leads to use canola protein on adhesive applications (Hale, 2013; Wang et al., 2014). However, limited number of research was conducted on canola protein based adhesives. Modifying canola protein with sodium bisulfite

showed strength values of 5.28 MPa, 4.07 MPa and 5.43 MPa for dry, wet and soaked adhesion respectively (Li et al., 2012). In another study, canola protein modification by 0.5% sodium dodecyl sulphate (SDS) increased adhesion up to 6.00, 3.52 MPa, and 6.66 MPa, for dry, wet and soaked adhesion respectively (Hale, 2013). Grafting poly (glycidyl methacrylate) into canola protein via free radically initiated reaction showed a dry, wet and soaked strength of 8.25 MPa, 3.80 MPa and 7.10 MPa respectively (Wang et al., 2014). However, the use of expensive poly (glycidyl methacrylate) polymer in excess amounts limits the future commercial exploration of this method. The promising results observed in limited number of research conducted on canola protein adhesive point out the importance of developing novel low cost technologies to further improve adhesion strength of canola protein based adhesives.

2.4 Nanotechnology in Wood Adhesive Research

Nanotechnology is a multidisciplinary field in applied sciences and technologies that usually deals with studying, fabrication and application of maters, structures and objects in atomic and molecular scale, usually in the size range of 1-100 nm for at least one dimension (Norde, 2011). Nanotechnology is comparatively new research area in many fields; similarly, applications of nanotechnology in wood adhesive research occurred very recently (Kaboorani & Riedl, 2011). Several studies were conducted on the application of nanomaterials in polymer based wood adhesives such as poly vinyl acetate; however, the applications in biobased adhesives, especially in protein based adhesives are extremely limited (Qi et al., 2016).

2.4.1 Nanomaterials

Materials at nanoscale dimensions exhibit unique and novel physical, chemical, and biological properties compared to their bulk material (Moon et al., 2006). Decrease in size of

nanomaterials results in a large increase in surface area (higher aspect ratio) in relation to its volume thereby increase the reactivity of material with other surfaces (Gatoo et al., 2014). The high aspect ratio also related to the surface charge and mechanical properties of the material (Gatoo et al., 2014). A large number of different nanomaterials were developed in the recent past; however, they can be categorized into several groups depending on their shape. Nanoparticles, nanotubes, fullerenes, nanofibers, nanowhiskers, and nanosheets are considered as the basic types of nanomaterials (Brody et al., 2008; Cushen et al., 2012).

Nanoparticles are defined as single particles with a diameter less than 100 nm; however agglomerates of nanoparticles can be larger than 100 nm (Cushen et al., 2012). Nanotubes shows a cylindrical lattice arrangement of the material with at least two dimensions in the nanometer scale, while fullerenes have a spherical molecular arrangement (Hoet et al., 2004; O'Brien & Cummins, 2008). Nanofibers generally have a length to diameter ratio of a least 3:1, and have two dimensions less than100 nm but the third (axial) dimension may or may not be larger than 100 nm (Hoet et al., 2004; Moon et al., 2006; O'Brien & Cummins, 2008). Nanowhiskers are fine fibers in the nano range with a 5-20 nm in diameter and several micrometers in length (Pandey et al., 2008). Nanosheets have only one dimension in the nanoscale and have a sheet like structure with other two dimensions can be in either nanometer or micrometer scale (Kumar et al., 2009).

Two main methods named "top down" and "bottom up" are available in terms of preparing nanomaterials (Cushen et al., 2012; Norde, 2011). Top down method involve in breaking down of larger particles into nanometer scale either by physical or chemical methods (Norde, 2011). Bottom up method produce nanomaterials from nanoscale, using methods such as layer by layer

deposition, crystallization, solvent extraction and evaporation, self-assembly, microbial synthesis and biomass reactions (Brody et al., 2008).

2.4.1.1 Nanoclay

Nanoclays are among the most studied nanomaterial for different applications such as composites, plastics, films and adhesives (Kaboorani & Riedl, 2011). Hydrous silicates formed by layers of tetrahedral sheets (made with silica as the main component) and octahedral sheets (made with diverse range of elements such as Al, Mg and Fe) are referred as nanoclays (Marquis et al., 2011). Nanoclays are categorized according to their crystalline structure, quantity & position of ions, and sheets stacking (Marquis et al., 2011; Wool, 2015). The ratio of tetrahedral and octahedral sheets stacks used to divide nanoclays into two main groups; 1:1 (tetrahedral:octahedral) kaolinite and 2:1 layer silicates (phyllosiclicates) (Wool, 2015).

Kaolinite stack layers consist with a metal hydroxide and silicon-oxygen network that held via hydrogen bonds while phyllosiclicates layers were held by interlayer cations. Phyllosiclicates include nanomaterials such as mica, vermiculite, chlorite, and smectite; where smectite group was further divided into nontronite, saponite, hectorite and montmorrilonite species (Marquis et al., 2011; Wool, 2015). Organomodified montmorrilonite is a natural phyllosilicate that are extracted from bentonite (Bilgiç et al., 2014). Generally, nanoclay surfaces are hydrophilic, therefore surface modification with hydrophobic polymers were carried out to improve hydrophobicity of nanoclay (Bilgiç et al., 2014).

2.4.1.2 Nanocrystalline Cellulose

Cellulose is the most abundant renewable biopolymer on earth with excellent biodegradability, non-toxicity and have an annual production volume of 7.5×10^5 metric tons

(Habibi et al., 2010). Cellulose is made up with repeating units of homopolysaccharide β-D-glucopyranose units linked via β-1-4 linkages (Brinchi et al., 2013). Each anhydrous glucose unit contains three hydroxyl groups that allows higher degree of functionality (Peng et al., 2011). Poly(β-D-glucopyranose) can form into hierarchical microstructure named as cellulose microfibrils, which again form into larger cellulose fibers with crystalline and amorphous regions (Kaboorani et al., 2012; Peng et al., 2011). Crystalline part of the cellulose fibrils are names as nanocellulose or nanowhiskers (Kaboorani et al., 2012). Generally, nanocrystalline cellulose (NCC) is extracted from cellulose biomasses using acid hydrolysis. Amorphous regions of the cellulose fibrils will selectively hydrolyzed to separate crystalline regions (Habibi et al., 2010; Peng et al., 2011). Resulting NCC will have an average diameter of 3-10 nm and length of 100-300 nm, and retain the natural cellulose crystalline structure (Brinchi et al., 2013). Nanoscale dimension, high specific strength and modulus, high surface area, and unique optical properties of NCC provides a completely different material properties than cellulose (Brinchi et al., 2013; Peng et al., 2011). NCC also have a unique advantages over mineral nanomaterials such as nanoclays due to its low density (~1.5 g cm^{-3}) high form factor (about 70), and higher surface area (~150 m^2 g^{-1}) (Brinchi et al., 2013; Kaboorani et al., 2012; Peng et al., 2011). The unique physicochemical properties of NCC allows scientist and industries to explore the novel material applications for variety of materials.

2.4.1.3 Graphite Oxide

Interest in the carbon nanomaterials increased rapidly in last decade with the isolation of graphene for the first time in 2004 that consist of two dimensional sheets of carbon molecules bonded via sp^2 bonds (Verdejo et al., 2011). Graphite oxide (GO) is an intermediate product of graphene production; where graphite is first chemically oxidized into GO, followed by

exfoliating in a liquid to make graphene nanosheets (Park & Ruoff, 2009). GO is a strongly oxygenated layered material; however GO have distinctive advantages over graphene, mainly due to the simplicity of production through wet chemical methods, hydrophilic properties that allows better exfoliation in aqueous media, and potential to convert into graphene or graphene oxide (Park & Ruoff, 2009; Zhong et al., 2015) either by chemical (Li et al., 2008; Xu et al., 2008) or thermal (González et al., 2012) reduction. The conversion of GO into graphene can be attained before or after exfoliating GO in the polymer matrix, which provide another unique advantage in material processing (González et al., 2012; Park & Ruoff, 2009; Xu et al., 2008). In comparison to other carbon based materials, graphene and GO have unique material properties where they shows high Young's modulus (~1 TPa), fracture strength (~130 GPa), thermal conductivity (~5000 $Wm^{-1}K^{-1}$) and specific surface area (2630 m^2g^{-1}) (Lee et al., 2008; Park & Ruoff, 2009). The oxidation of graphite will impart higher amount of oxygen containing functional groups, leading to improved hydrophilic properties that facilitate exfoliation of GO in polymer matrix (Shao et al., 2012). GO has been extensively studied in advanced nano-composites applications such as poly (vinyl acetate) (Liang et al., 2009; Liu et al., 2016), chitosan (Yang et al., 2010), natural rubber (Aguilar-Bolados & Lopez-Manchado, 2015), poly (methyl methacrylate) and epoxy (Shao et al., 2012; Shtein et al., 2015), but only one study found in adhesive applications (Khan et al., 2013) where they used graphene to improve adhesion of PVA adhesive.

2.4.2 Recent Advances in Nanotechnology Based Adhesive Development

Among the large number of available nanomaterials, only a handful of nanomaterials were used in adhesive preparations. Nanoclay (sepiolite, montmorrilonite) (Kaboorani & Riedl, 2011; Li et al., 2016; Qi et al., 2016), nano Al_2O_3 (Kaboorani & Riedl, 2012), SiO_2 (Salari et al., 2013),

and nanocrystalline cellulose (Kaboorani et al., 2012) are the main nanomaterials studied in adhesive preparations. Even though nanomaterials have extensively explored in composite applications to improve flexural strength, elasticity, toughness, and stability of materials (Santulli, 2016), the potential of nanomaterials in adhesive applications has not been fully explored. Specifically for biobased adhesives, very few studies were carried out on using nanomaterials to improve adhesion (Kaboorani & Riedl, 2011, 2012). Kaboorani et al (2011, 2012) observed an improvement in adhesion and water resistance of polyvinyl acetate (PVA) adhesives after adding montmorillonite (Kaboorani & Riedl, 2011), nano aluminum oxide (Kaboorani & Riedl, 2012), and nanocrystalline cellulose (Kaboorani et al., 2012) at low nanomaterial concentrations. Zhang et al (2014) exfoliated montmorillonite in polyisocyanate modified soy protein and reported a decrease in adhesion strength instead of increase, probably due to a nano scale blocking mechanism (Zhang et al., 2014). In a recent study, exfoliating sepiolite nanoclay into soybean meal creating sepiolite-based united crosslinked network showed an improvement in wet strength from 0.81 MPa to 1.18 MPa (Li et al., 2016). A improved wet adhesion from 2.9 MPa to 4.3 MPa were observed by exfoliating sodium montmorrilonite at 8% w/w addition rate into soy protein isolate (Qi et al., 2016). The improvement in adhesion was attributed to “physical filling effect” of sepiolite (Li et al., 2016), and nanomaterial induced crosslinking of protein network (Li et al., 2016; Qi et al., 2016).

2.5 Biomimetics in Wood Adhesive Research

Nature is considered as the best engineer of materials, where it provide ample examples on ordered and hierarchical arrangement of materials to serve specific functions (Lee et al., 2006). Specifically biological materials and composites shows properties far beyond the materials properties that can be achieved by present technological advances (Sarikaya, 1994). Biological

composites shows highly ordered yet hierarchical structures that contain both organic and inorganic materials and are synthesized at atmospheric conditions (Lee et al., 2006; Sarikaya, 1994). Scientist have been fascinated by the structure and functionality of biological materials; therefore, trying to develop materials that are structurally and functionally similar to the natural materials (Bandara et al., 2013). Biomimetics is a novel interdisciplinary research area of material science, that use investigation of structure & functions of biological materials in order to develop novel materials with similar functionality (Lee et al., 2006; Sarikaya, 1994). Adhesive development has focused on biomimetic approaches in recent past mainly due to the presence of unique and excellent adhesive materials derived from natural organisms like mussels, geckos, tube warms, and barnacles (Dalsin et al., 2003; Lee et al., 2006). Among them, mussel adhesion has inspired many researchers to develop high end adhesive for biomedical applications.

2.5.1 Mussel Adhesion

Common blue mussel (*Mytilus edulis*) is a marine organism that produce proteinaceous adhesive with an excellent underwater adhesion into a wide array of organic and inorganic surfaces (Bandara et al., 2013). Mussels adhere to surface via an exogenous structure called byssus. Mussel byssus is made up with two components; byssal plaque and byssal threads (Brown, 1952; Cha et al., 2008). Byssal thread is made with polyphenolic protein Mefp-1 (Filpula et al., 1990) and three collagen proteins named proximal collagen, gradient distal collagen, non-gradient distal collagen (Waite et al., 1998). Byssal plaque is made up with five different phenolic proteins; Mefp-2, Mefp-3, Mefp-4, Mefp-5 and Mefp-6 (Bandara et al., 2013). The presence of 3,4-dihydroxy phenylalanine (DOPA) in excess amounts is a common feature in most of the phenolic proteins present in the byssal plaque. For example, Mefp-5 contain 30% DOPA (mol%) in its composition while Mefp-1, Mefp-2, Mefp-3, Mefp-4, and Mefp-6 contains

10-15%, 3-5%, 20-25%, 5%, and 4% mol% DOPA respectively (Bandara et al., 2013). Interestingly, the proteins present in adhesive plaque, that are in direct contact with the surface such as Mefp-3 and Mefp-5 shows the highest DOPA content among other mussel adhesive proteins (Lee et al., 2006).

2.5.1.1 Mussel Adhesion Mechanism

The strong underwater adhesion of mussel adhesive proteins inspired scientist to study the potential adhesion mechanism; however the exact adhesion mechanism is still largely unknown (Bandara et al., 2013; Waite, 2002). The recent research progress of mussel adhesion mechanism indicates an contributing roles from DOPA content (Waite, 2002), redox chemistry (Burzio & Waite, 2000; Haemers et al., 2003), metal interactions (Hwang et al., 2010; Taylor et al., 1996; Zeng et al., 2010) and synergistic effect (Hight & Wilker, 2007; Sever et al., 2004) of several other factors. Presence of basic isoelectric point (pI), and post-translationally modified Tyr and Pro amino acids are the common features in all mussel adhesive proteins (Lee et al., 2006; Lin et al., 2007). Specifically, the proteins that are in contact with adhesion surface and outside environment shows higher degree of post-translational modifications; 42% of Mefp-3 and 37% of Mefp-5 amino acids were post-translationally modified (Waite et al., 2005). In addition, both Mefp-3 and Mefp-5 have comparatively smaller molecular weight (MW) of 5-7 KDa and 9.5 KDa respectively, compared to other mussel proteins (Waite, 2002); low MW allows easy conformational changes enabling crosslinking and hydrogen bond formation, thereby acting as primers in adhesion (Even et al., 2008; Silverman & Roberto, 2007). Post- or co-translationally modified amino acids such as DOPA, 4-hydroxyproline (Waite, 1983), 3,4-dihydroxyproline (Taylor et al., 1994), 4-hydroxyarginine (Papov et al., 1995), and *o*-phosphoserine (Waite & Qin, 2001) increase the hydrogen bonding and crosslinking potential of mussel proteins.

The exact role of DOPA in mussel adhesion is not fully understood to date, but several adhesion theories were proposed. The direct interactions of catechol side chains of DOPA with adhesion surface functional groups (Deshmukh, 2004), oxidation of DOPA into DOPA-quinone and DOPA-semiquinone via catechol oxidase followed by crosslinking of DOPA and DOPA-quinones with adhesion surface are considered to be some of the adhesion mechanisms (Burzio & Waite, 2000; Haemers et al., 2003; Monahan & Wilker, 2003; Monahan & Wilker, 2004; Yu et al., 1999).

Unoxidized DOPA were reported to create strong yet reversible coordination bonds with inorganic surfaces, while oxidized DOPA-quinone can create covalent bonds with organic surfaces (Bandara et al., 2013; Lee et al., 2006). In addition, noncovalent interactions such as electrostatic interactions and hydrogen bonding were also observed with reactive surfaces like mica (Lin et al., 2007). Presence of metal ions such as copper, iron, manganese and zinc believed to play a vital role in mussel adhesion mainly through metal ion mediated crosslinking of proteins (Bandara et al., 2013; Liu et al., 2010). Specifically, Fe^{3+} can bind with thee mussel adhesive protein strands together creating $Fe(DOPA)_3$ (Sever et al., 2004), that can further react with oxygen to create reactive radical species (Sever et al., 2004). $Fe(DOPA)_3$ and resulting reactive radical species will play a major role in adhesive curing.

2.5.2 Recent Advances in Biomimetics Based Adhesive Development

Mimicking mussel adhesion have been explored in many research fields for uses in wound healing, tissue engineering, orthopedic cement applications, and dental composites (Bandara et al., 2013). However, the applications of mussel biomimetics in wood adhesive research are still at infancy. Renewable polymer based adhesives have limited water resistance properties; therefore, developing mussel inspired adhesives hold great promise for improving wet adhesion

(Liu et al., 2010). Most of the natural plant proteins do not contain DOPA functional groups. Therefore several researchers attempted to graft DOPA groups into proteins to develop high strength wood adhesives (Liu et al., 2010; Liu & Li, 2002, 2004; Song et al., 2016). A synthetic chemical route was developed to graft dopamine into soy protein via amide linkages (Liu & Li, 2002). At the optimum dopamine level of 8.95% a dry adhesion strength of ~3.5 MPa was observed, which retained after three water soaking and drying cycles (Liu & Li, 2002). The improvement in adhesion was attributed to dopamine mediated protein crosslinking. Another biomimetic wood adhesive was developed by grafting cysteamine into soy protein via amide linkages using a multistep chemical route to increase the free mercapto groups (–SH) content (Liu & Li, 2004). At an optimum –SH group content of 2.09% (w/w), a dry adhesion strength of ~5 MPa was observed up to three water soaking and drying cycles. The improvement in adhesion was a result of –SH mediated disulfide bond formation and crosslinking of cysteamine grafter soy protein (Liu & Li, 2004). Ionic crosslinking of sub-micron/nano size $CaCO_3$ crystalline arrays with soy protein improved the dry adhesion strength about ~6.2 MPa at 3% (w/w) $CaCO_3$ addition level (Liu et al., 2010). In a recent study, a recombinant mussel adhesive protein extracted from *Escherichia coli* BL21(DE23) reported a bulk adhesion strength about ~2.5-3.0 MPa (Song et al., 2016). However, further research on biomimetic adhesives is needed to develop cost-effective renewable protein adhesive with improved water resistance.

2.6 References

Aachary, A., Thiyam-Hollander, U., & Eskin, M. (**2015**). Canola/rapeseed proteins and peptides. In Z. Ustunol (Eds.), *Applied Food Protein Chemistry* (pp 194–218). Chichester, UK: John Wiley & Sons, Ltd.

Aguilar-Bolados, H., & Lopez-Manchado, M. (**2015**). Effect of the morphology of thermally reduced graphite oxide on the mechanical and electrical properties of natural rubber nanocomposites. *Composites Part B:*, ***87***, 350–356.

Aider, M., & Barbana, C. (**2011**). Canola proteins: composition, extraction, functional properties, bioactivity, applications as a food ingredient and allergenicity – A practical and critical review. *Trends in Food Science & Technology*, ***22***(***1***), 21–39.

Anderson, T. J., & Lamsal, B. P. (**2011**). Zein extraction from corn, corn products, and coproducts and modifications for various applications: a aeview. *Cereal Chemistry*, ***88***(***2***), 159–173.

ASA-American Soybean Association. (**2015**). World soybean production - 2015. Available at : http://soystats.com/international-world-soybean-production/ [2016/12/16]

Baier, R., Shafrin, E., & Zisman, W. (**1968**). Adhesion: mechanisms that assist or impede it. *Science*, ***162***, 1360–1368.

Baldan, A. (**2012**). Adhesion phenomena in bonded joints. *International Journal of Adhesion and Adhesives*, ***38***, 95–116.

Bandara, N., Chen, L., & Wu, J. (**2011**). Protein extraction from triticale distillers grains. *Cereal Chemistry*, ***88***(***6***), 553–559.

Bandara, N., Chen, L., & Wu, J. (**2013**). Adhesive properties of modified triticale distillers grain

proteins. *International Journal of Adhesion and Adhesives*, ***44***, 122–129.

Bandara, N., Esparza, Y., & Wu, J. (**2017**). Exfoliating nanomaterials in canola protein derived adhesive improves strength and water resistance. *RSC Advances*, ***7(11)***, 6743-6752.

Bandara, N., Zeng, H., & Wu, J. (**2013**). Marine mussel adhesion: biochemistry, mechanisms, and biomimetics. *Journal of Adhesion Science and Technology*, ***27***(***18***–***19***), 2139–2162.

Bilgiç, C., Topaloğlu Yazıcı, D., Karakehya, N., Çetinkaya, H., Singh, A., & Chehimi, M. M. (**2014**). Surface and interface physicochemical aspects of intercalated organo-bentonite. *International Journal of Adhesion and Adhesives*, ***50***, 204–210.

Böhm, R., Hauptmann, M., Pizzi, A., Friedrich, C., & Laborie, M. P. (**2016**). The chemical, kinetic and mechanical characterization of tannin-based adhesives with different crosslinking systems. *International Journal of Adhesion and Adhesives*, ***68***, 1–8.

Bonnardeaux, J. (**2007**). Uses for canola meal. Available at: https://www.agric.wa.gov.au/canola/Western-Australian-canola-industry [2016/12/20]

Brinchi, L., Cotana, F., Fortunati, E., & Kenny, J. M. (**2013**). Production of nanocrystalline cellulose from lignocellulosic biomass: Technology and applications. *Carbohydrate Polymers*, ***94***(***1***), 154–169.

Brody, A., Bugusu, B., Han, J., & Sand, C. (**2008**). Innovative food packaging solutions - scientific status summary. *Journal of Food Science*, ***73***(***8***), R107–R116.

Brown, C. H. (**1952**). Some structural proteins of *Mytilus edulis*. *Microscale Science*, ***93***, 487–489.

Burzio, L. A., & Waite, J. H. (**2000**). Cross-linking in adhesive quinoproteins: studies with model decapeptides. *Biochemistry*, ***39***(***36***), 11147–11153.

Canola Council of Canada. (**2016**). Canadian canola production 2016. Available at: http://www.canolacouncil.org/markets-stats/statistics/tonnes/ [2016/12/28]

Cha, H. J., Hwang, D. S., & Lim, S. (**2008**). Development of bioadhesives from marine mussels. *Biotechnology Journal*, ***3***(***5***), 631–638.

Chupin, L., Motillon, C., Charrier-El Bouhtoury, F., Pizzi, A., & Charrier, B. (**2013**). Characterisation of maritime pine (*Pinus pinaster*) bark tannins extracted under different conditions by spectroscopic methods, FTIR and HPLC. *Industrial Crops and Products*, ***49***, 897–903.

COPA-Canadian Oilseed Processors Association. (**2016**). Canadian oilseed processing industry. Available at: http://copacanada.com/crush-oil-meal-production/ [2016/12/25]

Coyne, K. J., Qin, X.X., & Waite, J. H. (**1997**). Extensible collagen in mussel byssus: a natural block copolymer. *Science*, ***277***(***5333***), 1830–1832.

Cui, J., Lu, X., Zhou, X., Chrusciel, L., Deng, Y., Zhou, H., Brosse, N. (**2015**). Enhancement of mechanical strength of particleboard using environmentally friendly pine (*Pinus pinaster L.*) tannin adhesives with cellulose nanofibers. *Annals of Forest Science*, ***72***(***1***), 27–32.

Cushen, M., Kerry, J., Morris, M., Cruz-Romero, M., & Cummins, E. (**2012**). Nanotechnologies in the food industry – Recent developments, risks and regulation. *Trends in Food Science & Technology*, ***24***(***1***), 30–46.

D'Amico, S., Müller, U., & Berghofer, E. (**2013**). Effect of hydrolysis and denaturation of wheat gluten on adhesive bond strength of wood joints. *Journal of Applied Polymer Science*, ***129***(***5***), 2429–2434.

Dalsin, J. L., Hu, B. H., Lee, B. P., & Messersmith, P. B. (**2003**). Mussel adhesive protein

mimetic polymers for the preparation of nonfouling surfaces. *Journal of the American Chemical Society*, ***125***(***14***), 4253–4258.

Damodaran, S., & Zhu, D. (**2016**). A formaldehyde-free water-resistant soy flour-based adhesive for plywood. *Journal of the American Oil Chemists' Society*, ***93***(***9***), 1311–1318.

Deak, N. A., Murphy, P. A., & Johnson, L. A. (**2006**). Fractionating soybean storage proteins using Ca^{2+} and $NaHSO_3$. *Journal of Food Science*, ***71***(***7***), C413–C424.

Denbow, D. M., Ravindran, V., Kornegay, E. T., Yi, Z., & Hulet, R. M. (**1995**). Improving phosphorus availability in soybean meal for broilers by supplemental phytase. *Poultry science*, ***74***(***11***), 1831–42.

Desai, S., Patel, J., & Sinha, V. (**2003**). Polyurethane adhesive system from biomaterial-based polyol for bonding wood. *International Journal of Adhesion and Adhesives*, ***23***(***5***), 393–399.

Deshmukh, M. V. (**2004**). *Synthesis and Characterization of Mussel Adhesive Peptides*. (Doctoral dissertation) Department of chemistry, Universität Regensburg, Phillips Universität, Germany.

Detlefsen, W. (**2002**). Phenolic resins: some chemistry technology and history. In D. Dillard & Pocius AV (Eds.), *Adhesive Science and Engineering–2: Surfaces, Chemistry and Applications* (pp 869-946). Amsterdam: Elsevier.

Dhimiter, B., Herrick, C. A., Smith, T. J., Woskie, S. R., Streicher, R. P., Cullen, M. R., Redlich, C. A. (**2007**). Skin exposure to isocyanates: reasons for concern. *Environmental Health Perspective*, ***115***(***3***), 328–335.

Ebnesajjad, S. (**2008**). Introduction and adhesion theories. In S. Ebnesajjad (Eds.), *Adhesives*

Technology Handbook (pp 1–26). Norwich, NY: William Andrew Inc.

Efhamisisi, D., Thevenon, M. F., Hamzeh, Y., Karimi, A. N., Pizzi, A., & Pourtahmasi, K. (**2016**). Induced tannin adhesive by boric acid addition and its effect on bonding quality and biological performance of poplar plywood. *ACS Sustainable Chemistry & Engineering*, ***4***(***5***), 2734–2740.

El-Thaher, N., Mussone, P., Bressler, D., & Choi, P. (**2014**). Kinetics study of curing epoxy resins with hydrolyzed proteins and the effect of denaturants urea and sodium dodecyl sulfate. *ACS Sustainable Chemistry & Engineering*, ***2***(***2***), 282–287.

Even, M. A., Wang, J., & Chen, Z. (**2008**). Structural information of mussel adhesive protein mefp-3 acquired at various polymer/mefp-3 solution interfaces. *Langmuir*, ***24***(***11***), 5795–5801.

FAO - Food and Agriculture Organization. (**2016**). Food Outlook - 2016. Available at : http://www.fao.org/3/a-I5703E.pdf [2016/12/26]

FAOSTAT. (**2010**). Agricultural data. *Food and Agricultural Organization, United Nations,* Available at: http://faostat.fao.org [2016/12/18]

Filpula, D. R., Lee, S. M., Link, R. P., Strausberg, S. L., & Strausberg, R. L. (**1990**). Structural and functional repetition in a marine mussel adhesive protein. *Biotechnology progress*, ***6***(***3***), 171–177.

Freedonia Group. (**2016**). *World adhesives and sealents - Industry study with forcast for 2019 & 2024*. Available at: http://www.freedoniagroup.com/industry-study/world-adhesives-sealants-3377.htm [2016/12/20].

Frihart, C. (**2013**). Wood Adhesion and Adhesives. In R. M. Rowell (Eds.), *Handbook of Wood*

Chemistry and Wood Composites (pp 255–319). Boca Raton, FL: CRC.

Frihart, C. (**2016**). Potential for biobased adhesives in wood bonding. In *International Convention of Society of Wood Science and Technology* (or. 84–91). Curitiba, Brazil: Society of Wood Science and Technology.

Frihart, C. R., Birkeland, M. J., Frihart, C. R., & Birkeland, M. J. (**2014**). Soy properties and soy wood adhesives. In R. Brentin (Eds.), *Soy-Based Chemicals and Materials* (pp 167–192). Washington, DC.: American Chemical Society .

Frihart, C. R., & Hunt, C. G. (**2010**). Adhesives with wood materials: bond formation and performance. *US Department of Agriculture Forest Service, general technical report*: 508.

Gardner, D. (**2006**). Adhesion mechanisms of durable wood adhesive bonds. In D. Stokke & L. Groom (Eds.), *Characterization of the cellulosic cell wall* (pp 254–265). Ames, Iowa: Wiley-Blackwell.

Gatoo, M., Naseem, S., Arfat, M., Dar, A., Qasim, K., & Zubair, S. (**2014**). Physicochemical properties of nanomaterials: implication in associated toxic manifestations. *BioMed research international*, ***2014***(***498420***), 1–9.

González, Z., Botas, C., Álvarez, P., Roldán, S., Blanco, C., Santamaría, R., Menéndez, R. (**2012**). Thermally reduced graphite oxide as positive electrode in vanadium redox flow batteries. *Carbon*, ***50***(***3***), 828–834.

Grundmeier, G., & Stratmann, M. (**2005**). Adhesion and de-adhesion mechanism polymer/metal interfaces: Mechanistic understanding based on in situ studies of buried interfaces. *Annual Review of Materials Research*, ***35***(***1***), 571–615.

Guo, M., & Wang, G. (**2016**). Whey protein polymerisation and its applications in

environmentally safe adhesives. *International Journal of Dairy Technology*. ***69(4)***, 481-488.

Habibi, Y., Lucia, L. A., & Rojas, O. J. (**2010**). Cellulose nanocrystals: chemistry, self-assembly, and applications. *Chemical Reviews*, ***110***(***6***), 3479–3500.

Haemers, S., Koper, G. J. M., & Frens, G. (**2003**). Effect of oxidation rate on cross-linking of mussel adhesive proteins. *Biomacromolecules*, ***4***(***3***), 632–640.

Hale, K. (**2013**). *The potential of canola protein for bio-based wood adhesives*. (Master's dissertation). Kansas State University.

Hasegawa, Y., Shikinaka, K., Katayama, Y., Kajita, S., Masai, E., Nakamura, M., Shigehara, K. (**2009**). Tenacious epoxy adhesives prepared from lignin-derived stable metabolic intermediate. *Sen'i Gakkaishi*, ***65***(***12***), 359–362.

He, Z., Chapital, D. C., Cheng, H. N., & Dowd, M. K. (**2014**). Comparison of adhesive properties of water- and phosphate buffer-washed cottonseed meals with cottonseed protein isolate on maple and poplar veneers. *International Journal of Adhesion and Adhesives*, ***50***, 102–106.

Heendeniya, R. G., Christensen, D. A., Maenz, D. D., McKinnon, J. J., & Yu, P. (**2012**). Protein fractionation byproduct from canola meal for dairy cattle. *Journal of Dairy Science*, ***95***(***8***), 4488–4500.

Herrero, A. M., Carmona, P., Cofrades, S., & Jiménez-Colmenero, F. (**2008**). Raman spectroscopic determination of structural changes in meat batters upon soy protein addition and heat treatment. *Food Research International*, ***41***(***7***), 765–772.

Hettiarachchy, N. S., Kalapathy, U., & Myers, D. J. (**1995**). Alkali-modified soy protein with improved adhesive and hydrophobic properties. *Journal of the American Oil Chemists'*

Society, ***72***(***12***), 1461–1464.

Hight, L. M., & Wilker, J. J. (**2007**). Synergistic effects of metals and oxidants in the curing of marine mussel adhesive. *Journal of Materials Science*, ***42***(***21***), 8934–8942.

Hoet, P., Bruske-Hohlfeld, I., & Salata, O. (**2004**). Nanoparticles – known and unknown health risks. *Journal of Nanobiotechnology*, ***2***(***1***), 1–12.

Huang, W., & Sun, X. (**2000**a). Adhesive properties of soy proteins modified by sodium dodecyl sulfate and sodium dodecylbenzene sulfonate. *Journal of the American Oil Chemists' Society*, *77*(*7*), 705–708.

Huang, W., & Sun, X. (**2000**b). Adhesive properties of soy proteins modified by urea and guanidine hydrochloride. *Journal of the American Oil Chemists' Society*, ***77***(***1***), 101–104.

Hüttermann, A., Mai, C., & Kharazipour, A. (**2001**). Modification of lignin for the production of new compounded materials. *Applied Microbiology and Biotechnology*, ***55***(***4***), 387–384.

Hwang, D. S., Zeng, H., Masic, A., Harrington, M. J., Israelachvili, J. N., & Waite, J. H. (**2010**). Protein- and metal-dependent interactions of a prominent protein in mussel adhesive plaques. *The Journal of biological chemistry*, ***285***(***33***), 25850–25858.

Imam, S. H., Bilbao-Sainz, C., Chiou, B.-S., Glenn, G. M., & Orts, W. J. (**2013**). Biobased adhesives, gums, emulsions, and binders: current trends and future prospects. *Journal of Adhesion Science and Technology*, ***27***(***18***–***19***), 1972–1997.

Johns, W. (**1982**). Isocyanates as Wood Binders—A Review. *The Journal of Adhesion*, ***15***(***1***), 59–67.

Kaboorani, A., & Riedl, B. (**2011**). Effects of adding nano-clay on performance of polyvinyl acetate (PVA) as a wood adhesive. *Composites Part A: Applied Science and Manufacturing*,

42(***8***), 1031–1039.

Kaboorani, A., & Riedl, B. (**2012**). Nano-aluminum oxide as a reinforcing material for thermoplastic adhesives. *Journal of Industrial and Engineering Chemistry*, ***18***(***3***), 1076–1081.

Kaboorani, A., Riedl, B., Blanchet, P., Fellin, M., Hosseinaei, O., & Wang, S. (**2012**). Nanocrystalline cellulose (NCC): A renewable nano-material for polyvinyl acetate (PVA) adhesive. *European Polymer Journal*, ***48***(***11***), 1829–1837.

Kadota, J., Fukuoka, T., Uyama, H., Hasegawa, K., & Kobayashi, S. (**2004**). New positive-type photoresists based on enzymatically synthesized polyphenols. *Macromolecular Rapid Communications*, ***25***(***2***), 441–444.

Kalapathy, U., Hettiarachchy, N. S., Myers, D., & Hanna, M. A. (**1995**). Modification of soy proteins and their adhesive properties on woods. *Journal of the American Oil Chemists' Society*, ***72***(***5***), 507–510.

Kalapathy, U., Hettiarachchy, N. S., Myers, D., & Rhee, K. C. (**1996**). Alkali-modified soy proteins: effect of salts and disulfide bond cleavage on adhesion and viscosity. *Journal of the American Oil Chemists' Society*, ***73***(***8***), 1063–1066.

Kalapathy, U., Hettiarachchy, N. S., & Rhee, K. C. (**1997**). Effect of drying methods on molecular properties and functionalities of disulfide bond-cleaved soy proteins. *Journal of the American Oil Chemists' Society*, ***74***(***3***), 195–199.

Kasran, M., Cui, S. W., & Goff, H. D. (**2013**). Emulsifying properties of soy whey protein isolate–fenugreek gum conjugates in oil-in-water emulsion model system. *Food Hydrocolloids*, ***30***(***2***), 691–697.

Kendall, K. **(1994)**. Adhesion: molecules and mechanics. *Science*, ***263*****(5154)**, 1720-1726.

Keimel, F. (**2003**). Historical development of adhesive and adhesive bonding. In A. Pizzi & K. Mittal (Eds.), *Handbook of Adhesive Technology* (pp 1–12). Boca Raton, FL: CRC Press.

Khajali, F., & Slominski, B. A. (**2012**). Factors that affect the nutritive value of canola meal for poultry. *Poultry Science*, ***91***(***10***), 2564–2575.

Khan, U., May, P., Porwal, H., Nawaz, K., & Coleman, J. N. (**2013**). Improved adhesive strength and toughness of polyvinyl acetate glue on addition of small quantities of graphene. *ACS Applied Materials & Interfaces*, ***5***(***4***), 1423–1428.

Khosravi, S., Khabbaz, F., Nordqvist, P., & Johansson, M. (**2010**). Protein-based adhesives for particleboards. *Industrial Crops and Products*, ***32***(***3***), 275–283.

Khosravi, S., Khabbaz, F., Nordqvist, P., & Johansson, M. (**2014**). Wheat gluten based adhesives for particle boards: effect of crosslinking agents. *Macromolecular Materials and Engineering*, ***299***(***1***), 116–124.

Khosravi, S., Nordqvist, P., Khabbaz, F., & Johansson, M. (**2011**). Protein-based adhesives for particleboards-Effect of application process. *Industrial Crops and Products*. ***32(3)***, 275-283.

Kinloch, A. J. (**1980**). The science of adhesion - Part 1: Surface and interfacial aspects. *Journal of Materials Science*, ***15***(***9***), 2141–2166.

Kinloch, A. J. (**1982**). The science of adhesion - Part 2: Mechanics and mechanisms of failure. *Journal of Materials Science*, ***17***(***3***), 617–651.

Kinsella, J. E. (**1979**). Functional properties of soy proteins. *Journal of the American Oil Chemists' Society*, ***56***(***3***), 242–258.

Kishi, H., Fujita, A., Miyazaki, H., Matsuda, S., & Murakami, A. (**2006**). Synthesis of wood-based epoxy resins and their mechanical and adhesive properties. *Journal of Applied Polymer Science*, ***102***(***3***), 2285–2292.

Klockeman, D., Toledo, R., & Sims, K. (**1997**). Isolation and characterization of defatted canola meal protein. *Journal of Agricultural and Food Chemistry*, ***45***(***10***), 3867–3870.

Kolster, P., de Graaf, L. A., & Vereijken, J. M. (**1997**). Application of cereal proteins in technical applications. *Cereals: Novel uses and processes*, 107–116.

Kong, X., Liu, G., & Curtis, J. M. (**2011**). Characterization of canola oil based polyurethane wood adhesives. *International Journal of Adhesion and Adhesives*, ***31***(***6***), 559–564.

Krishnan, H. (**2001**). Biochemistry and molecular biology of soybean seed storage proteins. *Journal of New Seeds*, ***2***(***3***), 1–25.

Kumar, A., Depan, D., Singh Tomer, N., & Singh, R. (**2009**). Nanoscale particles for polymer degradation and stabilization—Trends and future perspectives. *Progress in Polymer Science*, ***34***(***6***), 479–515.

Kumar, R., Choudhary, V., Mishra, S., Varma, I. K., & Mattiason, B. (**2002**). Adhesives and plastics based on soy protein products. *Industrial Crops and Products*, ***16***(***3***), 155–172.

Lagrain, B., Goderis, B., Brijs, K., & Delcour, J. A. (**2010**). Molecular basis of processing wheat gluten toward biobased materials. *Biomacromolecules*, ***11***(***3***), 533–541.

Lambuth, A. L. (**1994**). Protein adhesives for wood. *Handbook of adhesive technology*, 259–268.

Lambuth, A. L. (**2001**). Blood and casein glues. In D. Satas & A. A. Tracton (Eds.), *Coatings Technology Handbook* (pp 519–530). New York: Marcel Dekker Inc.

Lee, B., Dalsin, J., & Messersmith, P. (**2006**). Biomimetic adhesive polymers based on mussel adhesive proteins. In A. Smith & J. Callow (Eds.), *Biological Adhesives* (pp 257–278). Berlin, Heidelberg: Springer.

Lee, C., Wei, X., Kysar, J. W., & Hone, J. (**2008**). Measurement of the elastic properties and intrinsic strength of monolayer graphene. *Science*, ***321***(***5887***), 385–388.

Lee, H., Scherer, N. F., & Messersmith, P. B. (**2006**). Single-molecule mechanics of mussel adhesion. *Proceedings of the National Academy of Sciences of the United States of America*, ***103***(***35***), 12999–13003.

Lei, H., Du, G., Wu, Z., Xi, X., & Dong, Z. (**2014**). Cross-linked soy-based wood adhesives for plywood. *International Journal of Adhesion and Adhesives*, ***50***, 199–203.

Lei, H., Pizzi, A., Navarrete, P., Rigolet, S., Redl, A., & Wagner, A. (**2010**). Gluten protein adhesives for wood panels. *Journal of Adhesion Science and Technology*, ***24***(***8***–***10***), 1583–1596.

Li, D., Müller, M. B., Gilje, S., Kaner, R. B., & Wallace, G. G. (**2008**). Processable aqueous dispersions of graphene nanosheets. *Nature Nanotechnology*, ***3***(***2***), 101–105.

Li, J. Y., Yeh, A. I., & Fan, K. L. (**2007**). Gelation characteristics and morphology of corn starch/soy protein concentrate composites during heating. *Journal of Food Engineering*, ***78***(***4***), 1240–1247.

Li, N., Qi, G., Sun, X. S., Stamm, M. J., & Wang, D. (**2011**). Physicochemical properties and adhesion performance of canola protein modified with sodium bisulfite. *Journal of the American Oil Chemists' Society*, ***89***(***5***), 897–908.

Li, N., Qi, G., Sun, X. S., & Wang, D. (**2012**). Effects of sodium bisulfite on the

physicochemical and adhesion properties of canola protein fractions. *Journal of Polymers and the Environment*, ***20***(***4***), 905–915.

Li, X., Luo, J., Gao, Q., & Li, J. (**2016**). A sepiolite-based united cross-linked network in a soybean meal-based wood adhesive and its performance. *RSC Advances*, ***6***(***51***), 45158–45165.

Liang, J., Huang, Y., Zhang, L., & Wang, Y. (**2009**). Molecular level dispersion of graphene into poly (vinyl alcohol) and effective reinforcement of their nanocomposites. *Advanced Functional Materials*, ***19***(***14***), 2297–2302.

Lin, Q., Gourdon, D., Sun, C., Holten-Andersen, N., Anderson, T. H., Waite, J. H., & Israelachvili, J. N. (**2007**). Adhesion mechanisms of the mussel foot proteins mfp-1 and mfp-3. *Proceedings of the National Academy of Sciences of the United States of America*, ***104***(***10***), 3782–3786.

Liu, D., Bian, Q., Li, Y., Wang, Y., Xiang, A., & Tian, H. (**2016**). Effect of oxidation degrees of graphene oxide on the structure and properties of poly (vinyl alcohol) composite films. *Composites Science and Technology*, ***129***, 146–152.

Liu, D., Chen, H., Chang, P. R., Wu, Q., Li, K., & Guan, L. (**2010**). Biomimetic soy protein nanocomposites with calcium carbonate crystalline arrays for use as wood adhesive. *Bioresource technology*, ***101***(***15***), 6235–6241.

Liu, H., Li, C., & Sun, X. S. (**2015**). Improved water resistance in undecylenic acid (UA)-modified soy protein isolate (SPI)-based adhesives. *Industrial Crops and Products*, ***74***, 577–584.

Liu, K. (**2012**). *Soybeans: chemistry, technology, and utilization*. Liu, K. (Eds). New York, USA:

Chapman an Hall.

Liu, Y., & Li, K. (**2002**). Chemical modification of soy protein for wood adhesives. *Macromolecular Rapid Communications*, ***23***(***13***), 739–742.

Liu, Y., & Li, K. (**2004**). Modification of soy protein for wood adhesives using mussel protein as a model: The influence of a mercapto group. *Macromolecular Rapid Communications*, ***25***(***21***), 1835–1838.

Luo, J., Li, C., Li, X., Luo, J., Gao, Q., & Li, J. (**2015**). A new soybean meal-based bioadhesive enhanced with 5,5-dimethyl hydantoin polyepoxide for the improved water resistance of plywood. *RSC Advances*, ***5***(*77*), 62957–62965.

Luo, J., Luo, J., Bai, Y., Gao, Q., & Li, J. (**2016**). A high performance soy protein-based bio-adhesive enhanced with a melamine/epichlorohydrin prepolymer and its application on plywood. *RSC Advances*, ***6***(***72***), 67669–67676.

Maeva, E., Severina, I., Bondarenko, S., Chapman, G., O'Neill, B., Severin, F., & Maev, R. G. (**2004**). Acoustical methods for the investigation of adhesively bonded structures: A review. *Canadian Journal of Physics*, ***82***(***12***), 981–1025.

Malik, M., & Kaur, R. (**2016**). Mechanical and thermal properties of castor oil-based polyurethane adhesive: effect of tio 2 filler. *Advances in Polymer Technology*, ***35***(***4***), 21637–21644.

Manamperi, W. A. R., Chang, S. K. C., Ulven, C. A., & Pryor, S. W. (**2010**). Plastics from an improved canola protein isolate: preparation and properties. *Journal of the American Oil Chemists' Society*, ***87***(***8***), 909–915.

Mansouri, N., Pizzi, A., & Salvado, J. (**2007**). Lignin-based polycondensation resins for wood

adhesives. *Journal of Applied Polymer Science*, ***103***(***3***), 1690–1699.

Marquis, D., Chivas-Joly, C., & Guillaume, É. (**2011**). *Properties of nanofillers in polymer*. INTECH Open Access Publisher.

Marra, A. (**1992**). *Technology of wood bonding: Principles in practice*. Newyork: Van Nostrand Reinhold.

Mathias, J., Grédiac, M., & Michaud, P. (**2016**). Bio-based adhesives. In Pacheco-Torgal F, V. Ivanov, N. Karak, & H. Jonkers (Eds.), *Biopolymers and Biotech Admixtures for Eco-Efficient Construction Materials* (pp 369–385). Waltham, MA: Elsevier Ltd.

McBain, J. W., & Hopkins, D. G. (**1924**). On adhesives and adhesive action. *The Journal of Physical Chemistry*, ***29***(***2***), 188–204.

Mekonnen, T. H., Mussone, P. G., Choi, P., & Bressler, D. C. (**2014**). Adhesives from waste protein biomass for oriented strand board composites: development and performance. *Macromolecular Materials and Engineering*, ***299***(***8***), 1003–1012.

Mo, X., Sun, X. S., & Wang, Y. (**1999**). Effects of molding temperature and pressure on properties of soy protein polymers. *Journal of Applied Polymer Science*, ***73***(***13***), 2595–2602.

Mo, X., Sun, X., & Wang, D. (**2004**). Thermal properties and adhesion strength of modified soybean storage proteins. *Journal of the American Oil Chemists' Society*, ***81***(***4***), 395–400.

Mojica, L., Dia, V., & Mejia, E. (**2015**). Soy proteins. In Z. Ustunol (Eds.), *Applied Food Protein Chemistry* (pp 141–191). Chichester, UK: John Wiley & Sons, Ltd.

Monahan, J., & Wilker, J. J. (**2003**). Specificity of metal ion cross-linking in marine mussel adhesives. *Chemical Communications*, ***2003***(***14***), 1672–1673.

Monahan, J., & Wilker, J. J. (**2004**). Cross-linking the protein precursor of marine mussel adhesives: Bulk measurements and reagents for curing. *Langmuir*, ***20***(***9***), 3724–3729.

Moon, R. J., Frihart, C. R., Wegner, T., Moon, R. J., Frihart, C. R., & Wegner, T. (**2006**). Nanotechnology applications in the forest products industry. *Forest products journal*, ***56***(***5***), 4–10.

Moubarik, A., Mansouri, H. R., Pizzi, A., Charrier, F., Allal, A., & Charrier, B. (**2013**). Corn flour-mimosa tannin-based adhesives without formaldehyde for interior particleboard production. *Wood Science and Technology*, ***47***(***4***), 675–683.

Nagano, T., Hirotsuka, M., Mori, H., Kohyama, K., & Nishinari, K. (**1992**). Dynamic viscoelastic study on the gelation of 7 S globulin from soybeans. *Journal of Agricultural and Food Chemistry*, ***40***(***6***), 941–944.

Newkirk, R. (**2015**). Canola meal - Feed industry guide. Available at : http://www.canolacouncil.org/media/516716/2015_canola_meal_feed_industry_guide.pdf [2016/12/27]

Nicholson, C., Abercrombie, J., Botterill, W., & Brocato, R. (**1991**). *History of adhesives*. *ESC Reports*.

Nietzel, T., Dudkina, N. V, Haase, C., Denolf, P., Semchonok, D. A., Boekema, E. J., Sunderhaus, S. (**2013**). The native structure and composition of the cruciferin complex in Brassica napus. *The Journal of biological chemistry*, ***288***(***4***), 2238–2245.

Norde, W. (**2011**). Intermolecular interactions. In L. Frewer, A. Fischer, W. Norde, & F. Kampers (Eds.), *Nanotechnology in the Agri-Food Sector* (pp 5–22). Weinheim, Germany: Wiley-VCH.

Nordqvist, P., Khabbaz, F., & Malmstroem, E. (**2010**). Comparing bond strength and water resistance of alkali-modified soy protein isolate and wheat gluten adhesives. *International Journal of Adhesion and Adhesives*, ***30***(***2***), 72–79.

Nordqvist, P., Thedjil, D., Khosravi, S., Lawther, M., Malmström, E., & Khabbaz, F. (**2012**). Wheat gluten fractions as wood adhesives-glutenins versus gliadins. *Journal of Applied Polymer Science*, ***123***(***3***), 1530–1538.

O'Brien, N., & Cummins, E. (**2008**). Recent developments in nanotechnology and risk assessment strategies for addressing public and environmental health concerns. *Human and Ecological Risk Assessment: An International Journal*, ***14***(***3***), 568–592.

OECD, & FAO. (**2016a**). OECD-FAO Agricultural outlook 2016-2025. Available at: http://www.oecd-ilibrary.org/agriculture-and-food/oecd-fao-agricultural-outlook-2016_agr_outlook-2016-en [2016/12/25].

OECD, & FAO. (**2016b**). OECD-FAO Agricultural Outlook 2016-2025. Oilseed industry. Availabe at: http://www.oecd-ilibrary.org/agriculture-and-food/oecd-fao-agricultural-outlook-2016_agr_outlook-2016-en [2016/12/25].

Pandey, J., Lee, J., Chu, W., Kim, C., Ahn, S., & Lee, C. (**2008**). Cellulose nano whiskers from grass of Korea. *Macromolecular Research*, ***16***(***5***), 396–398.

Papov, V. V, Diamond, T. V, Biemann, K., & Waite, J. H. (**1995**). Hydroxyarginine-containing Polyphenolic Proteins in the Adhesive Plaques of the Marine Mussel Mytilus edulis. *Journal of Biological Chemistry*, ***270***(***34***), 20183–20192.

Park, S., & Ruoff, R. S. (**2009**). Chemical methods for the production of graphenes. *Nature Nanotechnology*, ***4***(***4***), 217–224.

Peng, B. L., Dhar, N., Liu, H. L., & Tam, K. C. (**2011**). Chemistry and applications of nanocrystalline cellulose and its derivatives: A nanotechnology perspective. *The Canadian Journal of Chemical Engineering*, ***89***(***5***), 1191–1206.

Pizzi, A. (**1994a**). *Advanced Wood Adhesives Technology*. New York, NY. CRC Press.

Pizzi, A. (**1994b**). Urea-formaldehyde adhesives. In *Pizzi A.* (Eds) *Advanced wood adhesives technology.* (pp 19-66). *New York: Marcel Dekker*.

Pizzi, A. (**2003a**). Melamine-formaldehyde adhesives. In A. Pizzi & K. Mittal (Eds.), *Handbook of Adhesive Technology* (pp 653-680). *New York: Marcell Dekker.*

Pizzi, A. (**2003b**). Natural phenolic adhesives I: Tannin. In A. Pizzi & K. Mittal (Eds.), *Handbook of adhesive technology* (pp 573-588). *New York: Marcel Dekker.*

Pizzi, A. (**2003c**). Resorcinol Adhesives. In A. Pizzi & K. Mittal (Eds.), *Handbook of Adhesive Technology* (pp 599-614). *New York: Marcel Dekker.*

Pizzi, A. (**2006**). Recent developments in eco-efficient bio-based adhesives for wood bonding: opportunities and issues. *Journal of Adhesion Science and Technology*, ***20***(***8***), 829–846.

Pizzi, A. (**2013**). Bioadhesives for wood and fibres. *Reviews of Adhesion and Adhesives*, ***1***(***1***), 88–113.

Pizzi, A. (**2016**). Wood products and green chemistry. *Annals of Forest Science*, ***73***(***1***), 185–203.

Popa, V., Ungureanu, E., & Todorciuc, T. (**2007**). On the interaction of lignins, furan resins and furfuryl alcohol in adhesive systems. *Cellulose Chemistry and Technology*, ***41***, 119–123.

Qi, G., Li, N., Wang, D., & Sun, X. S. (**2013**). Physicochemical properties of soy protein adhesives modified by 2-octen-1-ylsuccinic anhydride. *Industrial Crops and Products*, ***46***,

165–172.

Qi, G., Li, N., Wang, D., & Sun, X. S. (**2016**). Development of high-strength soy protein adhesives modified with sodium montmorillonite clay. *Journal of the American Oil Chemists' Society*, ***93***(***11***), 1509–1517.

Qi, H. (**2013**). Growing Bioeconomy-Alberta Activities and Capacities. In M. Bruins & T. Boxtel (Eds.), *Biorefinery for Food, Fuel and Materials* (pp 103). Wageningen, The Netherlands: Proceedings of Symposium Biorefinery for food fuel and materials.

Qiao, W., Li, S., Guo, G., Han, S., Ren, S., & Ma, Y. (**2015**). Synthesis and characterization of phenol-formaldehyde resin using enzymatic hydrolysis lignin. *Journal of Industrial and Engineering Chemistry*, ***21***, 1417–1422.

Raftery, G., Harte, A., & Rodd, P. D. (**2009**). Bonding of FRP materials to wood using thin epoxy gluelines. *International Journal of Adhesion and Adhesives*, ***29***(***5***), 580–588.

Rajasekar, R., Moganapriya, C., Sathish Kumar, P., & Navaneethakrishnan, P. (**2016**). Binders such as adhesives, gums, wallpaper paste, resins or any subclass in polymer division. In Inamuddin Y (Eds.), *Green Polymer Composites Technology: Properties and Applications* (pp 49–62). Boca Raton, FL: CRC Press.

Salari, A., Tabarsa, T., Khazaeian, A., & Saraeian, A. (**2013**). Improving some of applied properties of oriented strand board (OSB) made from underutilized low quality paulownia (Paulownia fortunie) wood employing nano-SiO_2. *Industrial Crops and Products*, ***42***, 1–9.

Santulli, C. (**2016**). Nanoclay based natural fibre reinforced polymer composites: mechanical and thermal properties. In M. Jawaid, A. K. Qaiss, & R. Bouhfid (Eds.), *Nanoclay reinforced polymer composites* (pp 81–101). Singapore: Springer Singapore.

Sarikaya, M. (**1994**). An introduction to biomimetics: A structural viewpoint. *Microscopy Research and Technique*, ***27***(***5***), 360–375.

Schultz, J., & Nardin, M. (**2003**). Theories and mechanisms of adhesion. In A. Pizzi & K. Mittal (Eds.), *Handbook of Adhesive Technology* (pp 53–68). Boca Raton, FL: CRC Press.

Sever, M. J., Weisser, J. T., Monahan, J., Srinivasan, S., & Wilker, J. J. (**2004**). Metal-mediated cross-linking in the generation of a marine-mussel adhesive. *Angewandte Chemie, International Edition*, ***43***(***23***), 2986.

Shao, G., Lu, Y., Wu, F., Yang, C., Zeng, F., & Wu, Q. (**2012**). Graphene oxide: the mechanisms of oxidation and exfoliation. *Journal of Materials Science*, ***47***(***10***), 4400–4409.

Sharpe, L., & Schonhorn, H. (**1964**). Surface energetics, adhesion and adhesive joints. *Advances in Chemistry Series*, ***43***, 189–201.

Shtein, M., Nadiv, R., Buzaglo, M., Kahil, K., & Regev, O. (**2015**). Thermally conductive graphene-polymer composites: size, percolation, and synergy effects. *Chemistry of Materials*, ***27***(***6***), 2100–2106.

Silverman, H. G., & Roberto, F. F. (**2007**). Understanding marine mussel adhesion. *Marine Biotechnology*, ***9***(***6***), 661–681.

Somani, K. P., Kansara, S. S., Patel, N. K., & Rakshit, A. K. (**2003**). Castor oil based polyurethane adhesives for wood-to-wood bonding. *International Journal of Adhesion and Adhesives*, ***23***(***4***), 269–275.

Song, Y., Seo, J., Choi, Y., Kim, D., & Choi, B. (**2016**). Mussel adhesive protein as an environmentally-friendly harmless wood furniture adhesive. *International Journal of Adhesion and Adhesives*, ***70***, 260–264.

SoyCanada. (**2016**). Canada's growing soybean industry. Available at : http://soycanada.ca/industry/industry-overview/ [2016/12/22]

Staffas, L., Gustavsson, M., & McCormick, K. (**2013**). Strategies and policies for the bioeconomy and bio-based economy: An analysis of official national approaches. *Sustainability*, ***5***(***6***), 2751–2769.

Staswick, P. E., Hermodson, M. A., & Nielsen, N. C. (**1981**). Identification of the acidic and basic subunit complexes of glycinin. *The Journal of biological chemistry*, ***256***(***16***), 8752–8755.

Staswick, P. E., Hermodson, M. A., & Nielsen, N. C. (**1984**a). Identification of the cystines which link the acidic and basic components of the glycinin subunits. *The Journal of biological chemistry*, ***259***(***21***), 13431–1345.

Staswick, P. E., Hermodson, M. A., & Nielsen, N. C. (**1984**b). The amino acid sequence of the A2B1a subunit of glycinin. *The Journal of biological chemistry*, ***259***(***21***), 13424–13430.

Stoeckel, F., Konnerth, J., & Gindl-Altmutter, W. (**2013**). Mechanical properties of adhesives for bonding wood-A review. *International Journal of Adhesion and Adhesives*, ***45***, 32–41.

Sun, X., & Bian, K. (**1999**). Shear strength and water resistance of modified soy protein adhesives. *Journal of the American Oil Chemists' Society*, ***76***(***8***), 977–980.

Suppavorasatit, I., De Mejia, E. G., & Cadwallader, K. R. (**2011**). Optimization of the enzymatic deamidation of soy protein by protein-glutaminase and its effect on the functional properties of the protein. *Journal of Agricultural and Food Chemistry*, ***59***(***21***), 11621–11628.

Tan, H., Zhang, Y., & Weng, X. (**2011**). Preparation of the plywood using starch-based adhesives modified with blocked isocyanates. *Procedia Engineering*, ***15***, 1171–1175.

Tan, S., Mailer, R., Blanchard, C., & Agboola, S. (**2011**). Canola proteins for human consumption: extraction, profile, and functional properties. *Journal of Food Science*, ***76***(***1***), R16-28.

Tandang-Silvas, M. R. G., Fukuda, T., Fukuda, C., Prak, K., Cabanos, C., Kimura, A., Maruyama, N. (**2010**). Conservation and divergence on plant seed 11S globulins based on crystal structures. *Biochimica et Biophysica Acta*, ***1804***(***7***), 1432–1442.

Taylor, S. W., Chase, D. B., Emptage, M. H., Nelson, M. J., & Waite, J. H. (**1996**). Ferric Ion Complexes of a DOPA-Containing Adhesive Protein from Mytilus edulis. *Inorganic chemistry*, ***35***(***26***), 7572–7577.

Taylor, S. W., Luther III, G. W., & Waite, J. H. (**1994**). Polarographic and spectrophotometric investigation of iron (III) complexation to 3, 4-dihydroxyphenylalanine-containing peptides and proteins from Mytilus edulis. *Inorganic chemistry*, ***33***(***25***), 5819–5824.

Thanh, V., & Shibasaki, K. (**1976**). Major proteins of soybean seeds. A straightforward fractionation and their characterization. *Journal of Agricultural and Food Chemistry*, ***24***(***6***), 1117–1121.

Thanh, V., & Shibasaki, K. (**1977**). Beta-conglycinin from soybean proteins. Isolation and immunological and physicochemical properties of the monomeric forms. *Biochimica et Biophysica Acta (BBA) - Protein Structure*, ***490***(***2***), 370–384.

Thanh, V., & Shibasaki, K. (**1979**). Major proteins of soybean seeds. Reversible and irreversible dissociation of β-conglycinin. *Journal of Agricultural and Food Chemistry*, ***27***(***4***), 805–809.

Tzeng, Y., Diosady, L., & Rubin, L. (**1990**). Production of Canola Protein Materials by Alkaline Extraction, Precipitation, and Membrane Processing. *Journal of Food Science*, ***55***(***4***), 1147–

1151.

Updegraff, I. (**1990**). Amino resin adhesives. In I. Skeist (Eds.), *Handbook of Adhesives* (pp 341–346). Boston, MA: Springer US.

Ustunol, Z. (**2015**). Amino acids, peptides and proteins. In Z. Ustunol (Eds.), *Applied Food Protein Chemistry* (pp 12–15). Singapore: John Wiley & Sons.

Van Doosselaere, P. (**2013**). Production of Oils. In G. Calliauw, R. Hamilton, & W. Hamm (Eds.), *Edible Oil Processing* (pp 55–96). Chichester, UK: John Wiley & Sons, Ltd.

Van Nhiem, D., Berg, J., Kjos, N. P., Trach, N. X., & Tuan, B. Q. (**2013**). Effects of replacing fish meal with soy cake in a diet based on urea-treated rice straw on performance of growing Laisind beef cattle. *Tropical Animal Health and Production*, ***45***(***4***), 901–909.

Veraverbeke, W. S., & Delcour, J. A. (**2002**). Wheat protein composition and properties of wheat glutenin in relation to breadmaking functionality. *Critical reviews in food science and nutrition*, ***42***(***3***), 179–208.

Verdejo, R., Bernal, M. M., Romasanta, L. J., & Lopez-Manchado, M. A. (**2011**). Graphene filled polymer nanocomposites. *Journal of Material Chemistry*, ***21***(***10***), 3301–3310.

Waite, J., Andersen, N., Jewhurst, S., & Sun, C. (**2005**). Mussel adhesion: finding the tricks worth mimicking. *Journal of Adhesion*, ***81***(***3***–***4***), 297–317.

Waite, J. H. (**1983**). Evidence for a repeating 3,4-dihydroxyphenylalanine- and hydroxyproline-containing decapeptide in the adhesive protein of the mussel, Mytilus edulis L. *Journal of Biological Chemistry*, ***258***(***5***), 2911–2915.

Waite, J. H. (**2002**). Adhesion a la moule. *Integrative and Comparative Biology*, ***42***(***6***), 1172–1180.

Waite, J. H., & Qin, X. (**2001**). Polyphosphoprotein from the adhesive pads of *Mytilus edulis*. *Biochemistry*, ***40***(***9***), 2887–2893.

Waite, J. H., Qin, X. X., & Coyne, K. J. (**1998**). The peculiar collagens of mussel byssus. *Matrix Biology*, ***17***(***2***), 93–106.

Wanasundara, J. P. D. (**2011**). Proteins of Brassicaceae oilseeds and their potential as a plant protein source. *Critical Reviews in Food Science and Nutrition*, ***51***(*7*), 635–677.

Wang, C., Wu, J., & Bernard, G. M. (**2014**). Preparation and characterization of canola protein isolate–poly(glycidyl methacrylate) conjugates: A bio-based adhesive. *Industrial Crops and Products*, ***57***, 124–131.

Wang, P., Cheng, L., Gu, Z., Li, Z., & Hong, Y. (**2015**). Assessment of starch-based wood adhesive quality by confocal Raman microscopic detection of reaction homogeneity. *Carbohydrate Polymers*, ***131***, 75–79.

Wang, W., Bringe, N. A., Berhow, M. A., & Gonzalez de Mejia, E. (**2008**). B-Conglycinins among sources of bioactives in hydrolysates of different soybean varieties that inhibit leukemia cells in vitro. *Journal of Agricultural and Food Chemistry*, ***56***(***11***), 4012–4020.

Wang, Y., Mo, X., Sun, X. S., & Wang, D. (**2007**). Soy protein adhesion enhanced by glutaraldehyde crosslink. *Journal of Applied Polymer Science*, ***104***(***1***), 130–136.

Wang, Y., Sun, X. S., & Wang, D. (**2006**). Performance of soy protein adhesive enhanced by esterification. *Transactions of the ASAE-American Society of Agricultural Engineers*, ***49***(***3***), 713.

Wang, Z., Gu, Z., Hong, Y., Cheng, L., & Li, Z. (**2011**). Bonding strength and water resistance of starch-based wood adhesive improved by silica nanoparticles. *Carbohydrate Polymers*,

86(***1***), 72–76.

Wang, Z., Gu, Z., Li, Z., Hong, Y., & Cheng, L. (**2013**). Effects of urea on freeze–thaw stability of starch-based wood adhesive. *Carbohydrate Polymers*, ***95***(***1***), 397–403.

Wang, Z., Li, Z., Gu, Z., Hong, Y., & Cheng, L. (**2012**). Preparation, characterization and properties of starch-based wood adhesive. *Carbohydrate Polymers*, ***88***(***2***), 699–706.

Widsten, P., & Kandelbauer, A. (**2008**). Adhesion improvement of lignocellulosic products by enzymatic pre-treatment. *Biotechnology Advances*, ***26***(***4***), 379–386.

Woerfel, J. (**1995**). Extraction. In D. Erickson (Eds.), *Practical Handbook of Soybean Processing and Utilization* (pp 65–92). Champaign, Illinois: AOCS Press.

Wool, R. P. (**2015**). Nanoclay biocomposites. In R. P. Wool & X. S. Sun (Eds.), *Bio-based polymers and composites* (pp 523–550). Cambridge, Massachusetts: Academic Press.

Wu, S., Murphy, P., Johnson, L., & Fratzke, A. (**1999**). Pilot-plant fractionation of soybean glycinin and β-conglycinin. *Journal of the American Oil Chemists Society*, ***76***(***3***), 285–293.

Xia, Y., & Larock, R. C. (**2010**). Vegetable oil-based polymeric materials: synthesis, properties, and applications. *Green Chemistry*, ***12***(***11***), 1893–1909.

Xu, Y., Bai, H., Lu, G., Li, C., & Shi, G. (**2008**). Flexible graphene films via the filtration of water-soluble noncovalent functionalized graphene sheets. *Journal of the American Chemical Society*, ***130***(***18***), 5856–5857.

Yang, X., Tu, Y., Li, L., Shang, S., & Tao, X. (**2010**). Well-dispersed chitosan/graphene oxide nanocomposites. *ACS Applied Materials & Interfaces*, ***2***(***6***), 1707–1713.

Yu, M., Hwang, J., & Deming, T. J. (**1999**). Role of L-3,4-Dihydroxyphenylalanine in Mussel

Adhesive Proteins. *Journal of the American Chemical Society*, ***121***(***24***), 5825–5826.

Yuan, C., Luo, J., Luo, J., Gao, Q., & Li, J. (**2016**). A soybean meal-based wood adhesive improved by a diethylene glycol diglycidyl ether: properties and performance. *RSC Advances*, ***6***(***78***), 74186–74194.

Zeng, H., Hwang, D. S., Israelachvili, J. N., & Waite, H. (**2010**). Strong reversible Fe^{3+}-mediated bridging between dopa-containing protein films in water. *Proceedings of the National Academy of Sciences of the United States of America, Early Edition*, ***107(29)***, 12850-12853.

Zhang, Y., Ding, L., Gu, J., Tan, H., & Zhu, L. (**2015**). Preparation and properties of a starch-based wood adhesive with high bonding strength and water resistance. *Carbohydrate Polymers*, ***115***, 32–37.

Zhang, Y., Zhu, W., Lu, Y., Gao, Z., & Gu, J. (**2014**). Nano-scale blocking mechanism of MMT and its effects on the properties of polyisocyanate-modified soybean protein adhesive. *Industrial Crops and Products*, ***57***, 35–42.

Zhao, L., Liu, Y., Xu, Z., Zhang, Y., Zhao, F., & Zhang, S. (**2011**). State of research and trends in development of wood adhesives. *Forestry Studies in China*, ***13***(***4***), 321–326.

Zhao, Y., Yan, N., & Feng, M. W. (**2013**a). Bark extractives-based phenol–formaldehyde resins from beetle-infested lodgepole pine. *Journal of Adhesion Science and Technology*, ***27***(***18***–***19***), 2112–2126.

Zhao, Y., Yan, N., & Feng, M. W. (**2013**b). Biobased phenol formaldehyde resins derived from beetle-infested pine barks—structure and composition. *ACS Sustainable Chemistry & Engineering*, ***1***(***1***), 91–101.

Zhong, Y. L., Tian, Z., Simon, G. P., & Li, D. (**2015**). Scalable production of graphene via wet

chemistry: progress and challenges. *Materials Today*, ***18***(***2***), 73–78.

Zhu, D., & Damodaran, S. (**2014**). Chemical phosphorylation improves the moisture resistance of soy flour-based wood adhesive. *Journal of Applied Polymer Science*, ***131***(***13***), 40451–40457.

CHAPTER 3 - Exfoliating Nanomaterials in Canola Protein Derived Adhesive Improves Strength and Water Resistance[1]

[1]A version of this chapter has been published: Bandara, N., Esparza, Y., & Wu, J. (**2017**). Exfoliating nanomaterials in canola protein derived adhesive improves strength and water resistance. *RSC Advances*, ***7(11)***, 6743-6752.

3.1 Introduction

The wood adhesive industry is dominated by petrochemical-derived resins, such as urea formaldehyde (UF), phenol formaldehyde (PF) and melamine urea formaldehyde (MUF) (Li et al., 2016; Pizzi, 2006, 2013). However, increasing concerns on petrochemical based wood adhesives such as environmental impact, potential health hazard due to formaldehyde emission, and non-renewability have renewed the interest in developing green, renewable alternatives (Bandara et al., 2013; Kaboorani et al., 2012; Li et al., 2015; Li et al., 2016). Biobased adhesives, derived from protein, and polysaccharides were widely used before they were replaced by synthetic ones during the World War II (Bandara et al., 2013; Kaboorani et al., 2012; Pizzi, 2006, 2013). However, the challenge remains with regard to developing cost-effective and performance comparative adhesives from these biobased materials (Pizzi, 2013). Proteins are preferred among other biobased polymers for preparing adhesives, due to their versatile functionalities as well as flexibility for modifications (Pizzi, 2013; Wang et al., 2014). Historically, casein, gelatin, blood and soy proteins were applied for various adhesive applications (Li et al., 2015; Luo et al., 2015; Pizzi, 2013). More recently, the possibility of using other protein sources such as wheat gluten (Khosravi et al., 2014), cottonseed protein (He et al., 2014), triticale protein (Bandara et al., 2011, 2013), and canola protein (Wang et al., 2014) were studied. Without exception, canola protein derived adhesives also showed poor water resistance and low adhesion strength (Wang et al., 2014). Canola is the second largest oil seed crop in the world and oil processing generates a great deal of meal, containing 35-40% w/w proteins. Irrespective to its high protein content, canola meal has limited uses mainly as a low value animal feed or as a fertilizer (Manamperi et al., 2010; Wang et al., 2014). Canola meal mainly consists of cruciferin (12S), napin (2S) and oleosin with approximate proportions of ~60%,

~20% and ~8% respectively (Li et al., 2011). Cruciferin is a neutral protein (PI – 7.2) with molecular weight of ~ 300-310 KDa while napin is strongly basic (PI ~11.0) protein because of high proportion of amidated amino acids present in its structure with a molecular weight of ~ 12.5-14.5 KDa (Aider & Barbana, 2011). Canola protein adhesive prepared by modifying with sodium bisulfite showed dry, wet and soaked adhesion strength values of 5.28 ± 0.47 MPa, 4.07 ± 0.16 MPa and 5.43 ± 0.28 MPa, respectively (Li et al., 2012). Canola adhesive prepared with 0.5% sodium dodecyl sulphate (SDS) showed dry, wet, and soaked adhesion strength of 6.00 ± 0.69, 3.52 ± 0.48 MPa, and 6.66 ± 0.07 MPa, respectively (Hale, 2013). By grafting poly (glycidyl methacrylate) into canola protein, our study showed improved dry, wet and soaked strength of 8.25 ± 0.12 MPa, 3.80 ± 0.15 MPa and 7.10 ± 0.10 MPa for respectively (Wang et al., 2014). However, the use of high amount of expensive poly (glycidyl methacrylate) polymer (2.7 g/2 g protein, w/w) prevents its future commercial exploration. Therefore, there is a need to look for new methods to improve water resistance and adhesion strength of canola protein.

Nanomaterials are widely used in material science in order to change mechanical, electrical and chemical properties of the bulk material (Kaboorani et al., 2012). For example, in composites research, adding nanomaterials were reported to improve flexural strength, elasticity, toughness and stability of the material (Santulli, 2016). The potential of nanomaterials in improving adhesive performance was recently explored but with limited success. Kaboorani et al (2011, 2012) observed slight improvement in adhesion and water resistance after adding montmorillonite (Kaboorani & Riedl, 2011), nano aluminum oxide (Kaboorani & Riedl, 2012), and nanocrystalline cellulose (Kaboorani et al., 2012) into polyvinyl acetate adhesives at low nanomaterial concentrations. Research on nanomaterial addition into protein based adhesives was extremely limited. Zhang et al., (2014) reported a decreased adhesion strength of

polyisocyanate modified soy protein with the addition of montmorillonite, probably due to a nano scale blocking mechanism. Li et al., (2016) recently studied the effect of modified sepiolite-based united crosslinked network in improving adhesion of soybean meal-based wood adhesive and reported an improvement of wet strength from 0.81 MPa to 1.18 MPa. Another recent study by Qi et al (2016) reported an improvement of wet adhesion from 2.9 MPa to 4.3 MPa by exfoliating sodium montmorrilonite at 8% w/w addition rate into soy protein isolate (Qi et al., 2016). Both studies suggest that "physical filling effect" of sepiolite (Li et al., 2016), and nanomaterial induced crosslinking of protein network as the key factors contributing towards improving adhesion (Li et al., 2016; Qi et al., 2016). It is well recognized that proper dispersion and exfoliation of nanomaterials is a critical factor in their applications (Arshad et al., 2016). Therefore, it is necessary to develop new methods for exfoliating nanomaterials in use of protein-based adhesives matrix.

We hypothesized that a proper dispersion of nanomaterials into canola protein adhesive would improve water resistance and adhesion strength. The main objective of this study is to develop and characterize nano-material reinforced canola protein adhesive with improved water resistance and adhesive strength. Effects of addition levels and intercalation conditions of nanomaterials such as hydrophilic bentonite (Bento), surface modified montmorillonite (with 25-30 %, w/w trimethyl octadecylammonium chloride - SM-MMT), nanocrystalline cellulose (NCC), and graphite oxide (GO) were studied in this research. These nanomaterials have been selected based on the strong evidence found in literature in improving functional properties of adhesives, composites and plastic research (Kaboorani et al., 2012; Kaboorani & Riedl, 2011; Reddy et al., 2013; Stankovich et al., 2006). Nanoclays are hydrated material made with either tetrahedral or octahedral stacks of silicate sheets (Sapalidis et al., 2011). Bentonite is typically

considered as an impure form of clays that contain both montmorillonite and other crystalline structures, arranged in a octahedral sheet sandwich between two tetrahedral plates and an isolated additional octahedral plate (Marquis et al., 2011). Montmorillonite is a naturally hydrophilic and inorganic material that made with two stacked layers of tetrahedral sheets around a middle octahedral sheet, and usually contains hydrated Na+ or K+ ions (Marquis et al., 2011; Sapalidis et al., 2011). Montmorillonite used for this study is modified with 25-30 (%, w/w) trimethyloctadecylammonium chloride to improve interlayer spacing and hydrophobicity. GO consists of oxidized graphite sheets (or graphene oxide sheets) as their basal planes while surface of the sheet is decorated mostly with epoxide, hydroxyl, carbonyl and carboxyl groups (Stankovich et al., 2007). Nanocrystalline cellulose (NCC) is derived from acid hydrolysis of native cellulose and shows a rigid rod-like crystals with diameter in the range of 10–20 nm and lengths of a few hundred nanometers (Peng et al., 2011).

3.2 Materials and Methods

3.2.1 Materials and Chemicals

Canola meal was a generous gift from Richardson Oilseed Ltd. (Lethbridge, AB, Canada). Hydrophilic bentonite (Bento), surface modified montmorillonite (SM-MMT), graphite and cellulose were purchased from Sigma-Aldrich (Sigma Chemical Co, St. Louise, MO, USA). All chemicals were from Fisher Scientific (Ottawa, ON, Canada) unless otherwise noted.

3.2.2 Method

3.2.2.1 Canola Protein Extraction

Proteins were extracted from canola meal as described by Manamperi et al., (2010) with slight modifications. Canola meal was ground to pass through 100-mesh size using a Hosokawa

milling and classifying system (Hosokawa Micron Powder Systems, Summit, NJ, USA). Canola meal was mixed with mili-Q water in 1:10 (w/v) ratio; pH was adjusted to 12.0 using 3 M NaOH and stirred for 30 m followed by centrifugation (10000g, 15 min, 4ºC). The supernatant was collected, readjust pH to 4.0 using 3 M HCl and centrifuged as above after 30 m stirring. The resulting precipitate was collected, freeze-dried and stored at -20 ºC until further use.

3.2.2.2 Graphite Oxide Preparation

Graphite oxide nanoparticles (GO) were prepared according to Hummers & Offeman, (1958) method with slight modifications. In brief, 5 g of graphite and 2.5 g of $NaNO_3$ was mixed in a glass beaker where 120 mL of concentrated H_2SO_4 was slowly added while stirring for 30 m (200 RPM) in an ice bath to oxidize graphite. Then, 15g of $KMnO_4$ was slowly added to the mixture while maintaining temperature at 35 ± 3 ºC and stirred for 1 hrs. After the reaction, 92 mL of deionized water was added to the reaction mixture, and stirred for 15 min. Leftover $KMnO_4$ was neutralized by adding another 80 mL of hot (60 ºC) deionized water containing 3% H_2O_2. After cooling to room temperature, the sample was centrifuged (10000g, 15 min, 4 ºC) to remove any remaining chemicals. The precipitate was washed for three times as above to prepare oxidized graphite, followed by 5 m sonication (at 50% power output), before freeze drying.

3.2.2.3 Nanocrystalline Cellulose Preparation

Nanocrystalline cellulose (NCC) was prepared from cellulose samples as described by Cranston & Gray, (2006) with slight modifications. Cellulose hydrolysis was carried out by mixing 20 g of cellulose powder with 350 mL of 64% (w/w) sulfuric acid under continuous stirring for 45 m at 45 ºC. The mixture was diluted 10 times with deionized water in order to suspend the reaction and centrifuged (10000 g, 4 ºC, 10 min) to remove excessive acid. The

resulting precipitate was washed with deionized water, and centrifuged to remove any remaining chemicals. Extracted NCC was dialyzed for three days against deionized water until neutral pH achieved, freeze-dried, and stored at -20 ºC until further use.

3.2.2.4 Exfoliation of Nano Materials and Adhesive Preparation

A solution intercalation method was developed to exfoliate nanomaterials into canola protein matrix. In brief, 3 g of canola protein was mixed with 20 mL of deionized water to make 15% w/v dispersion. Samples were stirred for 6 h (300 rpm, RT) to disperse canola protein, and pH was readjusted to 5.0 using 1 M HCl solution. Nanomaterials at various concentrations (to have final concentrations of 0%, 1%, 3%, 5%, and 10% w/w, nanomaterial/protein) were separately dispersed in 10 mL deionized water, stirred for 5 h at room temperature (300 rpm) and another 1 h at 45 ± 3 ºC. Dispersed nanomaterials were sonicated for 3 m using a medium size tapered tip attached to a high intensity ultrasonic dismembrator (Model 500, Thermo Fisher Scientific INC, Pittsburg, PA, USA) providing intermittent pulse dispersion of 5 s at 3 s intervals and 60% amplitude. Resulting nanomaterial dispersions were homogenized for 2 m at 20,000 rpm using digital ULTRA TURRAX high shear homogenizer (Model T25 D S1, IKA® Works, Wilmington, NC, USA). Then, prepared nanomaterial dispersions were slowly added to protein dispersions dropwise while stirring for 15 m to have a final protein concentration of 10% w/v. Following the intercalation, protein-nanomaterial mixture was sonicated and homogenized as above and the pH of the adhesive mixture was readjust to 12.0 by adding 6 M NaOH solution. Negative controls were prepared by dispersing canola protein in deionized water at 10% w/v ratio and used as is. In the pH controls, canola protein samples were dispersed in deionized water at 10% w/v ratio, but adjust the pH to 12.0 similar to nanomaterial reinforced samples, without adding nanomaterials. Solution intercalation method developed by Zhang et al., (2014) was used

to produce canola protein adhesives from SM-MMT and NCC for the purpose of comparing water resistance and adhesion of the method developed in our lab.

3.2.2.5 Adhesion Strength Measurement

Birch veneer samples with a thickness of 1.2 mm were cut into a dimension of 20 mm × 120 mm (width and length) using a cutting device (Adhesive Evaluation Systems, Corvallis, OR, USA). They were conditioned according to the requirement of ASTM (American Society for Testing and Materials) standard method D2339-98 (2011) (ASTM, 2011) at 23 ºC and 50% relative humidity in a controlled environment chamber (ETS 5518, Glenside, PA, USA). The prepared adhesive samples were spread at an amount of 40 uL/veneer strand in a contact area of 20 mm × 5 mm using a micropipette. After adhesive application, veneer samples were air dried for 5 min, followed by hot pressing at 120 ºC and 3.5 MPa for 10 m using Carver manual hot press (Model 3851-0, Carver Inc, In, USA). Dry adhesion strength (DAS) was measured according to ASTM standard method D2339-98 (2011) by measuring tensile loading required to pull bonded veneer using Instron machine (Model 5565, Instron, MA, USA) equipped with a 5 kN load cell and data was collected using Bluhill 3.0 software (Instron, MA, USA). Wet adhesion strength (WAS) and soaked adhesion strength (SAS) were measured according to ASTM standard D1151-00 (2013) (ASTM, 2013) using Instron tensile loading. WAS values were measured after submerging bonded veneer samples for 48 h in water (23 ºC) while SAS was measured after reconditioning submerged wet samples for another seven days at 23 ºC and 50% relative humidity in a controlled environment chamber. In each strength testing (DAS, WAS and SAS) minimum four bonded veneer samples per replicate was used. All samples were clamped to instron with a 35 mm gauge length and tested at 10 mm/min cross head speed.

3.2.2.6 Differential Scanning Calorimetry (DSC)

Thermal properties in prepared nanomaterials and adhesive samples were analyzed using differential scanning calorimeter (Perkin-Elmer, Norwalk, CT, USA). Temperature and heat flow were calibrated using pure indium samples. Moisture in the samples was removed by freeze-drying followed by drying in a hermetic desiccator containing P_2O_5 for two weeks before analysis. Nanomaterial and adhesive samples were accurately weighed into T-Zero hermetic aluminum pans (~6 mg each), mixed with 60 µL of 0.01 M phosphate buffer, hermetically sealed with lids, and analyzed against an empty reference pan under continuous nitrogen purging. All samples were equilibrated at 0 ^oC for 10 m and heated from 0 to 250 ^oC at a ramping rate of 10 ^oC min^{-1}. Thermodynamic data was collected and analyzed using Universal Analysis 2000 software for thermal transition changes in adhesives and nanomaterials (Perkin-Elmer, Norwalk, CT, USA).

3.2.2.7 Fourier Transform Infrared Spectroscopy (FTIR)

FTIR was used to characterize nanomaterial induced secondary structural changes of canola proteins using Nicolet 8700 Fourier transform infrared spectrometer (Thermo Eletron Co. WI, USA). Moisture in the samples was removed by freeze drying followed by drying in a hermetic desiccator containing P_2O_5 for two weeks before analysis. Graphite, GO, NCC, and nanomaterial reinforced adhesive samples were mixed with potassium bromide (KBr), and milled to make a fine powder before FTIR analysis. IR Spectra in the range of 400-4000 cm^{-1} were collected using 128 scans at a resolution of 4 cm^{-1}. Collected data were processed and analyzed with Origin 2016 software (OriginLab Corporation, MA, USA), where the second derivative of FTIR spectra was used to identify the protein secondary structural changes.

3.2.2.8 X-ray Diffraction

X-ray diffraction (XRD) of nanomaterial reinforced adhesive samples was performed using Rigaku Ultima IV powder diffractometer (Rigaku Co. Japan). Cu-Kα radiation (0.154 nm) was used to collect the angle data (2Θ) from 5 to 50 degrees. XRD data was processed using Origin 2016 software (OriginLab Corporation, MA, USA) for nanomaterial-reinforced adhesives to identify the dispersion pattern at different nanomaterial concentrations. Interlayer distance of nanomaterials were calculated using the Bragg's equation (Bragg & Bragg, 1913); $\sin \theta = n\lambda/2d$, where λ is the wavelength of X-ray radiation used in the experiment, d is the spacing between diffraction lattice (interlayer spacing), and θ is the glancing angle (measured diffraction angle) (Alexandre & Dubois, 2000; Kaboorani & Riedl, 2011).

3.2.2.9 Transmission Electron Microscopy (TEM)

Transmission electron microscopy analysis was performed using Philips/FEI transmission electron microscope (Model Morgagni, FEI Co, OR, USA) coupled with Getan digital camera (Getan Inc, CA, USA). For nanomaterials, samples were dispersed in ethanol at a concentration of 0.5% w/w whereas adhesive samples were diluted to 100 fold with ethanol before TEM imaging. A drop of prepared solution was casted onto 200 mesh holey copper grid covered with carbon film and allowed for air drying before imaging. For NCC sample and adhesive containing NCC, 1% w/w uranyl acetate drop was added onto air dried drop in the copper grid in order to improve the contrast of NCC fibres.

3.2.3 Statistical Analysis

Data were analyzed using analysis of variance (ANOVA) followed by Duncan's Multiple Range (DMR) test to identify the effects of each nanomaterial concentration on adhesion

strength (Dry, Wet, Soaked) using Statistical Analysis System Software (SAS version 9.4, SAS Institute, Cary, NC). Effect of nanomaterial concentrations on adhesion strength of each nanomaterial was evaluated at the 95% confidence level.

3.3 Results and Discussion

3.3.1 Characterization of Nanomaterials

Fig. 3.1 shows the diffraction angles and interlayer spacing of nanomaterials used in this study. Both bentonite and SM-MMT show similar crystalline peaks around diffraction angles of 19.7º, 34.9º, and 54.0º with interlayer spacing of 0.450 nm, 0.257 nm, and 0.167 nm, respectively. Kaboorani & Riedl, (2011) also observed similar intense peaks in unmodified montmorillonite clay.

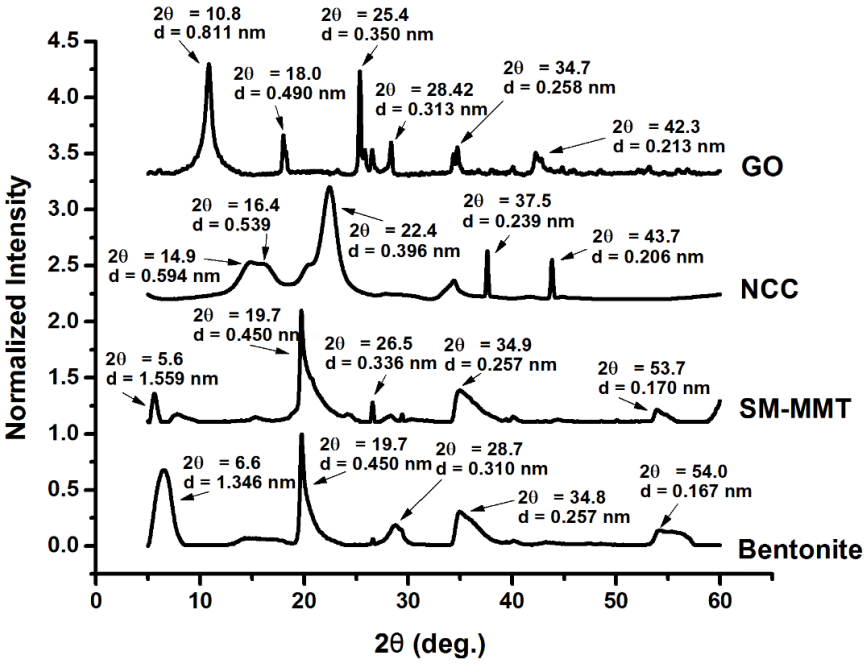

Figure 3.1. X-ray diffraction patterns show glancing angle (θ) and interlayer spacing (*d*) of bentonite, SM-MMT (surface modified montmorrilonite), NCC (nanocrystalline cellulose) and GO (graphite oxide) used in the adhesive preparation. [*Notes: X-ray diffraction data of the*

nanomaterials were collected at the glancing angle (2θ) range of 5-60º and interlayer spacing (d) was calculated according to the Bragg's equation: Sin θ = nλ/2d.]

The crystalline peaks at 6.6 º and 28.7 º in bentonite has shifted to 5.6 º and 26.5 º in SM-MMT whereas their corresponding interlayer spacing have shifted from 1.346 and 0.310 nm to 1.559 and 0.336 nm, respectively. Surface modification of montmorillonite with 25-30% (w/w) trimethyloctadecylammonium chloride polymer is known to cause changes of diffraction angle and the increase in interlayer spacing (Han et al., 2004; Zhou et al., 2009).

Crystallinity and interlayer spacing of NCC depend on the method of preparation (Chen et al., 2012; Liu et al., 2011). NCC samples show three characteristic cellulose crystalline peaks at 14.9º, 16.4 and 22.4º with interlayer spacing of 0.594 nm, 0.539 nm and 0.396 nm, respectively. Cellulose crystalline peaks at similar diffraction angels were previously reported (Chen et al., 2012; Liu et al., 2011). In addition, two other minor peaks were shown at 37.5 º, and 43.7 º diffraction angles with interlayer spacing of 0.239 nm and 0.213 nm, respectively. GO samples show two major peaks at 10.8º and 25.4º with interlayer spacing of 0.811 nm and 0.350 nm. In addition, three minor peaks were observed in the prepared GO at 18.0º, 34.7º and 42.3º angles with *d* space of 0.490 nm, 0.258 nm and 0.213 nm, respectively. The interlayer spacing of GO mainly depends on their oxidation level and C:O ratio (Krishnamoorthy et al., 2013); GO prepared for this study has a C:O ratio of 2.18 *(Appendix 1: supplementary Fig 3.1)*. Krishnamoorthy et al., (2013) identified similar crystalline peaks for graphite oxide prepared under different oxidation conditions. They attributed the peak at 10.8º to an oxidation product whereas the peak at ~25.4º to crystallinity of graphite. In the same study they observed changes in diffraction angle and interlayer spacing with different oxidation conditions. TEM images of nanomaterials are shown in Fig. 3.2. Both bentonite and SM-MMT showed the platelet like

structure at ~80 -150 nm whereas NCC samples appear to be in a long rod like fibers at ~60-90 nm diameters. GO appeared to be thin sheets stacked one another with average width of ~600-800 nm.

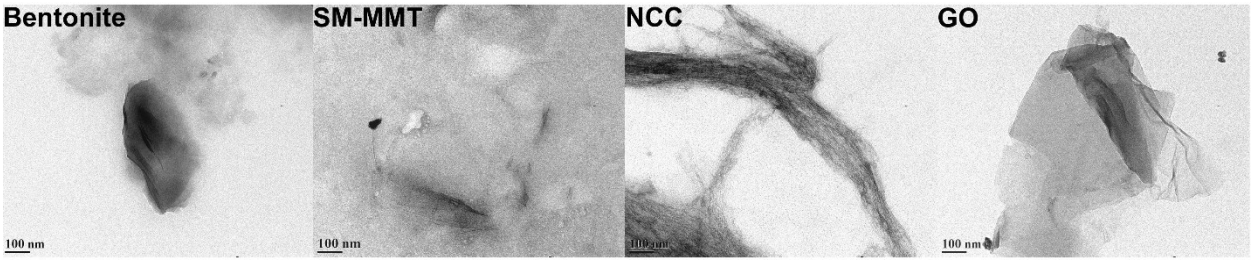

Figure 3.2. Transmission electron microscopic images of bentonite, SM-MMT (surface modified montmorrilonite), NCC (nanocrystalline cellulose) and GO (graphite oxide) used for adhesive preparation.

3.3.2 Dispersion of Nanomaterials in Canola Protein

Previous studies on dispersing NCC, nanoclay, and Al_2O_3 nano particle in PVA adhesives suggested that homogeneous dispersion/exfoliation of nanomaterials is the key to improve adhesion strength (Kaboorani et al., 2012; Kaboorani & Riedl, 2011, 2012). Fig 3.3 shows the TEM images of nanomaterial dispersion in canola adhesive samples at different concentrations. At a 1% addition level, all four nanomaterials were exfoliated where they dispersed completely and randomly in the protein matrix (Kaboorani & Riedl, 2011; Xu et al., 2011). However, aggregation of clay platelets started to be visible at 3, 5 and 10% (w/w of protein) addition levels in bentonite and SM-MMT samples. Similar results were observed in previous studies on nanoclay and Al_2O_3 dispersed PVA adhesives where aggregation of nanoclay platelets were reported at concentrations greater than 4% (Kaboorani & Riedl, 2011, 2012). In terms of NCC and GO, exfoliation was observed up to 5% (w/w of protein) addition level whereas aggregation

was visible at 10% (w/w of protein) addition level. The presence of surface hydrophilic groups such as –OH and –COOH in NCC and GO might be the reason for better exfoliation in canola protein matrix than those of bentonite and SM-MMT.

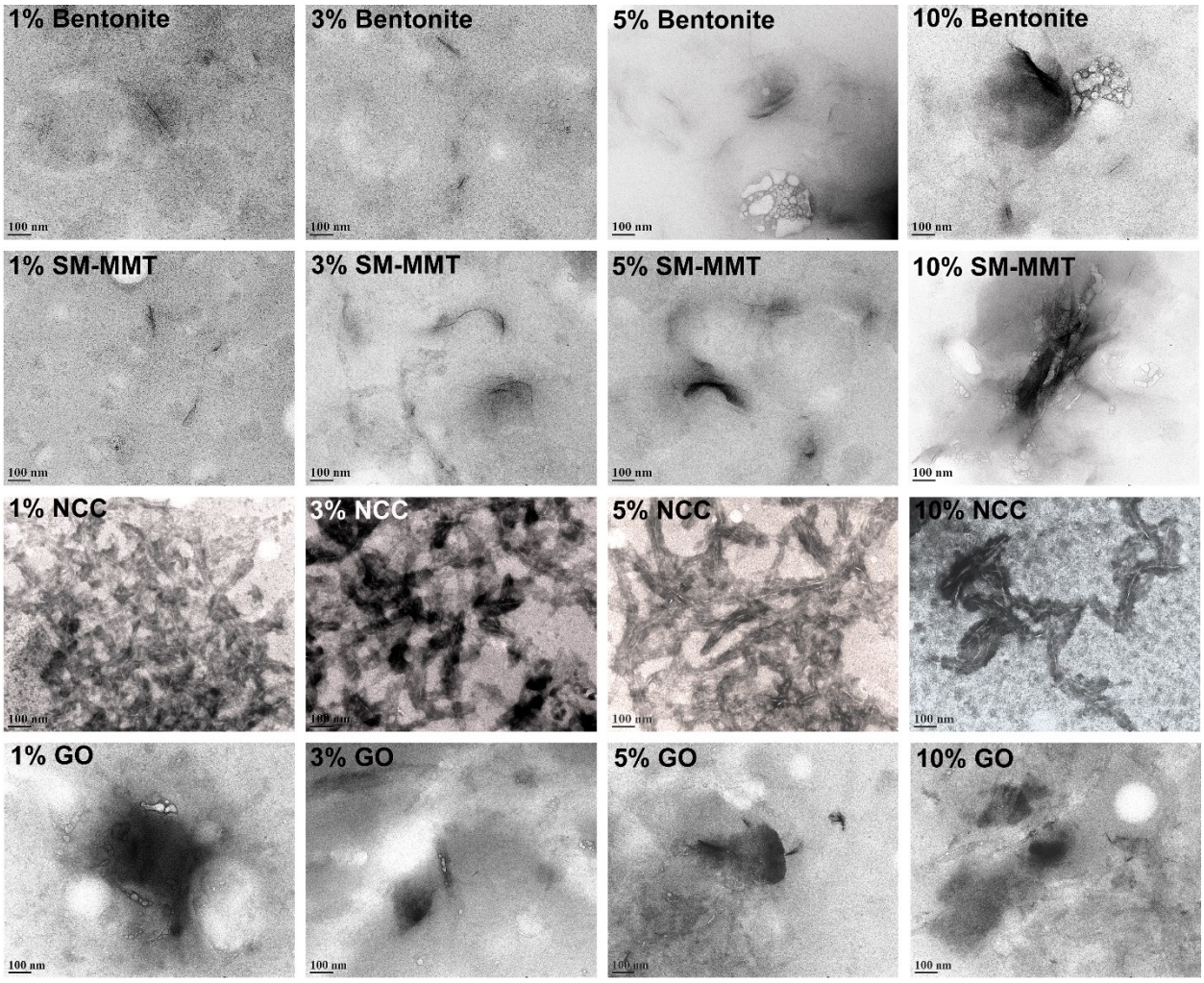

Figure 3.3. Transmission electron microscopic images of canola protein adhesives after exfoliating 1%, 3%, 5%, and 10% (w/w nanomaterial/canola protein) levels of bentonite, SM-MMT (surface modified montmorrilonite), NCC (nanocrystalline cellulose) and GO (graphite oxide).

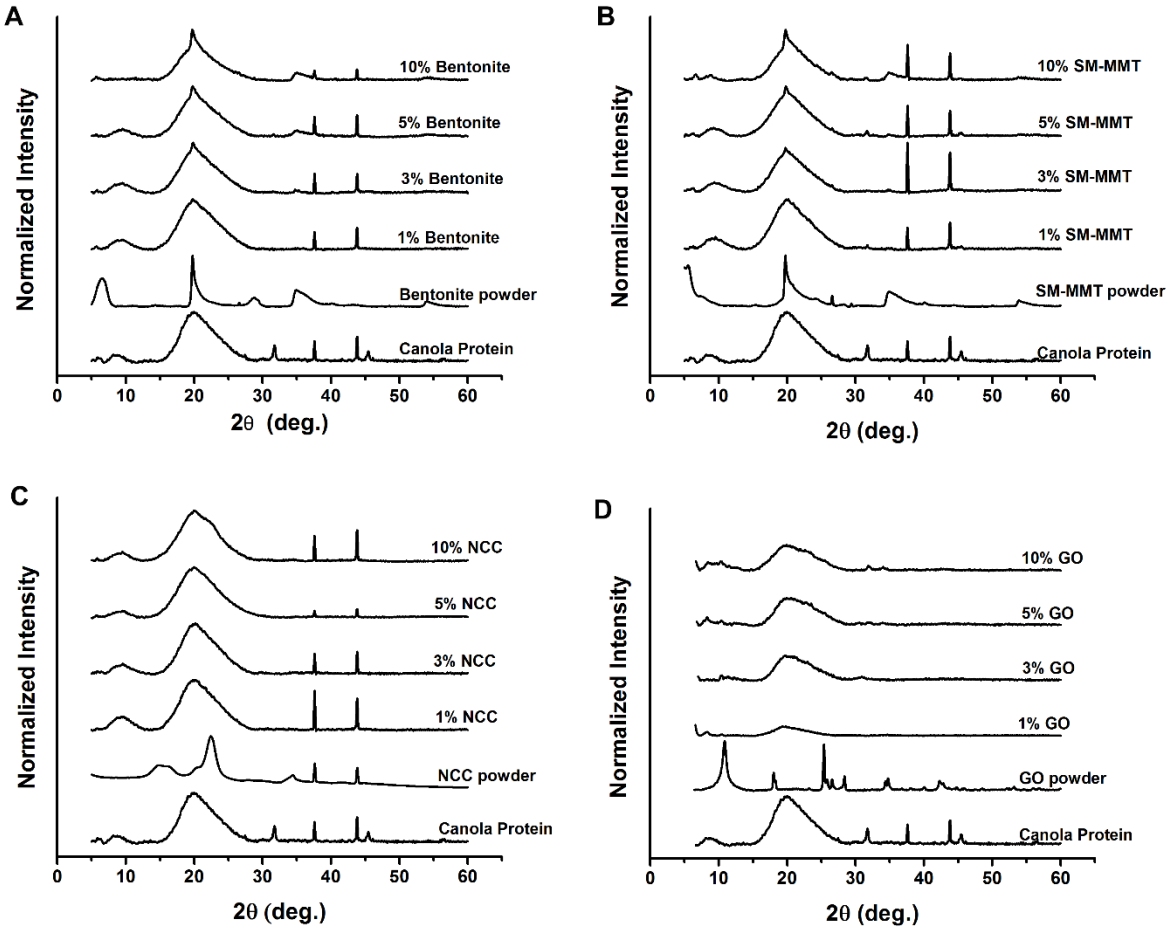

Figure 3.4. X-ray diffraction patterns of canola protein adhesives after exfoliating 1%, 3%, 5%, and 10% (w/w nanomaterial/canola protein) levels of bentonite, SM-MMT (surface modified montmorrilonite), NCC (nanocrystalline cellulose) and GO (graphite oxide).

X-ray diffraction of nanomaterial dispersed canola protein adhesives are shown in Fig 3.4. XRD patterns of dispersed nanomaterials supported the results observed in TEM. In a situation where nanomaterials are properly exfoliated in the matrix, crystalline peaks of original nanomaterial should not be visible since exfoliated nanomaterial since it could not generate identical peaks due to the absence of similar crystal lattice (Kaboorani & Riedl, 2011; Xu et al., 2011). XRD patterns of bentonite and SM-MMT exhibit a similar trend where the exfoliation of

nanomaterials was observed only in 1% (w/w of protein) addition level. Characteristic nanoclay peaks arising at 5.6°, 19.7°, and 34.8° start to appear in bentonite and SM-MMT incorporated adhesives after increasing the nanomaterial addition up to 3% or above. This can be due to partial exfoliation of nanomaterials or aggregation of nanoclay platelets at higher concentrations. Kaboorani & Riedl, (2011, 2012) observed similar trend in XRD patterns where, nanomaterial loading above 4% exhibit crystalline peaks similar to their original nanomaterials in montmorillonite and nano Al_2O_3 dispersed in PVA adhesives.

In comparison, NCC and GO show better exfoliation in canola protein as original NCC and GO crystalline peaks were not visible in XRD patterns up to 5% addition level. However, at 10% (w/w of protein) addition level, both NCC and GO exhibit respective crystalline peaks in XRD patterns of prepared adhesives. In a previous study with NCC reinforced PVA adhesive, NCC showed exfoliation only up to 3% addition with improved wet adhesion than PVA adhesives reinforced with nanoclay (Kaboorani et al., 2012; Kaboorani & Riedl, 2011). The improved solution intercalation method we used to disperse nanomaterials in canola protein might be the reason for improved exfoliation observed in NCC and GO up to 5% addition level.

3.3.3 Effect of Nanomaterial Type and Their Concentration on Adhesion Strength

Effects of different nanomaterials and concentrations on adhesion strength are shown in Fig. 3.5. Adding nanomaterials at low concentrations significantly improved adhesion strength compared to both pH and negative controls. Bentonite significantly increased dry strength from 6.38 ± 0.84 MPa to 7.65 ± 1.33 MPa at 1% (w/w) addition and to 8.50 ± 1.27 MPa at 3% (w/w) addition (Fig. 3.5A). The wet strength was also increased from 1.98 ± 0.22 MPa (pH control) to 2.80 ± 0.50 MPa and 2.44 ± 0.29 MPa at 1% and 3% (w/w) addition respectively. However, the soaked strength was not affected by bentonite addition.

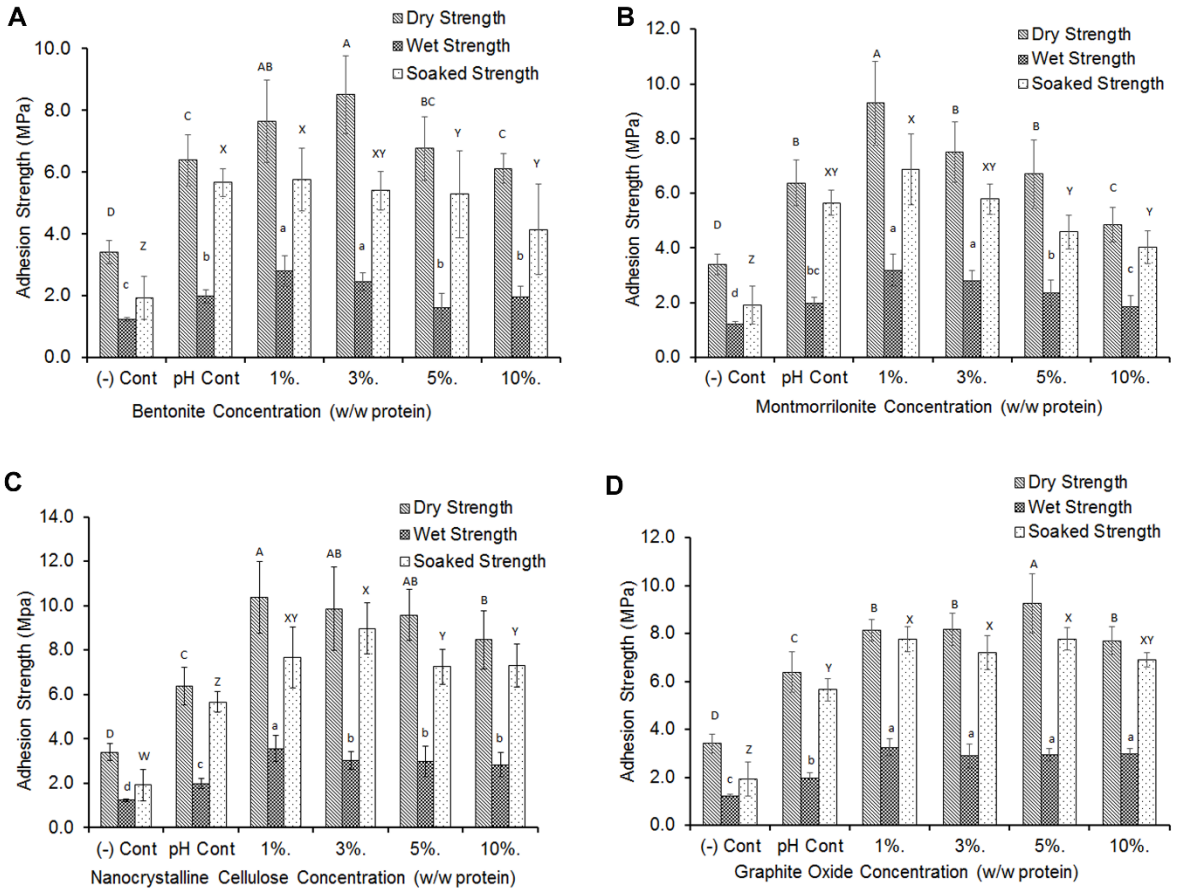

Figure 3.5. Adhesion strength of nanomaterial exfoliated canola protein adhesives after exfoliating 1%, 3%, 5%, and 10% (w/w nanomaterial/canola protein) levels of bentonite, SM-MMT (surface modified montmorrilonite), NCC (nanocrystalline cellulose) and GO (graphite oxide). Adhesion data was analyzed using one-way ANOVA followed by Duncan test for mean separation. Different letters on the bar represent significantly different adhesion strength ($p < 0.05$). Error bars represent standard deviations. All adhesive samples were prepared in triplicate ($n=3$) and minimum 5 wood samples per replicate were used for each strength measurement.

A similar trend was observed with the addition of SM-MMT (Fig 3.5B). At 1% SM-MMT addition, the dry, wet and soaked strengths were significantly increased up to 9.29 ± 1.53 MPa, 3.19 ± 0.57 MPa, and 6.87 ± 1.29 MPa respectively. However, the strength values were reduced

at increasing bentonite/SM-MMT addition levels, which may be due to partial exfoliation or aggregation of nanomaterials at higher concentration as evidenced by TEM and XRD. Aggregation of nanomaterials at higher concentrations were previously reported in metal oxide nanomaterials and carbon nanotubes in different matrixes, mainly due to interaction with functional groups in polymer (Hatchett & Josowicz, 2008; Keller et al., 2010). Similarly, aggregation of bentonite and SM-MMT might reduce the functional groups available for interacting with wood surface, thereby decreasing adhesion strength.

In comparison, both NCC and GO exhibited a better exfoliation even under higher addition levels up to 5% as evidenced by TEM and XRD, which was in good agreement with improved adhesion strength with NCC and GO addition (Fig 3.5C & 3.5D.). NCC significantly increased both dry and wet strength (10.37 ± 1.63 MPa and 3.57 ± 0.57 MPa respectively) at 1% (w/w) addition level while the highest soaked strength (8.98 ± 1.15 MPa) was observed at 3% (w/w) NCC addition. Unlike bentonite and SM-MMT, all tested NCC and GO addition levels significantly increased the adhesion and water resistance compared to negative and pH control samples. The highest dry and soaked strength for GO (9.27 ± 1.24 MPa, 7.78 ± 0.45 MPa respectively) was observed at 5% (w/w) concentration whereas the highest wet strength for GO (3.25 ± 0.36 MPa) was observed at 1% (w/w) concentration. Adhesive prepared by our exfoliation method exhibited significantly higher water resistance and adhesion than that prepared by the method reported by Zhang et al (2014) (*Appendix 1: supplementary Table 3.1).* Our study further supported the importance of uniform dispersion/exfoliation of nanomaterial in adhesive application, which was in good agreement with previous reports in improving mechanical properties of polymer matrix (Kaboorani et al., 2012; Kaboorani & Riedl, 2011, 2012). The adhesive strength of soy protein adhesive was not improved when SiO_2 nano particles

was not homogenously dispersed and exfoliated (Xu et al., 2011). Adding high level of montmorillonite could even reduce the adhesive strength, due to a nano scale blocking mechanism (Zhang et al., 2014). Zhang et al (2014) suggested that enhanced interactions between MMT and soy protein could make functional groups unavailable for reacting with wood surface, thus reducing adhesion strength. Adhesion between adhesive-wood interface results from various interactions including chemical bonding and mechanical interlocking (Schultz & Nardin, 2003). The exfoliated nanomaterials have the potential to affect both chemical bonding and mechanical interlocking thereby increasing adhesion. The presence of nanomaterials in an exfoliated state in the adhesive matrix could act as a physical barrier for water penetration (Li et al., 2016); it may also improve cohesion by increasing protein-protein interactions as a cross linker (Li et al., 2016; Qi et al., 2016; Zhang et al., 2014) which ultimately improves wet and dry adhesion strength. In addition, adding nanomaterials would also induce protein structural changes by exposing hydrophobic and other berried functional groups (Lynch & Dawson, 2008) enabling reaction with functional groups present in surface and inner layers of the wood during adhesive penetration and subsequent curing.

3.3.4 Effect of Nanomaterial on Structural Changes in Canola Protein Based Wood Adhesives

Effects of nanomaterial addition on protein secondary structure are shown in Fig 3.6. Protein secondary structural changes after modifications can be identified by processing amide I peak, typically generated by C=O and C-N stretching vibrations at 1600 – 1700 cm^{-1} wavelength (Barth, 2007; Kong & Yu, 2007). The CPI pH control samples are predominated by β sheet structure (Barth, 2007; Kong & Yu, 2007) with fitted peaks allocated at 1626 cm^{-1}, 1639 cm^{-1}, and 1676 cm^{-1} in the second derivative spectra, followed by α-helix and turns with peaks found

at 1657 cm^{-1} and 1695 cm^{-1} respectively (Barth, 2007) (*Appendix 1: supplementary Fig 3.2*). In all nanomaterial added samples, in particular at concentrations over 3%, there is an increase in unordered structure as the peak at 1641 cm^{-1} increased (Barth, 2007; Kong & Yu, 2007).

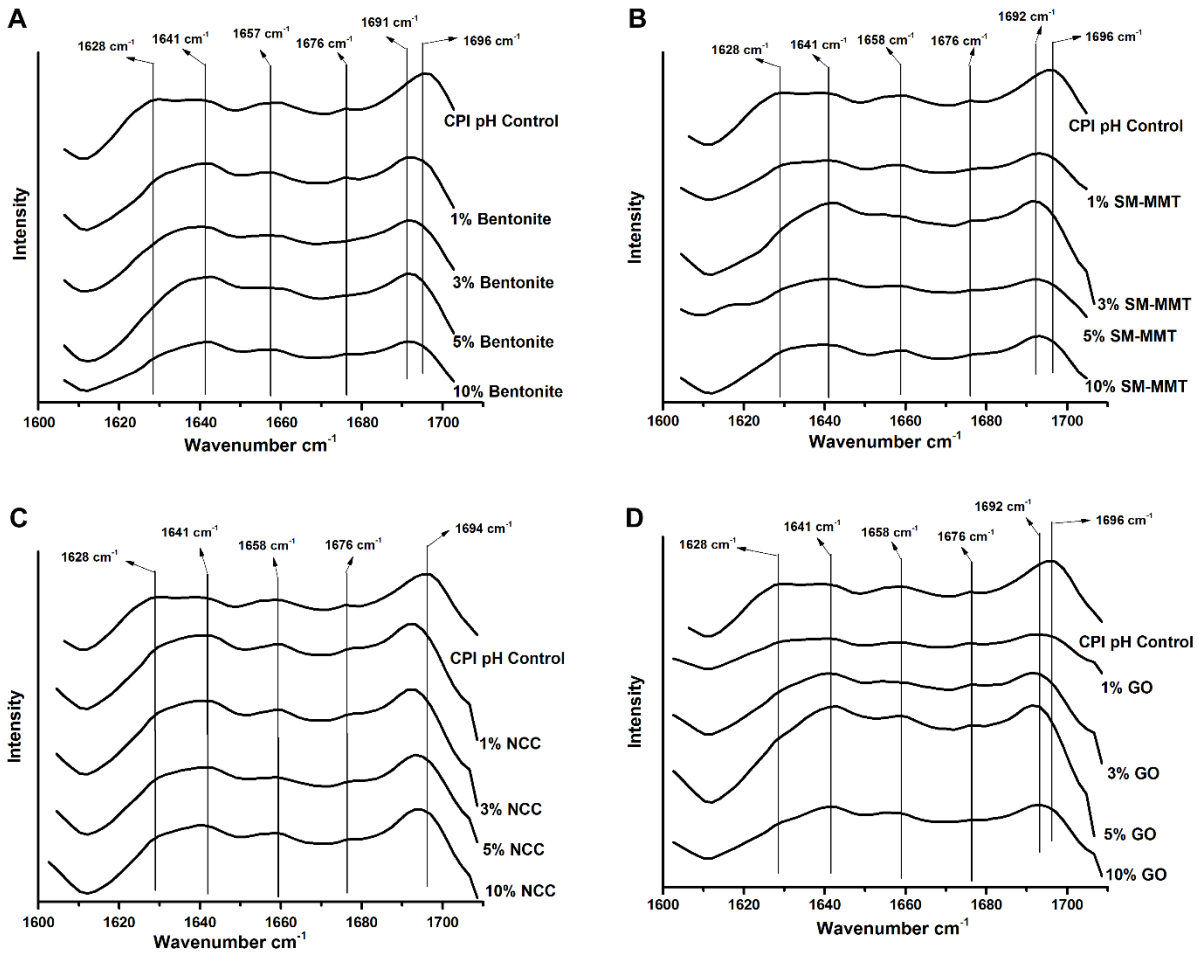

Figure 3.6. Second derivative spectra of amide I peak in FTIR spectra showing protein secondary structural changes of adhesives prepared either with canola protein (CPI pH Control), or by exfoliating bentonite, SM-MMT (surface modified montmorrilonite), NCC (nanocrystalline cellulose), and GO (graphite oxide), at different nanomaterial addition levels (1%, 3%, 5%, and 10% w/w nanomaterial/canola protein).

At increasing bentonite addition, the relative proportion of β sheet structures (1628 cm^{-1}, 1676 cm^{-1}) was decreasing while that of unordered structures (1641 cm^{-1}) was increasing (Fig 3.6a). Similar trend was also observed with SM-MMT addition (Fig 3.6b, *Appendix 1: supplementary Fig 3.2, Appendix 1: supplementary 3.3*). In addition, at high nanomaterial concentrations, a peak shift from 1695 cm^{-1} towards 1691 cm^{-1} also represent turns in secondary structure of modified proteins (Barth, 2007). In both type of nanoclay, increasing nanomaterial did reduce the relative proportion of α-helical structures as well (*Appendix 1: supplementary Fig 3.2, Appendix 1: supplementary Fig 3.3*).

NCC addition reduced the relative proportion of β sheet structure (1628 cm^{-1} and 1675 cm^{-1} wavelengths) while the proportion of α-helical structure (1657 cm^{-1}) increased at high NCC concentrations (Fig 3.6c). Unlike nanoclay, the unordered structure (1641 cm^{-1}) was not visible in second derivative spectra after peak fitting until concentrations up to 3% or above. At increasing GO concentrations, increase in unordered structure (1641 cm^{-1}) was more obvious compared to other nanomaterials, mainly at the expense of the relative proportions of α-helix and β sheet structure (*Appendix 1: supplementary Fig 3.4, Appendix 1: supplementary Fig 3.5*). Nanomaterial induced protein secondary structural changes were observed in previous studies as well (Linse et al., 2007; Lynch & Dawson, 2008; Norde & Giacomelli, 2000) where they reported decreased α-helix and β sheet structures (Norde & Giacomelli, 2000) but increased β turns and unordered structures (Lynch & Dawson, 2008; Norde & Giacomelli, 2000). These changes were attributed to the protein nanomaterial interactions such as nanomaterial induced the protein-protein interactions and exposed hydrophobic functional groups as a result of protein nanomaterial interactions, which was packed in core of protein structure (Lynch & Dawson, 2008).

Results obtained from FTIR analysis of modified adhesives support the trends observed in the adhesion strength of nanomaterial incorporated canola protein adhesives. At lower nanomaterial concentration, changes in secondary structure would expose more hydrophobic functional groups and enhance interactions with the wood surface thereby increasing adhesion strength and, specifically water resistance. Increasing nanomaterial concentrations, however, would lead to drastic change of secondary structure and promote strong nanomaterial-protein interactions, thereby reducing the potential functional groups available to react with wood surface (Zhang et al., 2014), which ultimately reduce adhesion strength and water resistance. Therefore choosing an appropriate level of nanomaterial addition into canola protein matrix is important in improving adhesion strength and water resistance of canola protein adhesives.

3.3.5 Effect of Nanomaterial on Thermal Properties of Adhesives

Effects of nanomaterial additions at different concentrations on the thermal stability and enthalpy required for adhesive denaturation were shown in Table 3.1. Denaturation temperature (T_d) of a protein is an indication of thermal stability of protein (Wu & Muir, 2008). Extracted canola protein used for this study exhibits an onset temperature of 72.20 ± 0.16 ºC and T_d value of 90.91 ± 2.09 ºC, which was comparable to previously reported onset temperature of 77.9 ºC and denaturation temperature of 83.9 ºC, by Wu and Muir (2008). The slight variations of denaturation temperatures are attributed to the method of protein extraction and compositional changes of extracted protein, which has an effect on thermal stability of the protein (Wu & Muir, 2008) . Thermal stability is one of the properties required in developing wood adhesives where hot pressing is required in adhesive curing. In general, adding nanomaterials increased the T_d of CPI adhesives compared to the controls which could be due to strong protein-nanomaterial and protein-protein interactions.

Table 3.1. Changes in thermal transitions (Mean + standard deviations ; *n=4*) of canola protein based adhesives after exfoliating bentonite, surface modified montmorrilonite (SM-MMT), nanocrystalline cellulose (NCC) and graphite oxide (GO) at different nanomaterial concentrations (1%, 3%, 5%, and 10% w/w nanomaterial/canola protein).

Sample	Onset T^o (^{o}C)	Peak T^o (^{o}C)	Specific heat (J/g.C)
CPI – Control	72.20 ± 0.16	90.91 ± 2.09	1.44 ± 0.03
CPI pH Control	88.55 ± 4.82	103.16 ± 4.74	2.53 ± 0.02
1% Bentonite	86.25 ± 2.62	103.79 ± 2.28	2.69 ± 0.12
3% Bentonite	91.75 ± 0.69	107.42 ± 0.18	2.60 ± 0.07
5% Bentonite	90.32 ± 1.75	105.58 ± 2.51	2.20 ± 0.01
10% Bentonite	87.69 ± 1.53	103.35 ± 2.14	2.14 ± 0.06
1% SM-MMT	85.98 ± 2.04	102.54 ± 2.41	2.32 ± 0.02
3% SM-MMT	85.80 ± 1.32	100.53 ± 1.61	1.92 ± 0.03
5% SM-MMT	78.22 ± 3.48	93.02 ± 4.82	2.12 ± 0.15
10% SM-MMT	84.34 ± 5.18	98.86 ± 3.44	1.84 ± 0.04
1% NCC	91.84 ± 1.73	105.15 ± 2.14	2.43 ± 0.04
3% NCC	85.40 ± 2.40	100.63 ± 2.82	2.12 ± 0.03
5% NCC	87.82 ± 1.28	101.69 ± 1.40	1.55 ± 0.06
10% NCC	84.34 ± 5.18	104.18 ± 0.08	1.56 ± 0.05
1% GO	79.17 ± 0.83	96.02 ± 0.88	2.88 ± 0.09
3% GO	80.66 ± 0.47	97.62 ± 1.32	2.52 ± 0.01
5% GO	82.39 ± 0.18	98.20 ± 1.64	2.11 ± 0.06
10% GO	80.50 ± 1.03	95.55 ± 2.94	1.48 ± 0.02

Linse et al., (2007) attributed increased thermal stability and denaturation temperatures of graphite oxide nano sheet incorporated soybean peroxidase to protein secondary structural changes. However, further increasing nanomaterial concentrations resulted in decreasing T_d values of CPI adhesives. This can be a result of drastic changes in protein secondary structures as evidenced by FTIR data, where they created higher degree of unordered structures, resulting lower temperature requirement for denaturation.

3.4 Conclusions

A solution intercalation method was developed to exfoliate nanomaterials in canola protein matrix as evidenced by TEM and XRD analysis. Our study showed that nanomaterials at lower addition levels (at 1% w/w addition) could significantly improve the adhesion strength and water resistance of canola protein adhesives. However, decrease in adhesion strength at increasing nanomaterial addition levels were observed with the exception of NCC and GO, where adhesion was improved even at 3% and 5% w/w levels, respectively. Our study further supported the significance of uniform dispersion and exfoliation of nanomaterial in the protein matrix. Adding nanomaterials exposed more hydrophobic and other functional groups to react with wood surface, which would increase water resistance and adhesion strength. The Improvement could also be attributed to the nanomaterial-induced cohesion. In addition, the properly exfoliated nanomaterials could act as physical barriers for water penetration, contributing to improved water resistance. Among four nanomaterials tested in this study, GO and NCC proved to be superior in terms of increasing functionality of canola protein adhesives compared to bentonite and SM-MMT. Results of this study provided evidence on the potential use of nanomaterial to improve the adhesive properties of biobased wood adhesives, which may replace traditional synthetic adhesives as green alternative adhesive materials.

3.5 References

Aider, M., & Barbana, C. (**2011**). Canola proteins: composition, extraction, functional properties, bioactivity, applications as a food ingredient and allergenicity – A practical and critical review. *Trends in Food Science & Technology*, ***22***(***1***), 21–39.

Alexandre, M., & Dubois, P. (**2000**). Polymer-layered silicate nanocomposites: preparation, properties and uses of a new class of materials. *Materials Science and Engineering: R: Reports*, ***28***(***1***–***2***), 1–63.

Arshad, M., Kaur, M., & Ullah, A. (**2016**). Green biocomposites from nanoengineered hybrid natural fiber and biopolymer. *ACS Sustainable Chemistry & Engineering*, ***4***(***3***), 1785–1793.

ASTM. (**2011**). D2339-98(2011) Standard test method for strength properties of adhesives in two-ply wood construction in shear by tension loading. *Annual Book of ASTM Standards.* Available at: http://compass.astm.org/EDIT/html_annot.cgi?D2339+98%5C [2012/12/04]

ASTM. (**2013**). D1151-00(2013) Standard practice for effect of moisture and temperature on adhesive bonds. *Annual Book of ASTM Standards.* Available at: http://compass.astm.org/EDIT/html_annot.cgi?D1151 +00%5C [2013/02/03]

Bandara, N., Chen, L., & Wu, J. (**2011**). Protein extraction from triticale distillers grains. *Cereal Chemistry*, ***88***(***6***), 553–559.

Bandara, N., Chen, L., & Wu, J. (**2013**). Adhesive properties of modified triticale distillers grain proteins. *International Journal of Adhesion and Adhesives*, ***44***, 122–129.

Barth, A. (**2007**). Infrared spectroscopy of proteins. *Biochimica et Biophysica Acta*, ***1767***(***9***), 1073–1101.

Bragg, W., & Bragg, W. (**1913**). The reflection of X-rays by crystals. *Proceedings of the Royal Society of London - Series A*, ***88***(***605***), 428–438.

Chen, X., Deng, X., Shen, W., & Jiang, L. (**2012**). Controled enzymolysis preparation of nanocrystalline cellulose from pretreated cotton fibers. *BioResources*, ***7***(***3***), 4237–4248.

Cranston, E. D., & Gray, D. G. (**2006**). Morphological and optical characterization of polyelectrolyte multilayers incorporating nanocrystalline cellulose. *Biomacromolecules*, ***7***(***9***), 2522–2530.

Hale, K. (**2013**). *The potential of canola protein for bio-based wood adhesives*. Masters dissertation. Kansas State University.

Han, B., Cheng, A., Ji, G., Wu, S., & Shen, J. (**2004**). Effect of organophilic montmorillonite on polyurethane/montmorillonite nanocomposites. *Journal of Applied Polymer Science*, ***91***(***4***), 2536–2542.

Hatchett, D. W., & Josowicz, M. (**2008**). Composites of intrinsically conducting polymers as sensing nanomaterials. *Chemical Reviews*, ***108***(***2***), 746–769.

He, Z., Chapital, D. C., Cheng, H. N., & Dowd, M. K. (**2014**). Comparison of adhesive properties of water- and phosphate buffer-washed cottonseed meals with cottonseed protein isolate on maple and poplar veneers. *International Journal of Adhesion and Adhesives*, ***50***, 102–106.

Hummers, W. S., & Offeman, R. E. (**1958**). Preparation of graphitic oxide. *Journal of the American Chemical Society*, ***80***(***6***), 1339–1339.

Kaboorani, A., & Riedl, B. (**2011**). Effects of adding nano-clay on performance of polyvinyl

acetate (PVA) as a wood adhesive. *Composites Part A: Applied Science and Manufacturing*, ***42***(***8***), 1031–1039.

Kaboorani, A., & Riedl, B. (**2012**). Nano-aluminum oxide as a reinforcing material for thermoplastic adhesives. *Journal of Industrial and Engineering Chemistry*, ***18***(***3***), 1076–1081.

Kaboorani, A., Riedl, B., Blanchet, P., Fellin, M., Hosseinaei, O., & Wang, S. (**2012**). Nanocrystalline cellulose (NCC): A renewable nano-material for polyvinyl acetate (PVA) adhesive. *European Polymer Journal*, ***48***(***11***), 1829–1837.

Keller, A. A., Wang, H., Zhou, D., Lenihan, H. S., Cherr, G., Cardinale, B. J., Ji, Z. (**2010**). Stability and aggregation of metal oxide nanoparticles in natural aqueous matrices. *Environmental Science & Technology*, ***44***(***6***), 1962–1967.

Khosravi, S., Khabbaz, F., Nordqvist, P., & Johansson, M. (**2014**). Wheat gluten based adhesives for particle boards: effect of crosslinking agents. *Macromolecular Materials and Engineering*, ***299***(***1***), 116–124.

Kong, J., & Yu, S. (**2007**). Fourier transform infrared spectroscopic analysis of protein secondary structures. *Acta Biochimica et Biophysica Sinica*, ***39***(***8***), 549–559.

Krishnamoorthy, K., Veerapandian, M., Yun, K., & Kim, S. J. (**2013**). The chemical and structural analysis of graphene oxide with different degrees of oxidation. *Carbon*, ***53***, 38–49.

Li, J., Li, X., Li, J., & Gao, Q. (**2015**). Investigating the use of peanut meal: a potential new resource for wood adhesives. *RSC Advances*, ***5***(***98***), 80136–80141.

Li, N., Qi, G., Sun, X. S., Stamm, M. J., & Wang, D. (**2011**). Physicochemical properties and adhesion performance of canola protein modified with sodium bisulfite. *Journal of the American Oil Chemists' Society*, ***89***(***5***), 897–908.

Li, N., Qi, G., Sun, X. S., & Wang, D. (**2012**). Effects of sodium bisulfite on the physicochemical and adhesion properties of canola protein fractions. *Journal of Polymers and the Environment*, ***20***(***4***), 905–915.

Li, X., Luo, J., Gao, Q., & Li, J. (**2016**). A sepiolite-based united cross-linked network in a soybean meal-based wood adhesive and its performance. *RSC Advances*, ***6***(***51***), 45158–45165.

Linse, S., Cabaleiro-Lago, C., Xue, W.-F., Lynch, I., Lindman, S., Thulin, E., Dawson, K. A. (**2007**). Nucleation of protein fibrillation by nanoparticles. *Proceedings of the National Academy of Sciences of the United States of America*, ***104***(***21***), 8691–8696.

Liu, D., Chen, X., Yue, Y., Chen, M., & Wu, Q. (**2011**). Structure and rheology of nanocrystalline cellulose. *Carbohydrate Polymers*, ***84***(***1***), 316–322.

Luo, J., Luo, J., Yuan, C., Zhang, W., Li, J., Gao, Q., & Chen, H. (**2015**). An eco-friendly wood adhesive from soy protein and lignin: performance properties. *RSC Advances*, ***5***(***122***), 100849–100855.

Lynch, I., & Dawson, K. A. (**2008**). Protein-nanoparticle interactions. *Nano Today*, ***3***(***1***–***2***), 40–47.

Manamperi, W. A. R., Chang, S. K. C., Ulven, C. A., & Pryor, S. W. (**2010**). Plastics from an improved canola protein isolate: preparation and properties. *Journal of the American Oil Chemists' Society*, ***87***(***8***), 909–915.

Marquis, D., Chivas-Joly, C., & Guillaume, É. (**2011**). *Properties of nanofillers in polymer*. INTECH Open Access Publisher.

Norde, W., & Giacomelli, C. E. (**2000**). BSA structural changes during homomolecular exchange between the adsorbed and the dissolved states. *Journal of Biotechnology*, ***79***(***3***), 259–268.

Peng, B. L., Dhar, N., Liu, H. L., & Tam, K. C. (**2011**). Chemistry and applications of nanocrystalline cellulose and its derivatives: A nanotechnology perspective. *The Canadian Journal of Chemical Engineering*, ***89***(***5***), 1191–1206.

Pizzi, A. (**2006**). Recent developments in eco-efficient bio-based adhesives for wood bonding: opportunities and issues. *Journal of Adhesion Science and Technology*, ***20***(***8***), 829–846.

Pizzi, A. (**2013**). Bioadhesives for wood and fibres. *Reviews of Adhesion and Adhesives*, ***1***(***1***), 88–113.

Qi, G., Li, N., Wang, D., & Sun, X. S. (**2016**). Development of high-strength soy protein adhesives modified with sodium montmorillonite clay. *Journal of the American Oil Chemists' Society*, ***93***(***11***), 1509–1517.

Reddy, M. M., Vivekanandhan, S., Misra, M., Bhatia, S. K., & Mohanty, A. K. (**2013**). Biobased plastics and bionanocomposites: Current status and future opportunities. *Progress in Polymer Science*, ***38***(***10***), 1653–1689.

Santulli, C. (**2016**). Nanoclay based natural fibre reinforced polymer composites: mechanical and thermal properties. In M. Jawaid, A. K. Qaiss, & R. Bouhfid (Eds.), *Nanoclay Reinforced Polymer Composites* (pp 81–101). Singapore: Springer Singapore.

Sapalidis, A., Katsaros, F., & Kanellopoulos, N. (**2011**). PVA/montmorillonite nanocomposites:

development and properties. *Nanocomposites and polymers with analytical methods*, 29–50.

Schultz, J., & Nardin, M. (**2003**). Theories and mechanisms of adhesion. In A. Pizzi & K. Mittal (Eds.), *Handbook of Adhesive Technology* (pp 53–68). Boca Raton, FL: CRC Press.

Stankovich, S., Dikin, D. A., Dommett, G. H. B., Kohlhaas, K. M., Zimney, E. J., Stach, E. A., Ruoff, R. S. (**2006**). Graphene-based composite materials. *Nature*, ***442***(***7100***), 282–286.

Stankovich, S., Dikin, D. A., Piner, R. D., Kohlhaas, K. A., Kleinhammes, A., Jia, Y., Ruoff, R. S. (**2007**). Synthesis of graphene-based nanosheets via chemical reduction of exfoliated graphite oxide. *Carbon*, ***45***(*7*), 1558–1565.

Wang, C., Wu, J., & Bernard, G. M. (**2014**). Preparation and characterization of canola protein isolate–poly(glycidyl methacrylate) conjugates: A bio-based adhesive. *Industrial Crops and Products*, ***57***, 124–131.

Wu, J., & Muir, A. D. (**2008**). Comparative structural, emulsifying, and biological properties of two major canola proteins, cruciferin and napin. *Journal of Food Science*, ***73***(***3***), 210–216.

Xu, H., Ma, S., Lv, W., & Wang, Z. (**2011**). Soy protein adhesives improved by SiO 2 nanoparticles for plywoods. *Pigment & Resin Technology*, ***40***(***3***), 191–195.

Zhang, Y., Zhu, W., Lu, Y., Gao, Z., & Gu, J. (**2014**). Nano-scale blocking mechanism of MMT and its effects on the properties of polyisocyanate-modified soybean protein adhesive. *Industrial Crops and Products*, ***57***, 35–42.

Zhou, L., Chen, H., Jiang, X., Lu, F., Zhou, Y., Yin, W., & Ji, X. (**2009**). Modification of montmorillonite surfaces using a novel class of cationic gemini surfactants. *Journal of Colloid and Interface Science*, ***332***(***1***), 16–21.

CHAPTER 4 - Graphite Oxide Improves Adhesion and Water Resistance of Canola Protein–Graphite Oxide Hybrid Wood Adhesive

CHAPTER 4

4.1 Introduction

Due to increasing concerns over environmental and human health implications of synthetic adhesives, researchers are looking for green materials/biobased adhesives using sustainable and renewable polymers (Kaboorani et al., 2012; Pizzi, 2013). Proteins are one of the most studied renewable polymers for adhesive applications (Wang et al., 2014). Canola is the farm-gate crop in Canada while its meal after oil extraction finds limited value-added applications other than feed and fertilizer uses; thus research on canola protein gains the momentum as an alternative polymer source for adhesive preparation (Li et al., 2011; Wang et al., 2014). However, similar to other proteins, canola protein derived adhesives also suffered from weak water resistance and adhesion strength, which might limit their widespread applications (Hale, 2013; Wang et al., 2014). Therefore, improving water resistance and adhesion strength of canola protein-derived adhesives is essential to succeed as a competitive alternative over synthetic ones. Our previous study found that exfoliating nanomaterials at lower addition levels could significantly increase the adhesion strength and water resistance of canola protein; especially, graphite oxide (GO) and nano crystalline cellulose (NCC) showed superior improvement over other nanomaterials (Bandara et al., 2017). The dry, wet and soaked adhesion strength of canola protein adhesives was increased from 6.38 ± 0.84 MPa, 1.98 ± 0.22 MPa, and 5.65 ± 0.46 MPa in the pH control samples to 10.37 ± 1.63 MPa, 3.56 ± 0.57 MPa, and 7.66 ± 1.37 MPa, respectively, for the 1% NCC addition (w/w, NCC/protein), and to 8.14 ± 0.45 MPa, 3.25 ± 0.36 MPa, and 7.76 ± 0.53 MPa for the 1% GO (w/w ,GO/protein) addition (Bandara et al., 2017).

Although NCC showed greater improvement than GO, NCC is more expensive than that of GO. Furthermore, GO shows excellent exfoliation properties in aqueous and organic solvents, as well as in different polymer matrixes due to hydrophilic nature of GO (Han et al., 2016).

Previous studies on composite materials showed that the improvements in mechanical, thermal and electrical properties were directly related to the exfoliation properties of nanomaterials in polymer matrix (Kaboorani et al., 2012; Shtein et al., 2015). Therefore, it is essential to use a nanomaterial with better exfoliation properties for adhesive preparation to improve mechanical strength of the adhesive (Kaboorani et al., 2012).

First isolated in 2004, graphene consists of two dimensional sheets of carbon molecules bonded via sp^2-bonds (Verdejo et al., 2011). Pristine graphene has unique material properties such as extremely high Young's modulus (~1 TPa), fracture strength (~130 GPa), thermal conductivity (~5000 $Wm^{-1}K^{-1}$) and specific surface area (2630 m^2g^{-1}) compared to other carbon based materials (Lee et al., 2008; Park & Ruoff, 2009). Graphite oxide (GO), an intermediary product in mass scale production of graphene, possess similar material properties to graphene (Park & Ruoff, 2009). GO represents advantages over graphene, mainly due to their simplicity of production through chemical methods, hydrophilic properties, and potential to convert into graphene or graphene oxide (Park & Ruoff, 2009; Zhong et al., 2015) either by chemical (Li et al., 2008; Y. Xu et al., 2008) or thermal (González et al., 2012) reduction methods before or after exfoliating in the polymer matrix. In addition, GO can form liquid crystals (Xu & Gao, 2011a) and microscopic assembly of graphene once incorporated in polymer matrix (Xu & Gao, 2011b), which could help develop homogeneous polymer composite with improved mechanical properties (Kim et al., 2010; Verdejo et al., 2011). The presence of oxygen containing functional groups imparts GO excellent hydrophilic properties, facilitating exfoliation in a polymer matrix (Shao et al., 2012). Hydrophilic nature of GO is a vital property in preparing GO exfoliated adhesives using the solution intercalation method.

GO has been extensively explored in developing advanced nano-composites in combination with different polymers such as poly (vinyl acetate) (Liang et al., 2009; Liu et al., 2016), chitosan (Yang et al., 2010), natural rubber (Aguilar-Bolados & Lopez-Manchado, 2015), poly (methyl methacrylate) and epoxy (Shao et al., 2012; Shtein et al., 2015). However, there is scanty information available in literature on GO based adhesives, except one study found in literature regarding applicability of graphene in adhesive preparation. Khan et al (2013) reported that incorporated 3% of graphene (dissolved in tetrahydrofuran) into poly (vinyl acetate) (PVA) adhesives improved both tensile strength (from 0.3 MPa to 0.75 MPa) and shear strength (from 0.5 MPa to 2.2 MPa). However, they did not study the effect of graphene in improving water resistance of the adhesive (Khan et al., 2013). It is well known that the functionality of GO largely depends on the level of its oxidation (Han et al., 2016; Shao et al., 2012; Wang et al., 2012); therefore, there is a need to study the effect of different GO oxidation levels on adhesion strength and water resistance. We hypothesized that adding GO with different oxidation levels will change adhesion strength and water resistance of canola protein derived adhesives. The objectives of this research were to prepare GO with different oxidation levels under various oxidation time, to determine the effect of GO with different oxidation levels on adhesion properties, and to explore the mechanism of GO in adhesion improvement.

In this study, GO with different oxidation levels were prepared by oxidizing graphite at different oxidation times. Prepared GO samples were exfoliated in canola protein to produce canola protein-graphite oxide (CPA-GO) hybrid wood adhesive. The effect of oxidation time on C/O ratio, surface functional groups, interlayer spacing, and thermal properties were characterized to identify their effect on GO dispersion in protein matrix, structural and thermal changes, adhesion strength and water resistance of CPA-GO.

4.2 Materials and Methods

4.2.1 Materials and Chemicals

Canola meal was provided by Richardson Oilseed Ltd. (Lethbridge, AB, Canada). All chemicals were purchased from Fisher Scientific (Ottawa, ON, Canada) unless otherwise noted. Graphite and cellulose were purchase from Sigma-Aldrich (Sigma Chemical Co, St. Louise, MO, USA). Birch wood veneer with thickness of 0.7 mM was purchased from Windsor Plywood Co (Edmonton, AB, Canada).

4.2.2 Methods

4.2.2.1 Canola Protein Extraction

Proteins were extracted from defatted canola meal as described by Manamperi et al., (2010) with slight modifications. Meal was ground to a fine powder using a Hosokawa milling and classifying system (Hosokawa Micron Powder Systems, Summit, NJ, USA) and then passed through a 100-mesh size sieve. Ground canola meal was mixed with mili-Q water in 1:10 (w/v) ratio; pH was adjusted to 12.0 by adding 3M NaOH and stirred for 30 m (300 RPM, room temperature). The resulting dispersion was centrifuged for 15 m (10000g, 4ºC). The supernatant was collected, pH was readjusted to 4.0 by adding 3 M HCl, stirred for another 30 min, and centrifuged at the same condition above to collect protein precipitate. The precipitate was washed with deionized water, freeze-dried, and stored at -20 ºC for further use.

4.2.2.2 Graphite Oxide Preparation

Graphite oxide nanoparticles (GO) were prepared as described by Hummers & Offeman, (1958) with modification for oxidation time to produce GO with different oxidation levels. In brief, 5 g of graphite and 5 g of $NaNO_3$ were mixed in a glass beaker and 120 mL of

concentrated H_2SO_4 was slowly added while stirring in an ice bath at 200 RPM for 0.5 hr, 2 hrs, and 4 h to prepare GO-A, GO-B and GO-C samples respectively. Then, 15 g of $KMnO_4$ was slowly added to the reaction mixture while maintaining the temperature at 35 ± 3 ºC with stirring for 1 hrs. At the end of the reaction, 92 mL of deionized water was added and stirred for 15 min. Unreacted $KMnO_4$ and other leftover chemicals were neutralized by adding 80 mL of hot (60 ºC) deionized water containing 3% H_2O_2. After cooling to room temperature, samples were centrifuged (10000g, 15 min, 4 ºC) and washed with deionized water to remove any leftover chemicals. Collected GO samples were sonicated for 5 m (at 50% power output); freeze dried and stored at -20 ºC for further use.

4.2.2.3 Preparation of Canola Protein-Graphite Oxide Hybrid Wood Adhesive (CPA-GO)

GO with different C/O ratios was exfoliated in canola protein matrix according to our previously reported method (Bandara et al., 2017). In brief, 3 g of canola protein was mixed with 20 mL of deionized water (15% w/v solution) and stirred for 6 h (300 rpm) at room temperature to disperse canola proteins; and then the pH was adjusted to 5.0 using 1 M HCl solution. GO samples (GO-A, GO-B and GO-C) were separately dispersed in 10 mL of deionized water (equivalent to a final GO/protein ratio of 1%, w/w, GO/protein) by stirring (300 rpm) 5 h at room temperature and another 1 h at 45 ± 3 ºC, sonicated for 3 m by providing intermittent pulse dispersion of 5 s (at 3 s intervals and 60% amplitude) using medium size tapered tip attached to a high intensity ultrasonic dismembrator (Model 500, Thermo Fisher Scientific INC, Pittsburg, PA, USA), and then homogenized for 2 m (2000 rpm) using ULTRA TURRAX high shear homogenizer (Model T25 D S1, IKA® Works, Wilmington, NC, USA). The prepared GO dispersions were slowly added to the protein dispersions dropwise while stirring for 15 m (300 rpm) to have a final protein concentration of 10% (w/v) in the adhesive mixture. The resulting

adhesive mixtures were sonicated and homogenized as above and the pH of the adhesive was adjusted to 12.0 by adding 6 M NaOH solution. Negative control was prepared by dispersing canola protein (10% w/v) in deionized water and use as is while pH control was prepared by adjusting the pH of canola protein dispersions (10% w/v) to 12.0 similar to GO dispersed samples, without adding GO.

4.2.2.4 Adhesion Strength Measurement

Hardwood veneer samples (Birch, 1.2 mm thickness) were cut into a dimension of 20 mm × 120 mm (width and length) using a cutting device (Adhesive Evaluation Systems, Corvallis, OR, USA). Veneer samples were conditioned for seven days at 23 ºC and 50% humidity in a controlled environment chamber (ETS 5518, Glenside, PA, USA) according to the specifications of ASTM D2339-98 (2011) standard method (ASTM, 2011). CPA-GO hybrid adhesives were spread at an amount of 40 uL/veneer strand in a contact area of 20 mm × 5 mm using a micropipette. Veneer samples were air dried for 5 m and hot pressed for 10 m (at 120 ºC and 3.5 MPa) using Carver manual hot press (Model 3851-0, Carver Inc., In, USA). Dry adhesion strength (DAS) was measured according to the ASTM standard method D2339-98 (2011) by measuring tensile loading required to pull bonded veneer using Instron machine (Model 5565, Instron, MA, USA) equipped with 5 kN load cell. Tensile strength data was collected using Bluhill 3.0 software (Instron, MA, USA). Wet adhesion strength (WAS) and soaked adhesion strength (SAS) was measured according to the ASTM standard method D1151-00 (2013) (ASTM, 2013) using instron tensile loading. WAS values were measured after submerging bonded veneer samples for 48 h in water (23 ºC) where SAS was measured after reconditioning submerged veneer samples for seven days at 23 ºC and 50% relative humidity in a controlled environment chamber (ETS 5518, Glenside, PA, USA). Minimum of four bonded veneer

samples per formulation were used in testing strength (DAS, WAS, SAS). All samples were clamped to Instron with a 35 mm gauge length and tested at 10 mm/min cross head speed.

4.2.2.5 X-ray Photoelectron Spectroscopy (XPS)

GO samples were characterized using X-ray photoelectron spectroscopy (XPS) for their elemental composition, carbon/oxygen (C/O) ratio and changes in the functional groups according to their oxidation time. Samples were analyzed using monochromatic Al K α radiation (1486.6 eV) generated from Kratos Axis 165 X-ray spectrometer (Kratos Analytical Ltd. UK). Resulting spectra's were analyzed by CasaXPS software V2.3.16 PR 1.6 (Casa Software Ltd) for elemental composition and C/O ratio. Binding energy of neutral carbon C1s spectra was adjusted to 284.5 eV as a reference. Oxidation time dependent changes in surface functional groups were characterized by curve fitting of high-resolution C1s spectra assuming a Shirley background and 70%/30% Gaussian/Lorentzian distribution shape. Four peaks were fitted for all other GO samples while five peaks were used in GO-A sample with a lower oxidation time.

4.2.2.6 X-ray Diffraction (XRD)

X-ray diffraction (XRD) of GO and CPA-GO samples were performed using Rigaku Ultima IV powder diffractometer (Rigaku Co. Japan). Cu-Kα radiation (0.154 nm) was used to collect angle data (2Θ) from 5 to 50 degrees. Interlayer spacing of graphite oxide was calculated using Bragg's equation (Bragg & Bragg, 1913); $\sin \theta = n\lambda/2d$ where, λ, d and θ represent wavelength of the radiation, spacing between diffraction lattice (interlayer space), and glancing angle (measured diffraction angle) respectively (Alexandre & Dubois, 2000; Kaboorani & Riedl, 2011). XRD data was analyzed using Origin 2016 software (OriginLab Corporation, MA, USA) to identify effect of oxidation time on exfoliation of GO.

4.2.2.7 Differential Scanning Calorimetry (DSC)

Thermal transitions of GO and CPA-GO adhesives were studied using differential scanning calorimeter (Perkin-Elmer, Norwalk, CT, USA). DSC instrument was calibrated for temperature and heat flow using a pure indium reference sample. Sample moisture was first removed by freeze-drying followed by drying with P_2O_5 for two weeks in a hermetically sealed desiccator. GO and hybrid adhesive samples were accurately weighed into T-Zero hermetic aluminum pans (~6 mg each), mixed with 60 µL of 0.01 M phosphate buffer, and hermetically sealed with lids. Heat flow differential of samples were recorded against the empty reference pan under continuous nitrogen purging. All samples were equilibrated at 0 ºC for 10 m and thermodynamic data was collected while heating from 0 to 250 ºC at a ramping rate of 10 ºC min^{-1}. Data was analyzed using Universal Analysis 2000 software for thermal transition changes in adhesives and GO samples (Perkin-Elmer, Norwalk, CT, USA).

4.2.2.8 Fourier Transform Infrared Spectroscopy (FTIR)

Effect of oxidation time on GO functional groups and GO induced protein secondary structural changes in adhesive samples were characterized using Nicolet 8700 Fourier transform infrared spectrometer (Thermo Eletron Co. WI, USA). Sample moisture was removed prior to FTIR analysis by freeze-drying and further drying with P_2O_5 in a hermetic desiccator for two weeks. Samples were mixed with potassium bromide (KBr), milled into a powdered pellet prior to FTIR analysis. IR spectra were collected in 400-4000 cm^{-1} range using 128 scans at a resolution of 4 cm^{-1}. Collected data was analyzed using Origin 2016 software (OriginLab Corporation, MA, USA) to identify changes in functional groups. Second derivative spectra were generated using Savitzky-Golay smooth function (7 points window) and used for curve fitting to identify GO induced protein structural changes.

4.2.2.9 Transmission Electron Microscopy (TEM)

Effect of GO samples on exfoliation in canola protein matrix were characterized using transmission electron microscopy (TEM). Images were collected using Philips/FPI transmission electron microscope (Model Morgagni, FEI Co, OR, USA) coupled with Getan digital camera (Getan Inc, CA, USA). Adhesive samples were diluted to 100 fold with ethanol, and a single drop was casted onto 200 mesh holey copper grid covered with carbon film. After 30 seconds of air-drying, the remaining liquid was removed and copper grid was used for collecting TEM images.

4.2.3 Statistical Analysis

Adhesion strength data (DAS, WAS, and SAS) was analyzed using analysis of variance (ANOVA) followed by Duncan's Multiple Range (DMR) test to identify the effects of graphite oxidation time on adhesion strength. Collected data was processed using Statistical Analysis System Software (SAS version 9.4, SAS Institute, Cary, NC). Effects of different GO samples on adhesion strength were evaluated at the 95% confidence level.

4.3 Results and Discussion

The functionality of GO depends largely on the methods of preparation and conditions used in the process such as oxidation time and amount of oxidizer (Shao et al., 2012; Wang et al., 2012). In composite research, tailoring conditions of GO preparation have proven to change material properties such as flexural strength and conductivity (Wang et al., 2012). However, to best of our knowledge, there were no previous reports in the literature regarding the effect of GO on adhesives derived from biobased polymers/protein based polymers.

4.3.1 Adhesion Strength of Canola Protein-GO Hybrid Adhesives

Adhesives failure can happen in two occasions, either adhesively at adhesive-wood interface or cohesively within bulk adhesive material (Khan et al., 2013). Since amorphous polymer generally has a limited mechanical strength (Khan et al., 2013), cohesive failure is more prominent in biobased adhesives. The effects of adding GO on adhesion strength of canola protein are shown in Fig 4.1.

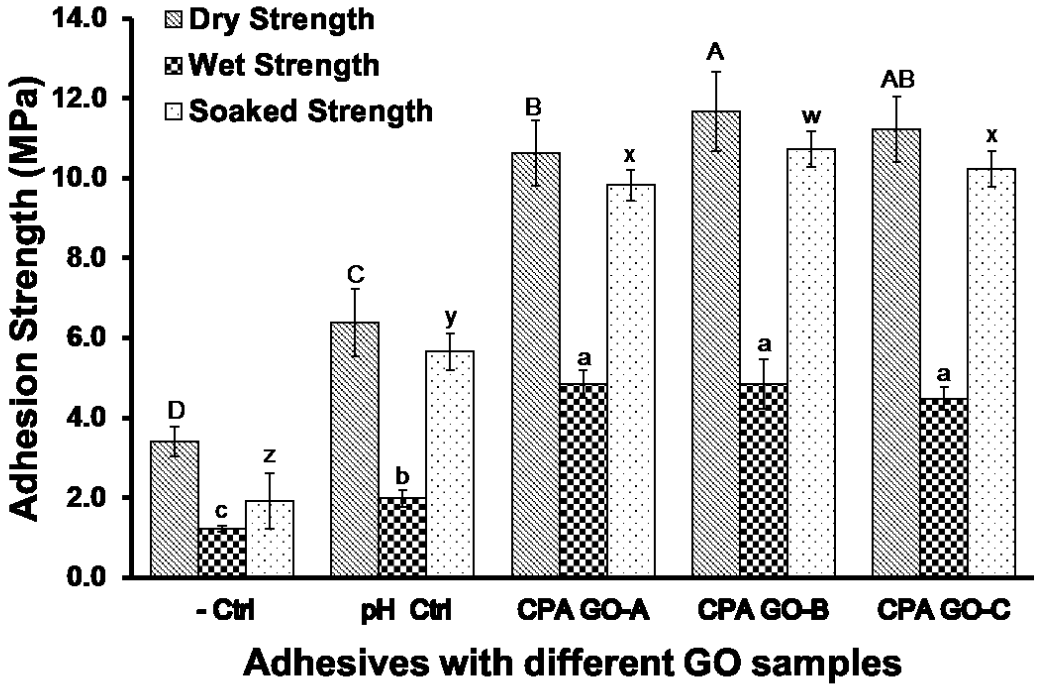

Figure 4.1. Adhesion strength of canola protein-graphite oxide hybrid wood adhesives prepared by exfoliating 1% (w/w GO:canola protein) GO prepared at various oxidation times (0.5 h – CPA GO-A, 2 h – CPA GO-B, 4 h – CPA GO-C). Adhesion data was analyzed using one-way ANOVA followed by Duncan test for mean separation. Different letters on the bar represent significantly different adhesion strength ($p < 0.05$). Error bars represent standard deviations. All adhesive samples were prepared in triplicate ($n=3$) and minimum 5 wood samples per replicate were used for each strength measurement.

All GO samples used in this study significantly increased ($p < 0.05$) the adhesion strength and water resistance compared to the negative control and the pH control samples. GO prepared at 05, 2, and 4 h of oxidation showed a dry adhesion strength of 10.63 ± 0.81, 11.67 ± 1.00, and 11.22 ± 0.82 MPa, respectively. Increasing oxidation time reduced the C/O ratio of GO samples, but showed an increasing trend in dry adhesion strength. Similar trend was also observed in soaked strength, where the highest strength of 10.73 ± 0.45 MPa was observed in GO-B (2 h of oxidation) followed by GO-C and GO-A samples (10.22 ± 0.45, 9.82 ± 0.38 MPa respectively). The wet adhesion was significantly increased from 1.98 ± 0.22 MPa in the pH control sample to 4.85 ± 0.35, 4.85 ± 0.61 and 4.48 ± 0.28 MPa for GO-A, GO-B and GO-C samples respectively, but did not differ among different oxidation times.

Protein contains both hydrophilic and hydrophobic residues which makes it an excellent amphiphilic biopolymer with well-known adhesiveness to various solid surfaces (Liu et al., 2010). Liu et al (2010) studied the interactions of GO with bovine serum albumin (BSA) and suggested that conjugated GO-protein complex can act as an adhesive matrix to interact with other solid materials. Studies on PVA polymer composites showed improved interactions and mechanical strength after exfoliating graphene oxide at low concentrations (Khan et al., 2013; Zhao et al., 2010). Therefore, GO induced cohesive (protein-protein) and adhesive (protein-wood surface) interactions might be the main contributor in increased adhesion and water resistance observed in this study. Conversion of GO into more hydrophobic and stable reduced graphene oxide (rGO) might be another reason for improved water resistance. Several authors reported thermal (Héctor Aguilar-Bolados et al., 2016) or protein aided reduction (Liu et al., 2010) of GO into rGO in composite research, which improved the mechanical properties. Adhesive curing at

elevated temperature, and the presence of canola protein might trigger the reduction of GO into rGO, thereby improve water resistance of the CPA-GO adhesive.

In comparison, canola protein modified with sodium bisulfite showed dry, wet and soaked adhesion strength of 5.28 ± 0.47, 4.07 ± 0.16, and 5.43 ± 0.28 MPa, respectively (Li et al., 2011). In another study, modifying canola protein with 0.5% sodium dodecyl sulphate (SDS) had dry, wet and soaked adhesion of 6.00 ± 0.69, 3.52 ± 0.48, and 6.66 ± 0.07 MPa, respectively (Li et al., 2012). Grafting poly(glycidyl methacrylate) in canola protein was reported to improve the dry, wet and soaked adhesion to 8.25± 0.12, 3.80 ± 0.15, and 7.10 ± 0.10 MPa, respectively (Wang et al., 2014). Canola protein adhesives prepared with GO as developed in this study substantially improved both adhesion strength and water resistance.

4.3.2 Changes in Elemental Composition, and Surface Functional Groups of GO and Their Effect on Adhesion

GO with variable elemental composition, C/O ratio and functional groups were previously developed via manipulating oxidation conditions (Han et al., 2016; Jeong et al., 2009; Shao et al., 2012). In this study, we prepared GO with variable properties by changing oxidation time while maintaining other conditions constant. Oxidation conditions used in this study, elemental composition and C/O ratio of prepared GO samples are shown in Table 4.1. Native graphite mainly consists of carbon and oxygen at percentages of 97.65% and 2.35%, respectively, according to the XPS data (*Appendix 2: supplementary Fig 4.1*). Graphite showed a C/O ratio of 41.55 while oxidizing graphite for 0.5, 2 and 4 h reduced C/O ratio to 2.06, 1.40 and 1.49, respectively. In addition, GO also contains small amount of sulfur (~2%) and trace amounts of sodium, and manganese, as the residuals from GO processing.

Table 4.1. – Conditions used for oxidation of graphite and their effect on C/O ratio and elemental composition of prepared GO samples

Sample	Oxidation time	Oxidizer Amount ($NaNO_3$)	C %	O%	S%	C/O ratio
Graphite	-	-	97.65	2.35	-	41.55
GO-A	0.5 hrs	5 g	65.60	31.85	2.54	2.06
GO-B	2 hrs	5 g	57.37	40.81	1.81	1.40
GO-C	4 hrs	5 g	57.06	38.20	2.32	1.49

The presence of oxygen containing functional groups was confirmed by analyzing XPS high-resolution C1s spectra of graphite and GO samples. The original high-resolution C1s spectra and fitted peaks are shown in Fig 4.2. XPS data processing for C1s spectra of graphite only showed a major peak centered at 284.5 eV which is attributed to sp^2 hybridized carbon, derived from C=C and C-C bonds with delocalized π electrons (Jeong et al., 2009; Wang et al., 2012). The other small peak at a binding energy of 285.3 eV resembles to sp^3 carbon hybridization (Jackson & Nuzzo, 1995), which attributed to oxidation of graphite in the presence of atmospheric oxygen (Hontoria-Lucas et al., 1995)

GO-A sample shows four new peaks at binding energies around 285.5-288.5 eV, representing oxygen functional groups in addition to the characteristic sp^2 peak at 284.5 eV. Shift of binding energies from 284.5 eV to 285.4 eV, 286.5 eV, 287.2 eV, and 288.5 eV are attributed to the occurrence of carbon sp^3, C–OH, C–O–C, and C=O functional groups respectively. Previous studies reported similar binding energy shift in GO (Schniepp et al., 2006; Shin et al., 2009; Tien et al., 2011).

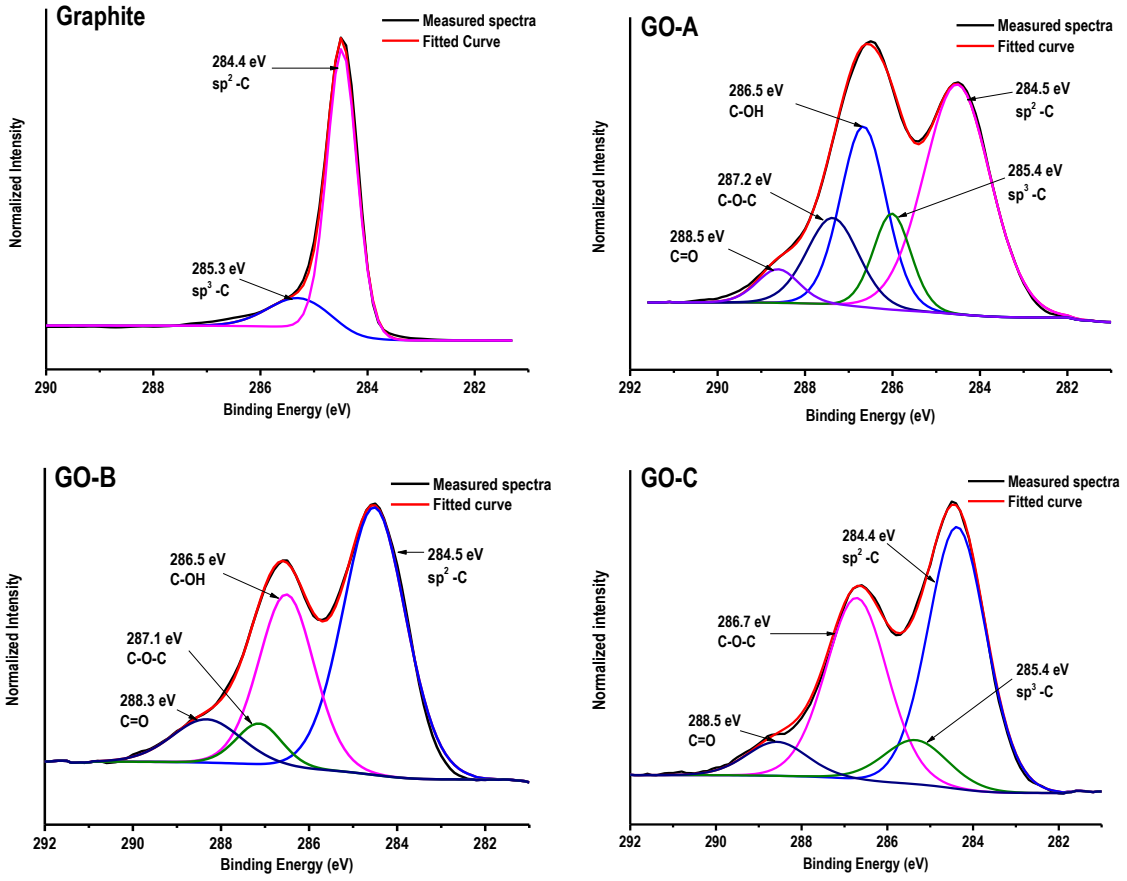

Figure 4.2. High-resolution carbon C 1s scans of graphite and GO prepared with different oxidation times (Graphite – Without oxidation, GO-A – 0.5 hrs, GO-B – 2 hrs, and GO-C – 4 h oxidation) obtained from X-ray photoelectron spectroscopy, and peak fitting showing oxidation time dependent changes in surface functional groups after graphite oxidation.

Increasing oxidation time to 2 h (GO-B sample) further changed the composition of surface functional groups. Peak corresponding to the carbon sp^3 was disappeared while the relative proportion of C–OH and C=O peaks (286.5 eV and 288.3 eV respectively) increased. Furthermore, C–O–C peak appeared at the binding energy of 287.1 eV. Wang et al. (2012) also reported an increased proportion of C=O and C–OH groups at higher oxidation conditions in graphite oxide (Wang et al., 2012). Further oxidation of graphite up to 4 h in GO-C increased the

relative proportion of carbon sp^2, C–O–C, and C=O groups, at the expense of C-OH groups; interestingly, the carbon sp^3 peak re-appeared at 285.4 eV binding energy. Degradation of oxygen functional groups in prolonged oxidation might be the reason for sp^3 hybridization observed in GO-C sample (Jeong et al., 2009).

FTIR spectra of GO samples prepared under different oxidation times are shown in Fig 4.3. FTIR peaks were assigned to respective functional groups according to the previous data reported in the literature.

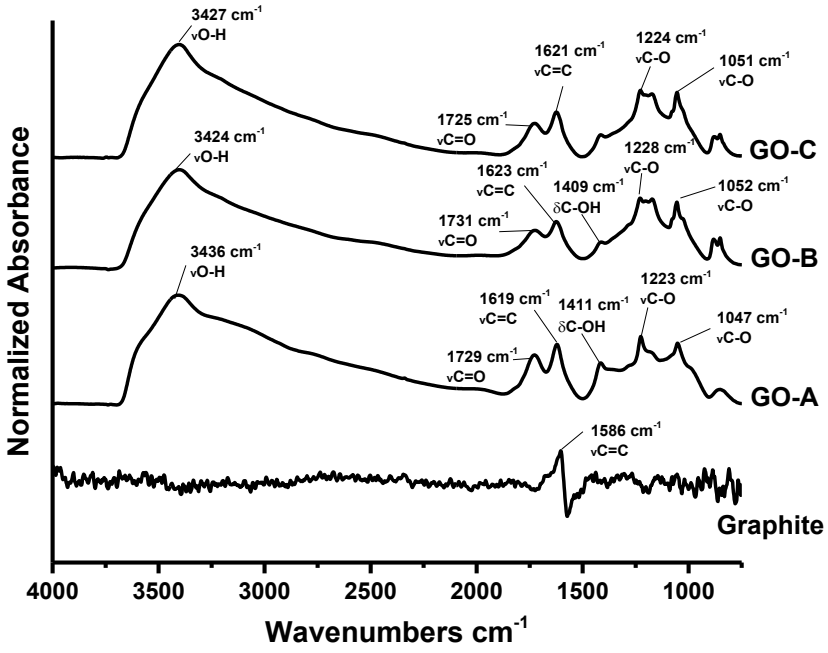

Figure 4.3. – FTIR spectra of graphite and GO (graphite – Without oxidation, GO-A – 0.5 hrs, GO-B – 2 hrs, and GO-C – 4 h oxidation) samples prepared with variable oxidation times showing oxidation dependent changes in GO functional groups.

In graphite, the peak appearing at 1586 cm^{-1} generally represents the stretching vibration of C=C bond (νC=C) (Hontoria-Lucas et al., 1995; Paredes et al., 2008; Posudievsky & Khazieieva, 2012). However; after oxidation, the C=C stretching vibrations shifted to 1619 cm^{-1}, 1623 cm^{-1},

and 1621 cm^{-1} wavelengths for GO-A, GO-B and GO-C respectively. Chen et al., (2010 and Stankovich et al., (2006) also reported similar peak shifts in the range of 1618 cm^{-1} - 1626 cm^{-1} probably due to the oxygen functional groups present in GO. The absorption peaks of GO samples at 3424 cm^{-1}-3436 cm^{-1} are attributed to the stretching vibration of –OH groups (νO–H) either from –OH groups of absorbed water or –OH groups formed during the oxidation (Hontoria-Lucas et al., 1995; Lee & Park, 2014; Stankovich et al., 2006).

Following oxidation, the presence of new peaks at 1729 cm^{-1}, 1731 cm^{-1}, and 1725 cm^{-1} wavelengths respectively in GO-A, GO-B, and GO-C samples was observed; probably due to the formation of oxygen containing functional groups, causing the C=O stretching vibrations (νC=O) (Chen et al., 2010; Stankovich et al., 2006; Wang et al., 2012). The intensity of νC=O in GO samples was increasing at increasing oxidation level. Wang et al (2012) also reported similar trend at increasing oxidation levels (Wang et al., 2012). Higher degree of oxidation and oxidation induced cracks in GO edges were reported as the main reasons for increased intensity of νC=O (Li et al., 2009; Wang et al., 2012; Yuge et al., 2008). C-OH bending vibration (δC-OH) peaks were observed in both GO-A and GO-B samples at 1411 cm^{-1} and 1423 cm^{-1} respectively, however the intensity was reduced in GO-C. Vibrations from either alcohols or carboxylic groups of GO were reported as the main contributors to δC-OH (Paredes et al., 2008; Posudievsky & Khazieieva, 2012). The peaks appeared at 1220 cm^{-1} – 1230 cm^{-1} range were usually assigned to C–O stretching vibrations (νC–O) (Hontoria-Lucas et al., 1995; Paredes et al., 2008; Posudievsky & Khazieieva, 2012; Stankovich et al., 2006), which attributed to carboxylic acid groups (Wang et al., 2012), hydroxyl groups (Paredes et al., 2008; Stankovich et al., 2006), or epoxy groups (Posudievsky & Khazieieva, 2012; Zhou et al., 2011) present in GO.

The formation of various oxygen containing functional groups in GO might be responsible for the improved adhesion strength. For example, –OH groups in GO might increase –H bonding between adhesive matrix and wood surface; the epoxy groups (C–O–C) in GO can either homopolymerize with another epoxy group in GO, or react with functional groups such as –OH, –COOH on the wood surface, and $–NH_2$, –SH in canola protein (Tanaka & Kakiuchi, 1964), thus improving both adhesive and cohesive strength.

4.3.3 Effect of Different GO Samples on Protein Structural Changes

Effect of different GO samples on secondary structure of canola protein was studied by creating second derivative of FTIR spectra followed by peak fitting of Amide I peak (Barth, 2007; Kong & Yu, 2007). GO induced protein secondary structural changes are shown in Fig 4.4. Exfoliating GO in canola protein has increased the relative proportions of unordered structures (1639-1642 cm^{-1} wavelength) and turn structures (at wavelength range of 1694-1697 cm^{-1}) at the expense of β-sheets in the wavelengths of 1625 cm^{-1}, 1636 $cm^{-1}$and 1673-1675 cm^{-1} (Barth, 2007; Kong & Yu, 2007).

In comparison, GO-B and GO-C samples showed the highest relative proportions of unordered structures and turn structures, compared to the pH control and GO-A samples (*Appendix 2: supplementary Fig 4.2*). The results observed in protein structural changes were compliment to the changes in adhesion strength of CPA-GO prepared with different GO samples. Increase in unordered structures will exposes more hydrophobic functional groups buried inside protein molecules which increase the hydrophobic interactions with wood surface (Zhang et al., 2014), thereby increase the water resistance and adhesion strength.

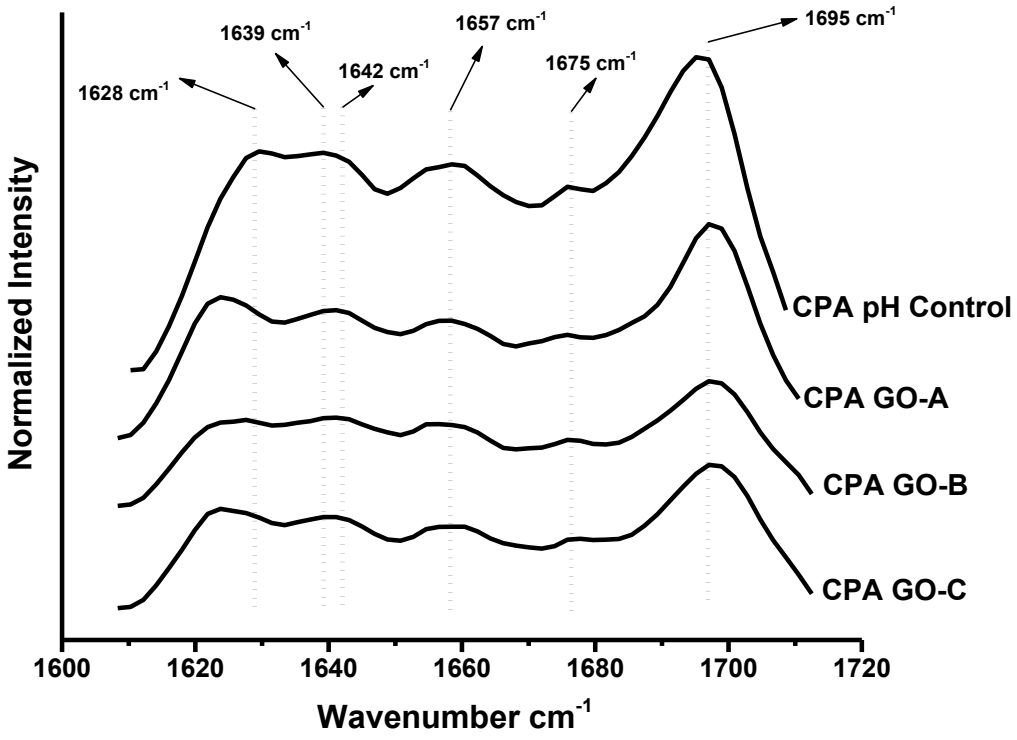

Figure 4.4. – FTIR second derivative spectra showing changes in protein secondary structure of CPA-GO adhesives prepared by exfoliating GO (1% w/w GO:canola protein) with different oxidation levels. CPA pH Control – 10% w/v canola protein adhesive at pH 12.0; CPA GO-A – 10% w/v canola protein adhesive with 1% w/w (GO/protein) GO-A, CPA GO-B – 10% w/v canola protein adhesive with 1% w/w (GO/protein) GO-B, and CPA GO-C – 10% w/v canola protein adhesive with 1% w/w (GO/protein) GO-C

4.3.4 Changes in GO Crystallinity and Their Effect on GO Dispersion in Protein Matrix

The effect of oxidation time on glancing angle (2θ) and interlayer spacing (*d*) of GO samples are shown in Fig 4.5. X-ray diffraction of graphite showed one major crystalline peak at a glancing angle of 26.28º with *d* spacing of 0.338 nm. Shao et al. (2012) also reported a similar peak for graphite at a glancing angle of 26.54º and *d* spacing of 0.334 nm (Shao et al., 2012).

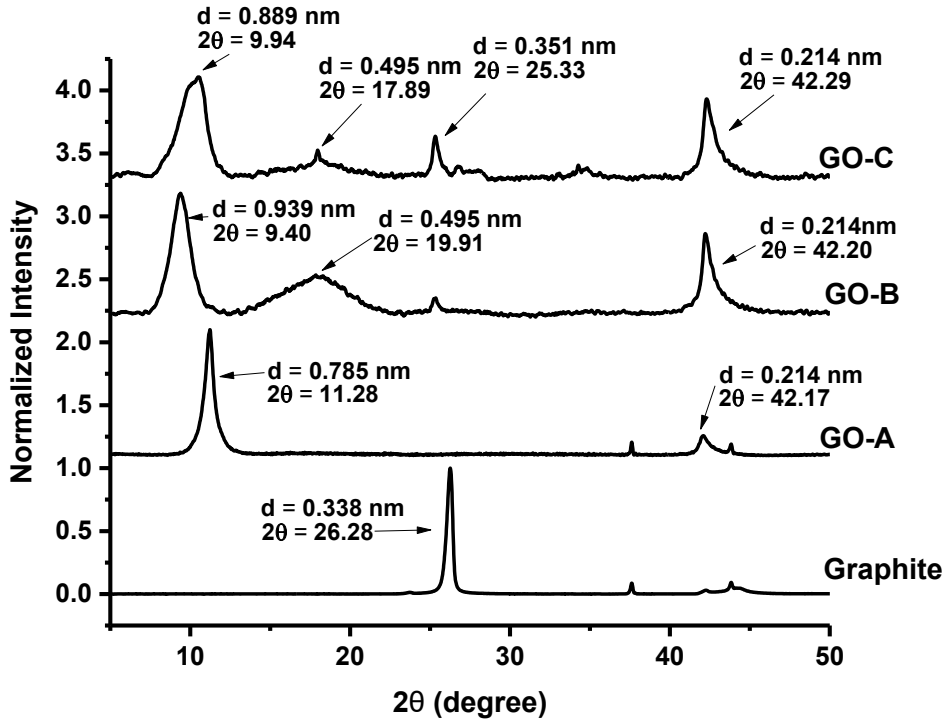

Figure 4.5. – X-ray diffraction patterns, changes in glancing angle and interlayer spacing (calculated according to the Bragg's equation : Sin θ = nλ/2d) of graphite and graphite oxide samples prepared with different oxidation times.

After oxidation, the graphite crystalline peak was disappeared in GO-A (0.5 h) but two new peaks appeared at different glancing angles: the first major peak was appeared at glancing angle of 11.28° with *d* spacing of 0.785 nm while another minor peak was observed at glancing angle of 42.17° with *d* spacing of 0.214 nm. Shao et al. (2012) also reported the disappearance of the characteristic graphitic peak after oxidation and the formation of a new peak at a glancing angle of 11.3° with increased interlayer spacing of 0.80 nm (Shao et al., 2012). Increasing graphite oxidation time from 0.5 h to 2 h significantly changed the crystallinity and *d* spacing of GO-B sample. Glancing angle of the characteristic GO peak has shifted from 11.28° to 9.40° while *d* spacing increased from 0.785 nm to 0.939 nm (for GO-A and GO-B respectively).

Similar to GO-A, GO-B sample showed another peak at a glancing angle of 42.20° (d = 0.214 nm), and a new crystalline peak at 19.91° (d = 0.495 nm). Further increasing oxidation time to 4 h slightly shifted the glancing angle towards 9.94° while decreased d spacing to 0.889 nm. The reduction in interlayer spacing has been previously reported due to the decomposition of oxygen containing functional groups in GO samples at prolonged oxidation (Jeong et al., 2009; Mcallister et al., 2007). In GO-C, another two peaks were visible at glancing angles of 42.29°, and 17.89° with d spacing of 0.214 nm and 0.495 nm respectively. In addition, the new peak at a glancing angle of 25.33° (d = 0.351 nm) in GO-C showed similarity to the characteristic graphite peak appeared in un-oxidized graphite. The re-appearance of graphite like crystalline peak at higher oxidation level indicate the decomposition of oxygen containing functional groups, re-forming carbon sp^2 bonds and reduction in crystallinity of GO-C samples (Jeong et al., 2009; Mcallister et al., 2007).

Proper exfoliation of GO in polymer matrix is one of the major factors affecting the improvement of adhesion strength and water resistance. Aggregation of nanomaterial upon mixing with protein will not improve adhesion strength (Kaboorani et al., 2012; Kaboorani & Riedl, 2011); therefore it is important to produce GO with appropriate exfoliation properties. All three GO samples prepared in this study exhibit improved exfoliation in canola protein matrix. X-ray diffraction patterns of GO samples and their dispersion in canola protein are shown in Fig 4.6. Two common crystalline peaks were appeared in all three GO samples with diffraction angles (2θ value) around ~9-11° and ~42° and one additional crystalline peak was found at ~25° diffraction angle for GO-C. The disappearance of crystalline peaks after exfoliation of GO in canola protein clearly indicated the uniform exfoliation of GO within protein matrix.

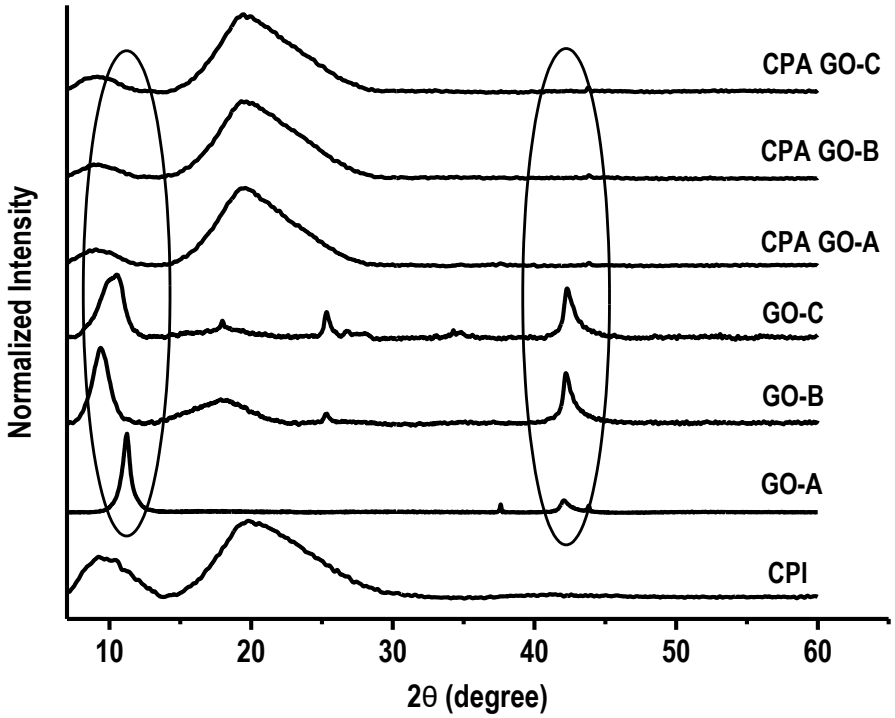

Figure 4.6. – X-ray diffraction data showing the crystallinity of prepared graphite oxide samples under different oxidation time, and exfoliation properties of GO in canola protein matrix after adhesive preparation. CPI – Canola protein isolate, GO-A, GO-B and GO-C – starting graphite oxide samples prepared by oxidizing graphite for 0.5 h, 2 h, and 4 h respectively. CPA GO-A, CPA GO-B and CPA GO-C are prepared by exfoliating 1% w/w (GO/protein) GO-A, GO-B and GO-C respectively in 10% w/v canola protein dispersion.

As shown in TEM images of exfoliated GO samples (Fig 4.7), the appearance of single GO sheets in both CPA GO-A and CPA GO-B adhesive samples further supported the uniform exfoliation of GO in canola protein matrix. However, a slight aggregation of GO was visible in CPA GO-C. Addition of hydrophilic functional groups during graphite oxidation is the major reason for increased interlayer spacing of GO (Jeong et al., 2009). It was reported that increased interlayer space reduces binding energies of GO, which would facilitate the exfoliation of GO

layers in the matrix (Yoon et al., 2015). Therefore, the uniform exfoliation of GO observed in this study, in particular for GO-B might be due to reduced binding energy resultant from increased interlayer spacing. Ultimately, proper exfoliation of GO will help in improving both adhesion strength and water resistance of the CPA-GO adhesive.

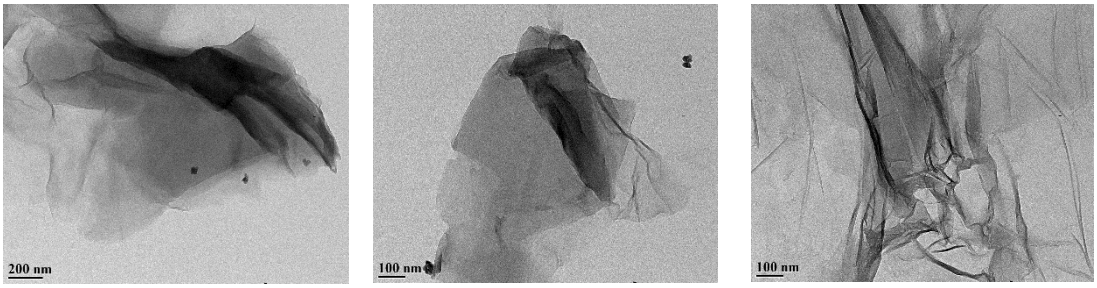

CPA GO-A **CPA GO-B** **CPA GO-C**

Figure 4.7. – Transmission electron microscopic (TEM) images of exfoliated graphite oxide samples prepared under different oxidation time in canola protein matrix. CPA GO-A, CPA GO-B and CPA GO-C are prepared by exfoliating 1% w/w (GO/protein) GO-A, GO-B and GO-C respectively in 10% w/v canola protein dispersion.

4.3.5 Change in Thermal Properties of Graphite Oxide and Effect on Thermal Stability of Prepared Adhesive

Effect of graphite oxidation time on GO thermal transitions is shown in Fig 4.8. An exothermic transition was observed in all GO samples, but with different enthalpy requirement and temperature range. In GO-A (0.5 h) exothermic transition was observed at extrapolated onset and peak temperatures of 159.7 ºC 190.0 ºC respectively with 1.57 KJ/g ΔH.

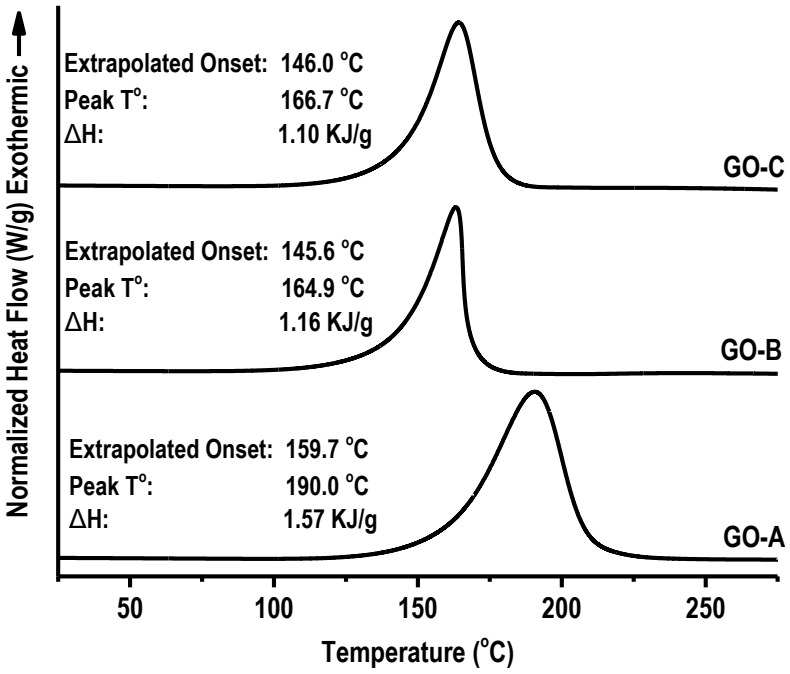

Figure 4.8. – Changes in thermal properties of different graphite oxide samples prepared under different oxidation times (0.5 h – GO-A; 2 h – GO-B; 4 h – GO-C).

Increasing oxidation time to 2 h (GO-B) has changed the thermal transition to 145.6 ºC, 164.9 ºC and 1.16 KJ/g for extrapolated onset, peak temperature and ΔH respectively. Increasing oxidation time to 4 h (GO-C) shifted extrapolated onset and peak temperatures to 146.0 ºC and 166.7 Cº respectively where ΔH changed to 1.10 KJ/g. The reduction in ΔH and transition temperatures is a result of increased amount of oxygen containing functional groups. Schniepp et al., (2006) also reported similar changes in thermal transitions around ~200 ºC in graphite oxide and attributed them to decomposition of oxygen containing functional groups. They have further analyzed the outlet gas generated from DSC, and showed that major products as CO_2 and H_2O that were generated during decomposition of oxygen containing functional groups (Schniepp et al., 2006).

Table 4.2. – Effect GO exfoliation on thermal transitions (Mean + standard deviation; *n=4*) of canola protein-GO hybrid wood adhesives (CPA GO). CPA GO-A, CPA GO-B and CPA GO-C are prepared by exfoliating 1% w/w (GO/protein) GO-A, GO-B and GO-C respectively in 10% w/v canola protein dispersion.

Adhesive Sample	**Onset T^o (^{o}C)**	**Midpoint T^o (^{o}C)**	**Specific heat (J/g.C)**
Canola Protein (-Control)	72.31 ± 1.86	89.43 ± 0.23	0.449 ± 0.07
Canola Protein (+ Control)	85.14 ± 0.79	99.81 ± 2.01	1.202 ± 0.01
CPA GO-A	88.26 ± 1.67	105.64 ± 1.27	0.979 ± 0.13
CPA GO-B	83.44 ± 0.99	102.48 ± 1.83	1.260 ± 0.06
CPA GO-C	80.13 ± 1.94	99.25 ± 068	1.199 ± 0.10

Effect of different GO samples on thermal transitions of CPA-GO are shown in Table 4.2. Adding GO into canola protein increased both onset and peak temperatures, as well as the specific heat in transitions. The increased thermal stability is an essential property for adhesive application, as it required to process under higher temperature for adhesive curing (Khan et al., 2013). Adding nanomaterials, especially graphene oxide, have been proven to increase thermal stability of protein in previous studies mainly due to improved protein-protein/protein-GO interactions, and inherent thermal properties of GO. Linse et al., (2007) also reported an increased thermal stability and denaturation temperatures of soybean peroxidase enzyme conjugated with graphene oxide nanosheets. Addition of GO into canola protein increased the thermal stability of all CPA-GO samples compared to control samples, which can be related with

the increased protein-protein/protein-GO interactions. CPA GO-A showed slightly higher onset and peak temperatures than that of CPA GO-B and CPA GO-C which can be a result of GO induced protein structural changes. Increased unordered structures were observed after adding GO-B and GO-C, at the expense of β-sheets and α-helix which can potentially reduce the thermal stability compared to GO-A.

4.4 Conclusions

GO samples with various C/O ratio and surface functional groups were prepared at different oxidation time. Oxidation of graphite for 0.5, 2 and 4 h reduced the C/O ratio of graphite from 41.55 to 2.06, 1.40, and 1.49, respectively. The relative proportion of C-OH and C=O groups as well as interlayer spacing of GO were increased at increasing oxidation time from 0.5 h to 2 h whereas both C-OH content and interlayer spacing were reduced at 4 h of oxidation. GO prepared with different oxidation times improved both adhesion strength and water resistance in all three GO samples; the dry, wet and soaked strength was increased from 6.38 ± 0.84 MPa, 1.98 ± 0.22 MPa, 5.65 ± 0.46 MPa in the pH control sample to 11.67 ± 1.00 MPa, 4.85 ± 0.61 MPa, and 10.73 ± 0.45 MPa, respectively for GO-B added adhesive. The improved adhesive and water resistance in GO added canola adhesive was due to increased interlayer spacing, improved exfoliation properties, and increased adhesive and cohesive interactions (protein-protein, protein-GO and adhesive-wood surface), hydrophobic interactions and thermal stability. Graphite oxide, instead of graphene, as we proposed for the first time in the study, is easier to process and more cost-effective in preparing protein based wood adhesives.

4.5 References

Aguilar-Bolados, H., & Lopez-Manchado, M. (**2015**). Effect of the morphology of thermally reduced graphite oxide on the mechanical and electrical properties of natural rubber nanocomposites. *Composites Part B:*, ***87***, 350–356.

Aguilar-Bolados, H., Lopez-Manchado, M. A., Brasero, J., Avilés, F., & Yazdani-Pedram, M. (**2016**). Effect of the morphology of thermally reduced graphite oxide on the mechanical and electrical properties of natural rubber nanocomposites. *Composites Part B: Engineering*, ***87***, 350–356.

Alexandre, M., & Dubois, P. (**2000**). Polymer-layered silicate nanocomposites: preparation, properties and uses of a new class of materials. *Materials Science and Engineering: R: Reports*, ***28***(***1***–***2***), 1–63.

ASTM. (**2011**). D2339-98(2011) Standard test method for strength properties of adhesives in two-ply wood construction in shear by tension loading. *Annual Book of ASTM Standards.* Available at: http://compass.astm.org/EDIT/html_annot.cgi?D2339+98%5C [2012/12/04]

ASTM. (**2013**). D1151-00(2013) Standard practice for effect of moisture and temperature on adhesive bonds. *Annual Book of ASTM Standards.* Available at: http://compass.astm.org/EDIT/html_annot.cgi?D1151 +00%5C [2013/02/03]

Bandara, N., Esparza, Y., & Wu, J. (**2017**). Exfoliating nanomaterials in canola protein derived adhesive improves strength and water resistance. *RSC Advances*, ***7(11)***, 6743-6752.

Barth, A. (**2007**). Infrared spectroscopy of proteins. *Biochimica et Biophysica Acta*, ***1767***(***9***),

1073–1101.

Bragg, W., & Bragg, W. (**1913**). The reflection of X-rays by crystals. *Proceedings of the Royal Society of London - Series A*, ***88***(***605***), 428–438.

Chen, W., Yan, L., & Bangal, P. (**2010**). Preparation of graphene by the rapid and mild thermal reduction of graphene oxide induced by microwaves. *Carbon*, ***48***(***4***), 1146–1152.

González, Z., Botas, C., Álvarez, P., Roldán, S., Blanco, C., Santamaría, R., Menéndez, R. (**2012**). Thermally reduced graphite oxide as positive electrode in vanadium redox flow batteries. *Carbon*, ***50***(***3***), 828–834.

Hale, K. (**2013**). *The potential of canola protein for bio-based wood adhesives*. (Master's dissertation). Kansas State University.

Han, C., Zhang, N., & Xu, Y.-J. (**2016**). Structural diversity of graphene materials and their multifarious roles in heterogeneous photocatalysis. *Nano Today*, ***11***(***3***), 351–372.

Hontoria-Lucas, C., López-Peinado, A. J., López-González, J. d. D., Rojas-Cervantes, M. L., & Martín-Aranda, R. M. (**1995**). Study of oxygen-containing groups in a series of graphite oxides: Physical and chemical characterization. *Carbon*, ***33***(***11***), 1585–1592.

Hummers, W. S., & Offeman, R. E. (**1958**). Preparation of graphitic oxide. *Journal of the American Chemical Society*, ***80***(***6***), 1339–1339.

Jackson, S., & Nuzzo, R. G. (**1995**). Determining hybridization differences for amorphous carbon from the XPS C 1s envelope. *Applied Surface Science*, ***90***(***2***), 195–203.

Jeong, H. K., Jin, M. H., So, K. P., Lim, S. C., & Lee, Y. H. (**2009**). Tailoring the characteristics

of graphite oxides by different oxidation times. *Journal of Physics D: Applied Physics*, ***42***(***65418***), 1–6.

Kaboorani, A., & Riedl, B. (**2011**). Effects of adding nano-clay on performance of polyvinyl acetate (PVA) as a wood adhesive. *Composites Part A: Applied Science and Manufacturing*, ***42***(***8***), 1031–1039.

Kaboorani, A., Riedl, B., Blanchet, P., Fellin, M., Hosseinaei, O., & Wang, S. (**2012**). Nanocrystalline cellulose (NCC): A renewable nano-material for polyvinyl acetate (PVA) adhesive. *European Polymer Journal*, ***48***(***11***), 1829–1837.

Khan, U., May, P., Porwal, H., Nawaz, K., & Coleman, J. N. (**2013**). Improved adhesive strength and toughness of polyvinyl acetate glue on addition of small quantities of graphene. *ACS Applied Materials & Interfaces*, ***5***(***4***), 1423–1428.

Kim, H., Abdala, A., & Macosko, C. (**2010**). Graphene/polymer nanocomposites. *Macromolecules*, ***43***(***16***), 6515–6530.

Kong, J., & Yu, S. (**2007**). Fourier transform infrared spectroscopic analysis of protein secondary structures. *Acta Biochimica et Biophysica Sinica*, ***39***(***8***), 549–559.

Lee, C., Wei, X., Kysar, J. W., & Hone, J. (**2008**). Measurement of the elastic properties and intrinsic strength of monolayer graphene. *Science*, ***321***(***5887***), 385–388.

Lee, S., & Park, S. (**2014**). Isothermal exfoliation of graphene oxide by a new carbon dioxide pressure swing method. *Carbon*, ***68***, 112–117.

Li, D., Müller, M. B., Gilje, S., Kaner, R. B., & Wallace, G. G. (**2008**). Processable aqueous

dispersions of graphene nanosheets. *Nature Nanotechnology*, ***3***(***2***), 101–105.

Li, N., Qi, G., Sun, X. S., Stamm, M. J., & Wang, D. (**2011**). Physicochemical properties and adhesion performance of canola protein modified with sodium bisulfite. *Journal of the American Oil Chemists' Society*, ***89***(***5***), 897–908.

Li, Z., Zhang, W., Luo, Y., & Yang, J. (**2009**). How graphene is cut upon oxidation? *Journal of the American Chemical Society*, ***131***(***18***), 6320–6321.

Liang, J., Huang, Y., Zhang, L., & Wang, Y. (**2009**). Molecular-level dispersion of graphene into poly (vinyl alcohol) and effective reinforcement of their nanocomposites. *Advanced Functional Materials*, ***19***(***14***), 2297–2302.

Linse, S., Cabaleiro-Lago, C., Xue, W.-F., Lynch, I., Lindman, S., Thulin, E., Dawson, K. A. (**2007**). Nucleation of protein fibrillation by nanoparticles. *Proceedings of the National Academy of Sciences of the United States of America*, ***104***(***21***), 8691–8696.

Liu, D., Bian, Q., Li, Y., Wang, Y., Xiang, A., & Tian, H. (**2016**). Effect of oxidation degrees of graphene oxide on the structure and properties of poly (vinyl alcohol) composite films. *Composites Science and Technology*, ***129***, 146–152.

Liu, J., Fu, S., Yuan, B., Li, Y., & Deng, Z. (**2010**). Toward a universal adhesive nanosheet for the assembly of multiple nanoparticles based on a protein-induced reduction/decoration of graphene oxide. *Journal of the American Chemical Society*, ***132***(***21***), 7279–7281.

Manamperi, W. A. R., Chang, S. K. C., Ulven, C. A., & Pryor, S. W. (**2010**). Plastics from an improved canola protein isolate: preparation and properties. *Journal of the American Oil*

Chemists' Society, ***87***(***8***), 909–915.

Mcallister, M. J., Li, J.-L., Adamson, D. H., Schniepp, H. C., Abdala, A. A., Liu, J., Aksay, I. A. (**2007**). Single sheet functionalized graphene by oxidation and thermal expansion of graphite. *Chemistry of Materials*, ***19***(***18***), 4396–4404.

Paredes, J., Villar-Rodil, S., & Martínez-Alonso, A. (**2008**). Graphene oxide dispersions in organic solvents. *Langmuir*, ***24***(***19***), 10560–10564.

Park, S., & Ruoff, R. S. (**2009**). Chemical methods for the production of graphenes. *Nature Nanotechnology*, ***4***(***4***), 217–224.

Pizzi, A. (**2013**). Bioadhesives for wood and fibres. *Reviews of Adhesion and Adhesives*, ***1***(***1***), 88–113.

Posudievsky, O., & Khazieieva, O. (**2012**). Preparation of graphene oxide by solvent-free mechanochemical oxidation of graphite. *Journal of Materials Chemistry*, ***22***(***25***), 12465–12467.

Schniepp, H. C., Li, J.-L., McAllister, M. J., Sai, H., Herrera-Alonso, M., Adamson, D. H., … Aksay, I. A. (**2006**). Functionalized single graphene sheets derived from splitting graphite oxide. *The Journal of Physical Chemistry B*, ***110***(***17***), 8535–8539.

Shao, G., Lu, Y., Wu, F., Yang, C., Zeng, F., & Wu, Q. (**2012**). Graphene oxide: the mechanisms of oxidation and exfoliation. *Journal of Materials Science*, ***47***(***10***), 4400–4409.

Shin, H., Kim, K., Benayad, A., & Yoon, S. (**2009**). Efficient reduction of graphite oxide by sodium borohydride and its effect on electrical conductance. *Advanced Functional*

Materials, ***19***(***12***), 1987–1992.

Shtein, M., Nadiv, R., Buzaglo, M., Kahil, K., & Regev, O. (**2015**). Thermally conductive graphene-polymer composites: size, percolation, and synergy effects. *Chemistry of Materials*, ***27***(***6***), 2100–2106.

Stankovich, S., Piner, R. D., Nguyen, S. T., & Ruoff, R. S. (**2006**). Synthesis and exfoliation of isocyanate-treated graphene oxide nanoplatelets. *Carbon*, ***44***(***15***), 3342–3347.

Tanaka, Y., & Kakiuchi, H. (**1964**). Study of epoxy compounds. Part VI. Curing reactions of epoxy resin and acid anhydride with amine, acid, alcohol, and phenol as catalysts. *Journal of Polymer Science Part A: General Papers*, ***2***(***8***), 3405–3430.

Tien, H., Huang, Y., Yang, S., Wang, J., & Ma, C. (**2011**). The production of graphene nanosheets decorated with silver nanoparticles for use in transparent, conductive films. *Carbon*, ***49***(***5***), 1550–1560.

Verdejo, R., Bernal, M. M., Romasanta, L. J., & Lopez-Manchado, M. A. (**2011**). Graphene filled polymer nanocomposites. *Journal of Material Chemistry*, ***21***(***10***), 3301–3310.

Wang, C., Wu, J., & Bernard, G. M. (**2014**). Preparation and characterization of canola protein isolate–poly(glycidyl methacrylate) conjugates: A bio-based adhesive. *Industrial Crops and Products*, ***57***, 124–131.

Wang, Y., Shi, Z., Yu, J., Chen, L., Zhu, J., & Hu, Z. (**2012**). Tailoring the characteristics of graphite oxide nanosheets for the production of high-performance poly (vinyl alcohol) composites. *Carbon*, ***50***(***15***), 5525–5536.

Xu, Y., Bai, H., Lu, G., Li, C., & Shi, G. (**2008**). Flexible graphene films via the filtration of water-soluble noncovalent functionalized graphene sheets. *Journal of the American Chemical Society*, ***130***(***18***), 5856–5857.

Xu, Z., & Gao, C. (**2011**a). Aqueous liquid crystals of graphene oxide. *ACS nano*, ***5***(***4***), 2908–2915.

Xu, Z., & Gao, C. (**2011**b). Graphene chiral liquid crystals and macroscopic assembled fibres. *Nature Communications*, ***2***(***571***), 1–9.

Yang, X., Tu, Y., Li, L., Shang, S., & Tao, X. (**2010**). Well-dispersed chitosan/graphene oxide nanocomposites. *ACS Applied Materials & Interfaces*, ***2***(***6***), 1707–1713.

Yoon, G., Seo, D.-H., Ku, K., Kim, J., Jeon, S., & Kang, K. (**2015**). Factors affecting the exfoliation of graphite intercalation compounds for graphene synthesis. *Chemistry of Materials*, ***27***(***6***), 2067–2073.

Yuge, R., Zhang, M., Tomonari, M., Yoshitake, T., Iijima, S., & Yudasaka, M. (**2008**). Site identification of carboxyl groups on graphene edges with Pt derivatives. *ACS Nano*, ***2***(***9***), 1865–1870.

Zhang, Y., Zhu, W., Lu, Y., Gao, Z., & Gu, J. (**2014**). Nano-scale blocking mechanism of MMT and its effects on the properties of polyisocyanate-modified soybean protein adhesive. *Industrial Crops and Products*, ***57***, 35–42.

Zhao, X., Zhang, Q., Chen, D., & Lu, P. (**2010**). Enhanced mechanical properties of graphene-based poly(vinyl alcohol) composites. *Macromolecules*, ***43***(***5***), 2357–2363.

Zhong, Y. L., Tian, Z., Simon, G. P., & Li, D. (**2015**). Scalable production of graphene via wet chemistry: progress and challenges. *Materials Today*, ***18***(***2***), 73–78.

Zhou, X., Zhang, J., Wu, H., Yang, H., Zhang, J., & Guo, S. (**2011**). Reducing graphene oxide via hydroxylamine: a simple and efficient route to graphene. *The Journal of Physical Chemistry C*, ***115***(***24***), 11957–11961.

CHAPTER 5 - Chemically Modified Canola Protein-Nanomaterial Hybrid Wood Adhesive Shows Improved Adhesion and Water Resistance

CHAPTER 5

5.1 Introduction

Engineered wood products (EWP) are widely used for structural and non-structural purposes (Kaboorani et al., 2012). Urea formaldehyde (UF), phenol formaldehyde (PF), melamine urea formaldehyde (MUF), or isocyanates (MDI) are the most common adhesives applied to produce EWP (Pizzi, 2013). However, there are concerns over synthetic adhesives with regard to emission of volatile organic compounds, potential health hazards and non-renewability (Bandara et al., 2013). Various proteins, including soy protein, wheat gluten, cottonseed protein, triticale protein, and spent hen proteins, have been explored as the alternatives (Bandara et al., 2013; Cheng et al., 2013; Khosravi et al., 2014; Wang & Wu, 2012; Zhu & Damodaran, 2014). Among them, soy protein and wheat gluten show promising potential in commercial uses. Canola is the second largest oil seed crop in the world and oil extraction generates a great deal of meal with a protein content of 35-40% w/w (Wang et al., 2014). In comparison, canola proteins are not traditionally used for human consumption (Wang et al., 2014); therefore developing adhesives from canola proteins represent advantages over soy proteins as they are compete for human food uses (Manamperi et al., 2010; Wang et al., 2014).

Canola storage proteins mainly consist of cruciferin (12S), napin (2S) and oleosin with approximate proportions of ~60%, ~20% and ~8% respectively (Li et al., 2011). Cruciferin is a neutral protein (PI – 7.2) with a molecular weight of ~ 300-310 KDa. It consists of six sub-units with a molecular weight ~ 50 KDa each (Tan et al., 2011; Wanasundara, 2011). Each subunit is made of two polypeptide chains, a ~30 KDa acidic α-chain (254-296 amino acid residues) and a ~20 KDa basic β-chain (189-191 amino acid residues) linked via a single disulfide bond between amino acid side chains (Aider & Barbana, 2011; Tandang-Silvas et al., 2010; Wanasundara, 2011). The hydrophobic β-sheets (~50% of total secondary structure) located inside the

cruciferin molecule whereas hydrophilic α-helix structures (~10%) are located on the surface of molecule. Napin is strongly basic (2S) protein because of higher level of amidated amino acids present in its structure. It has a molecular weight of ~ 12.5-14.5 KDa with an isoelectric point of ~11.0 (Aider & Barbana, 2011; Nietzel et al., 2013). It consists of two polypeptide chains, a ~4.5 KDa polypeptide with ~40 amino acid residues and 9.5 KDa polypeptide with ~90 amino acid residues which stabilized by two inter-chain and two intra-chain disulfide bonds (Aider & Barbana, 2011; Wanasundara, 2011). Unlike cruciferin, napin contains a higher degree of α-helix (~40-46%) than β-sheet structures (~12%) (Tan et al., 2011).

Chemical modification have been previously used to improve the adhesion properties of protein based adhesives (Khosravi et al., 2014; Li et al., 2011, 2012; Wang et al., 2014). Li et al., (2012) studied the adhesion strength of canola protein fractions extracted by solubilizing at higher pH (12.0) and sequentially precipitated at pH 7.0, 5.5, and 3.5. Canola protein fraction precipitated at pH 3.5 showed dry, wet and soaked adhesion strength of 5.28 ± 0.47 MPa, 4.07 ± 0.16 MPa and 5.43 ± 0.28 MPa, respectively after modifying with sodium bisulfite (Li et al., 2012). Sodium bisulfite modified canola protein without fractionation showed dry, wet and soaked strength of 5.44 ± 0.12 MPa, 3.97 ± 0.53 MPa and 5.24 ± 0.21 MPa, respectively (Li et al., 2011). Grafting poly (glycidyl methacrylate) into canola protein using ammonium persulphate (APS) as a free radical initiator showed dry, wet and soaked adhesion strength of 8.25 ± 0.12 MPa, 3.80 ± 0.15 MPa and 7.10 ± 0.10 MPa respectively (Wang et al., 2014). However, further investigations showed that APS itself improved the adhesion strength comparable to poly (glycidyl methacrylate) grafted adhesive. Our previous work on nanomaterial reinforced canola adhesives showed that exfoliating graphite oxide (GO) and nano crystalline cellulose (NCC) at low concentrations could significantly increase the adhesion and water

resistance. At 1% addition level, NCC improved the strength to 10.37 ± 1.63 MPa, 3.56 ± 0.57 MPa and 7.66 ± 1.37 MPa where GO increased the adhesion up to 8.14 ± 0.45 MPa, 3.25 ± 0.36 MPa and 7.76 ± 0.53 MPa for dry, wet and soaked strength respectively (Bandara et al., 2017a). Tailoring oxidation conditions of GO further improved the adhesion of canola adhesive to 11.67 ± 1.00 MPa, 4.85 ± 0.35 MPa and 10.73 ± 0.45 MPa respectively at 1% GO addition level.

We hypothesize that preparing hybrid wood adhesive by exfoliating GO and NCC in chemically modified canola protein (CMCP) will further increase the adhesion strength and water resistance. The objectives of the study were to develop APS modified canola protein – nanomaterial hybrid adhesive by exfoliating GO or NCC, and to study the effect of APS and synergistic effect of APS/NCC and APS/GO on adhesion and water resistance. For this purpose, canola protein was chemically modified using APS at different concentrations to identify the effective modifier concentration, and then GO and NCC at optimum addition levels (1% w/w nanomaterial/protein (Bandara et al., 2017a) were exfoliated in the chemically modified canola protein to develop canola protein-nanomaterial hybrid wood adhesive (CMCP-NM – either CMCP-GO or CMCP-NCC).

5.2 Materials and Methods

5.2.1 Materials and Chemicals

Defatted canola meal was provided as a gift from Richardson Oilseed Ltd. (Lethbridge, AB, Canada). All chemicals and other materials were purchased from Fisher Scientific (Ottawa, ON, Canada) unless otherwise noted. Ammonium persulphate (APS), graphite and cellulose were purchased from Sigma-Aldrich (Sigma Chemical Co, St. Louise, MO, USA). Wood veneer samples were purchased from Windsor Plywood Ltd (Edmonton, AB, Canada).

5.2.2 Methods

5.2.2.1 Canola Protein Extraction

Canola protein was extracted from defatted canola meal using pH shifting method as described by Manamperi et al (2010) with slight modifications (Manamperi et al., 2010). Canola meal was finely ground using Hosokawa milling and classifying system (Hosokawa Micron Powder Systems, Summit, NJ, USA) and passed through a 150 μM sieve. Ground canola meal was mixed with 1:10 (w/v) mili-Q water, pH was adjusted to 12.0 using 3 M NaOH, and stirred for 30 m (300 rpm) followed by centrifugation (10000g, 15 m, 4 ºC). Supernatant was collected, readjust pH to 4.0 using 3 M HCl and stirred for 15 m (300 rpm) to allow protein precipitation. Resulting slurry was centrifuged as above, precipitate was collected, freeze dried and stored at -20 ºC until further use.

5.2.2.2 Graphite Oxide Preparation

Graphite oxide nanoparticles (GO) were prepared as described by Hummers and Offeman method (Hummers & Offeman, 1958) with modifications according to our previous study (Bandara et al., 2017b). In a glass beaker, 5g of graphite was mixed with 5g of $NaNO_3$ and 120 mL of concentrated H_2SO_4 was slowly added while stirring for 2 h in an ice bath (200 rpm, 20 ± 3 ºC). Then, 15 g of $KMnO_4$ was slowly added to the reaction mixture and temperature was gradually increased to 35 ± 3 ºC while stirring (200 RPM) for another 1 h. After reaction, 92 mL of deionized water was added and stirred for 15 m (200 RPM). Following reaction, unreacted $KMnO_4$ was neutralized by adding 80 mL of hot (80 ºC) deionized water containing 3% H_2O_2. Final solution was allowed to cool up to room temperature, and centrifuged (10000g, 15 m, 4ºC) to remove any remaining acids or chemicals. The precipitate was collected, washed three times with deionized water, and sonicated for 5 m (at 50% power output) prior to freeze-drying.

5.2.2.3 Nanocrystalline Cellulose Preparation

Nano crystalline cellulose (NCC) was prepared as described by Cranston & Gray (2006) with slight modifications. In brief, 20g of cellulose powder was mixed with 350 mL of H_2SO_4 (64% w/w), and stirred for 45 m (300 RPM at 45 ^oC). Cellulose hydrolysis was terminated by diluting reaction mixture to 10 fold with deionized water and excess acid was removed by centrifugation (10000g, 4 ^oC, 10 m). Precipitate was collected, washed with deionized water for three times, and centrifuged to remove any remaining acids. The collected NCC precipitate was dialyzed against deionized water for three days until achieving a neutral pH, freeze dried and stored at -20 ^oC until further use.

5.2.2.4 Optimizing Ammonium Persulphate (APS) Modification Conditions

Canola proteins were modified with APS as described by Wang et al., (2014) with modifications. CPI was measured into 10 beakers (3g each), mixes with 90 mL of deionized water and pH was adjusted to 7.0 using 1 M NaOH. Protein dispersions were transferred to round bottom flasks and placed in a water bath. All samples were purged with N_2 gas for 5 m prior to adding APS and temperature of water bath was maintained at 30 ± 2 ^oC during the experiment. The required amounts of APS was measured (0%, 1%, 3%, 5%, 7% and 10% w/w APS/protein), added into flask, and purged with N_2 gas for another 5 m. Flasks were sealed, stirred for 4 h (300 rpm, 30 ^oC) and centrifuged (10000g, 15 m, 4 ^oC) to collect the precipitate. Resulting APS modified CPI samples were freeze dried and stored at -20 ^oC until further use.

Optimum APS concentration in improving adhesion strength was measured by preparing APS modified canola protein adhesives. In brief, 2 g of modified canola protein samples were measured into in duplicate, mixed with 20 mL of deionized water (10% w/v protein dispersions), stirred for 2 h (300 rpm) and pH was adjusted to 5.0 using 1 M NaOH. Following pH adjustment,

samples were stirred for another 1 h and pH was readjusted to 12.0 by adding 30 μL/(mL of adhesive) of 6 M NaOH with vigorous mixing. Negative controls were prepared by dispersing canola protein in deionized water at 10% w/v ratio. The pH controls were prepared by dispersing canola protein in deionized water at 10% w/v ratio, and adjusting the pH to 12.0 (without APS modification).

5.2.2.5 Preparing CMCP-NM Hybrid Adhesive

Optimum APS concentration (1% w/w APS/protein) for highest adhesion improvement was selected to prepare CMCP-NM hybrid adhesive. The nanomaterial were exfoliated in CMCP as described in our previous work (Bandara et al., 2017a). In brief, 3g of APS modified canola protein was measured into six beakers, mixed with 20 mL (to make 15% w/w) of deionized water. Samples were stirred for 6 h (300 rpm, RT) to disperse canola protein, and pH was readjusted to 5.0 using 1 M HCl solution. NCC and GO was measured at 1% w/w nanomaterial/protein addition level and separately dispersed in 10 mL of deionized water, stirred for 5 h at room temperature (300 rpm) and another 1 h at 45 ± 3 ºC. After stirring, dispersed NCC and GO were sonicated for 3 m by providing intermittent pulse dispersions (5 s at 3 s intervals, 60% amplitude) using a medium size tapered tip attached to a high intensity ultrasonic dismembrator (Model 500, Thermo Fisher Scientific INC, Pittsburg, PA, USA). Following sonication, nanomaterial dispersions were homogenized for 2 m (20,000 rpm) using digital ULTRA TURRAX high shear homogenizer (Model T25 D S1, IKA® Works, Wilmington, NC, USA). Then, prepared nanomaterial dispersions were slowly added to protein dispersions dropwise while stirring for 15 m to have a final protein concentration of 10% w/v. Following the exfoliation of nanomaterials, prepared adhesive samples were sonicated and homogenized as above, and the pH of the adhesive mixture was readjusted to 12.0 by adding 6 M NaOH solution.

Negative controls and pH controls were prepared as described above while APS Control adhesives were prepared by dispersing APS modified canola protein in deionized water at 10% w/v ratio, and adjusting the pH to 12.0 (without dispersing GO or NCC).

5.2.2.6 Adhesion Strength Measurement

Birch veneer samples (1.2 mm thick) were cut into a size of 20 mm × 120 mm using a cutting device (Adhesive Evaluation Systems, Corvallis, OR, USA), and conditioned as per requirement of ASTM (American Society for Testing and Materials) standard method D2339-98(2011) by placing them in a controlled environmental chamber (ETS 5518, Glenside, PA, USA) at 23 ^{o}C and 50% humidity (ASTM, 2011).

Prepared adhesives were spread on veneer surface using a micropipette at an amount of 40 µL/veneer strands in a contact area of 20 mm × 5 mm. Following adhesive application, veneer samples were air dried for 5 min, and hot pressed (120 ^{o}C, 3.5 MPa temperature and pressure respectively) for 10 min using Carver manual hot press (Model 3851-0, Carver Inc, In, USA). Dry adhesion strength (DAS) was measured according to the ASTM S2339-98 (2011) standard method, where tensile loading required to break bonded veneer was measured using Instron (Model 5565, Instron, MA, USA) equipped with 5 kN load cell and recorded using Bluhill 3.0 software (Instron, MA, USA). Wet adhesion strength (WAS), and soaked adhesion strength (SAS) was measured according to ASTM standard method ASTM D1151-00 (2013) using tensile loading. WAS values were measured after submerging bonded veneer samples for 48 h in water (23 ^{o}C) while SAS was measured after conditioning submerged veneer samples for 7 days at 25 ^{o}C and 50% relative humidity in a controlled environment chamber (ETS 5518, Glenside, PA, USA). Each measurement was carried out with minimum of four bonded veneer per

replicate. All bonded veneer samples were clamped to instron with 35 mm gauge length and tested at 10 mm/m cross head speed.

5.2.2.7 Characterization of Structure and Crystallinity of Modified Canola Protein

Fourier transformed infrared spectroscopy (FTIR) was used to characterize APS modified canola protein and CMCP-NM hybrid adhesive samples. Sample moisture was removed by freeze drying followed by drying with P_2O_5 for two weeks in hermetically sealed desiccator. Dried samples were mixed with potassium bromide (KBr), and milled into a fine powder before analyzing using a Nicolet 8700 (Thermo Eletron Co. WI, USA) Fourier transform infrared spectrometer. IR Spectra in the range of 400-4000 cm^{-1} were collected using 128 scans at a resolution of 4 cm^{-1}. Collected IR spectra was processed and analyzed with Origin 2016 software (OriginLab Corporation, MA, USA).

Crystallinity of starting GO / NCC and their exfoliation properties in CMCP samples were analyzed using Rigaku Ultima IV powder diffractometer (Rigaku Co. Japan). Diffraction angle (2θ) data was collected in the range 5 to 50 degrees using Cu-Kα radiation (0.154 nm) and interlayer spacing (*d*) of nanomaterial was calculated using the Bragg's equation (Bragg & Bragg, 1913). Collected diffraction data was processed using Origin 2016 software (OriginLab Corporation, MA, USA).

5.2.2.8 Characterization of Changes in Particle Size

CMCP (with different APS concentrations) were dissolved in 1 M urea at a concentration of 2 mg/mL, mixed with a 1:1 (v/v) sample buffer which contains 5% β-mercaptoethanol (950 μL Laemmli sample buffer + 50 μL of β-mercaptoethanol). Prepared samples were heated for 5 m at 95 ºC in an Eppendorf Thermomixer Dry Heating Block (Eppendorf Canada, Mississauga,

ON, Canada), and centrifuged for 2 m using a minicentrifuge (Fisher Scientific, Ottawa, ON, Canada). 15 μL of prepared samples were loaded on a Tris-HCl 4-20% linear gradient gel, and run at 200 V for 0.5 h in a Mini-PROTEAN II electrophoresis cell (Bio-Rad, Hercules, Canada). Gels were stained with Coomassie brilliant blue for 0.5 h, and destained for 2 h in a solution containing 50% methanol, 10% acetic acid and water. The molecular weight of protein bands were analyzed using GelAnalyzer 2010 image analysis software (http://www.gelanalyzer.com).

Changes in particle size of protein after APS modification was characterized using Litesizer™ 500 (Anton Paar Instruments, Austria) at 25 °C. Modified canola proteins were dispersed in deionized water at a concentration of 0.5 mg/mL, and stirred for 2 h (300 rpm). Dispersed proteins were transferred into disposable plastic cuvettes (1 mL/cuvette in duplicate), and absorbance was measured using dynamic light scattering (DLS). The data was collected and analyzed using Kalliope™ software (Anton Paar Instruments, Austria).

5.2.2.9 Microscopy of Nanomaterials, Nanomaterial Exfoliation and Fracture Surface

Prepared nanomaterial (NCC and GO) samples, and CMCP-NM adhesive samples were examined under transmission electron microscopy (TEM) to determine nanomaterials properties and exfoliation in adhesive matrix. TEM imaging were performed using Philips/FEI transmission electron microscope (Model Morgagni, FEI Co, OR, USA) coupled with Getan digital camera (Getan Inc, CA, USA). A dilute solution of NCC and GO were prepared by dispersing them in ethanol at 0.5% w/w concentration. Adhesive samples were diluted by 100 fold with ethanol before TEM imaging. A drop of prepared solution was casted on the 200 mesh holey copper grid covered with carbon film and air dried before imaging. NCC and CPA adhesive with NCC were prepared by staining NCC with 1% w/w uranyl acetate to improve image quality.

The fracture surface between two wood veneer samples after lap shear testing was observed using a Hitachi S-2500 scanning electron microscope (SEM, Nis-sei Sangyo America Ltd., CA, USA). A thin layer of wood veneer was cut along the fracture surface for each adhesive group and coated with a thin layer of gold using a gold sputter unit (Denton Vacuum, Moorestown, NJ, USA) before microscopic observation.

5.2.2.10 Changes in Thermal Properties of Modified Protein

Changes in thermal properties of CMCP and CMCP-NM was characterized by differential scanning calorimeter (Perkin-Elmer, Norwalk, CT, USA). Sample moisture were removed by freeze drying and drying in a hermetically sealed desiccator with P_2O_5 for seven days. Approximately 6 mg sample (accurate weight recorded) was weighed into T-Zero hermetic aluminum pans, mixed with 60 μL of 0.01 M phosphate buffer, and hermetically sealed with lids. Samples were equilibrated at 0 ºC for 10 m, heated from 0 to 250 ºC at a ramping rate of 10 ºC min^{-1} under continuous nitrogen purging and heat flow differential of samples were measured against and empty reference pan. Thermodynamic data was collected and analyzed using Universal Analysis 2000 software (Perkin-Elmer, Norwalk, CT, USA).

5.2.3 Statistical Analysis

Effect of different APS concentrations on adhesion strength, and effect of exfoliating NCC or GO at 1% (w/w NM:canola protein) addition level in APS modified canola protein were analyzed using analysis of variance (ANOVA) followed by Duncan's Multiple Range (DMR) test. Dry, Wet, Soaked strength changes were analyzed using Statistical Analysis System Software (SAS version 9.4, SAS Institute, Cary, NC). Effect of APS and nanomaterial addition on adhesion strength of each nanomaterial was evaluated at the 95% confidence level.

5.3 Results and Discussion

5.3.1 Effect of Ammonium Persulphate Modification on Adhesion Strength

Weak water resistance of protein-based adhesives is one of major factors limiting their widespread commercial applications (Pizzi, 2013). Our preliminary study showed that APS modified canola proteins had comparable adhesive performance as that of poly (glycidyl methacrylate) grafted one Therefore, effect of APS concentrations on adhesion was further studied. Fig 5.1 shows the dry, wet and soaked adhesion strengths of canola protein modified at different APS concentrations.

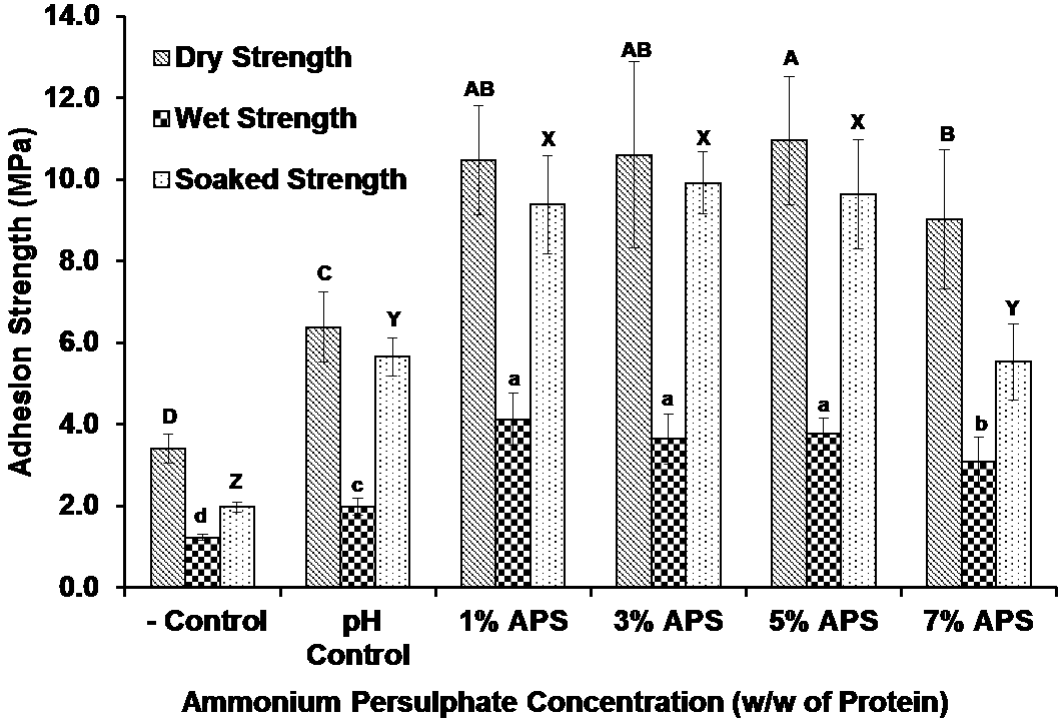

Figure 5.1 - Adhesion strength of canola protein adhesive (10% w/v canola protein:water) modified with different concentrations (0%, 1%, 3% 5%, & 7% w/w APS:protein) of ammonium persulphate. Adhesion data was analyzed using one-way ANOVA followed by Duncan test for mean separation for dry, wet and soaked strength separately. Different letters on the bar represent significantly different adhesion strength ($p < 0.05$). Error bars represent standard deviations. All

adhesive samples were prepared in triplicate ($n=3$) and minimum 5 wood samples per replicate were used for each strength measurement.

Dry, wet and soaked adhesion strength increased from 6.38 ± 0.86 MPa, 1.98 ± 0.20 MPa, and 5.65 ± 0.46 MPa in pH control sample to 10.47 ± 1.35 MPa, 4.12 ± 0.64 MPa, and 9.39 ± 1.20 MPa (dry, wet and soaked strength respectively) at 1% (w/w APS/protein), leveled off at increasing concentrations up to 5%, and then started to decrease at 7%. The decreased adhesion and water resistance at concentrations over 7% might be due to protein aggregation and or gelation, which may limit penetration of adhesive into wood surface, thus interfering interactions between protein functional groups and functional groups in wood surface. Proper wetting and adhesive penetration are considered as one of the main requirements in developing adhesion (Kamke & Lee, 2007). 10% (w/w APS/protein) concentration was removed from adhesion strength testing due to poor followability, and gelation occurred after modifying with APS that caused technical issues in adhesive application. The adhesion strengths observed in this study shows a significant improvement ($p<0.05$) over the method develop by Wang et al (2014), where they reported dry, wet and soaked strength of 8.25 ± 0.12 MPa, 3.80 ± 0.15 MPa, and 7.10 ± 0.10 MPa respectively by grafting a functional polymer at 1:1.35 ratio (protein : poly glycidyl methacrylate). Based on the results of APS concentration optimization, 1% APS (w/w APS/protein) was selected to prepare CMCP-NM adhesives by exfoliating either NCC or GO.

APS has been used as an electron acceptor in chemical/photochemical oxidation, oxidative crosslinking reactions of proteins, and especially for site selective protein modifications. However, the exact role of APS in protein modification is still not completely understood (Antos & Francis, 2006; Fancy & Kodadek, 1999; Kodadek et al., 2005; Sato & Nakamura, 2013). Fancy & Kodadek (1999), reported a 20 fold increase in crosslinking, for several proteins when

APS is present in the reaction mixture with a metal catalyst. They suggested that a APS mediated free radical reaction, where Tyr residue crosslinks with another nearby Tyr residue in protein chain (Fancy & Kodadek, 1999). Tyr, Trp, His and Cys residues were identified as the specific amino acid residues that can undergo chemical/photochemical oxidation of proteins in the presence of APS (Antos & Francis, 2006; Fancy & Kodadek, 1999; Kodadek et al., 2005). Crosslinking of protein has previously been used as a method to improve adhesion of wheat gluten and soy proteins (Bandara et al., 2013; Khosravi et al., 2014; Wang et al., 2007). The improvement in adhesion and water resistance of crosslinked proteins were attributed to the crosslinking induced covalent bonds, reduction in hydrophilic nature of crosslinked protein and improved thermal stability (Khosravi et al., 2014; Wang et al., 2007). Similarly, the improvement of adhesion and water resistance observed in the APS modified canola protein might be due to the chemical crosslinking. However, the formation of gel at higher APS concentrations might be the reason for decreased adhesion and water resistance, similar to previous adhesion studies on crosslinked proteins (Bandara et al., 2013).

5.3.2 Effect of APS Modification on Chemical and Structural Properties of Canola Protein

Effect of APS concentrations on protein structure and chemical/functional groups was studied using FTIR (Fig 5.2). Amino acid side chain vibrations observed in FTIR spectra can be used as a tool to identify site specific modification of proteins (Abaee et al., 2017; Kong & Yu, 2007). Especially, Tyr, His, Arg, Asn, Gln, and Lys shows significant absorbance in the FTIR spectra compared to other amino acids (Kong & Yu, 2007). As seen in Fig 5.2 (b), absorbance intensities of Tyr ring –OH group vibrations (1518 cm^{-1}, and 1602 cm^{-1} - Kong & Yu, 2007) were reduced at increasing APS concentration up to 5% (w/w APS/protein).

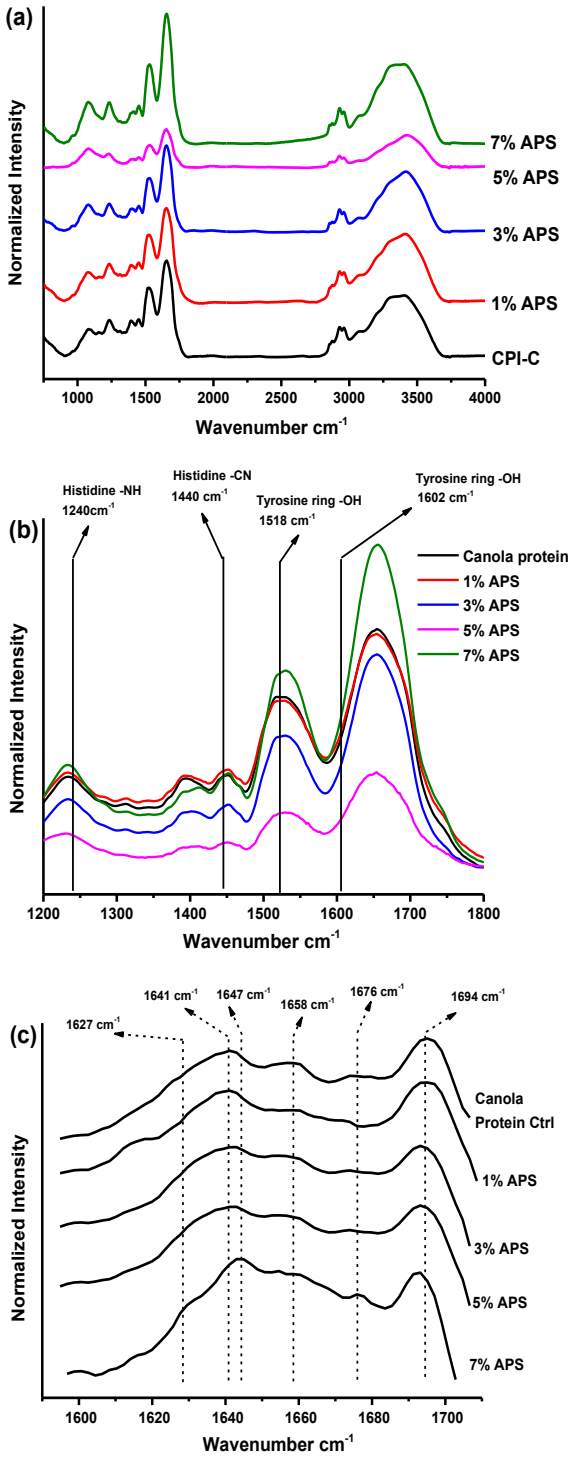

Figure 5.2 (a) - FTIR spectra of modified canola protein with different APS concentrations, (b) enlarge FTIR spectra showing changes in tyrosine and histidine residues in canola protein after APS modifications, (c) second derivative spectra of Amide I peak showing protein secondary structural changes after APS modification.

APS initiated crosslinking between Tyr-Tyr and Tyr-His residues during APS modification (Fancy & Kodadek, 1999; Kodadek et al., 2005), might be the reason for reduced –OH ring vibration of Tyr residue. However, Tyr ring –OH group vibration was increased at 7% APS concentration (w/w APS/ protein). Crosslinking induced protein structural changes might expose additional Tyr residues at higher APS concentrations, thereby contributing to the increased Tyr ring vibration occurred at 1518 cm^{-1}. Similar to Tyr, absorption intensities of –NH vibration at 1240 cm^{-1}, and –CN vibrations at 1440 cm^{-1} wavelengths of His residue were also reduced at increasing APS concentrations. Abaee et al (2017) also reported crosslinking induced reduction of absorption intensities at similar wavelength for His residues in cold gelation of whey protein (Abaee et al., 2017). These reduction in His and Tyr residues provide a strong evidence on APS induced crosslinking reaction that may have triggered due to oxidation. Such covalent crosslinking reaction might be one of the major reason for improved water resistance and adhesion observed in APS modified proteins.

Fig 5.2 (c) shows the second derivative spectra for amide I peak of APS modified canola protein and the effect of APS concentration on protein secondary structure. Increasing APS concentration changed the absorbance of peaks resembling to β sheets (1627 cm^{-1}, 1676 cm^{-1}), α-helix (1647 $cm^{-1,}$ 1658 cm^{-1}), unordered (1641 cm^{-1}) and turn structures (1694 cm^{-1}) (Kong & Yu, 2007) at different degrees. A new peak at 1627 cm^{-1} resembling to β sheets was observed at 7% APS concentration, but did not appear at low APS concentrations. However, the other peak corresponds to β sheets was appeared at 1676 cm^{-1} wavelength showed an increase in intensity with increased APS concentration. The intensity of the peak appeared at 1658 cm^{-1} (α-helix) deceased while peak intensity of 1641 cm^{-1} (unordered structures) increased at increasing APS concentration. Similar to our results, an increase in aggregated β sheet structures, which was

mainly attributed to increased intramolecular interactions during crosslinking; increased unordered structures at a expense of α-helix structures were previously observed in crosslinked proteins (Koichi & Tomida, 2004).

5.3.3 Effect of APS on Physical and Thermal Properties of Canola Protein

Changes in particle size and molecular weight of modified proteins can provide further evidence on APS induced protein crosslinking. Changes in particle size of APS modified proteins were studied by measuring hydrodynamic diameter of modified protein in a dispersion using dynamic light scattering method as shown in Table 5.1.

Table 5.1 - Effect of APS concentration on hydrodynamic diameter (particle size), and polydispersity index of modified canola protein (Mean + standard deviation; *n=6*). Hydrodynamic diameter and PDI data was analyzed using one-way ANOVA followed by Duncan test for mean separation. Different letters on the each column represent significantly different value ($p < 0.05$).

Sample	**Hydrodynamic diameter (μnm)**	**Polydispersity index**
Canola Protein Ctrl	3.03 ± 0.23 ^{A}	0.24 ± 0.02^{a}
1% APS modified	3.26 ± 0.34 ^{A}	0.26 ± 0.03^{a}
3% APS modified	3.20 ± 0.22 ^{A}	0.12 ± 0.02^{a}
5% APS modified	5.03 ± 0.28 ^{B}	0.23 ± 0.03^{a}
7% APS modified	5.36 ± 0.20 ^{B}	0.18 ± 0.09^{a}

Increasing APS concentrations to 3% (w/w APS/protein) did not showed a significant change in hydrodynamic diameter, but significantly increased at further increasing of APS

concentrations. Unmodified canola protein showed a hydrodynamic diameter of 3.02 ± 0.23 μm with a polydispersity index (PDI) of 0.24 ± 0.02 in a water dispersion while modified proteins showed a hydrodynamic diameters of 3.26 ± 0.34 nm, 3.20 ± 0.22 μm, 5.03 ± 0.28 μm, 5.36 ± 0.20 μm respectively, at 1% APS, 3% APS, 5% APS and 7% APS (w/w APS/protein) respectively. However, PDI of APS modified canola protein did not affect among the APS concentrations. Increased particle size is another indication of APS induced protein crosslinking (Khosravi et al., 2014).

SDS-PAGE analysis was performed to identify the effect of APS on protein molecular weight as shown in Fig 5.3. Native canola proteins (Lane -a) showed several protein bands at molecular weights (MW) of 7 KDa, 9.5 KDa, 23 KDa, 27 KDa, and 44 KDa as calculated compared to the protein marker MW. Similar MW bands were previously identified in several studies where they attributed 7 KDa and 9.5 KDa to short and long polypeptide chains respectively, 27.5 KDa band to a dimer of napin, and 44 KDa band to a subunit of cruciferin (Aluko & McIntosh, 2001; Krzyzaniak et al., 1998; Wu & Muir, 2008).

Modification of canola protein with different concentrations of APS has changed the MW profile of modified protein. The band intensity of 43 KDa and 27 KDa was decreasing at increasing APS concentrations while a new minor band with a MW of 75 KDs appeared, probably due to crosslinked subunits of cruciferin and napin. Unlike the canola protein control sample (lane - b), a protein band was observed in the sample loading area (MW above 250 KDa) for all APS modified canola protein samples. These can be a result of APS induced protein crosslinking, as larger MW aggregates could not travel through the SDS-PAGE gel and stuck in sample loading area. The results observed in SDS-PAGE also provide further evidence on APS

induced protein crosslinking that contributed to improvement in adhesion of modified canola protein.

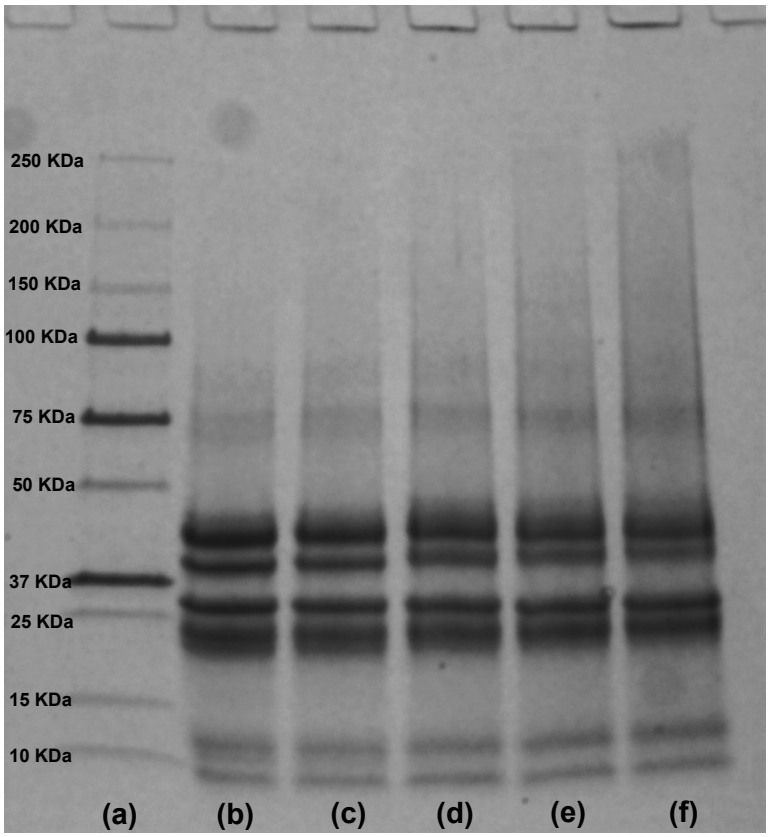

Figure 5.3 - SDS-PAGE of canola proteins modified with different APS concentrations. (a) molecular weight marker, (b) canola protein control, (c) canola protein modified with 1% w/w APS, (d) canola protein modified with 3% w/w APS, (e) canola protein modified with 5% w/w APS, (f) canola protein modified with 7% w/w APS.

Effect of APS concentrations on thermal properties of APS modified canola protein was shown in Table 5.2. Onset temperature and denaturation temperature (T_d) are two important properties for wood adhesives due to the requirement of hot pressing during adhesive curing step (Mo et al., 2004). Unmodified canola protein showed an onset temperature of 71.89 ± 0.59 ºC

and T_d of 89.59 ± 0.22 ºC. However, both onset temperature and T_d of APS modified proteins are increasing at increasing APS concentrations up to 5% (w/w APS/protein), but decreased at 7% APS (w/w APS/protein) concentration. These changes in T_d might be due to the improved thermal stability of crosslinked canola protein. However, the drastic changes of protein secondary structures as observed in FTIR might be the reason for decreased T_d in canola protein modified with 7% APS (w/w APS/protein). Similar increase in thermal stability was previously reported in other crosslinked proteins as well (Gerrard, 2002; Wang et al., 2007).

Table 5.2 - Thermal transitional changes of wood adhesive prepared with APS modified canola protein (Mean + standard deviations; *n=4*).

Sample	**Onset temperature (Tº)**	**Denaturation temperature (Tº)**	**Specific heat (J/(g.ºC)**
Canola Protein Ctrl	71.89 ± 0.59	89.59 ± 0.22	1.38 ± 0.09
1% APS modified	78.81 ± 3.80	97.95 ± 7.07	1.30 ± 0.17
3% APS modified	81.26 ± 6.10	101.25 ± 5.30	1.25 ± 0.02
5% APS modified	81.75 ± 2.68	104.51 ± 2.81	1.24 ± 0.04
7% APS modified	75.57 ± 1.48	93.62 ± 1.97	1.17 ± 0.21

5.3.4 Exfoliation of Nanomaterials in APS Modified Canola Protein

NCC and GO were selected based on our previous study for further improving adhesion of chemically modified canola protein (with optimum APS concentration of 1% w/w APS) (Bandara et al., 2017a). Fig 5.4a shows the interlayer spacing (*d*) and glancing angles (2θ) of two nanomaterials used for adhesive preparation, where Fig 5.4b and 5.4c shows the TEM images of GO and NCC respectively. NCC samples prepared for this study showed typical NCC crystalline

peaks similar to previously published literature (Chen et al., 2012; Liu et al., 2011) at glancing angles of 14.9°, 16.4°, and 22.4° with a interlayer spacing of 0.594 nm, 0.539 nm, and 0.396 nm respectively.

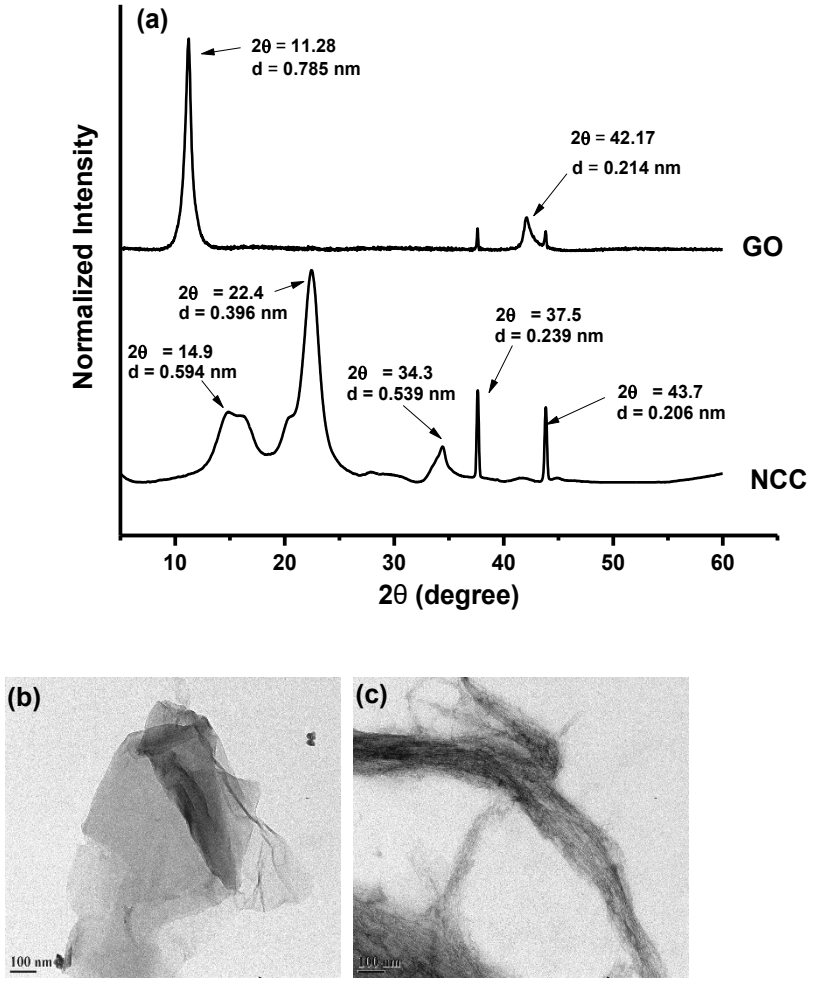

Figure 5.4 - Properties of the nanomaterials used in the study (a) XRD showing interlayer spacing and glancing angels of peaks in NCC and GO, (b) TEM images of GO (c) TEM image of NCC

In addition, two other minor peaks were appeared at glancing angle of 37.5° and 43.7° (0.239 nm and 0.213 nm respectively). GO sample (C/O ratio – 1.40) showed two major crystalline peaks at glancing angles of 11.28° and 42.17° with a interlayer spacing of 0.785 nm

and 0.214 nm respectively. Krishnamoorthy et al., (2013) also reported similar crystalline peaks in GO at glancing angles of 10.8° with similar interlayer spacing and attributed it to the crystallinity of oxidized graphite. TEM characterization showed a long rod like fibrous structure for NCC with a diameter of ~60-90 nm, while GO appeared as single layer sheets and stacked nano sheets with an average width of 600-800 nm.

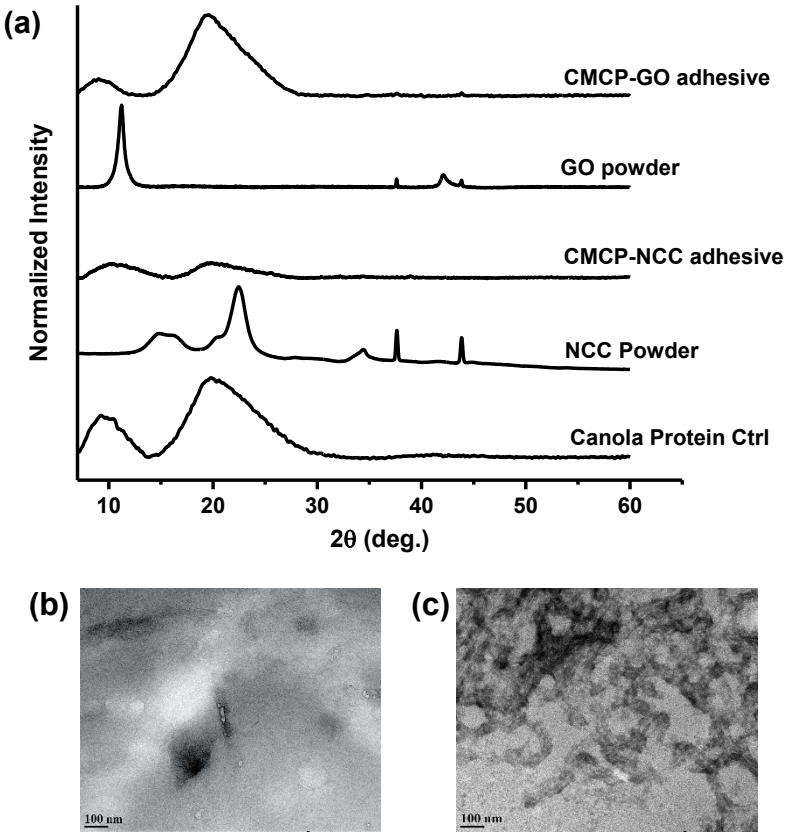

Figure 5.5 (a) X-ray diffraction patterns of NCC powder, GO powder, CMCP-NCC adhesive, and CMCP-GO adhesive samples showing their dispersion properties, (b) TEM image of exfoliated GO in CMCP-GO adhesive, and (c) TEM image of exfoliated NCC in CMCP-NCC adhesive

Prepared NCC and GO were dispersed in chemically modified (with 1% w/w APS) canola protein at optimized addition levels (1% w/w; nanomaterial/protein) as determined in our

previous study (Bandara et al., 2017a). Nanomaterial dispersion and proper exfoliation in adhesive matrix is a critical factor in improving adhesion and water resistance of the adhesive (Bandara et al., 2017a; Kaboorani et al., 2012; Kaboorani & Riedl, 2011, 2012). Therefore, exfoliation of GO and NCC was characterized using XRD and TEM as shown in Fig 5.5. Crystalline peaks corresponding to both NCC and GO disappeared in XRD spectrum of CMCP-NCC/CMCP-GO adhesives indicating a random exfoliation of NCC and GO in the adhesive matrix. When nanomaterials are exfoliated in a polymer matrix, they will lose their crystalline structure due to increased interlayer spacing (Kaboorani et al., 2012; Xu et al., 2011). TEM images of exfoliated nanomaterials provides further confirmation on the exfoliation of NCC and GO in canola protein matrix, where NCC fibers and GO sheets were seen as individually dispersed in protein matrix.

5.3.5 Adhesion of Chemically Modified Canola Protein-Nanomaterial Hybrid Wood

In our previous studies, exfoliating GO and NCC at low addition level (1% w/w, NM/protein) proved to be effective in increasing adhesion and water resistance of canola protein based adhesives (Bandara et al., 2017a, 2017b). First part of this study showed that chemical modification of canola protein with APS can also improve the adhesion and water resistance. Therefore, in the next step of this study we combined chemical modification (with 1% w/w APS/protein) and nanomaterial exfoliation (NCC and GO at 1% w/w addition) to produce CMCP-NM adhesive, as a means to synergistically improve adhesion and water resistance. The adhesion strength and water resistance properties of CMCP-NM adhesives (CMCP-GO and CMCP-NCC) are shown in Fig 5.6.

CMCP (with 1% APS) showed adhesion strength of 10.47 ± 1.29 MPa, 4.12 ± 0.64 MPa, and 9.39 ± 1.20 MPa for dry, wet and soaked adhesion respectively. Exfoliation of both NCC

and GO at 1% w/w (NCC or GO/protein) addition level has significantly increased ($p < 0.05$) dry, wet and soaked adhesion strength of CMCP-NCC and CMCP-GO adhesives compared to negative control, pH control and APS control sample, but did not showed a difference among them. 1% NCC addition to CMCP has increased the adhesion up to 12.50 ± 0.71 MPa, 4.79 ± 0.40 MPa, and 10.92 ± 0.75 MPa while 1% GO addition increased the adhesion up to 11.82 ± 1.15 MPa, 4.99 ± 0.28 MPa, and 10.74 ± 0.72 MPa for dry, wet and soaked adhesion respectively.

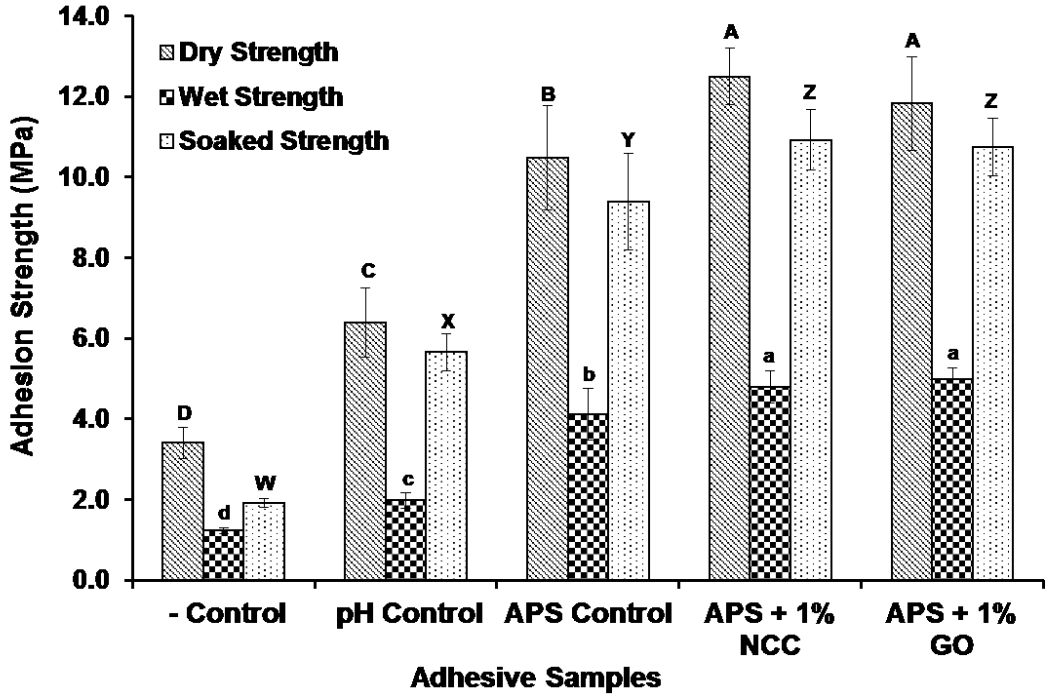

Figure 5.6 - Adhesion strength of chemically modified canola protein-nanomaterial hybrid wood adhesive. Adhesion data was analyzed using one-way ANOVA followed by Duncan test for mean separation for dry, wet and soaked strength separately. Different letters on the bar represent significantly different adhesion strength ($p < 0.05$). Error bars represent standard deviations. All

adhesive samples were prepared in triplicate ($n=3$) and minimum 5 wood samples per replicate were used for each strength measurement.

These significant increase ($p < 0.05$) in adhesion and water resistance might be due to the synergistic effect of chemical modification with APS, protein crosslinking due to APS modification which provides stable protein network, and uniform exfoliation of NCC/GO in protein matrix as evidenced in XRD and TEM. Nanomaterials such as NCC (Bandara et al., 2017a; Kaboorani et al., 2012), GO (Bandara et al., 2017a; Khan et al., 2013), nanoclay and nano Al_2O_3 (Kaboorani & Riedl, 2012) were previously reported to improve adhesion at low addition levels, at exfoliated state. Increased thermal stability (Bandara et al., 2017a, 2017b) and cohesive strength (Khan et al., 2013) of NCC and GO exfoliated adhesives as observed in previous studies might be another reason for improved adhesion in CMCP-NM adhesives.

Amorphous polymers such as protein generally have limited mechanical strength; therefore, cohesive failure is predominant in protein based adhesives (Khan et al., 2013). As a result, increasing cohesive interactions is a critical factor in improving adhesion and water resistance of protein based adhesives. Both GO and NCC have showed improved cohesion after exfoliating in polyvinyl acetate adhesive matrix (Kaboorani et al., 2012; Khan et al., 2013). Studying the morphology of wood fracture surface using scanning electron microscopy (SEM) can provide an indication on the type of adhesive failure.

Fig 5.7 shows the SEM images of wood fracture surface for control adhesive, CMCP-NCC and CMCP-GO adhesive samples at different magnifications (50X, 1000X and 4500X). Wood surfaces that used CMCP-NCC and CMCP-GO adhesives showed a wood failure and fiber pulling/breaking compared to smooth surface on veneer that used control adhesive at 50X magnification. Adhesive penetration into the wood pores, and fiber pulling were visible higher

magnification (both 1000X and 4500X) for CMCP-NCC and CMCP-GO adhesives. These results suggest an adhesive failure in CMCP-NCC/CMCP-GO adhesives compared to a cohesive failure observed in control adhesive sample. These improvement in cohesive interactions might be one of the major reasons for significantly improved adhesion and water resistance observed in CMCP-NM adhesives.

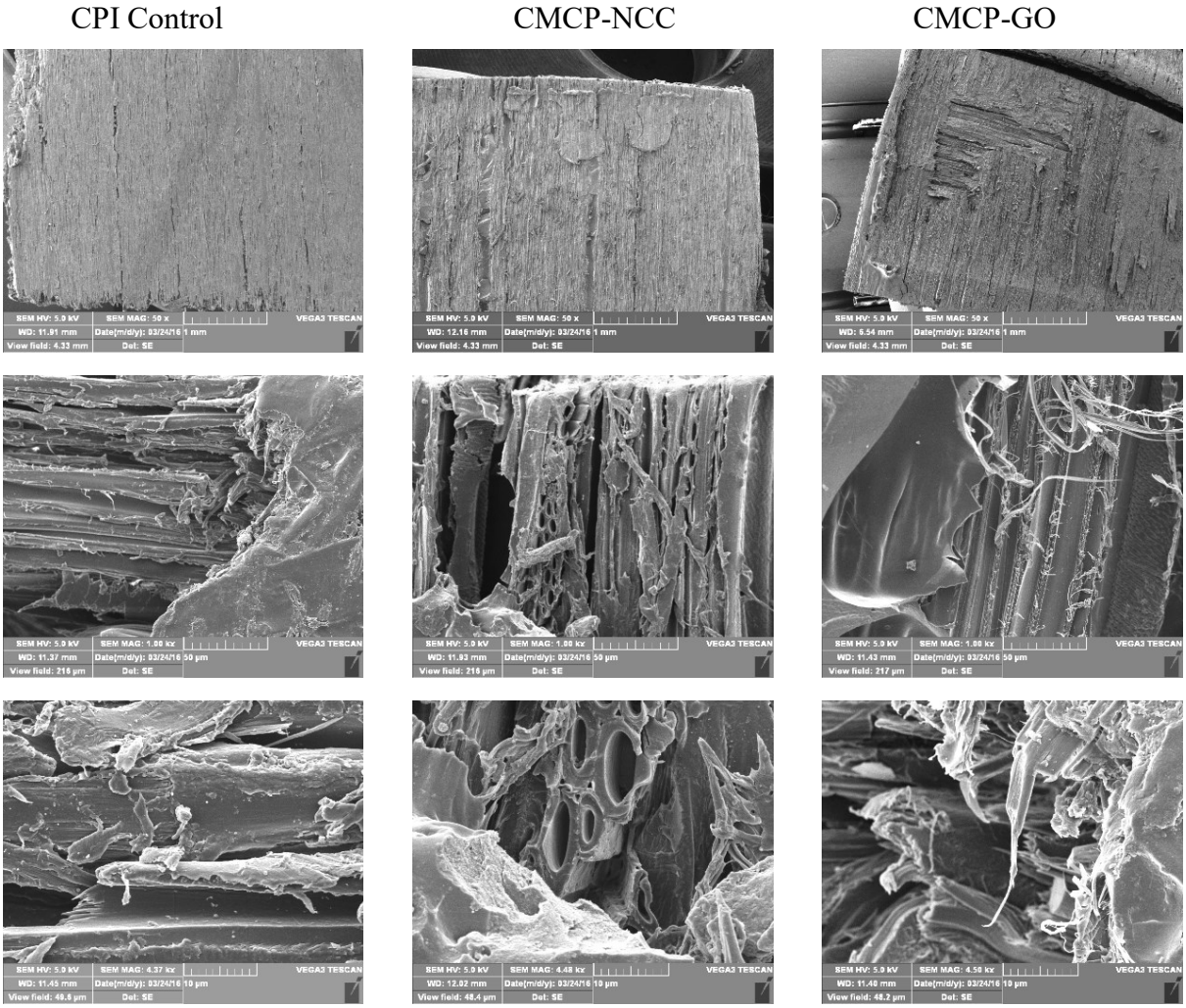

Figure 5.7 - Scanning electron microscopy of wood veneer surface showing the surface properties after bond pulling

5.3.6 Changes in Structural Properties of CMCP-NM Adhesives

Effect of NCC/GO addition on chemically modified canola protein secondary structures are shown in Fig 5.8. Changes to canola protein secondary structure was studied by processing Amide I peak into second derivative followed by peak fitting to respective structures.

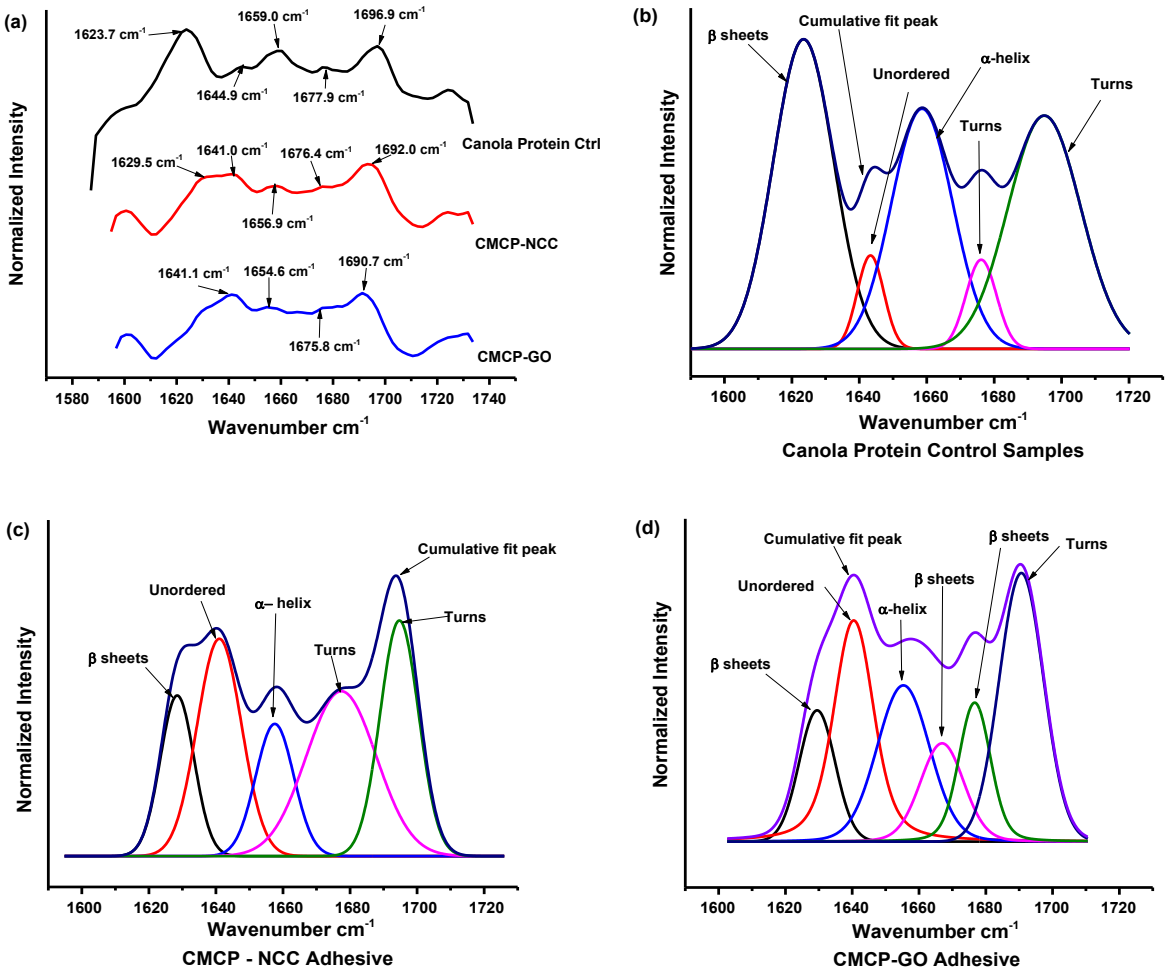

Figure 5.8 - Protein structural changes of chemically modified canola protein adhesive (a) second derivative spectra of modified adhesives (b,c,d)- peak fitting of Amide I peak showing relative proportion of each secondary structure of (b) – canola protein control sample, (c) – CMCP-GO adhesive, (d) – CMCP-GO adhesive

Secondary structures of Amide I peak was assigned based on the previously published literature(Grdadolnik, 2002; Haris & Severcan, 1999; Kong & Yu, 2007). As observed in Fig 5.8b, relative proportion of the β sheets (1623 cm^{-1}, 1676 cm^{-1}) and α-helix (1659 cm^{-1}) structures of modified canola protein decreased while relative proportion of unordered structures (1641 cm^{-1}) increased significantly. In addition, the relative proportion of turn structures located at 1696 cm^{-1} also increased in CMCP-NM adhesive samples compared to control canola protein. These results were consistent with the results observed in our previous studies on nanomaterial exfoliated canola protein adhesive (Bandara et al., 2017a, 2017b). Increasing unordered structures in CMCP increase the availability hydrophobic functional groups that were originally buried inside protein structure, thereby increasing hydrophobic interactions with the functional groups in wood surface (Bandara et al., 2017a; Zhang et al., 2014).

5.4 Conclusions

A chemically modified canola protein-nanomaterial hybrid wood adhesive (CMCP-NM) was developed with significantly improved adhesion and water resistance compared to previously reported canola protein adhesives. APS modification significantly increased ($p < 0.05$) dry, wet and soaked adhesion (10.47 ± 1.35 MPa, 4.12 ± 0.64 MPa, and 9.39 ± 1.20 MPa respectively) at 1% w/w (APS/protein) concentration, due to APS induced oxidation reaction that leads to covalently crosslinked protein network (via Tyr-Tyr, and Tyr-His covalent bonds). The results observed in FTIR, hydrodynamic diameter, and SDS-PAGE provide further evidence on APS mediated protein crosslinking. Crosslinked protein showed better thermal stability and increased hydrophobic functional groups, which also contributed to the improved adhesion and water resistance. Exfoliating NCC or GO in CMCP at 1% w/w (NCC or GO/CMCP) addition level further increased ($p < 0.05$) the adhesion to 12.50 ± 0.71 MPa, 4.79 ± 0.40 MPa, and 10.92

± 0.75 MPa (for NCC) and to 11.82 ± 1.15 MPa, 4.99 ± 0.28 MPa, and 10.74 ± 0.72 MPa (with GO) for dry, wet and soaked adhesion respectively. Proper exfoliation of NCC/GO in protein matrix improved cohesive interactions as observed in wood failure study; possibly increased hydrophobic functional groups due to protein structural changes in combination with stability of crosslinked protein network might be the major reasons for synergistic improvement in adhesion and water resistance observed in CMCP-NM adhesive. CMCP-NM hybrid adhesive prepared in this study with improved adhesion and water resistance can be used as a green alternative for synthetic adhesives in developing engineered wood products.

5.5 References

Abaee, A., Madadlou, A., & Saboury, A. (**2017**). The formation of non-heat-treated whey protein cold-set hydrogels via non-toxic chemical cross-linking. *Food Hydrocolloids*. ***63***, 43-49.

Aider, M., & Barbana, C. (**2011**). Canola proteins: composition, extraction, functional properties, bioactivity, applications as a food ingredient and allergenicity – A practical and critical review. *Trends in Food Science & Technology*, ***22***(***1***), 21–39.

Aluko, R., & McIntosh, T. (**2001**). Polypeptide profile and functional properties of defatted meals and protein isolates of canola seeds. *Journal of the Science of Food and Agriculture,* ***81***(***4***), 391–396.

Antos, J., & Francis, M. (**2006**). Transition metal catalyzed methods for site-selective protein modification. *Current Opinion in Chemical Biology*, ***10***, 253–262.

ASTM. (**2011**). D2339-98(2011) Standard test method for strength properties of adhesives in two-ply wood construction in shear by tension loading. *Annual Book of ASTM Standards.* Available at: http://compass.astm.org/EDIT/html_annot.cgi?D2339+98%5C [2012/12/04]

ASTM. (**2013**). D1151-00(2013) Standard practice for effect of moisture and temperature on adhesive bonds. *Annual Book of ASTM Standards.* Available at: http://compass.astm.org/EDIT/html_annot.cgi?D1151 +00%5C [2013/02/03]

Bandara, N., Chen, L., & Wu, J. (**2013**). Adhesive properties of modified triticale distillers grain proteins. *International Journal of Adhesion and Adhesives*, ***44***, 122–129.

Bandara, N., Esparza, Y., & Wu, J. (**2017**a). Exfoliating nanomaterials in canola protein derived adhesive improves strength and water resistance. *RSC Advances*, ***7(11)***, 6743-6752.

Bandara, N., Esparza, Y., & Wu, J. (**2017**b). Graphite oxide improves adhesion and water resistance of protein–graphite oxide hybrid wood adhesive (Unpublished).

Bragg, W., & Bragg, W. (**1913**). The reflection of X-rays by crystals. *Proceedings of the Royal Society of London - Series A*, ***88***(***605***), 428–438.

Chen, X., Deng, X., Shen, W., & Jiang, L. (**2012**). Controled enzymolysis preparation of nanocrystalline cellulose from pretreated cotton fibers. *BioResources*, ***7***(***3***), 4237–4248.

Cheng, H. N., Dowd, M. K., & He, Z. (**2013**). Investigation of modified cottonseed protein adhesives for wood composites. *Industrial Crops and Products*, ***46***, 399–403.

Cranston, E. D., & Gray, D. G. (**2006**). Morphological and optical characterization of polyelectrolyte multilayers incorporating nanocrystalline cellulose. *Biomacromolecules*, ***7***(***9***), 2522–2530.

Fancy, D. A., & Kodadek, T. (**1999**). Chemistry for the analysis of protein-protein interactions: rapid and efficient cross-linking triggered by long wavelength light. *Proceedings of the National Academy of Sciences*, ***96***(***11***), 6020–6024.

Gerrard, J. A. (**2002**). Protein–protein crosslinking in food: methods, consequences, applications. *Trends in Food Science & Technology*, ***13***(***12***), 391–399.

Grdadolnik, J. (**2002**). A FTIR investigation of protein conformation. *Bulletin of the Chemists and Technologists of Macedonia*, ***21***, 23–34.

Haris, P. I., & Severcan, F. (**1999**). FTIR spectroscopic characterization of protein structure in aqueous and non-aqueous media. *Journal of Molecular Catalysis B: Enzymatic*, ***7***(***1–4***),

207–221.

Hummers, W. S., & Offeman, R. E. (**1958**). Preparation of graphitic oxide. *Journal of the American Chemical Society*, ***80***(***6***), 1339–1339.

Kaboorani, A., & Riedl, B. (**2011**). Effects of adding nano-clay on performance of polyvinyl acetate (PVA) as a wood adhesive. *Composites Part A: Applied Science and Manufacturing*, ***42***(***8***), 1031–1039.

Kaboorani, A., & Riedl, B. (**2012**). Nano-aluminum oxide as a reinforcing material for thermoplastic adhesives. *Journal of Industrial and Engineering Chemistry*, ***18***(***3***), 1076–1081.

Kaboorani, A., Riedl, B., Blanchet, P., Fellin, M., Hosseinaei, O., & Wang, S. (**2012**). Nanocrystalline cellulose (NCC): A renewable nano-material for polyvinyl acetate (PVA) adhesive. *European Polymer Journal*, ***48***(***11***), 1829–1837.

Kamke, F. A., & Lee, J. N. (**2007**). Adhesive penetration in wood—a review. *Wood and Fiber Science*, ***39***(***2***), 205–220.

Khan, U., May, P., Porwal, H., Nawaz, K., & Coleman, J. N. (**2013**). Improved adhesive strength and toughness of polyvinyl acetate glue on addition of small quantities of graphene. *ACS Applied Materials & Interfaces*, ***5***(***4***), 1423–1428.

Khosravi, S., Khabbaz, F., Nordqvist, P., & Johansson, M. (**2014**). Wheat gluten based adhesives for particle boards: effect of crosslinking agents. *Macromolecular Materials and Engineering*, ***299***(***1***), 116–124.

Kodadek, T., Duroux-Richard, I., & Bonnafous, J.-C. (**2005**). Techniques: Oxidative cross-linking as an emergent tool for the analysis of receptor-mediated signalling events. *Trends in Pharmacological Sciences*, ***26***(***4***), 210–217.

Koichi, M., & Tomida, M. (**2004**). Heat-induced secondary structure and conformation change of bovine serum albumin investigated by fourier transform infrared spectroscopy. *Bochemistry*, ***43***(***36***), 11526–11532.

Kong, J., & Yu, S. (**2007**). Fourier transform infrared spectroscopic analysis of protein secondary structures. *Acta Biochimica et Biophysica Sinica*, ***39***(***8***), 549–559.

Krishnamoorthy, K., Veerapandian, M., Yun, K., & Kim, S. J. (**2013**). The chemical and structural analysis of graphene oxide with different degrees of oxidation. *Carbon*, ***53***, 38–49.

Krzyzaniak, A., Burova, T., & Haertle, T. (**1998**). The structure and properties of Napin-seed storage protein from rape (*Brassica napus* L.). *Food/Nahrung*, ***42***(***3***–***4***), 201–204.

Li, N., Qi, G., Sun, X. S., Stamm, M. J., & Wang, D. (**2011**). Physicochemical properties and adhesion performance of canola protein modified with sodium bisulfite. *Journal of the American Oil Chemists' Society*, ***89***(***5***), 897–908.

Li, N., Qi, G., Sun, X. S., & Wang, D. (**2012**). Effects of sodium bisulfite on the physicochemical and adhesion properties of canola protein fractions. *Journal of Polymers and the Environment*, ***20***(***4***), 905–915.

Liu, D., Chen, X., Yue, Y., Chen, M., & Wu, Q. (**2011**). Structure and rheology of

nanocrystalline cellulose. *Carbohydrate Polymers*, ***84***(***1***), 316–322.

Manamperi, W. A. R., Chang, S. K. C., Ulven, C. A., & Pryor, S. W. (**2010**). Plastics from an improved canola protein isolate: preparation and properties. *Journal of the American Oil Chemists' Society*, ***87***(***8***), 909–915.

Mo, X., Sun, X., & Wang, D. (**2004**). Thermal properties and adhesion strength of modified soybean storage proteins. *Journal of the American Oil Chemists' Society*, ***81***(***4***), 395–400.

Nietzel, T., Dudkina, N. V, Haase, C., Denolf, P., Semchonok, D. A., Boekema, E. J., Sunderhaus, S. (**2013**). The native structure and composition of the cruciferin complex in *Brassica napus*. *The Journal of biological chemistry*, ***288***(***4***), 2238–2245.

Pizzi, A. (**2013**). Bioadhesives for wood and fibres. *Reviews of Adhesion and Adhesives*, ***1***(***1***), 88–113.

Sato, S., & Nakamura, H. (**2013**). Ligand-directed selective protein modification based on local single-electron-transfer catalysis. *Angewandte Chemie International*, ***52***, 8681–8684.

Tan, S., Mailer, R., Blanchard, C., & Agboola, S. (**2011**). Canola proteins for human consumption: extraction, profile, and functional properties. *Journal of food science*, ***76***(***1***), R16-28.

Tandang-Silvas, M. R. G., Fukuda, T., Fukuda, C., Prak, K., Cabanos, C., Kimura, A., Maruyama, N. (**2010**). Conservation and divergence on plant seed 11S globulins based on crystal structures. *Biochimica et Biophysica Acta*, ***1804***(***7***), 1432–1442.

Wanasundara, J. P. D. (**2011**). Proteins of Brassicaceae oilseeds and their potential as a plant

protein source. *Critical Reviews in Food Science and Nutrition*, ***51***(***7***), 635–677.

Wang, C., & Wu, J. (**2012**). Preparation and characterization of adhesive from spent hen proteins. *International Journal of Adhesion and Adhesives*, ***36***, 8–14.

Wang, C., Wu, J., & Bernard, G. M. (**2014**). Preparation and characterization of canola protein isolate–poly(glycidyl methacrylate) conjugates: A bio-based adhesive. *Industrial Crops and Products*, ***57***, 124–131.

Wang, Y., Mo, X., Sun, X. S., & Wang, D. (**2007**). Soy protein adhesion enhanced by glutaraldehyde crosslink. *Journal of Applied Polymer Science*, ***104***(***1***), 130–136.

Wu, J., & Muir, A. D. (**2008**). Comparative structural, emulsifying, and biological properties of two major canola proteins, cruciferin and napin. *Journal of Food Science*, ***73***(***3***), C210–C216.

Xu, H., Ma, S., Lv, W., & Wang, Z. (**2011**). Soy protein adhesives improved by SiO_2 nanoparticles for plywoods. *Pigment & Resin Technology*, ***40***(***3***), 191–195.

Zhang, Y., Zhu, W., Lu, Y., Gao, Z., & Gu, J. (**2014**). Nano-scale blocking mechanism of MMT and its effects on the properties of polyisocyanate-modified soybean protein adhesive. *Industrial Crops and Products*, ***57***, 35–42.

Zhu, D., & Damodaran, S. (**2014**). Chemical phosphorylation improves the moisture resistance of soy flour-based wood adhesive. *Journal of Applied Polymer Science*, ***131***(***13***), 40451–40457.

CHAPTER 6 - Randomly Oriented Strand Board Composites from Nanoengineered Protein Based Wood Adhesive

CHAPTER 6

6.1 Introduction

Demand for engineered composite products such as oriented strand boards (OSB), particle boards, medium density fiber boards (MDF), hard boards, and plywood has been increasing rapidly in recent years throughout the world (Salari et al., 2013; Schwarzkopf et al., 2010). Among many engineered composites, OSB has a wide range of applications in sheathing, roofing, subfloors, single layer floors, structural insulated panels in construction industry, packaging and furniture sectors (Mekonnen et al., 2014; Veigel et al., 2012). OSB is manufactured by pressing thin wood strands, which are premixed with a wood adhesive under heat and pressure (Canadian Standards Association, 1993). Depending on the orientation of wood strands, panels are classified either as oriented strand board (OSB) or randomly oriented strand boards (ROSB) (Schwarzkopf et al., 2009). In OSB panels, the direction of surface strands is perpendicular to that of core layers, whereas in ROSB the wood strands are randomly oriented in both core and surface layers (Schwarzkopf et al., 2009, 2010). Both OSB and ROSB panels have unique advantages, such as low cost of production, ability to manufacture with low quality wood logs, and higher production yield over other engineered wood products such as plywood and particleboards. (Rebollar et al., 2007; Salari et al., 2013).

Adhesives used in OSB/ROSB manufacturing play a key role in determining bond quality and mechanical strength (Salari et al., 2013; Veigel et al., 2012). In commercial scale OSB production, liquid phenol formaldehyde (LPF) resins are used on the surface layers whereas isocyanate adhesive (MDI) are used in the core layers of OSB panels (Luo et al., 2015; Mekonnen et al., 2014; Pizzi, 2013; Schwarzkopf et al., 2009; Yuan et al., 2016). MDI adhesives (ex: pMDI) are highly reactive and polymerize rapidly, which is essential for rapid and low temperature adhesive curing. Handling and application of pMDI adhesive is less welcomed due

to its' ability to react with human body and being potentially hazardous to human health as asthma inducers or sensitizers (Dhimiter et al., 2007; Jang et al., 2011). LPF, as another formaldehyde containing adhesives, was reclassified as a carcinogen in 2004 by the International Agency for Research on Cancer (Mekonnen et al., 2014; Schwarzkopf et al., 2009). Therefore, there is an increasing interest in exploring the potential of renewable biopolymers such as protein, tannin, lignin, and polysaccharides as the sources of wood adhesive preparations (Pizzi, 2013; Schwarzkopf et al., 2010; Sen et al., 2015). Proteins have gained special interest, mainly due to their versatile functionalities and flexibility for modifications (Pizzi, 2013). Soy (K. Li, 2007; Schwarzkopf et al., 2009, 2010; Yang et al., 2006), animal byproducts (Mekonnen et al., 2014), wheat gluten (Khosravi et al., 2014) and casein (Guo & Wang, 2016) have been used to prepare OSB panels with various levels of success. Protein-derived adhesives suffer mainly from their low internal bond strength (IB) and modulus of rupture (MOR), as well as weak water resistance (Mekonnen et al., 2014; Rebollar et al., 2007; Schwarzkopf et al., 2009, 2010); they are often used as a partial replacement of synthetic adhesives. For example, adhesive prepared from specified risk material hydrolysate (SRM) copolymerized with 60% MDI resin showed a modulus of elasticity (MOE), MOR, IB, and bond durability of 3.7 ± 0.35 GPa, 21.5 ± 1.0 MPa, 0.4 ± 0.1 MPa, and 3.2 ± 0.0 MPa, respectively, which is significantly lower compared to commercial MDI adhesive (Mekonnen et al., 2014). The lap shear strength of a hybridized adhesive prepared by mixing soy protein and a resin "Kymene® 736H" (polyamido-amine-epichlorohydrin, an underwater adhesive) at ratios of 2:1 or 4:1 (soy protein: Kymene® 736H resin) was increased compared to urea formaldehyde resin (UF) (Li, 2007; Schwarzkopf et al., 2009). A soy protein adhesive prepared by reacting polyethylenimine (245.55 g), maleic anhydride (MA – 39.68 g), sodium hydroxide (12.27 g), and soy protein (933.65 g)

(Schwarzkopf et al., 2010) showed IB, MOE and MOR values similar to commercial adhesive at 7% (w/w adhesive:wood strands) adhesive addition rate.

Canola (*Brassica Spp.*) is the second largest oil seed in the world (Manamperi et al., 2010). The potential of canola protein for preparing adhesive has been previously explored. Li et al., (2011) reported an dry, wet and soaked strengths of 5.28 ± 0.47 MPa, 4.07 ± 0.16 MPa and 5.43 ± 0.28 MPa, respectively, after modifying canola protein with sodium bisulfite. Canola protein modified by 0.5% sodium dodecyl sulphate (SDS) showed dry, wet, and soaked adhesion strengths of 6.00 ± 0.69, 3.52 ± 0.48 MPa, and 6.66 ± 0.07 MPa, respectively (Hale, 2013). Grafting poly (glycidyl methacrylate) into canola protein in our previous study showed dry, wet and soaked strength up to 8.25 ± 0.12 MPa, 3.80 ± 0.15 MPa and 7.10 ± 0.10 MPa, respectively (Wang et al., 2014). Our recent research progress on canola protein adhesives showed that both wet and dry strength of canola protein adhesive was significantly improved with the exfoliation of a nanomaterial, such as graphite oxide (GO) and nanocrystalline cellulose (NCC) (Bandara et al., 2017a, 2017b). Especially, adhesive prepared by exfoliating GO in chemically modified (1% w/w ammonium persulphate) canola protein showed promising adhesion strength (11.82 ± 1.15 MPa, 4.99 ± 0.28 MPa and 10.74 ± 0.72 MPa for dry, wet and soaked strength respectively) in lap shear testing. To evaluate the its potential for commercial applications, it is required to scale up adhesive preparation and produce engineered wood products in a pilot processing plant.

We hypothesize that CPA prepared by exfoliating GO (1% w/w GO/protein) in ammonium persulphate modified canola protein can replace LPF resin of ROSB surface layers without compromising the mechanical and water resistance properties of ROSB composites. Therefore, the objectives of this research were to prepare ROSB composites using nanoengineered canola

protein adhesive at pilot scale and to characterize the adhesive and mechanical properties of ROSB panels.

6.2 Materials and Methods

6.2.1 Materials and Chemicals

Canola meal was provided by Richardson Oilseed Ltd. (Lethbridge, AB, Canada). All chemicals and materials were purchased from Fisher Scientific (Ottawa, ON, Canada) unless otherwise noted. Ammonium persulphate (APS) and graphite were purchased from Sigma-Aldrich (Sigma Chemical Co, St. Louise, MO, USA). Slack wax (100% solid content), commercial liquid phenol formaldehyde (LPF - 57% solid content), polymeric diphenyl methane diisocyanate (pMDI – 100% solid content) and commercial aspen wood strands were provided by Alberta Innovates Technology Futures (AITF) (Edmonton, AB, Canada).

6.2.2 Methods

Pilot scale extraction of canola protein was carried out in the Agri-Food Discovery Place (AFDP) of the University of Alberta (Edmonton, Alberta, Canada). Fabrication, production and characterization of ROSB composites were carried out in a pilot processing plant at Engineered Composite division of Alberta Innovates Technology Futures (AITF, Edmonton, AB, Canada).

6.2.2.1 Canola Protein Extraction

Canola proteins were extracted from finely ground canola meal (100 mesh size), as described by Manamperi et al, (2010) with modifications. Canola meal (40 Kg) was mixed with 400 L of deionized water in a 500 L reactor tank attached with top mounted stirrer (Model XIP 50A, SPX FLOW Lightning Process Equipment, Rochester, New York, USA). After stirring at 180 rpm for 15 m, the pH of the mixture was adjusted to 12.0 by adding 6 M NaOH solution and

stirred for 1 h at the same conditions. The supernatant was collected by centrifugation using continuous decanter (Model Optimum TFEC, Centrifuges Unlimited Inc, Calgary, AB, Canada) at 3000 rpm and 22.89% torque. Following centrifugation, the pH of the supernatant was readjusted to 4.00 using 6 M HCl solution and stirred for 15 m (180 rpm). Protein dispersion was centrifuged at 9000 rpm, at a 218-220 L/hr flow rate using a disc centrifuge (Model LAPX 404, Alpha Laval Inc, Toronto, ON, Canada). The precipitate was collected, mixed with deionized water to remove excess salt (1:10 ratio w/w %), stirred for 30 m, and centrifuged (9000 rpm at a flow rate of 245 L/h) using disc centrifuge (Model LAPX 404, Alpha Laval Inc, Toronto, ON, Canada). The resulting protein precipitate was freeze dried and stored at -20 ^{o}C until adhesive formulation.

6.2.2.2 Graphite Oxide (GO) Preparation

GO nanoparticles were prepared according to the Hummers and Offeman method (Hummers & Offeman, 1958) with slight modifications. Graphite and $NaNO_3$ (20 g each) were mixed in a glass beaker, and 480 mL of concentrated H_2SO_4 was slowly added to the mixture while stirring in an ice bath at 200 rpm for 2 h. Then 60 g of $KMnO_4$ powder was slowly added while maintaining the temperature at 20 ± 3 ^{o}C. After adding $KMnO_4$, the temperature was gradually increased to 35 ± 3 ^{o}C, stirred for 1 h, and then 368 mL of deionized water was added to the mixture, stirred for another 15 m. The remaining unreacted $KMnO_4$ was neutralized by adding 320 mL of hot deionized water (60 ^{o}C) containing 3% H_2O_2. After cooling to room temperature, leftover chemicals were removed by centrifugation (10000g, 15 m, 4 ^{o}C) followed by three cycle washing with deionized water. The final GO precipitate was sonicated for 5 m (at 50% power output), freeze dried and stored at -20 ^{o}C for further use.

6.2.2.3 Formulation of Nanoengineered Canola Protein Adhesive (CPA)

CPA was prepared according to the method developed in our previous study (Bandara & Wu, 2017) with modifications to accommodate pilot scale processing requirements. In a 10 L container 50 g of NaCl (5% w/w, NaCl/protein), 50 g of sodium benzoate (5% w/w, $NaC_6H_5CO_2$ /protein), and 20 g of sodium dodecyl sulphate (2% w/w, SDS/protein) were mixed with 4800 mL of deionized water and stirred for 30 m at 300 rpm. After dissolving, 1 kg of canola protein isolate was added while stirring for 1 h (500 rpm) and the pH was adjusted to 7.0 using 6 M NaOH. Then, 10 g of ammonium persulphate (1% w/w, APS/protein) was added, and stirred for another 4 h (700 rpm) under continuous N_2 purging. After adjusting pH to 5.0 using 6 M HCl, 300 g of $CaCO_3$ (as a filler to increase solid content of final adhesive mixture up to 30% w/v) was added while stirring for 1 h at 1000 rpm. In a separate beaker, 10 g of GO (equivalent to 1% w/w, GO/protein) was mixed with 200 mL deionized water, stirred for 3 h at room temperature (300 rpm) and another 1 h at 45 ± 3 ^oC (700 rpm). The prepared GO dispersion was sonicated for 3 m (5 s intermittent pulse dispersion with 3 s intervals) at 60% amplitude using high intensity ultrasonic dismembrator (Model 500, Thermo Fisher Scientific INC, Pittsburg, PA, USA). Following sonication, the GO dispersion was homogenized for 2 m (2000 rpm) using ULTRA TURRAX high shear homogenizer (Model T25 D S1, IKA® Works, Wilmington, NC, USA). The prepared GO dispersion was slowly added to protein dispersion and stirred for another 30 m (1000 rpm). The prepared canola protein-GO adhesive (CPA) was further sonicated and homogenized under the same conditions as above. The pH of the prepared adhesive was then adjusted to 12.0 by adding 126 g of NaOH pellets (equivalent solid content of NaOH for 30 uL of 6 M NaOH solution /mL adhesive mixture) while continuous stirring at 1000 rpm at room temperature. The final solid content of the adhesive formulation was 30% w/v.

6.2.2.4 Characterization of Exfoliation Properties of Graphite Oxide in Adhesive

Exfoliation of GO in canola protein adhesive was studied using X-ray diffraction (XRD). The experiments were performed using Rigaku Ultima IV powder diffractometer (Rigaku Co. Japan) where Cu-Kα radiation (0.154 nm) was used to collect angle data (2θ) from 5 to 50 degrees. Origin 2016 software (OriginLab Corporation, MA, USA) was used to process and analyze X-ray diffraction data to confirm exfoliation of GO in canola protein matrix.

6.2.2.5 Fabrications of Randomly Oriented Strand Board (ROSB)

ROSB were produced at the Alberta Innovates Technology Futures Engineered Composite Products Laboratory. The core layer of ROSB was fabricated using a commercial pMDI adhesive similar to commercial OSB production while the surface layers were prepared using a mixture of CPA adhesive and a commercial LPF resin at ratios of 0%, 20%, 40%, 60%, 80%, and 100% (w/w, canola adhesive/LPF resin). Three ROSB panels were prepared from each adhesive formulation. Detailed work plan including adhesive formulation and solid addition rates are shown in Table 6.1.

Table 6.1 – Composition of adhesive formulations, and adhesive addition levels used for surface and core layers in ROSB preparation.

Group ID	**Surface**				**Core**	**Surface & Core**
	LPF Resin (%)	**CPA Resin (%)**	**Resin mix solids content (%)**	**Resin addition rate (%)**	**pMDI resin addition (%)**	**Slack wax addition (%)**
LPF	100	0	57.0	3.5	2.2	1.0
20% CPA	80	20	51.6	3.5	2.2	1.0
40% CPA	60	40	46.2	3.5	2.2	1.0
60% CPA	40	60	40.8	3.5	2.2	1.0
80% CPA	20	80	35.4	3.5	2.2	1.0
100% CPA	0	100	30.0	3.5	2.2	1.0

Commercial aspen OSB strands were screened to a uniform size (> 0.48 cm) and air-dried to a moisture content of 3.5% w/w. The adhesive resins and other additives were mixed separately with OSB strands using a drum blender equipped with a spinning disc atomizer (Coil Manufacturing, Surrey, BC, Canada). For the core layer strands, pMDI resin (100% solid content) was added at a level of 2.20% w/w (resin/weight of strands). Surface strands were first mixed with appropriate amount of water (10500 rpm, 1.5 m) and then with each adhesive formulation (8000 rpm, 2 m) at 3.5% w/w solid addition level to reach a final moisture content of 8%. A commercial slack wax (100% solid content) was mixed (10500 rpm, 1.5 m) with both surface and core strands at a level of 1% w/w (weight of wax/weight of strands) following adhesive blending. ROSB mats were fabricated at 25-50-25 % w/w split rate for surface-core-surface strands, where 5.2 kg of blended strands were used to fabricate one randomly oriented mat with a target size, thickness and density of 865 mm × 865 mm, 11.1 mm, and 624 kg/m^3 respectively.

Fabricated mats were pressed at a pressure of 5000 kPa at 205 ^{o}C platen temperature for 4 m using 450 Ton Lab Press equipped with 864 mm × 864 mm platen (Diffenbacher North America Inc, Tecumesh, ON, Canada). The core temperatures and gas release properties of the panels were observed by inserting two thermocouples into the fabricated mat during hot pressing and data were collected using AITF's PressMann panel press monitoring software system. After hot pressing, prepared ROSB panels were trimmed to 711 mm × 711 mm and conditioned according to the panel test requirements as described in ASTM D1037-12 and CSA O437.0-93 (ASTM, 2013; Canadian Standards Association, 1993).

6.2.2.6 Performance Characterization of ROSB Panels

Performance characteristics of ROSB panels such as modulus of rupture (MOR), modulus of elasticity (MOE), internal bond strength (IB), bond durability, and vertical density profile were characterized according to ASTM D1037-12 (ASTM, 2013) standard method and Canadian Standard Association protocol for strand board - CSA O437.0-93 (Canadian Standards Association, 1993). All test specimens were conditioned at 65% relative humidity and 20 ºC temperature for 7 days prior to analysis.

6.2.2.6.1 Static Bending Test

Flexural properties of the prepared ROSB panels were measured using static bending test. Six specimens per ROSB panel were cut into a dimension of 75 mm × 315 mm (width and length respectively). Three point static bending test was conducted using Instron (Instron 4204, Norwood, MA, USA) attached with a 25 kN load cell. Tensile loading was applied at a cross head speed of 5 mm/m to obtain a load/deflection curve. The maximum load at linear range of the curve and the failure curve were used to calculate MOE and MOR using following equations where P_{max} is the maximum failure load (in N), L is the distance between centers of support (in mm), W is the width of test specimen (in mm), and t is the average thickness of test specimen (mm). Increment in load (N) on the straight line of load/deflection curve represents the ΔP, while ΔY represents the increment in deflection at mid-span (in mm) corresponding to P increment in load.

$$Modulus\ of\ rupture\ (MOR) = \frac{3P_{max}L}{2Wt^2}$$

$$Modulus\ of\ elasticity\ (MOE) = \left(\frac{L^3}{4Wt^3}\right) \times \left(\frac{\Delta P}{\Delta Y}\right)$$

6.2.2.6.2 Bond Durability (2 hour boil test)

Bond durability of ROSB specimens were tested using 2 hour boil test as described in CSA O437.0-93 standard specification for strand boards (Canadian Standards Association, 1993). Three test specimens (75 mm × 315 mm) per panel were cut from prepared ROSB panels, submerged in boiling water for 2 h and another 1 h in cold water before testing for MOR as described above.

6.2.2.6.3 Density Profile along Thickness

Six specimens (50 mm × 50 mm) per ROSB panel were prepared, and conditioned prior to the non-destructive density analysis. Each sample was placed in a cassette holder and loaded into density profiler separately. Density profile was measured using QDP X-ray profiler (QDP-01X, Quintek Measurement Systems Inc, Tennessee, USA) by transmitting automated X-ray (0.05 mm profile step resolution) through the specimen along thickness.

6.2.2.6.4 Internal Bond Strength (IB)

Specimens after density profile test were used for measuring IB according to the ASTM D1037-12 (ASTM, 2013) standard method. Specimens were conditioned as per standard method and glued into aluminum alloy sample holding block (50 mm × 50 mm) in Instron using hot melt adhesive. Tensile strength of the specimens were measured by applying tensile loading perpendicular to panel surface of ROSB specimens using Instron (Instron 4204, Norwood, MA, USA) attached with 10 kN load cell. Average IB value was calculated using the formula listed below.

$$Internal\ Bond\ Strength\ (IB) = \frac{Failing\ Load\ (N)}{Length\ (mm)\ \times Width\ (mm)}$$

6.2.2.6.5 24 Hour Soak Test (Thickness Swelling & Water Absorption)

24 h soak test was carried out according to ASTM D1037-12 (ASTM, 2013) standard method in order to determine thickness swelling and water absorption properties of prepared ROSB panels. Two test specimens per ROSB panel were cut into 150 mm × 150 mm size. The prepared specimens were conditioned, measured using a digital varnier caliper (four points in each side, 25 mm inside the edge), weighed and placed under 25 mm of water using a metal grid. Water temperature was maintained at 23 ^{o}C ± 2 ^{o}C during the experiment. After 24 h of submersion, the specimens were removed from water, drained for 10 m and wiped using a paper towel. The weight and thickness of test specimens were measured immediately after draining. Thickness swelling was calculated as the percentage of the original thickness to the swelled thickness, whereas the water absorption was calculated as percentage of the original weight to the swelled weight (Mekonnen et al., 2014).

6.2.3 Statistical Analysis

Mean values of mechanical strength data (MOR, MOE, bond durability, IB, water absorption and thickness swelling) were compared using one-way analysis of variance (ANOVA) followed by Duncan's Multiple Range test ($P < 0.05$) to identify the effects of CPA replacement levels. Statistical data was analyzed using Statistical Analysis System Software (SAS version 9.4, SAS Institute, Cary, NC).

6.3 Results and Discussion

Canola protein adhesive (CPA) was prepared according to the method developed in our previous study using APS and GO. In brief, APS (1%, w/w, APS/protein) was first used to

chemically modify canola protein and then GO (1%, w/w of GO/protein, C/O ratio of GO is 1.40) was added to reinforce adhesive.

6.3.1 Dispersion of GO in Prepared Adhesive

Effectiveness of a nanomaterial in reinforcing polymer matrix largely depends on the exfoliation properties of nanomaterial in the said polymer (Kaboorani et al., 2012; Kaboorani & Riedl, 2012). X-ray diffraction data of canola protein, GO, and dispersed GO sample in canola protein adhesive are shown in Fig 6.1.

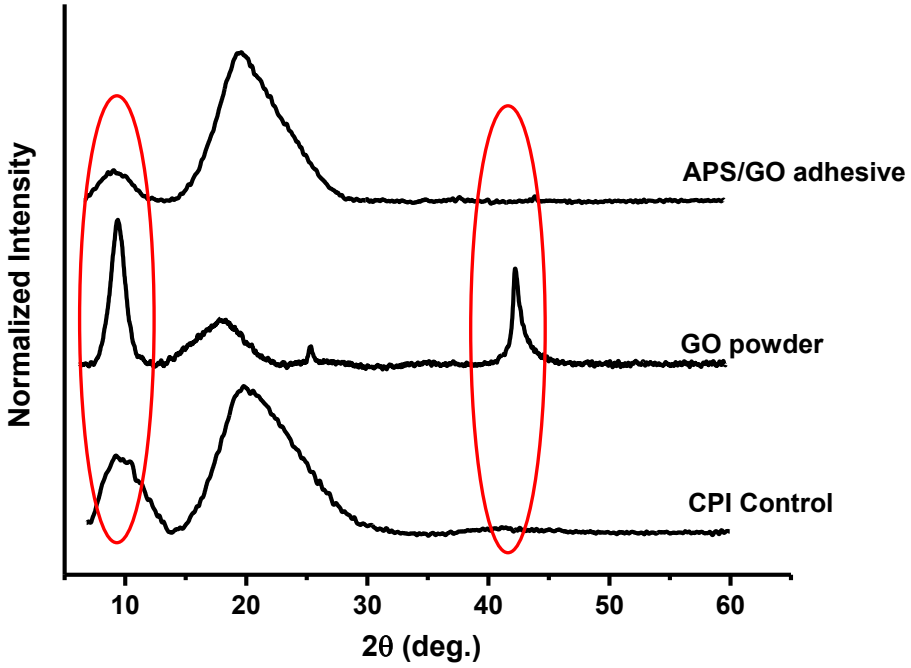

Figure 6.1 – X-ray diffraction pattern of canola protein used in the study (CPI Control), graphite oxide (GO Powder at C/O ratio of 1.40) and CPA adhesive prepared by exfoliating 1% GO (w/w, GO/canola protein) in APS modified canola protein (APS/GO adhesive).

GO sample used for adhesive preparation has three major characteristic crystalline peaks at glancing angles of 9.4°, 19.91° and 42.2° and interlayer spacing of 0.939 nm, 0.495 nm and 0.214

nm, respectively. The characteristic GO crystalline peaks disappeared after exfoliating GO in CPA, indicating the disruption of GO crystalline structure and appropriate exfoliation of GO. Similar results were also observed in other nanomaterials such as nanoclay (Kaboorani & Riedl, 2011), nanocrystalline cellulose (Kaboorani et al., 2012) and nano-SiO_2 (Salari et al., 2013; Xu et al., 2011). The presence of surface functional groups such as –COOH and –OH on GO facilitates the exfoliation of GO in canola protein matrix by increasing –H bonding, while oxidation induced increase in interlayer spacing of GO also facilitate GO exfoliation.

6.3.2 ROSB Composite Preparation

Six groups of ROSB panels were prepared in triplicate using different adhesive formulations. Fig 6.2 shows the representative press curves of ROSB panels prepared with 100% LPF adhesive (Fig 6.2a), 40% CPA (Fig 6.2b) and 100% CPA (Fig 6.2c), respectively. Adhesive formulations did not affect the mat thickness and core temperature of prepared ROSB panels, however, the core gas pressure increased at increasing CPA addition levels. The core gas pressure increased from ~110 KPag at 0% CPA level (100% LPF) to ~130 kPag and ~180 kPag, respectively, at 40% CPA and 100% CPA replacement levels.

The steam generated during the panel pressing at high temperature is the main reason for increasing core gas pressure observed in panels prepared with CPA. Since the moisture content of 100% CPA is ~70% compared to ~43% in LPF adhesive, the higher gas pressure in CPA was mainly due to the presence of a higher moisture content in the ROSB mats. The presence of a higher gas pressure can cause several problems such as steam blow of the panel, delamination, and prone to have higher thickness swelling etc. (Feipeng Liu & Joel Barker, 2007)

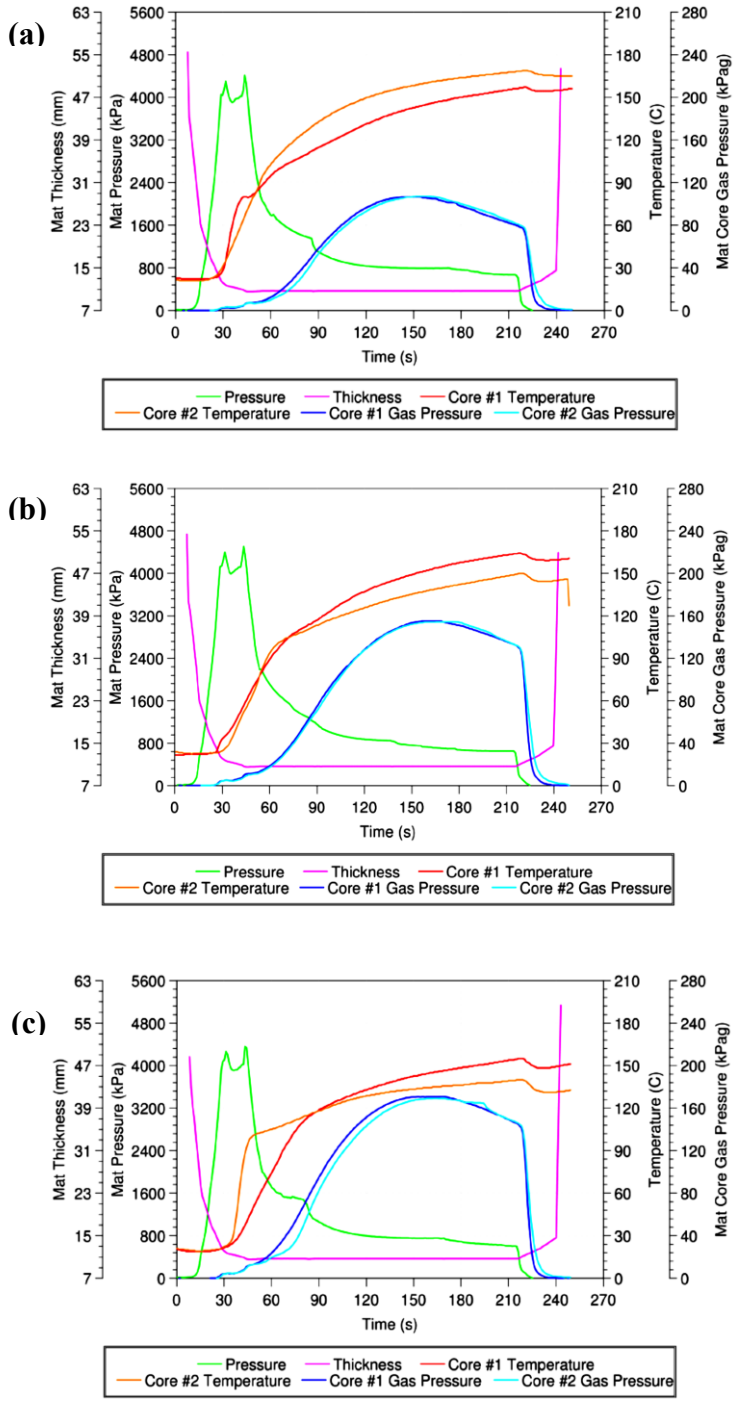

Figure 6.2 – Representative press cycle curves of ROSB fabrication with (a) 100% LPF adhesive, (b) 40% CPA adhesive and (c) 100% CPA adhesives showing mat thickness (mm), mat pressure (KPa), core temperature (^{o}C) and mat core gas pressure (KPag)

6.3.3 Mechanical Performance of ROSB Panels

MOR is an indication of the resistance of permanent bending deformation whereas MOE represents a mathematical description of panel's tendency on elastic deformation (non-permanent deformation) (Mekonnen et al., 2014). Fig 6.3 shows MOR and MOE values obtained from static bending test conducted according to ASTM D1037-12 method. ROSB panels prepared with 100% LPF showed a MOR value of 24.59 ± 3.20 MPa. Replacing LPF adhesive with CPA adhesive up to 60% did not affect MOR; at 80% and 100% CPA addition levels, MOR was significantly reduced to 21.21 ± 2.28 MPa and 20.32 ± 4.74 MPa, respectively.

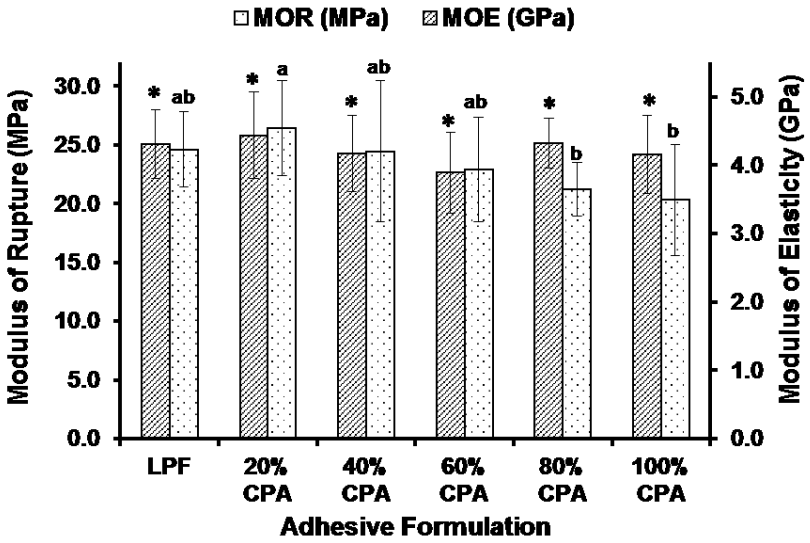

Figure 6.3 – Modulus of rupture (MOR) and modulus of elasticity (MOE) of ROSB panels prepared by replacing 0, 20, 40, 60, 80 & 100% of LPF resin with CPA adhesive. MOE and MOR values were analyzed using one-way ANOVA followed by Duncan test for mean separation. Different letters on the bar represent significantly different MOE and MOR ($p < 0.05$) values. Error bars represent standard deviations. For each CPA replacement level, three ROSB panels were prepared ($n=3$) and minimum 6 composite panel samples per replicate were used for each strength measurement.

A decreasing MOR at increasing CPA addition levels may be attributed to increased filler ($CaCO_3$) and water content in the formulated adhesive, which might interfere bonding at increasing core gas pressure during panel pressing. MOE was not affected by CPA at all addition levels, and values were ranged from 3.89 ± 0.55 GPa to 4.43 ± 0.63 GPa at different CPA addition levels. The minimum required MOR and MOE values for ROSB panels were 17.2 MPa and 3.1 GPa according to CSA 0439.0-93 (Canadian Standards Association, 1993) standard.

ROSB panels prepared with all six adhesive formulations showed MOE and MOR values well above the required standards. CPA at 100% replacement level showed MOR and MOE values of 20.32 ± 4.74 MPa and 4.16 ± 0.57 GPa respectively, which is favorably better than the results of previous OSB panel trials with protein based adhesives found in literature (Mekonnen et al., 2014; Schwarzkopf et al., 2009, 2010). Schwarzkopf *et al* (2010) observed a sharp decrease in both MOE (~ 3.4 GPa) and MOR (~ 15 MPa) values at increasing soy flour content in formulated adhesive up to ~66% (2:1 soy flour / curing agent). Schwarzkopf *et al* (2009) reported an improved MOE and MOR value up to ~4.5 GPa, and ~27 MPa respectively at a 7% (w/w, weight of adhesive/ weight of wood strands) adhesive addition rate for soy adhesive prepared at 1/1 ratio of soy flour and a curing agent; but showed a drastic reduction at 3% adhesive addition rate (~3.2 GPa, and ~17 MPa for MOE and MOR respectively). However, 7% addition rate is higher than the regular adhesive addition levels used in industry which are in the range of 2.5 – 4% (w/w of wood strands) based on the type of panel product (Rowell, 2005). OSB panels prepared with a specified risk material hydrolysate (SRM, copolymerized with MDI adhesive) showed a decreasing MOE values at increasing SRM contents in the formulation; the highest MOE of 3.9 GPa was observed at 60% SRM addition level (Mekonnen et al., 2014). At 70% SRM addition level, both MOE and MOR decreased up to ~3.6 GPa, and ~16.0 MPa

respectively (Mekonnen et al., 2014). The variation of mechanical performance in different adhesive mixtures can be attributed to the spreadability of adhesive, degree of adhesive curing, and the type of chemical bonds formed during curing process (Baier et al., 1968). Adhesive strength of protein based adhesives were generally attributed to chemical bonds such as –H bonds, electrostatic bonds, hydrophobic interactions and mechanical interlocking of cured adhesive (Mekonnen et al., 2014; Pizzi, 2013). The CPA used in this study contain –OH, –COOH, and $–NH_2$ groups that are capable of making –H bonding with wood surface (Mekonnen et al., 2014). The presence of hydrophobic amino acids in canola protein also facilitates the hydrophobic interactions (Wang et al., 2014).

APS mediated chemical modification of canola protein might be another reason for improved panel properties as a strong protein-protein interaction may be achieved due to the APS induced protein cross linking (Fancy & Kodadek, 1999). The GO can contribute to the panel performance either by reinforcing adhesive matrix, or by improving chemical bonding between wood surface and adhesive matrix due to added surface functional groups such as –OH, and –COOH available in GO (Bandara et al., 2017a; Khan et al., 2013). In addition, GO used in this study led to protein secondary structural changes upon exfoliating in canola protein (Bandara et al., 2017a); the exposed hydrophobic functional groups can potentially improve the adhesion and cohesion via hydrophobic interactions with wood surface. Also, GO can act as a crosslinking agent for protein molecules and enhance cohesive interactions (Bandara et al., 2017a), thereby improving mechanical performance of the panel.

6.3.4 Internal Bond Strength

Internal bond strength (IB) of ROSB is defined as the tensile strength required to rupture bonds perpendicular to the grain surface and is a direct indication of the cohesion between wood

strands (André et al., 2008). IB strength of six adhesive formulations used for ROSB fabrication in this study is shown in Fig 6.4. IB strength of ROSB specimens showed a similar trend of MOR, where adding CPA at a level of 20% did not showed a significant difference compared to 100% LPF (IB values of 0.55 ± 0.06 MPa to 0.59 ± 0.09 MPa for 100% LPF and 20% CPA respectively), and then started to decrease at increasing CPA levels. However, all six ROSB panel groups showed IB strength values above the standard requirement of 0.345 MPa according to CSA O437.0-93 standard specification (Canadian Standards Association, 1993) whereas the lowest IB strength reported in this study is 0.35 ± 0.08 MPa at 100% CPA content.

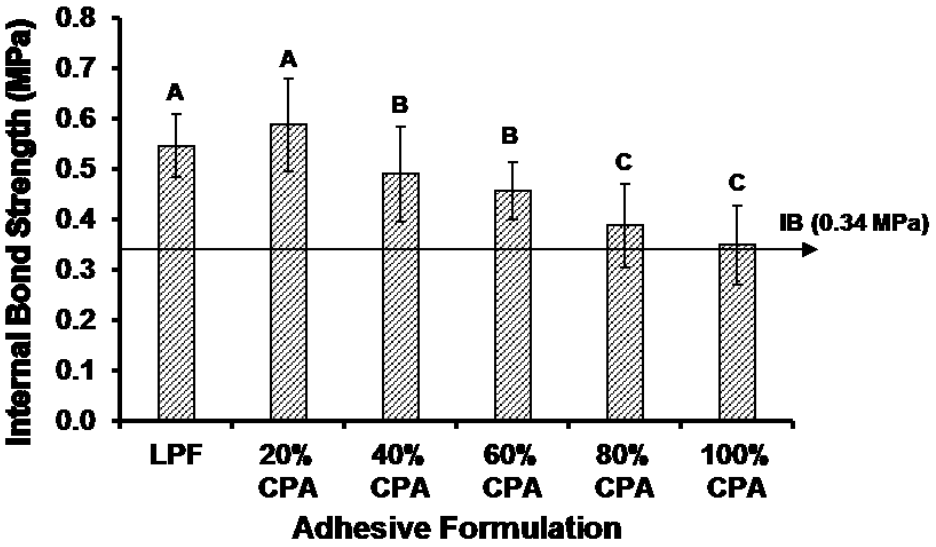

Figure 6.4 – Internal bond strength of ROSB panels prepared by replacing 0, 20, 40, 60, 80 & 100% of LPF resin with CPA adhesive. Internal bond strength values were analyzed using one-way ANOVA followed by Duncan test for mean separation. Different letters on the bar represent significantly different internal bond strength ($p < 0.05$). Error bars represent standard deviations. For each CPA replacement level, three ROSB panels were prepared ($n=3$) and minimum 6 composite panel samples per replicate were used for each strength measurement.

Mekonnen et al., (2014) reported a maximum IB strength of 0.4 ± 0.00 MPa at 50% SRM mixture with MDI adhesive, but a drastic reduction in IB was observed at increasing levels of SRM in the formulated adhesive. In two other studies, comparative IB strength to commercial adhesive was observed for OSB panels prepared using soy protein based adhesives (Schwarzkopf et al., 2009, 2010); however, they used 7% (w/w of wood strand) resin addition level which is significantly higher compared to the 3.5% (w/w of wood strand) addition level used in this study and commercial OSB plant adhesive addition levels (2.5 – 4% w/w of wood strands (Rowell, 2005)). Therefore, CPA adhesive developed in this study provide a significant advantage over previously reported protein based adhesives in preparing ROSB composites.

6.3.5 Bond Durability of ROSB Prepared with CPA

Water resistance or bond durability is a critically important parameter for OSB/ROSB panels for exterior structural applications such as roof sheathing or dry walls (Rebollar et al., 2007). Protein based adhesives generally have weak water resistance (Pizzi, 2013; Wang et al., 2014). Proteins are rich in hydrophilic functional groups such as primary and secondary amines (–NH2, –NH), –COOH (carboxyl), –SH (sulfhydryl), and –OH (hydroxyl) in both protein back bone and side chains (Mekonnen et al., 2014) whereas hydrophobic residues are mainly buried inside the protein structure; therefore hydrogen bonding is the main responsible factor for its adhesion strength. However, such –H bonds are easily disrupted upon exposure to water, thereby lowering water resistance properties of protein based adhesives (Mekonnen et al., 2014; Wang et al., 2014). Bond durability was determined via measuring MOR values of composite panel samples after boiling for 2 h, and effect of CPA addition on bond durability of prepared ROSB panels are shown in Fig 6.5. In all adhesive formulation groups, bond durability was reduced

after 2 h of boiling compared to MOR in dry ROSB panels. Panels prepared with 100% LPF adhesive showed a reduced MOR value of 11.90 ± 1.75 MPa compared to its original MOR of 24.59 ± 3.20 MPa. Replacement of LPF up to 40% in the adhesive formulation showed slight increase (but was not statistically different) in MOR from 11.90 ± 1.75 MPa to 14.06 ± 2.10 MPa and 13.83 ± 2.66 MPa, for 20% and 40% CPA addition levels respectively. Further increasing of CPA content decreased the MOR to 9.54 ± 2.68 MPa, 6.29 ± 1.86 MPa and 4.33 ± 1.99 MPa, for 60%, 80% and 100%, CPA addition respectively. CPA replacement up to 60% showed acceptable bond durability than that of minimum requirement of bond durability as specified by CSA O437.0-93 standard specification (8.6 MPa) (Canadian Standards Association, 1993).

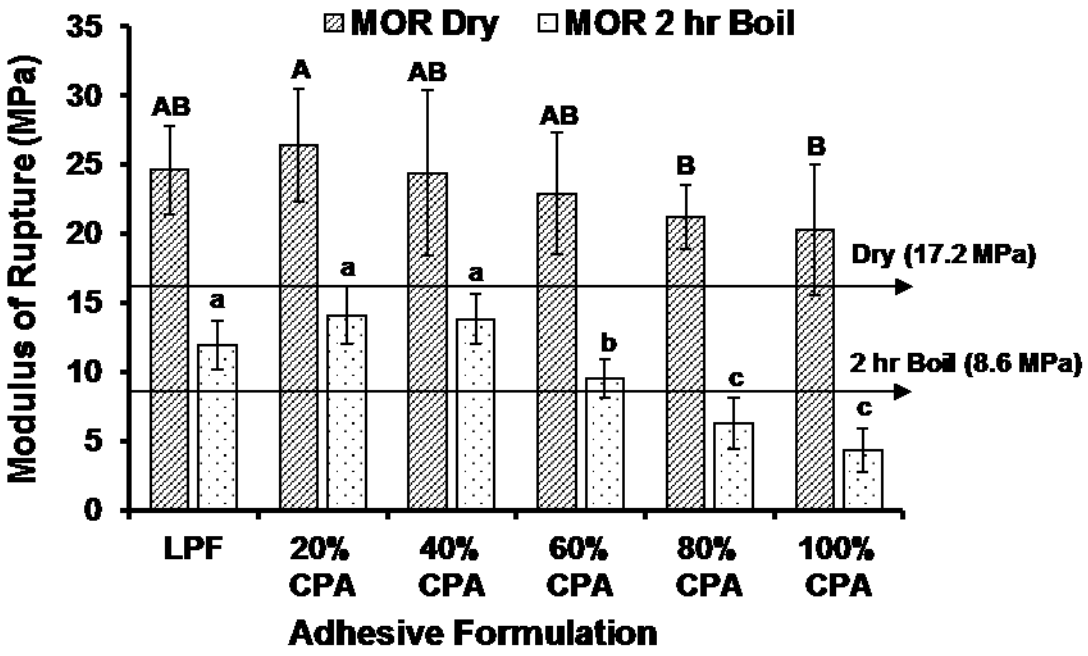

Figure 6.5 – Changes in MOR values of ROSB panels prepared under different LPF replacement levels in 2 hour boil test. MOR values of dry and 2 hour boil test were separately analyzed using one-way ANOVA followed by Duncan test for mean separation. Different letters on the bar represent significantly different MOR value ($p < 0.05$). Error bars represent standard deviations.

For each CPA replacement level, three ROSB panels were prepared (*n=3*) and minimum 3 and 6 sub samples per panel replicate were used for 2 hour boil test (MOR 2 h Boil) and static bending test (MOR Dry) respectively.

Generally, bond durability decreases after 2 h boiling, even in commercial adhesives (100% LPF), mainly due to the loss of –H bonding after exposing to external moisture and heat. Our results showed that adding CPA did not affect detrimentally the performance of CAP formulation up to 40% addition levels. The drastic reduction in bond durability at high CPA addition can be attributed to its low solid content and the presence of inorganic filler in adhesive formulation. Canola protein adhesive has a solid content of 30% (w/w) compared to 57% (w/w) in LPF adhesive; therefore the solid content of the formulation was substantially reduced at increasing CPA addition levels. In preparing CPA adhesive, $CaCO_3$ was added as an inorganic filler to maintain a solid content of 30% in CPA, which can interfere with the cohesion of ROSB strands, thereby reduce bond durability. Furthermore, to maintain the same resin solid addition rate of 3.5% (w/w of wood strand) in the experiment, a greater volume of CPA had to be applied, which added substantial quantity of water in the panels; at pressing, the excessive steam would interfere adhesive interactions with panels, weakening adhesive bonding within the panels.

6.3.6 Thickness Swelling and Water Absorption

Thickness swelling (TS), water absorption (WA) and initial moisture content (MC) of the ROSB panels prepared with different CPA addition levels are shown in Fig 6.6. Initial moisture content of ROSB panels was not affected up to 60% CPA addition, but significantly increased at increasing CPA levels. The hygroscopic nature of added $CaCO_3$ filler might increase the moisture content in the panel. WA of the prepared ROSB panels were slowly increased at

increasing CPA addition levels up to 40% and then rapidly increased at levels over 60% CPA addition. Both TS and WA showed positive correlations with CPA addition levels. Addition of CPA adhesive up to 40% did not showed a significant change in TS of ROSB panels compared to panels made with 100% LPF; but rapidly increased at CPA addition above 60%. The increasing trends in both TS and WA are related to the hydrophilic nature of protein based wood adhesives (Mekonnen et al., 2014; Salari et al., 2013) and the presence of $CaCO_3$ in higher concentration. In addition, the increased amount of moisture added to wood strands at higher CPA replacement levels might be another reason for increased TS and WA.

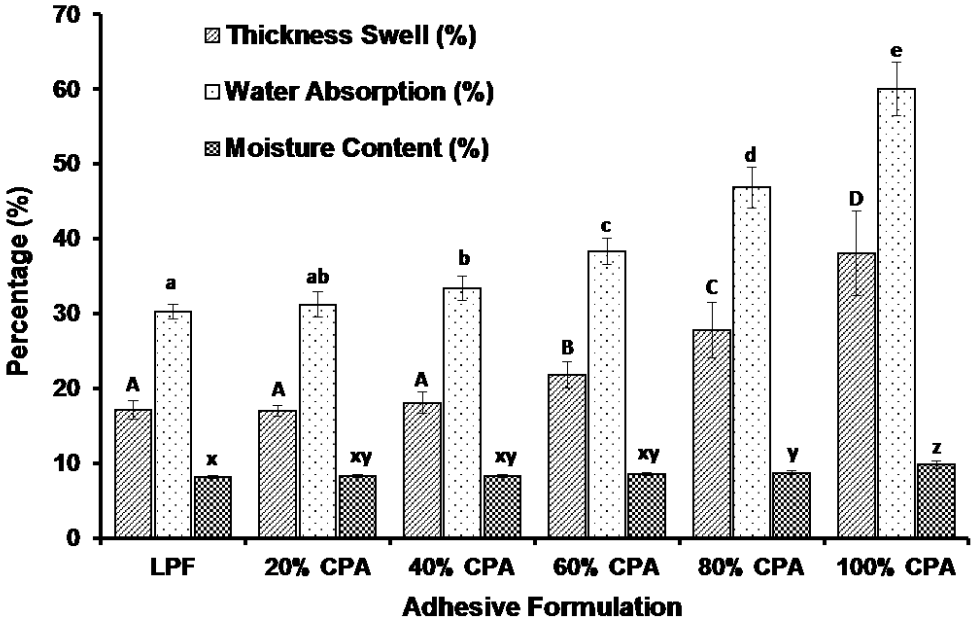

Figure 6.6 – Thickness swell (TS), water absorption (WA) and moisture content (MC) of ROSB panels prepared by replacing 0, 20, 40, 60, 80 & 100% of LPF resin with CPA adhesive. TS, WA, and MC values were analyzed using one-way ANOVA followed by Duncan test for mean separation. Different letters on the bar represent significantly TS, WA and MC ($p < 0.05$). Error bars represent standard deviations ($n=6$).

The highest TS value of 38.05% was observed for the ROSB panels prepared with 100% CPA replacement; in comparison, Mekonnen et al (2014) reported a 35% TS at 40% SRM replacement level (60% MDI) and 115% TS at 85% SRM replacement level. Yang et al (2006) reported a 26%, 35.2%, 84.1% TS values for soy protein adhesives mixed with LPF resin at 50:50, 60:40 and 70:30 (soy protein:LPF resin) ratios respectively. Therefore, the TS observed in this study compared favorably to previously published literature on protein based adhesives.

6.3.7 Density Profile of Prepared Panel

Fig 6.7 shows the representative density profile of ROSB panels prepared in this study with 100% LPF, 40% CPA and 100% CPA adhesive formulation. Vertical density profile of ROSB panels prepared with CPA adhesives also showed a similar density variations to typical composite panels, where it showed a symmetric "M" shape with a higher density in two surface of the panels, and a low density in the panel core (Kei et al., 2008; S. Wang et al., 2007). The presence of density profile is beneficial in improving the bending strength (MOE) of the composite panel. However, a very low density core has a detrimental effect on the internal bond strength of OSB panels (Wang et al., 2007).

The density profile of a wood composite panel depends on the wood fiber type, the moisture content, hot pressing conditions (temperature, closing speed, pressure and duration), and the adhesive type (Wang et al., 2007). Density profiles of six ROSB panels prepared with different CPA replacement levels are shown in Table 6.2. The control sample (100% LPF) exhibits a density of 702.73 ± 39.03 Kg m^{-3}, 543.17 ± 30.28 Kg m^{-3}, and 678.26 ± 34.94 Kg m^{-3} for surface (zone 1), core (zone 2) and surface (zone 3) respectively. The density profile was not

affected at increasing CPA levels, although a slight reduction trend was observed among each panel groups.

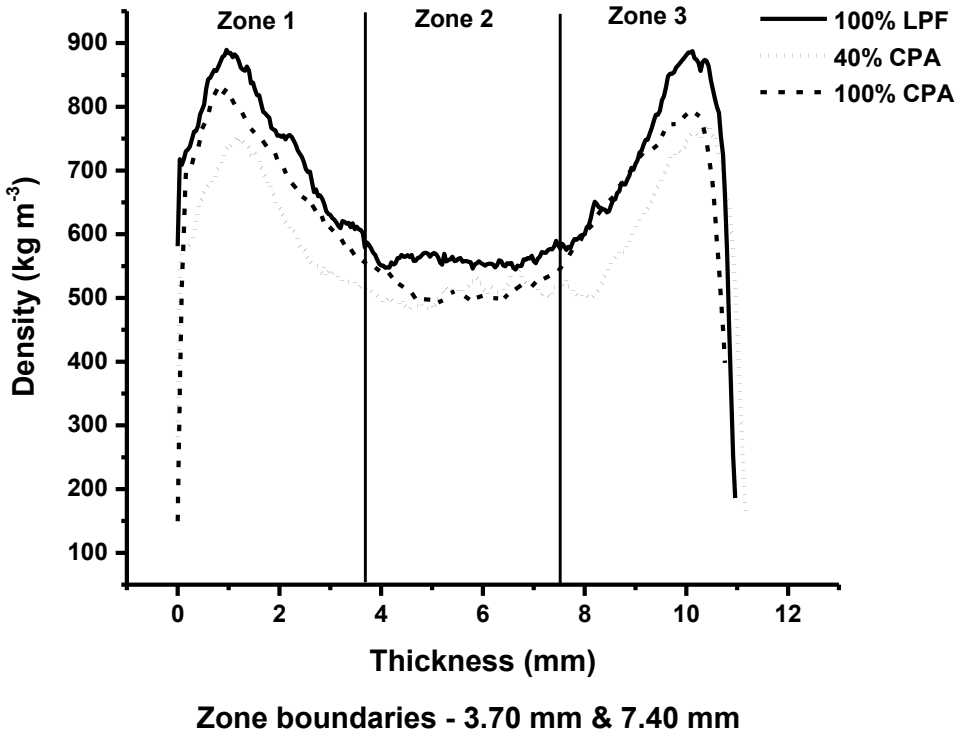

Figure 6.7 – Representative vertical density profiles of a)100% LPF and b) 40% CPA and c)100% CPA adhesives. Zone boundaries were marked at 3.70 mm and 7.40 mm.

In comparison, Mekonnen et al (2014), and Yang et al (2006) showed that the core and surface density of POSB/OSB panels were significantly reduced at increasing protein content in formulated adhesives compared to control adhesive sample. Improved cohesion of adhesive resin molecules occurred due to potential crosslinking induced by GO/APS and mechanical interlocking occurred following adhesive curing might be responsible for maintaining similar density profile among the ROSB panel groups prepared with CPA adhesives.

Table 6.2 – Mean density profile at different zones in ROSB panels prepared with different CPA replacement levels (Mean + standard deviations; *n=6*). Effect of CPA replacement levels on panel density was analyzed using one-way ANOVA followed by Duncan test for mean separation. Different letters in each column represent significantly different density profile ($p < 0.05$).

Adhesive formulation (w/w %)	**Density (Kg m^{-3})**		
	Zone 1	**Zone 2**	**Zone 3**
100% LPF	702.73 ± 39.03^{a}	543.17 ± 30.28^{a}	678.26 ± 34.94^{a}
20% CPA	690.42 ± 31.06^{a}	535.20 ± 25.42^{a}	646.74 ± 27.21^{a}
40% CPA	654.99 ± 60.47^{a}	503.23 ± 32.09^{a}	621.10 ± 42.65^{a}
60% CPA	692.54 ± 76.59^{a}	535.00 ± 55.15^{a}	671.47 ± 80.59^{a}
80% CPA	669.46 ± 45.78^{a}	522.77 ± 16.20^{a}	615.71 ± 27.51^{a}
100% CPA	683.56 ± 6.76^{a}	520.31 ± 15.01^{a}	654.39 ± 8.84^{a}

6.4 Conclusions

Our results showed that replacement of LPF resin with up to 40% of CPA adhesive can produce ROSB panels with comparable performance to that of commercial LPF; however further increasing CPA deteriorated the panel performance. All adhesive formulations including 100% CPA replacement showed mechanical properties well above the minimum requirement for OSB/ROSB panels as specified in CSA O437.0-93 (Canadian Standards Association, 1993). Bond durability met the minimum requirement of CSA O437.0-93 up to 60% CPA replacement, whereas TS and WA retained similar properties to LPF up to 40% CPA content. However, water resistance properties (TS and WA) and bond durability (in 2 h boil test) decreased rapidly at increasing CPA levels above 60% CPA addition level. The reduction in water resistance

properties at higher CPA content can be attributed to the hydrophilic nature of protein-based adhesives, increased filler ($CaCO_3$) and a high water content at high CPA addition levels. The CPA adhesive developed in this study showed improved ROSB panel performance compared to the previous studies with protein based adhesives (Mekonnen et al., 2014; Schwarzkopf et al., 2009, 2010). The improved functionality is a result of increase in hydrogen bonding, increased hydrophobic interactions due to protein structural changes, APS induced protein crosslinking, improved cohesive interactions due to APS and GO modifications and reinforcing effect of exfoliated GO. The ROSB panels prepared with nanoengineered canola protein adhesive has the potential to be used in internal applications at 100% replacement level based on the minimum requirement specified by CSA O437.0-93 standard method while up to 40% CPA replacement can be achieved without compromising mechanical or water resistance properties for exterior and structural applications. Therefore, CPA adhesive can be effectively used in commercial OSB productions, either as 100% resin for specific products or to replace up to 40% of LPF, which will reduce the detrimental effect of formaldehyde based LPF. Further improvements to the solid content in CPA adhesive is required to improve panel performance; therefore, finding alternate reactive filler with adhesive properties or increasing protein content in the adhesive without compromising panel performance is essential.

6.5 References

André, N., Cho, H.W., Baek, S. H., & Jeong, M.K. (**2008**). Prediction of internal bond strength in a medium density fiberboard process using multivariate statistical methods and variable selection. *Wood Science and Technology*, ***42***(***7***), 521–534.

ASTM. (**2013**). *ASTM D1037-13 Standard test methods for evaluating properties of wood-base fiber and particle*. *Annual Book of ASTM Standards*. Available at: https://doi.org/10.1520/D1037-06A.1.2 [2013/03/12]

Baier, R., Shafrin, E., & Zisman, W. (**1968**). Adhesion: mechanisms that assist or impede it. *Science*, ***162***, 1360–1368.

Bandara, N., Esparza, Y., & Wu, J. (**2017**a). Exfoliating nanomaterials in canola protein derived adhesive improves strength and water resistance. *RSC Advances*, ***7(11)***, 6743-6752.

Bandara, N., Esparza, Y., & Wu, J. (**2017**b). Graphite oxide improves adhesion and water resistance of protein–graphite oxide hybrid wood adhesive (Unpublished data).

Bandara, N., & Wu, J. (**2017**c). Chemically modified canola Protein-Nanomaterial Hybrid Wood Adhesive Shows Improved Adhesion and Water Resistance. (Unpublished data)

Canadian Standards Association. (**1993**). Canadian standard association protocol for strand board. *CSA O437-93*, 1–88.

Dhimiter, B., Herrick, C. A., Smith, T. J., Woskie, S. R., Streicher, R. P., Cullen, M. R., Redlich, C. A. (**2007**). Skin exposure to isocyanates: reasons for concern. *Environmental Health Perspective*, ***115***(***3***), 328–335.

Fancy, D. A., & Kodadek, T. (**1999**). Chemistry for the analysis of protein-protein interactions: rapid and efficient cross-linking triggered by long wavelength light. *Proceedings of the National Academy of Sciences*, ***96***(***11***), 6020–6024.

Feipeng Liu, & Joel Barker. (**2007**). Multi-step preheating processes for manufacturing wood based composites. US 7258761 B2. USPTO.

Guo, M., & Wang, G. (**2016**). Whey protein polymerization and its applications in environmentally safe adhesives. *International Journal of Dairy Technology*. ***69(4)***, 481-488.

Hale, K. (**2013**). *The potential of canola protein for bio-based wood adhesives*. (Master's dissertation). Kansas State University.

Hummers, W. S., & Offeman, R. E. (**1958**). Preparation of graphitic oxide. *Journal of the American Chemical Society*, ***80***(***6***), 1339–1339.

Jang, Y., Huang, J., & Li, K. (**2011**). A new formaldehyde-free wood adhesive from renewable materials. *International Journal of Adhesion and Adhesives*, ***31***(*7*), 754–759.

Kaboorani, A., & Riedl, B. (**2011**). Effects of adding nano-clay on performance of polyvinyl acetate (PVA) as a wood adhesive. *Composites Part A: Applied Science and Manufacturing*, ***42***(***8***), 1031–1039.

Kaboorani, A., & Riedl, B. (**2012**). Nano-aluminum oxide as a reinforcing material for thermoplastic adhesives. *Journal of Industrial and Engineering Chemistry*, ***18***(***3***), 1076–1081.

Kaboorani, A., Riedl, B., Blanchet, P., Fellin, M., Hosseinaei, O., & Wang, S. (**2012**).

Nanocrystalline cellulose (NCC): A renewable nano-material for polyvinyl acetate (PVA) adhesive. *European Polymer Journal*, ***48***(***11***), 1829–1837.

Kei, S., Shibusawa, T., Ohashi, K., Castellanos, J. R. S., & Hatano, Y. (**2008**). Effects of density profile of MDF on stiffness and strength of nailed joints. *Journal of Wood Science*, ***54***(***1***), 45–53.

Khan, U., May, P., Porwal, H., Nawaz, K., & Coleman, J. N. (**2013**). Improved adhesive strength and toughness of polyvinyl acetate glue on addition of small quantities of graphene. *ACS Applied Materials & Interfaces*, ***5***(***4***), 1423–1428.

Khosravi, S., Khabbaz, F., Nordqvist, P., & Johansson, M. (**2014**). Wheat gluten based adhesives for particle boards: effect of crosslinking agents. *Macromolecular Materials and Engineering*, ***299***(***1***), 116–124.

Li, K. (**2007**). Formaldehyde-free lignocellulosic adhesives and composites made from the adhesives. US 7722712 B2. USPTO.

Li, N., Qi, G., Sun, X. S., Stamm, M. J., & Wang, D. (**2011**). Physicochemical properties and adhesion performance of canola protein modified with sodium bisulfite. *Journal of the American Oil Chemists' Society*, ***89***(***5***), 897–908.

Luo, J., Luo, J., Yuan, C., Zhang, W., Li, J., Gao, Q., & Chen, H. (**2015**). An eco-friendly wood adhesive from soy protein and lignin: performance properties. *RSC Advances*, ***5***(***122***), 100849–100855.

Manamperi, W. A. R., Chang, S. K. C., Ulven, C. A., & Pryor, S. W. (**2010**). Plastics from an

improved canola protein isolate: preparation and properties. *Journal of the American Oil Chemists' Society*, ***87***(***8***), 909–915.

Mekonnen, T. H., Mussone, P. G., Choi, P., & Bressler, D. C. (**2014**). Adhesives from waste protein biomass for oriented strand board composites: development and performance. *Macromolecular Materials and Engineering*, ***299***(***8***), 1003–1012.

Pizzi, A. (**2013**). Bioadhesives for wood and fibres. *Reviews of Adhesion and Adhesives*, ***1***(***1***), 88–113.

Rebollar, M., Pérez, R., & Vidal, R. (**2007**). Comparison between oriented strand boards and other wood-based panels for the manufacture of furniture. *Materials & Design*, ***28***(***3***), 882–888.

Rowell, R. M. (**2005**). *Handbook of wood chemistry and wood composites*. Boca Raton, Florida: CRC Press.

Salari, A., Tabarsa, T., Khazaeian, A., & Saraeian, A. (**2013**). Improving some of applied properties of oriented strand board (OSB) made from underutilized low quality paulownia (*Paulownia fortunie*) wood employing nano-SiO_2. *Industrial Crops and Products*, ***42***, 1–9.

Schwarzkopf, M., Huang, J., & Li, K. (**2009**). Effects of adhesive application methods on performance of a soy-based adhesive in oriented strandboard. *Journal of the American Oil Chemists' Society*, ***86***(***10***), 1001–1007.

Schwarzkopf, M., Huang, J., & Li, K. (**2010**). A Formaldehyde-free soy-based adhesive for making oriented strandboard. *The Journal of Adhesion*, ***86***(***3***), 352–364.

Sen, S., Patil, S., & Argyropoulos, D. S. (**2015**). Thermal properties of lignin in copolymers, blends, and composites: a review. *Green Chemistry*, ***17***(***11***), 4862–4887.

Veigel, S., Rathke, J., Weigl, M., & Gindl-Altmutter, W. (**2012**). Particle board and oriented strand board prepared with nanocellulose-reinforced adhesive. *Journal of Nanomaterials*, ***2012***, 1–8.

Wang, C., Wu, J., & Bernard, G. M. (**2014**). Preparation and characterization of canola protein isolate–poly(glycidyl methacrylate) conjugates: A bio-based adhesive. *Industrial Crops and Products*, ***57***, 124–131.

Wang, S., Winistorfer, P. M., & Young, T. M. (**2007**). Fundamentals of vertical density profile formation in wood composites. Part III - MDF density formation during hot-pressing. *Wood and Fiber Science*, ***36***(***1***), 17–25.

Xu, H., Ma, S., Lv, W., & Wang, Z. (**2011**). Soy protein adhesives improved by SiO_2 nanoparticles for plywoods. *Pigment & Resin Technology*, ***40***(***3***), 191–195.

Yang, I., Kuo, M., Myers, D. J., & Pu, A. (**2006**). Comparison of protein-based adhesive resins for wood composites. *Journal of Wood Science*, ***52***(***6***), 503–508.

Yuan, C., Luo, J., Luo, J., Gao, Q., & Li, J. (**2016**). A soybean meal-based wood adhesive improved by a diethylene glycol diglycidyl ether: properties and performance. *RSC Advances*, ***6***(***78***), 74186–74194.

CHAPTER 7 - Biomimetic Soy protein Adhesive Inspired by Mussel Adhesion

CHAPTER 7

7.1 Introduction

Agricultural and food industries generate a great deal of byproducts and waste streams. Soybean meal (Kalapathy et al., 1996; Zhu & Damodaran, 2014), canola meal (Wanasundara, 2011), distillers grain (Anderson & Lamsal, 2011; Bandara et al., 2011), poultry feathers (Ullah et al., 2011) and livestock byproducts (Wang & Wu, 2012) are some of the major agricultural byproduct streams available in North America. These byproducts are abundantly available, low in cost and have limited value added applications. It is widely recognized that value addition to these low-value byproduct streams is essential to sustain the agri/food industries. In addition to food and feed uses, there is an increasing interest in exploring the potential of these materials as sources of industrial products such as plastics and adhesives (Bandara et al., 2013; Lambuth, 1994; Yuan et al., 2016).

Wood adhesives were historically made from animal and plant proteins such as bone meal, blood, fish meal, soy flour etc (Lambuth, 1994). However, the rise of low cost synthetic adhesives hinders the widespread applications of biobased adhesives. Petrochemical byproduct based phenol formaldehyde (PF), urea formaldehyde (UF), and melamine urea formaldehyde (MUF) dominate today's adhesive market (Pizzi, 2013). These synthetic adhesives are facing sustainability and environmental issues due to their non-renewability and emission of volatile organic compounds (Pizzi, 2013; Wang & Wu, 2012). Soy proteins have been extensively studied for the adhesive applications; however, the challenge remains in developing technologically applicable adhesive with high adhesion strength and water resistance (Liu et al., 2010; Qi et al., 2016).

Nature itself provides great examples of adhesives with high strength and water resistance such as mussel adhesion, barnacle adhesion, gecko adhesion, to name a few (Bandara, et al.,

2013). Biomimetics is an emerging research area where scientists are studying structure function relationship of complex biological systems in order to develop advanced materials by mimicking their properties (Lee et al., 2006). Mussel adhesion has fascinated many scientists in biomimetic research area over the time, due to its strong underwater adhesion and ability to bind into virtually any kind of surface (Bandara, et al., 2013; Liu et al., 2010; Liu & Li, 2002, 2004). The adhesion mechanism of mussel adhesive proteins were not fully understood, but the presence of post translationally modified amino acid 3,4-dihydroxyphenylalanine (DOPA) is considered to be the main contributing factor in strong mussel adhesion. DOPA is a highly reactive functional group that can adhere with both organic and inorganic surfaces (Bandara, et al., 2013). Fig 7.1 shows the schematic representation of possible DOPA oxidation and crosslinking reactions. Direct chemical interactions via catechol side chains of DOPA, or crosslinking of DOPA groups following oxidation into DOPA-quinone via aryl-aryl coupling or Michael additions in the presence of amine groups were considered to be the primary means of DOPA polymerization (Burzio & Waite, 2000; Haemers et al., 2003).

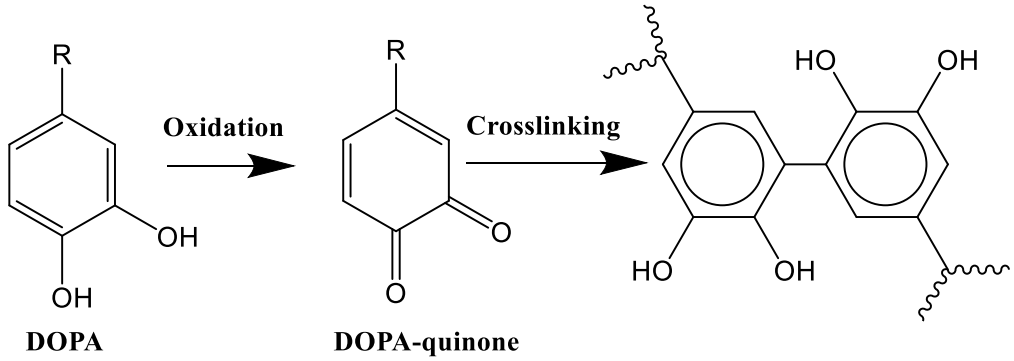

Figure 7.1: Schematic representation of DOPA, oxidation of DOPA into DOPA-quinone and crosslinking of DOPA-quinone

Unoxidized DOPA can create strong yet reversible coordination bonds with inorganic surfaces, while oxidized DOPA-quinones can create covalent bonds with organic surfaces which allows DOPA to be adhere with almost any surface (Bandara, et al., 2013; Lee et al., 2006). Noncovalent interactions such as electrostatic interactions and hydrogen bonding were also observed with more reactive surfaces like mica (Lin et al., 2007). In addition, the presence of metal ions such as copper, iron, manganese and zinc is believed to play a vital role in mussel adhesion, mainly in crosslinking of proteins (Bandara et al., 2013; Liu et al., 2010). The potential of DOPA in creating wide array of interactions, the presence of different type of polymerization mechanisms, and crosslinking ability allows DOPA to create strong adhesive interaction with the surface functional groups and cohesive interaction within bulk adhesive itself, thereby providing strong adhesion strength (Lee et al., 2006).

However, most proteins do not contain DOPA in their native peptide sequences. Therefore, several attempts have been made to use the knowledge on mussel adhesion to develop high strength wood adhesives (Liu et al., 2010; Liu & Li, 2002, 2004; Song et al., 2016). Liu & Li, (2002) successfully grafted DOPA residue into soy protein isolate via an amide linkage through a multistep chemical route. At 8.95% grafted DOPA content, a dry adhesion strength of ~3.5 MPa was retained even after three water soaking and drying (WSAD) cycles. They attributed the improvement of DOPA grafted soy protein adhesive to crosslinking between adjacent DOPA functional groups. Liu & Li, (2004) biomimetically modified soy protein by grafting cysteamine via amide linkages using another multistep chemical route to increase the free mercapto groups (–SH) content in soy protein. At 2.09% (w/w) –SH group content, a dry adhesion strength of ~5 MPa was retained up to three WSAD cycles, due to –SH mediated disulfide bond formation and crosslinking with DOPA-quinone. Liu et al., (2010) used sub-micron/nano size $CaCO_3$

crystalline arrays to improve adhesion of soy protein via ionic crosslinking and reported a dry adhesion strength about ~6.2 MPa at 3% (w/w) $CaCO_3$ addition level. In a more recent study, Song et al., (2016) used recombinant mussel adhesive protein extracted directly from *Escherichia coli* BL21(DE23) cell lines as a wood adhesive and reported a bulk adhesion strength about ~2.5-3.0 MPa.

Grafting of DOPA or –SH groups showed great potential in improving adhesive strength, however these modifications require a complex chemical route involving use of several toxic chemicals and multiple steps that are not cost-effective in wood adhesive applications. The use of recombinant mussel adhesive proteins is costly and has a low output, thus is impractical (Song et al., 2016). Therefore, there is a need to develop an alternative method to prepare cost-effective biomimetic adhesive. Although soy proteins do not contain DOPA residues, they are rich in tyrosine (Tyr) and phenylalanine (Phe), accounting for ~25 (g/kg dry matter), and ~37 (g/kg dry matter) respectively (Grala et al., 1998). Tyrosinase enzyme has been widely used in several biochemical reactions to convert Tyr residues into DOPA, specifically in biomedical research field (Ito et al., 1984; Zhang et al., 2010). We hypothesize that conversion of naturally present amino acids into DOPA residue followed by adding adhesion induced additives (NaOH and Fe^{3+}) will improve adhesion and water resistance of soy protein adhesive. Therefore, the objectives of this study were to convert existing Tyr residues into DOPA using enzymatic modification, to determine the effects of induced additives on adhesion, and to apply modified protein adhesive into wood and other surfaces.

7.2 Materials and Methods

7.2.1 Materials and Chemicals

All chemicals were purchased from Fisher Scientific (Ottawa, ON, Canada) unless otherwise noted. Ethylenediamine, 3,4-dihydroxy phenylalanine (DOPA), 3-methyl-2-benzothiazolinone hydrazine hydrochloride monohydrate (MBTH) and ethylenediamine dihydrochloride was purchased from Sigma-Aldrich (Sigma Chemical Co, St. Louise, MO, USA). Soy protein was purchased from MP Biomedicals (MP Biomedicals LLC, Irvine, CA, USA). Wood veneers were purchased from Windsor Plywood (Edmonton, AB, Canada).

7.2.2 Method

7.2.2.1 Biomimetic Modification of Soy Protein

Soy protein was weighed (10 g each) in triplicate and mixed with deionized water to make 10% w/v dispersion, pH was adjusted to 5.0 using 1 M HCl solution and stirred for 30 m (250 RPM) at room temperature. Soy protein dispersion was transferred to a mini reactor (Model: Trallero HME-R, Trallero and Schlee Inc, La Llagosta, Barcelona, Spain), temperature adjusted to 25 ^{o}C ± 2 ^{o}C, and stirred for another 15 m at 300 rpm under N_2 purging. Tyrosinase enzyme was added to the protein dispersion at a ratio of 50 μg/g (tyrosinase/protein), and stirred for 2 h (25 ^{o}C ± 2 ^{o}C, 250 rpm) under continuous N_2 purging. After the reaction, tyrosinase modified soy protein sample was stored at 4 ^{o}C in air-tight container until further use for adhesive application. Negative control sample (SPI) was prepared by dispersing soy protein in deionized water at 10% w/v, and following similar conditions to TSPI preparation except adding tyrosinase enzyme.

7.2.2.2 Optimizing Adhesive Application Conditions

Polymerization of DOPA functional groups depend on several external factors such as metal ions, pH of the reaction solution, and the presence of oxidants (Hight & Wilker, 2007;

Hwang et al., 2010). Specifically, Fe^{3+} plays a critical role in DOPA polymerization. Therefore, effects of NaOH and Fe^{3+} on adhesion were studied. The optimum NaOH concentration for the adhesive application was determined by preparing a series of tyrosinase modified soy protein adhesives with different NaOH additions ranging from 5 µl, 10 µl, 20 µl, 30 µl, and 50 µl of 6 M NaOH solution per mL of 10% (w/v – protein:water) DOPA converted soy protein solution (without $FeCl_3$ addition). The optimum Fe^{3+} ion concentration for adhesion improvement was determined by preparing another series of tyrosinase modified soy protein adhesives with different $FeCl_3$ addition levels (in the absence of NaOH) ranging from 10 µl, 20 µl, 30 µl, and 40 µl of 0.2 M $FeCl_3$ solution per mL of 10% (w/v – protein:water) DOPA converted soy protein solution.

7.2.2.3 Adhesion Strength Measurement

Biomimetic adhesive was prepared at optimum NaOH and Fe^{3+} concentrations using tyrosinase treated soy protein (TSPI). Veneer samples (Birch, 1.2 mm thickness) were cut into 20 mm × 120 mm (width and length) using a cutting device (Adhesive Evaluation Systems, Corvallis, OR, USA), and conditioned for seven days (23 ^{o}C and 50% humidity) in a controlled environment chamber (ETS 5518, Glenside, PA, USA) as per the specifications of ASTM D2339-98 (2011) standard method (ASTM, 2011). Adhesive samples were spread in a contact area of 20 mm × 5 mm at an amount of 40 µL/veneer strand. Following adhesive application, veneer samples were air dried for 5 min and hot pressed for 10 m (at 120 ^{o}C and 3.5 MPa) using Carver manual hot press (Model 3851-0, Carver Inc., In, USA). ASTM standard method D2339-98 (2011) (ASTM, 2011) was followed to measure dry adhesion strength (DAS) where tensile loading required to pull bonded veneer was measured using Instron machine (Model 5565, Instron, MA, USA) equipped with 5 kN load cell. ASTM standard method D1151-00 (2013) was

used to measure wet adhesion strength (WAS) and soaked adhesion strength (SAS) using instron tensile loading (ASTM, 2013). All tensile strength data was collected using Bluhill 3.0 software (Instron, MA, USA). Bonded veneer samples were submerged in 48 h in water (23 ºC) prior to measuring WAS values, while SAS was measured after reconditioning submerged veneer samples for seven days at 23 ºC and 50% relative humidity in a controlled environment chamber (ETS 5518, Glenside, PA, USA). To measure adhesion into mica, glass and polystyrene surfaces, samples were prepared in same size (20 mm × 120 mm) from each material, adhesive were applied in same volume to wood, but cold pressed at room temperature for 24 h while applying 1 MPa pressure. Each adhesive formulation was prepared in triplicate ($n=3$) and minimum of four bonded veneer samples per replicate were used in testing adhesion strength. Veneer samples were clamped to Instron with a 35 mm gauge length and tested at 10 mm/m cross head speed.

7.2.2.4 Characterization of DOPA Functional Groups in Modified Proteins

The presence of DOPA functional group after protein modification was determined using the method described by Kuboe et al (2004) (Jus et al., 2008; Kuboe et al., 2004). Tyrosinase modified (TSPI) and unmodified proteins (SPI) were dispersed in deionized water at a concentration of 5 mg/mL, and stirred for 2 h (300 rpm, room temperature). From each dispersion, 100 µL was pipetted out in duplicate, and mixed with 3920 µL deionized water, 280 µL of ethylenediamine and 200 µL of 2 M ethylenediamine dihydrochloride at pH 11.00, vigorously vortexed, and incubated at 50 ºC for 2 h in dark. The fluorescence intensity of prepared samples were measured at excitation and emission wavelength of 420 nm and 543 nm respectively, with a quartz cell (1 cm path length) and 5 nm slit width using Shimadzu RF-5301PC spectrofluorophotometer (Shimadzu Scientific Instruments, Kyoto, Japan). A series of DOPA standard solutions (0.05 mM, 0.025 mM, 0.01 mM, 0.005 mM, and 0.001 mM) were used

to generate a DOPA standard curve and the concentrations of DOPA residue in modified protein were calculated against the DOPA standard fluorescent curve.

7.2.2.5 Changes in Surface Hydrophobicity of Modified Proteins

The surface hydrophobicity of soy protein and tyrosinase modified soy proteins were measured using 1-anilinonaphthalene-8- sulfonic acid (ANS) fluorescent probe method (Alizadeh-Pasdar & Li-Chan, 2000). Modified and unmodified soy protein samples were diluted to five concentrations ranging from 0.0025 mg/ml to 0.05 mg/ml using citrate buffer. Then, 4 mL of diluted protein samples were mixed with 20 μL of 8 mM ANS solution, vortexed and fluorescence intensity was measured at excitation and emission wavelengths of 390 nm and 470 nm respectively with a quartz cell (1 cm path length and 5 nm slit width) using Shimadzu RF-5301PC spectrofluorophotometer (Shimadzu Scientific Instruments, Kyoto, Japan). The changes in fluorescence emission plot in the range of 400 nm to 625 nm were used as an indication of the changes in protein surface hydrophobicity.

7.2.2.6 Site-Specific Modifications and Protein Structural Changes

Site-specific protein modifications of Tyr and His amino acid residues and protein secondary structures of tyrosinase modified soy proteins and adhesive samples were characterized using Nicolet 8700 Fourier transform infrared spectrometer (Thermo Eletron Co. WI, USA). All samples were dried prior to FTIR analysis by freeze-drying and further drying with P_2O_5 in a hermetic desiccator for two weeks. Dried protein samples were mixed with potassium bromide (KBr), and milled into a powdered pellet. IR spectra of protein samples in the range of 400-4000 cm^{-1} were collected using 128 scans at a resolution of 4 cm^{-1}. IR spectral data was analyzed using Origin 2016 software (OriginLab Corporation, MA, USA) to identify

changes in specific functional groups, and protein secondary structures by deriving second derivative spectra using Savitzky-Golay smooth function followed by curve fitting.

7.2.2.7 Changes in Thermal Transitions

Effect of tyrosinase modification on thermal transitions of protein was characterized using differential scanning calorimeter (Perkin-Elmer, Norwalk, CT, USA). Protein samples were first freeze-dried and further dried with P_2O_5 in a hermetic desiccator for two weeks to remove sample moisture. DSC instrument was calibrated for temperature and heat flow using pure indium reference samples prior to sample analysis. Protein samples were accurately weighed (~6 mg each) into T-Zero hermetic aluminum pans. They were mixed with 60 µL of 0.01 M phosphate buffer, and hermetically sealed with lids. DSC samples were equilibrated at 0 ºC for 10 m and thermodynamic data was collected while heating samples from 0 to 250 ºC under continuous nitrogen purging at a ramping rate of 10 ºC m^{-1}. Heat flow differential of samples were recorded against the empty reference pan. Collected DSC data was analyzed using Universal Analysis 2000 software (Perkin-Elmer, Norwalk, CT, USA).

7.2.3 Statistical Analysis

All adhesive samples were prepared in triplicate (*n=3*) while minimum of five samples were tested for adhesion strength testing. Dry, wet and soaked adhesion strength data was analyzed using analysis of variance (ANOVA) followed by Duncan's Multiple Range (DMR) test to identify the effects of tyrosinase modification, and effect of additives (NaOH and Fe^{3+}) on adhesion strength. Adhesion data was processed using Statistical Analysis System Software (SAS version 9.4, SAS Institute, Cary, NC). Effects of tyrosinase modification and additives on adhesion strength were evaluated at the 95% confidence level.

7.3 Results and Discussion

7.3.1 Characterization of DOPA Functional Groups

The presence of DOPA functional groups after tyrosinase modification was characterized using spectrofluorometric method as shown in Fig 7.2. Catechol side chains of DOPA residues shows a condensation reaction with ethylenediamine to produce a fluorescent emitting compound that has optimum excitation and emission wavelengths of 420 nm and 543 nm, respectively (Kuboe et al., 2004; Ohkawa et al., 1999).

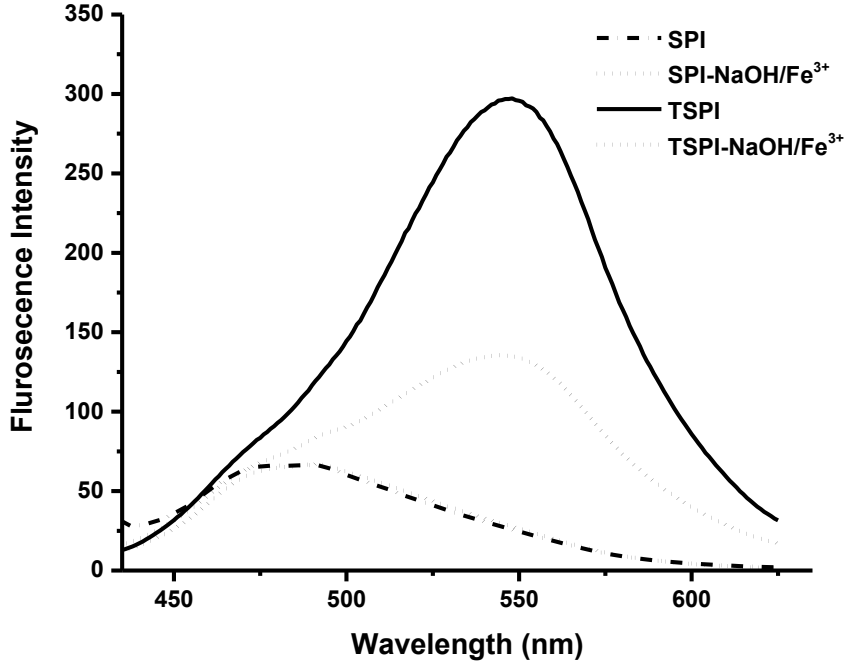

Figure 7.2: Fluorescence emission spectra (excitation wavelength: 390 nm, emission wavelength range: 400-625 nm) of soy protein (SPI), modified soy protein with tyrosinase enzyme (TSPI), adhesives prepared (by adding 30 µL/mL 6 M NaOH/adhesive, and 30 µL/mL 0.2 M $FeCl_3$/adhesive) with native soy protein (SPI-NaOH/Fe^{3+}) and modified soy protein with tyrosinase enzyme (TSPI-NaOH/Fe^{3+}) showing presence of DOPA functional group.

Unmodified DOPA samples showed a minor fluorescent intensity, which can be a result of intrinsic fluorescent emission of other amino acids present in the reaction mixture. At emission wavelength of 543 nm, DOPA condensation product shows optimum fluorescent absorption; while other fluorescent emitting amino acids such as Tyr, Trp and DOPA have minute amount of fluorescent emission at same wavelength (Ohkawa et al., 1999). Tyrosinase modification increased the fluorescent intensity of TSPI sample significantly compared to the SPI sample. However, after adding NaOH and Fe^{3+} ions into TSPI sample to make adhesive (TSPI-NaOH/Fe^{3+}), a reduction in fluorescent intensity was observed. DOPA is a highly reactive compound that can easily undergo through polymerization into DOPA-quinone, especially at higher pH values. Adding Fe^{3+} ions induced crosslinking of DOPA and DOPA-quinone's (Lee et al., 2006), altogether resulted a reduction in fluorescent intensity as observed in Fig 7.2.

Table 7.1 – DOPA content of soy protein (SPI), modified soy protein with tyrosinase enzyme (TSPI), adhesives prepared with native soy protein (SPI-NaOH/Fe^{3+}) and modified soy protein with tyrosinase enzyme (TSPI-NaOH/Fe^{3+}). Percentage conversion of Tyr to DOPA was calculated based on the estimated Tyr content of 25 g/Kg in soy protein isolate as reported by Grala et al (1998) [24].

Sample Name	**DOPA Content (mg/g)**	**Percentage conversion (%)**
SPI	-0.83 ± 0.01	~ -3.30
SPI-NaOH/Fe^{3+}	-0.23 ± 0.15	~ -1.02
TSPI	12.17 ± 0.03	~ 48.69
TSPI-NaOH/Fe^{3+}	7.08 ± 0.96	~ 28.32

Quantification experiments (Table 7.1.) showed a 12.17 ± 0.03 mg/g DOPA content in TSPI samples compared to negligible DOPA content in unmodified proteins. Tyr content of soy protein was reported to be 25 g/kg (DM basis) (Grala et al., 1998); therefore the estimated percentage of DOPA conversion is about ~48% of the total Tyr present in soy protein. Similar to our observation in the Fig 2, addition of NaOH and Fe^{3+} ions in TSPI- NaOH/Fe^{3+} adhesive samples reduced the available DOPA content to 7.08 ± 0.96 mg/g.

FTIR characterization of modified protein also provided further confirmation on the presence of DOPA in TSPI and TSPI- NaOH/Fe^{3+} adhesive samples. Fig 7.3a shows the IR absorbance intensities in the range of 1400 cm^{-1} to 1800 cm^{-1} wavelength highlighting site specific modifications of Tyr residues. Amino acid side chain vibrations can be used to identify site specific modifications of proteins (Grdadolnik, 2002; Kong & Yu, 2007). Especially, Tyr ring –OH group has the distinctive vibration at 1518 cm^{-1}, and 1602 cm^{-1} wavelengths which can be used to identify protein modifications (Kong & Yu, 2007).

The absorbance intensity of Tyr ring –OH group at both wavelengths (1518 cm^{-1}, and 1602 cm^{-1}) of TSPI samples increased significantly compared to SPI sample, indicating increased amount of Tyr ring –OH groups in modified proteins. As evidenced in the DOPA quantification results, protein modification with tyrosinase enzyme has modified the existing Tyr residues in soy protein into DOPA (Ito et al., 1984; Zhang et al., 2010). The increase in DOPA residues will increase the presence of –OH groups attached to Tyr ring as shown in Fig 7.3b. These added –OH groups can potentially contribute to the increased side chain IR absorbance observed in TSPI sample. However, preparing adhesive by adding NaOH and Fe^{3+} ions reduced the Tyr –OH side chain vibration of SPI-NaOH/Fe^{3+} and TSPI-NaOH/Fe^{3+} samples. As evidenced in several previous studies, presence of higher pH and Fe^{3+} ions catalyze DOPA polymerization into

DOPA-quinone and crosslinking (Guvendiren et al., 2007; Lee et al., 2006; Zeng et al., 2010), thereby reducing the –OH groups that can generate intrinsic IR absorbance at 1518 cm^{-1}, and 1602 cm^{-1} wavelengths.

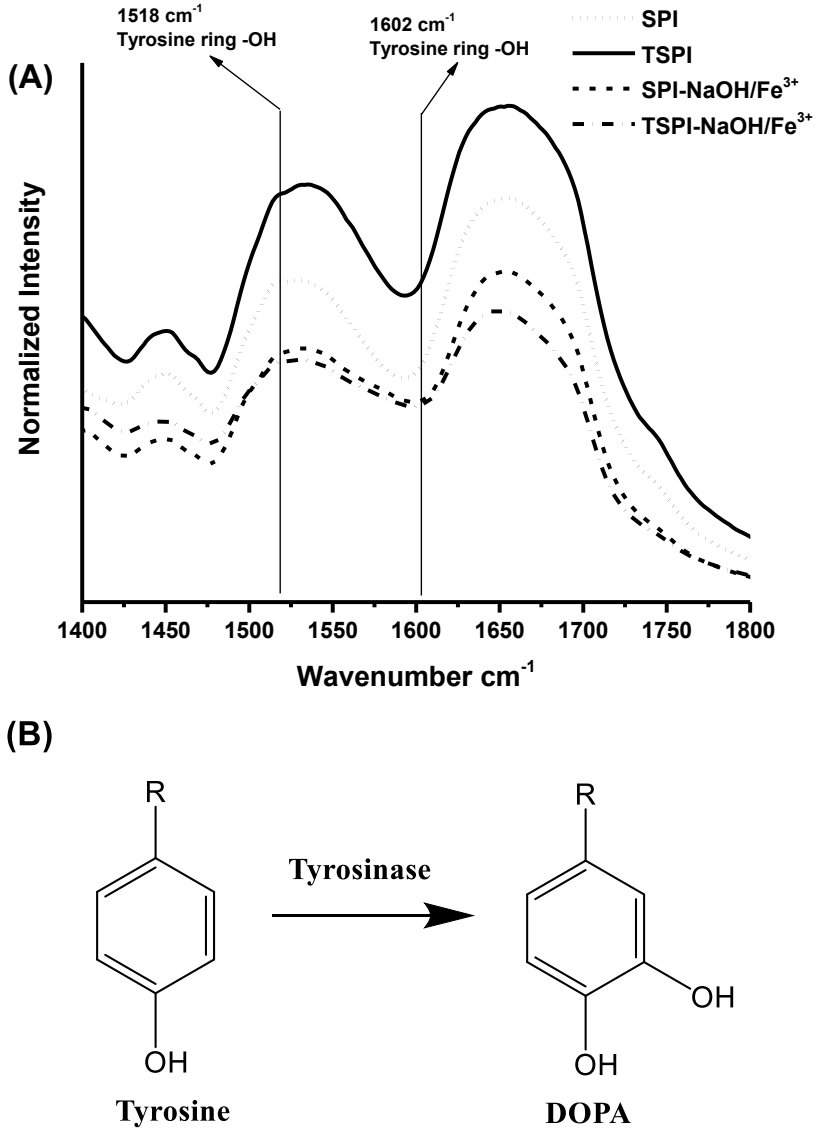

Figure 7.3: (A) Enlarged FTIR spectra (1400 -1800 cm^{-1}) showing changes in absorption intensities of tyrosine side chain –OH groups, (B) schematic representation of conversion of Tyr into DOPA.

7.3.2 Changes in Surface Hydrophobicity of Modified Protein

Effect of tyrosinase modification on surface hydrophobicity of soy protein is shown in Fig 7.4.

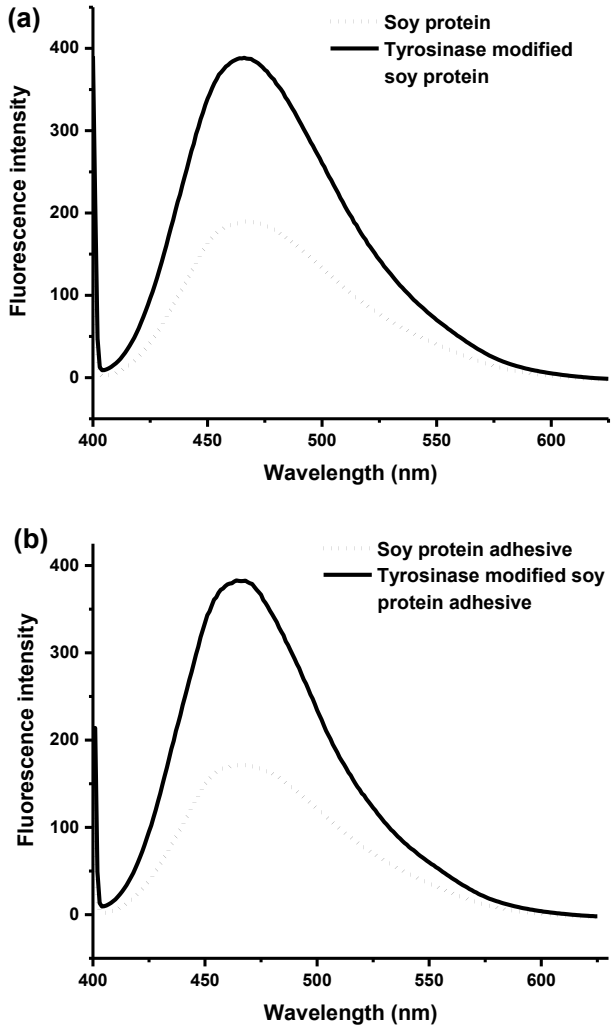

Figure 7.4: Fluorescence emission spectra (excitation wavelength: 390 nm, emission wavelength range: 400-625 nm) of (a) Soy protein and modified soy protein with tyrosinase enzyme (b) adhesives prepared with native soy protein and modified soy protein with tyrosinase enzyme (with 30 μL/mL 6 M NaOH/adhesive, and 30 μL/mL 0.2 M $FeCl_3$/adhesive) showing changes in surface hydrophobicity using ANS probe.

Proteins are amphiphilic molecules due to the presence of both hydrophobic and hydrophilic amino acids (Alizadeh-Pasdar & Li-Chan, 2000). Hydrophobic interactions plays a vital role in adhesives, mainly in water resistance properties (Bandara et al., 2017). ANS (1-anilinonaphthalene-8- sulfonic acid) fluorescent probe method is a widely used method in determining changes in protein hydrophobicity. ANS has a low fluorescence emission in solution, but upon binding to a hydrophobic region of a protein, fluorescence intensity increases indicating an increase in protein surface hydrophobicity (Alizadeh-Pasdar & Li-Chan, 2000).

As shown in Fig 7.4a, tyrosinase modification increased the fluorescence intensity of TSPI sample compared to unmodified SPI protein. Similar trend was observed in adhesives prepared using SPI and TSPI (Fig 7.4.b), where TSPI-NaOH/Fe^{3+} showed a higher fluorescence intensity than that of SPI-NaOH/Fe^{3+}. The changes observed in the fluorescence intensities are directly related to the conversion of Tyr into DOPA groups via tyrosinase enzyme. DOPA residues shows a strong hydrophobicity compared to Tyr residues, and adding DOPA residues into a polymers have been previously reported to increase surface hydrophobicity (Guvendiren et al., 2007). Even though, conversion of DOPA into DOPA-quinone occurred during adhesive preparation, surface hydrophobicity was not affected, mainly due to the strong hydrophobicity present in DOPA-quinone (Guvendiren et al., 2007).

7.3.3 Adhesion Strength of Biomimetic Adhesive

DOPA groups have the ability to go through oxidation and crosslinking reactions as seen in Fig 7.1. Higher pH and transition metal ions (Fe^{3+}) can mediate the oxidation and crosslinking reactions (Lee et al., 2006; Monahan & Wilker, 2003; Zeng et al., 2010). The optimum levels of NaOH and Fe^{3+} ion addition for improving adhesion were studied as shown in Fig 7.5. In the first step, four different levels of 0.2 M $FeCl_3$ solution were used to identify the effect of Fe^{3+} ions on

adhesion. Increasing Fe^{3+} ion addition up to 30 µL/mL (0.2 M $FeCl_3$ /Adhesive) showed an increasing trend in adhesion, but decreased at 40 µL/mL (0.2 M $FeCl_3$ /Adhesive). At 30 µL/mL (0.2 M $FeCl_3$ /Adhesive) addition level, adhesion strength of TSPI increased significantly ($p < 0.05$) to 10.36 ± 0.74 MPa compared to 7.71 ± 0.46 MPa strength observed in TSPI without Fe^{3+} ion addition.

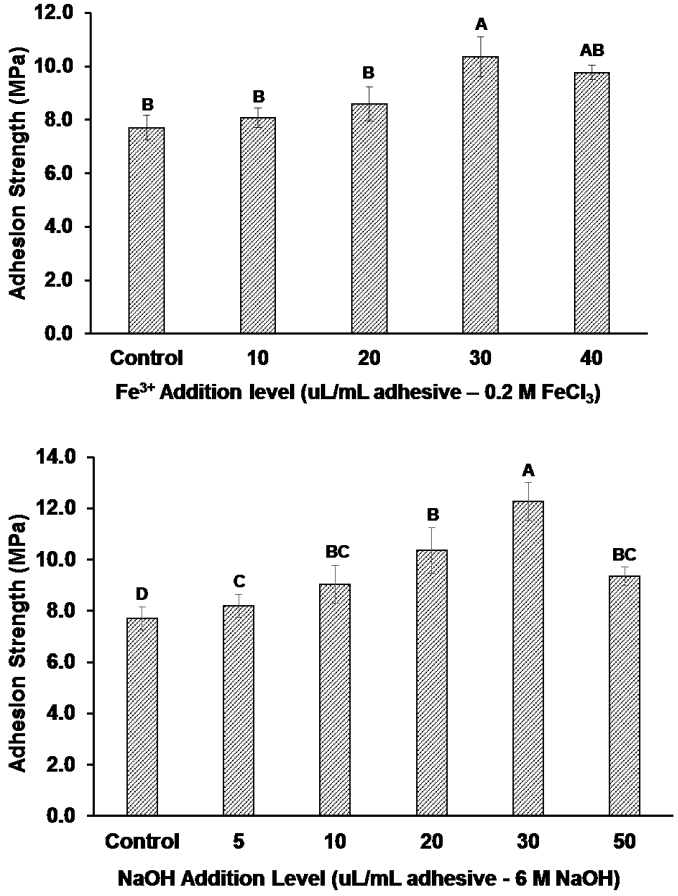

Figure 7.5: Optimization of NaOH and Fe^{3+} concentration for tyrosinase modified soy protein (TSPI). Different letters on the bar represent significantly different adhesion strength ($p < 0.05$). Error bras represent standard deviations. All adhesive samples were prepared in triplicate ($n=3$) and minimum 5 wood samples per replicate were used for each strength measurement.

The increase in adhesion with added Fe^{3+} ions was in a good agreement with previous reports on DOPA adhesion (Hight & Wilker, 2007; Hwang et al., 2010; Zeng et al., 2010). Fe^{3+} ions have the ability to bind with DOPA groups from adjacent protein molecules to create $Fe(DOPA)_3$ complex, thereby facilitating the formation of a strong crosslinked protein network that contribute towards a strong adhesion (Hight & Wilker, 2007; Hwang et al., 2010; Zeng et al., 2010). However, further increase in Fe^{3+} ions might induce excessive crosslinking in protein which can reduce the adhesion due to lack of reactive functional groups available to interact with wood surface.

In the second step of the study, effect of adding NaOH on adhesive performance of TSPI was studied. Addition of NaOH showed an increasing trend in adhesion strength up to 30 μL/mL (6 M NaOH/Adhesive) at a value of 12.28 ± 0.73 MPa, and started to decrease at 50 μL/mL (6 M NaOH/Adhesive) level. DOPA residues can readily oxidized into DOPA-quinone under higher pH values, initiating intramolecular crosslinking reactions (B. Lee et al., 2006; H. Lee et al., 2006) thereby strengthening the cohesiveness of the adhesive. Weak cohesion is considered to be one of the major factors associated with biobased adhesives, therefore strong cohesive forces created by DOPA will improve the adhesion strength of biobased adhesives. Reduced adhesion strength observed at low NaOH addition might be related to the high viscosity and low flowing ability of adhesives, which can decrease adhesive penetration into wood surface (Schultz & Nardin, 2003).

The adhesion of TSPI proteins at optimized NaOH and Fe^{3+} concentrations (30 μL/mL 0.2 M $FeCl_3$ and 30 μL/mL 6 M NaOH) is shown in Fig 7.6. Unmodified SPI adhesives showed a strength of 4.97 ± 0.94 MPa, 1.79 ± 0.52 MPa, and 5.62 ± 0.65 MPa for dry, wet and soaked adhesion respectively, while tyrosinase treated soy protein (TSPI) showed a significant increase

($p < 0.05$) in adhesion to 7.88 ± 0.48 MPa, 2.17 ± 0.20 MPa, and 7.44 ± 0.45 MPa for dry, wet and soaked strength respectively. At the optimized conditions, adhesion of TSPI-NaOH/Fe^{3+} sample has further increased ($p < 0.05$) to 13.21 ± 1.58 MPa, 3.93 ± 0.21 MPa, and 12.10 ± 0.46 MPa for dry, wet and soaked strength. The synergistic effect of NaOH and Fe^{3+} ions might be the reason for improved adhesion and water resistance.

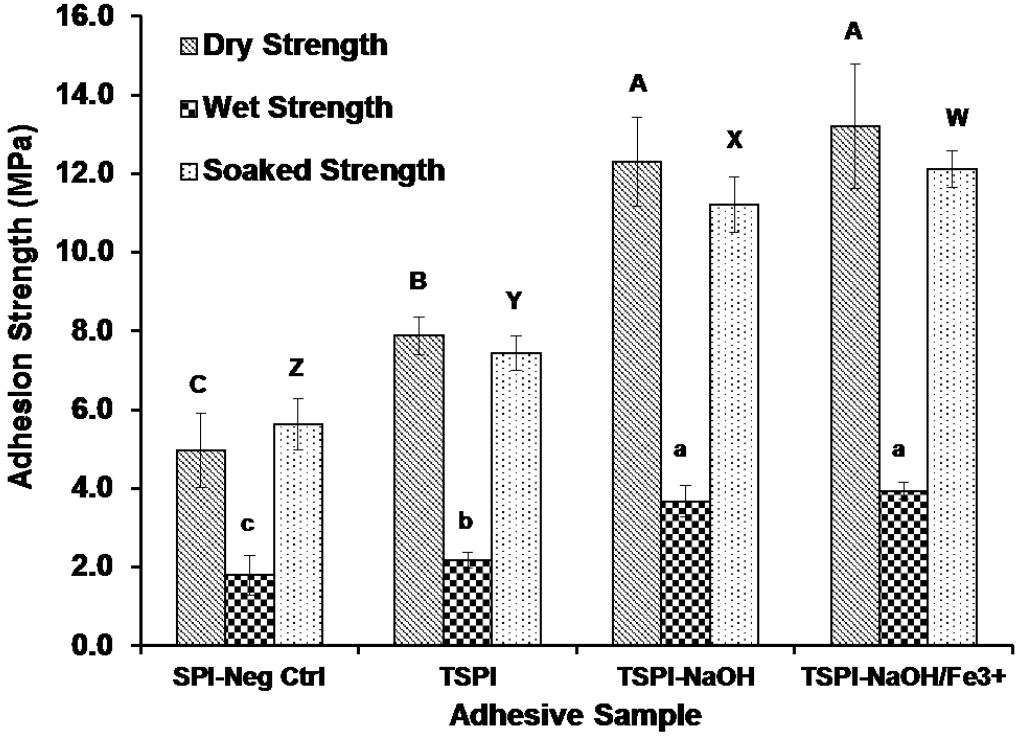

Figure 7.6: Adhesion strength of native soy protein adhesive (SPI-Neg Ctrl), tyrosinase treated soy protein (TSPI), tyrosinase treated soy protein with optimized NaOH addition level (TSPI-NaOH), and tyrosinase treated soy protein with optimized conditions for NaOH and Fe^{3+} ions (TSPI-NaOH/Fe^{3+}). Different letters on the bar represent significantly different adhesion ($p < 0.05$). Error bras represent standard deviations. All adhesive samples were prepared in triplicate ($n=3$) and minimum 5 wood samples per replicate were used for each strength measurement.

The improvement in adhesion observed in this study was well above the previously reported DOPA grafted soy protein adhesives, where they showed a dry adhesion up to ~4-5.5 MPa (Liu & Li, 2002, 2004). In addition, the present method is less complicated and use limited number of chemicals compared to the other DOPA grafting methods published in literature.

7.3.4 Adhesion of TSPI-NaOH/Fe^{3+} Adhesive to Different Surfaces

DOPA groups have a unique ability to bind to both organic and inorganic surface via different adhesion mechanisms (Bandara et al., 2013). As the modified soy proteins do contain DOPA functional groups, we studied the adhesion of TSPI-NaOH/Fe^{3+} samples to three different surfaces; glass, mica and polystyrene. Unlike the adhesives prepared with TSPI proteins, adhesives prepared with SPI samples (with similar NaOH and Fe^{3+} ion additions) did not showed an adhesion to any of the above surfaces (Fig 7.7).

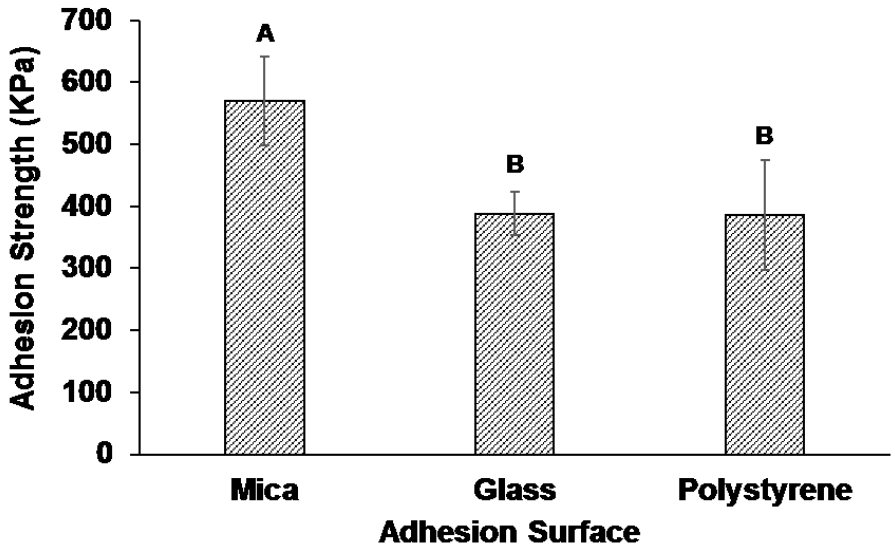

Figure 7.7: Adhesion of tyrosinase treated soy protein adhesive (TSPI-NaOH/Fe^{3+}) with optimized NaOH and Fe^{3+} additions, into different surfaces. Different letters on the bar represent significantly different adhesion strength ($p < 0.05$). Error bras represent standard deviations.

Adhesive sample was prepared in duplicate (*n=2*) and minimum 5 samples per replicate were used for strength measurement.

Among three different surface's studied in this experiment, mica showed the highest adhesion to TSPI-NaOH/Fe^{3+} with a strength of 570.04 ± 70.87 KPa, followed by glass (388.22 ± 34.54 KPa) and polystyrene (385.75 ± 89.15 KPa). Mica is considered to be more reactive than that of glass and polystyrene (Bandara et al., 2013), which can be a reason for higher adhesion observed with TSPI-NaOH/Fe^{3+} adhesive. In addition, –OH of DOPA can create –H bonds with oxygen atoms present in both mica and glass surface (Lu et al., 2013). In polystyrene surface, DOPA have previously showed hydrophobic interactions and cation–π interactions or π–π stacking (Lu et al., 2013). In comparison to, adhesion onto wood, three different surfaces tested for adhesion exhibit significantly lower adhesion values. In addition to the differences in type of interactions, the surface properties of wood can directly contribute to higher adhesion strength. Wood itself has an irregular surface with porous structures, where glass, mica and polystyrene have a smooth surface (Gardner, 2006). Porous nature of wood surface can increase adhesive penetration, thereby provide both mechanical interlocking and increased surface area for chemical interactions, which leads to increased adhesion strength.

7.3.5 Effect of Tyrosinase Modification on Protein Secondary Structure

The effect of tyrosinase modification and adhesive preparation on protein secondary structure was studied using FTIR. As shown in Fig 7.8., second derivative spectra of modified and unmodified soy proteins were used to identify secondary structural changes (Kong & Yu, 2007). Unmodified soy proteins predominantly showed α-helix structures (at wavelengths of 1654 cm^{-1}, and 1660 cm^{-1}), β sheet structures (1627 cm^{-1}, and 1676 cm^{-1}), and turn structures

(1695 cm^{-1}). These secondary structure assignments were similar to the previously published data on soy protein secondary structures, where α-helix were assigned in the range of 1650–1660 cm^{-1} and β sheets were assigned in the range of 1618–1640 cm^{-1} and 1670–1690 cm^{-1}, respectively (Kong & Yu, 2007; Zhao et al., 2008).

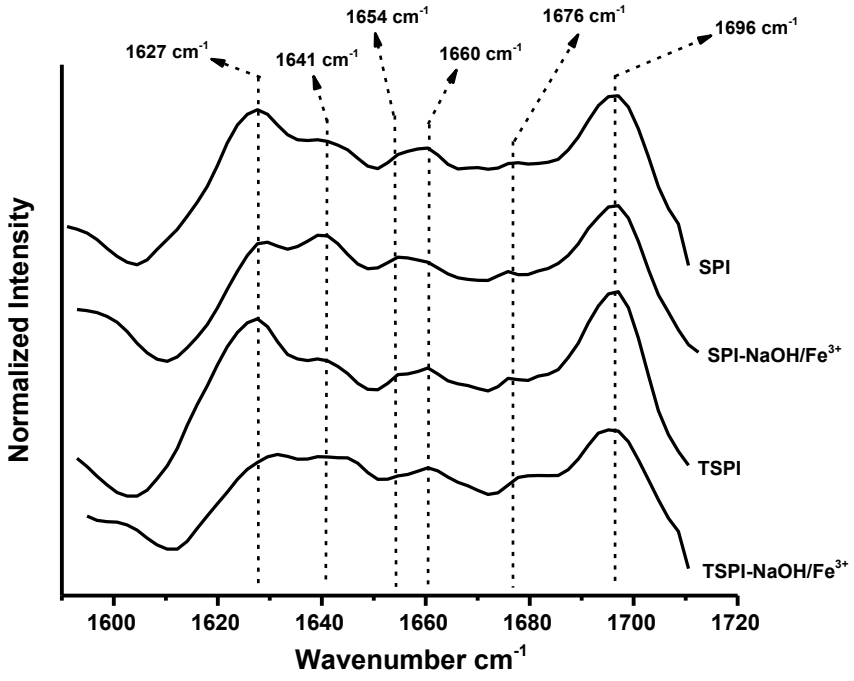

Figure 7.8: FTIR Characterization of protein secondary structural changes in unmodified (SPI) and tyrosinase modified soy proteins (TSPI) and their adhesives (SPI-NaOH/Fe^{3+}; TSPI-NaOH/Fe^{3+}).

Tyrosinase modification of soy proteins (TSPI sample) did not show a major change in protein secondary structure as observed in Fig 7.8. Tyrosinase is an site specific enzyme that act on Tyr residues present in protein structure [25], therefore the effect on protein secondary structure should be minimum. However, both SPI-NaOH/Fe^{3+} and TSPI-NaOH/Fe^{3+} samples exhibited secondary structural changes after adding NaOH and $FeCl_3$. A new peak was visible at 1641 cm^{-1}

wavelength at the expense of β sheets (1627 cm^{-1}) and α-helix (1654 cm^{-1}) structures in both adhesive samples. This new peak was assigned to unordered structures (Kong & Yu, 2007), which is a result of NaOH induced protein denaturation occurred during adhesive preparation. Increasing unordered structures can expose buried hydrophobic functional groups, thereby increase the hydrophobic interactions with wood surface, which may contribute to the increased water resistance observed in the SPI-NaOH/Fe^{3+} and TSPI-NaOH/Fe^{3+} adhesive samples. A drastic reduction of relative intensity of β sheets (1627 cm^{-1}) and increase in turn structures (1696 cm^{-1}) was observed in TSPI-NaOH/Fe^{3+} sample, which may be an effect of DOPA induced crosslinking of proteins.

7.3.6 Effect of Tyrosinase Modification on Thermal Properties of the Protein

The effect of tyrosinase modification on thermal transitions of soy protein and soy protein adhesives is shown in Table 7.2. Unmodified soy protein (SPI) samples showed an onset temperature of 71.43 ± 0.67 ºC and denaturation temperature of 86.43 ± 0.03 ºC. These values were comparable with the previously reported thermal transitions of soy proteins at a range of 74-76 ºC and 87-92 ºC for onset and denaturation temperatures respectively (Jiang et al., 2010; Sobral et al., 2010). Tyrosinase modification of soy protein has increased the thermal stability of soy protein where onset and denaturation temperatures increased up to 74.40 ± 5.13 ºC and 93.07 ± 5.54 ºC respectively, while adding NaOH and Fe^{3+} further increased thermal transitions up to 77.12 ± 0.43 ºC and 97.63 ± 0.24 ºC respectively. Crosslinking of protein molecules were reported to be increase the thermal stability of soy protein (Wang et al., 2007), therefore; DOPA mediated crosslinking might be responsible for increased thermal stability of TSPI sample. Addition of NaOH and Fe^{3+} ions accelerate protein crosslinking and improve cohesive interactions, thereby contribute to further increase in thermal stability of TSPI-NaOH/Fe^{3+}

sample. Increased thermal stability will positively impact on the adhesive application, especially due to higher temperature processing requirements in adhesive curing.

Table 7.2 – Changes in thermal transitions (Mean + standard deviations; *n=4*) of soy protein (SPI), modified soy protein with tyrosinase enzyme (TSPI), adhesives prepared (by adding 30 μL/mL 6 M NaOH/adhesive, and 30 μL/mL 0.2 M $FeCl_3$/adhesive) with native soy protein (SPI-NaOH/Fe^{3+}) and modified soy protein with tyrosinase enzyme (TSPI-NaOH/Fe^{3+}).

Sample	**Onset temperature (°C)**	**Denaturation temperature (°C)**	**Specific heat (J/(g. °C)**
SPI	71.43 ± 0.67	86.43 ± 0.03	1.35 ± 0.30
TSPI	74.40 ± 5.13	93.07 ± 5.54	1.58 ± 0.14
SPI-NaOH/Fe^{3+}	75.31 ± 3.62	94.52 ± 2.06	1.57 ± 0.05
TSPI-NaOH/Fe^{3+}	77.12 ± 0.43	97.63 ± 0.24	1.63 ± 0.01

7.4 Conclusions

A green biobased wood adhesive was developed from soy protein through biomimetic modifications. Tyrosinase enzyme was used to convert Tyr residues into DOPA. Fluorescence study showed a ~48% conversion of Tyr residues into DOPA groups after modification. Tyrosinase modification followed by addition of NaOH and Fe^{3+} significantly increased ($p < 0.05$) the adhesion strength of soy protein from 4.97 ± 0.94 MPa, 1.79 ± 0.52 MPa, and 5.62 ± 0.65 MPa to 13.21 ± 1.58 MPa, 3.93 ± 0.21 MPa, and 12.10 ± 0.46 MPa for dry, wet and soaked strength respectively. TSPI-NaOH/Fe^{3+} adhesive showed adhesion to mica (570.04 ± 70.87 KPa), glass (388.22 ± 34.50 KPa) and polystyrene (385.75 ± 89.15 KPa) as well indicating it's versatile applications. Increased thermal stability was also observed with tyrosinase

modification, which further improve adhesive stability. The increased adhesion is a result of increased amount of DOPA, leading to DOPA mediated crosslinking of soy protein that increase cohesive interactions, and polymerization with functional groups present in the wood surface. Adding NaOH and Fe^{3+} accelerate DOPA polymerization and crosslinking, thereby further improving adhesion and water resistance of soy adhesive. DOPA might increase hydrophobic and electrostatic interactions which might further contribute to improved adhesion (Bandara et al., 2013; Lee et al., 2006; Lin et al., 2007). The biomimetic adhesive prepared from byproduct soy protein shows promising potential in using as an alternative for petrochemical based adhesives.

7.5 References

Alizadeh-Pasdar, N., & Li-Chan, E. (**2000**). Comparison of protein surface hydrophobicity measured at various pH values using three different fluorescent probes. *Journal of Agricultural and Food Chemistry*, ***48***(***2***), 328–334.

Anderson, T. J., & Lamsal, B. P. (**2011**). Zein extraction from corn, corn products, and coproducts and modifications for various applications: a aeview. *Cereal Chemistry*, ***88***(***2***), 159–173.

ASTM. (**2011**). D2339-98(2011) Standard test method for strength properties of adhesives in two-ply wood construction in shear by tension loading. *Annual Book of ASTM Standards.* Available at: http://compass.astm.org/EDIT/html_annot.cgi?D2339+98%5C [2012/12/04]

ASTM. (**2013**). D1151-00(2013) Standard practice for effect of moisture and temperature on adhesive bonds. *Annual Book of ASTM Standards.* Available at: http://compass.astm.org/EDIT/html_annot.cgi?D1151 +00%5C [2013/02/03]

Bandara, N., Chen, L., & Wu, J. (**2011**). Protein extraction from triticale distillers grains. *Cereal Chemistry*, ***88***(***6***), 553–559.

Bandara, N., Chen, L., & Wu, J. (**2013**). Adhesive properties of modified triticale distillers grain proteins. *International Journal of Adhesion and Adhesives*, ***44***, 122–129.

Bandara, N., Esparza, Y., & Wu, J. (**2017**). Exfoliating nanomaterials in canola protein derived adhesive improves strength and water resistance. *RSC Advances*, ***7(11)***, 6743-6752.

Bandara, N., Zeng, H., & Wu, J. (**2013**). Marine mussel adhesion: biochemistry, mechanisms,

and biomimetics. *Journal of Adhesion Science and Technology*, ***27***(***18***–***19***), 2139–2162.

Burzio, L. A., & Waite, J. H. (**2000**). Cross-linking in adhesive quinoproteins: studies with model decapeptides . *Biochemistry*, ***39***(***36***), 11147–11153.

Grala, W., Verstegen, M. W., Jansman, A. J., Huisman, J., & van Leeusen, P. (**1998**). Ileal apparent protein and amino acid digestibilities and endogenous nitrogen losses in pigs fed soybean and rapeseed products. *Journal of Animal Science*, ***76***(***2***), 557.

Grdadolnik, J. (**2002**). A FTIR investigation of protein conformation. *Bulletin of the Chemists and Technologists of Macedonia*, ***21***, 23–34.

Guvendiren, M., Messersmith, P., & Shull, K. (**2007**). Self-assembly and adhesion of DOPA-modified methacrylic triblock hydrogels. *Biomacromolecules*, ***9***(***1***), 122–128.

Haemers, S., Koper, G. J. M., & Frens, G. (**2003**). Effect of oxidation rate on cross-linking of mussel adhesive proteins. *Biomacromolecules*, ***4***(***3***), 632–640.

Hight, L. M., & Wilker, J. J. (**2007**). Synergistic effects of metals and oxidants in the curing of marine mussel adhesive. *Journal of Materials Science*, ***42***(***21***), 8934–8942.

Hwang, D. S., Zeng, H., Masic, A., Harrington, M. J., Israelachvili, J. N., & Waite, J. H. (**2010**). Protein- and metal-dependent interactions of a prominent protein in mussel adhesive plaques. *The Journal of Biological Chemistry*, ***285***(***33***), 25850–25858.

Ito, S., Kato, T., Shinpo, K., & Fujita, K. (**1984**). Oxidation of tyrosine residues in proteins by tyrosinase. Formation of protein-bonded 3, 4-dihydroxyphenylalanine and 5-S-cysteinyl-3, 4-dihydroxyphenylalanine. *Biochemical Journal*, ***222***(***2***), 407–411.

Jiang, J., Xiong, Y., & Chen, J. (**2010**). PH shifting alters solubility characteristics and thermal stability of soy protein isolate and its globulin fractions in different pH, salt concentration, and temperature. *Journal of Agricultural and Food Chemistry*, ***58***(***13***), 8035–8042.

Jus, S., Kokol, V., & Guebitz, G. (**2008**). Tyrosinase-catalysed coupling of functional molecules onto protein fibres. *Enzyme and Microbial Technology*, ***42***(***7***), 535–542.

Kalapathy, U., Hettiarachchy, N. S., Myers, D., & Rhee, K. C. (**1996**). Alkali-modified soy proteins: effect of salts and disulfide bond cleavage on adhesion and viscosity. *Journal of the American Oil Chemists' Society*, ***73***(***8***), 1063–1066.

Kong, J., & Yu, S. (**2007**). Fourier transform infrared spectroscopic analysis of protein secondary structures. *Acta Biochimica et Biophysica Sinica*, ***39***(***8***), 549–559.

Kuboe, Y., Tonegawa, H., & Ohkawa, K. (**2004**). Quinone cross-linked polysaccharide hybrid fiber. *Biomacromolecules*, ***5***(***2***), 348–357.

Lambuth, A. L. (**1994**). Protein adhesives for wood. In A. Pizzi & K.L. Mittal (Eds.), *Handbook of Adhesive Technology*, (pp 457–478). New York: NY. Marcel Dekker Inc.

Lee, B., Dalsin, J., & Messersmith, P. (**2006**). Biomimetic adhesive polymers based on mussel adhesive proteins. In A. Smith & J. Callow (Eds.), *Biological Adhesives* (pp 257–278). Berlin, Heidelberg: Springer.

Lee, H., Scherer, N. F., & Messersmith, P. B. (**2006**). Single-molecule mechanics of mussel adhesion. *Proceedings of the National Academy of Sciences of the United States of America*, ***103***(***35***), 12999–13003.

Lin, Q., Gourdon, D., Sun, C., Holten-Andersen, N., Anderson, T. H., Waite, J. H., & Israelachvili, J. N. (**2007**). Adhesion mechanisms of the mussel foot proteins mfp-1 and mfp-3. *Proceedings of the National Academy of Sciences of the United States of America*, ***104***(***10***), 3782–3786.

Liu, D., Chen, H., Chang, P. R., Wu, Q., Li, K., & Guan, L. (**2010**). Biomimetic soy protein nanocomposites with calcium carbonate crystalline arrays for use as wood adhesive. *Bioresource technology*, ***101***(***15***), 6235–6241.

Liu, J., Fu, S., Yuan, B., Li, Y., & Deng, Z. (**2010**). Toward a universal adhesive nanosheet for the assembly of multiple nanoparticles based on a protein-induced reduction/decoration of graphene oxide. *Journal of the American Chemical Society*, ***132***(***21***), 7279–7281.

Liu, Y., & Li, K. (**2002**). Chemical modification of soy protein for wood adhesives. *Macromolecular Rapid Communications*, ***23***(***13***), 739–742.

Liu, Y., & Li, K. (**2004**). Modification of soy protein for wood adhesives using mussel protein as a model: The influence of a mercapto group. *Macromolecular Rapid Communications*, ***25***(***21***), 1835–1838.

Lu, Q., Danner, E., & Waite, J. (**2013**). Adhesion of mussel foot proteins to different substrate surfaces. *Journal of The Royal Society Interface*, ***10***(***70***), 2012–759.

Monahan, J., & Wilker, J. J. (**2003**). Specificity of metal ion cross-linking in marine mussel adhesives. *Chemical Communications*, ***2003***(***14***), 1672–1673.

Ohkawa, K., Nishida, A., Ichimiya, K., Matsui, Y., & Nagaya, K. (**1999**). Purification and

characterization of a DOPA-containing protein from the foot of the Asian freshwater mussel, *Limnoperna fortunei*. *Biofouling*, ***14***(***3***), 181–188.

Pizzi, A. (**2013**). Bioadhesives for wood and fibres. *Reviews of Adhesion and Adhesives*, ***1***(***1***), 88–113.

Qi, G., Li, N., Wang, D., & Sun, X. S. (**2016**). Development of high-strength soy protein adhesives modified with sodium montmorillonite clay. *Journal of the American Oil Chemists' Society*, ***93***(***11***), 1509–1517.

Schultz, J., & Nardin, M. (**2003**). Theories and mechanisms of adhesion. In A. Pizzi & K. Mittal (Eds.), *Handbook of Adhesive Technology* (pp 53–68). Boca Raton, FL: CRC Press.

Sobral, P., Palazolo, G., & Wagner, J. (**2010**). Thermal behavior of soy protein fractions depending on their preparation methods, individual interactions, and storage conditions. *Journal of agricultural and Food Chemistry*, ***58***(***18***), 10092–10100.

Song, Y., Seo, J., Choi, Y., Kim, D., & Choi, B. (**2016**). Mussel adhesive protein as an environmentally-friendly harmless wood furniture adhesive. *International Journal of Adhesion and Adhesives*, ***70***, 260–264.

Tandang-Silvas, M. R. G., Fukuda, T., Fukuda, C., Prak, K., Cabanos, C., Kimura, A., Maruyama, N. (**2010**). Conservation and divergence on plant seed 11S globulins based on crystal structures. *Biochimica et Biophysica Acta*, ***1804***(***7***), 1432–1442.

Ullah, A., Vasanthan, T., Bressler, D., Elias, A. L., & Wu, J. (**2011**). Bioplastics from feather quill. *Biomacromolecules*, ***12***(***10***), 3826–3832.

Wanasundara, J. P. D. (**2011**). Proteins of *Brassicaceae* oilseeds and their potential as a plant protein source. *Critical Reviews in Food Science and Nutrition*, ***51***(***7***), 635–677.

Wang, C., & Wu, J. (**2012**). Preparation and characterization of adhesive from spent hen proteins. *International Journal of Adhesion and Adhesives*, ***36***, 8–14.

Wang, Y., Mo, X., Sun, X. S., & Wang, D. (**2007**). Soy protein adhesion enhanced by glutaraldehyde crosslink. *Journal of Applied Polymer Science*, ***104***(***1***), 130–136.

Yuan, C., Luo, J., Luo, J., Gao, Q., & Li, J. (**2016**). A soybean meal-based wood adhesive improved by a diethylene glycol diglycidyl ether: properties and performance. *RSC Advances*, ***6***(***78***), 74186–74194.

Zeng, H., Hwang, D. S., Israelachvili, J. N., & Waite, H. (**2010**). Strong reversible Fe^{3+}-mediated bridging between DOPA-containing protein films in water. *Proceedings of the National Academy of Sciences of the United States of America, **107(29)***, 12850-12853.

Zhang, X., Monroe, M., Chen, B., Chin, M., Heibeck, T., Schepmoes, A., & Jacobs, J. (**2010**). Endogenious 3, 4 dihydroxyphenylalanine and dopaquinone modification on protein. *Molecular & Cellular Proteomics*, ***9***(***6***), 1199–1208.

Zhao, X., Chen, F., Xue, W., & Lee, L. (**2008**). FTIR spectra studies on the secondary structures of 7S and 11S globulins from soybean proteins using AOT reverse micellar extraction. *Food Hydrocolloids*, ***22***(***4***), 568–575.

Zhu, D., & Damodaran, S. (**2014**). Chemical phosphorylation improves the moisture resistance of soy flour-based wood adhesive. *Journal of Applied Polymer Science*, ***131***(***13***), 40451–40457.

CHAPTER 8 - Conclusions and Recommendations

8.1 Conclusions

In addition to Canola, Canada also produces considerable amount of soybean (Canola Council of Canada, 2016; OECD & FAO, 2016). The oilseed industry generates a great deal of meals as byproducts, that are used mainly as low value animal feeds, bio-fertilizer, or as an fuel (COPA, 2016; Newkirk, 2015). However, exploring value added applications are required to improve the sustainability of oilseed industry (Bandara et al., 2017). Protein based wood adhesives gain enormous research interest in the past two decades mainly due to the environmental and human health concerns over synthetic adhesives and consumer driven demand for green materials (Frihart, 2016; Pizzi, 2013, 2016).

Several attempts were made in the past to develop protein derived adhesives with improved adhesion (Frihart, 2016). Protein modification methods such as denaturation (Hettiarachchy et al., 1995; Kalapathy et al., 1996), crosslinking (Khosravi et al., 2014; Silva et al., 2004), chemical modification (Damodaran & Zhu, 2016; Liu & Li, 2004; Zhu & Damodaran, 2014), enzyme modification (Nordqvist et al., 2012), and nanotechnology (Qi et al., 2016) were applied to develop protein derived adhesives. To make protein-derived adhesives commercially competitive, it is inevitable to improve their adhesion and water resistance and to prepare in a cost-effective manner (Pizzi, 2016; Qi et al., 2016).

Nanotechnology studies materials and structures in atomic and molecular scale (1-100 nm) dimensions (Norde, 2011). Even though it has been extensively studied in the plastic and composite fields, its applications in adhesive research is extremely limited (Kaboorani et al., 2012; Kaboorani & Riedl, 2011). The effectiveness of nanomaterial in improving flexural strength, elasticity, toughness, and thermal stability of materials largely depends on the proper

exfoliation of nanomaterial (Santulli, 2016). “Biomimetics is the field of science and engineering that seeks to understand and use nature as a model for innovation and problem solving” (Bar-Cohen, 2012); for example, to develop mussel inspired adhesive for wood adhesive application (Liu et al., 2010). Therefore, the main objective of this thesis was to develop biobased wood adhesives with improved adhesion and water resistance properties using renewable proteins extracted from agricultural/food industry byproducts via nanotechnological and biomimetic approaches.

In this context, for the first time we developed nanomaterial exfoliated wood adhesives from canola protein with significantly improved functionalities. The solution intercalation method developed in this study effectively exfoliated all four nanomaterials, especially at lower addition levels (at 1% w/w addition), while significantly ($p < 0.05$) increasing adhesion strength and water resistance. Among the four different nanomaterials studied in first chapter; NCC and GO showed superior performance over bentonite and SM-MMT. Dry, wet and soaked adhesion strength (6.38 ± 0.84 MPa, 1.98 ± 0.22 MPa, and 5.65 ± 0.46 MPa respectively) of pH control samples were increased to 10.37 ± 1.63 MPa, 3.57 ± 0.57 MPa, and 7.66 ± 1.37 MPa for 1% NCC (w/w) addition and 8.14 ± 0.45 MPa, 3.25 ± 0.36 MPa, and 7.76 ± 0.53 MPa for 1% GO (w/w) addition (dry, wet and soaked strength respectively). Further increase of nanomaterial addition level showed a decrease in adhesion and water resistance, except for NCC and GO, where improved adhesion was observed up to 3% and 5% w/w addition levels respectively. Increase in thermal stability and unordered secondary structure was observed with nanomaterial addition. The improvement in adhesion and water resistance was due to the, nanomaterial induced cohesion and protein crosslinking, improved thermal stability, and increase in hydrophobic functional groups that can react with functional groups present in wood surface. In

addition properly exfoliated nanomaterials can act as a physical barrier for water penetration, thereby improve water resistance.

In the second chapter, GO with different chemical and functional properties were prepared by changing graphite oxidation time. In this study, we used GO for the first time in preparing adhesives instead of graphene that are widely used in composite research, with improved functionalities. The material and chemical properties of GO can be manipulated by changing oxidation conditions (Jeong et al., 2009). Changing graphite oxidation time to 0.5, 2, and 4 h (referred as GO-A, GO-B, and GO-C) reduced the C/O ratio of graphite from 41.55 to 2.06, 1.40, and 1.49 respectively. Changing oxidation time up to 2 h, increased the interlayer spacing of GO sheets, relative proportion of C–OH and C=O functional groups, thereby improved the exfoliation properties of GO, especially in GO-B sample. Addition of all GO samples at our optimized conditions from study 1, significantly ($p < 0.05$) increased the adhesion and water resistance, where GO showed the best results with dry, wet and soaked strength of 11.67 ± 1.00 MPa, 4.85 ± 0.61 MPa, and 10.73 ± 0.45 MPa, respectively. Improved exfoliation observed due to increased interlayer spacing and changes in surface functional groups of GO, increased adhesive and cohesive interactions, increased hydrophobic interactions and thermal stability are the main reason for improved adhesion and water resistance of GO-B exfoliated adhesives.

Chemical modification has been previously used in our group to improve adhesion of canola derived adhesive with success (Wang et al., 2014). In this study ammonium persulphate (APS) was used as a free radical initiator for grafting poly(glycidyl methacrylate). However, further studies on APS showed an excellent potential in improving adhesion itself without polymer grafting. Therefore, in the third chapter of this thesis, a chemically modified canola protein-nanomaterial hybrid wood adhesive (CMCP-NM) was developed with significantly

improved adhesion and water resistance. APS modification alone significantly increased ($p < 0.05$) dry wet and soaked adhesion (10.47 ± 1.35 MPa, 4.12 ± 0.64 MPa, and 9.39 ± 1.20 MPa respectively) at 1% w/w (APS/protein) concentration. Evidence of APS induced oxidation and crosslinking of protein network via Tyr-Tyr, and Tyr-His covalent bonds were observed in FTIR, hydrodynamic diameter, and SDS-PAGE analysis. The crosslinked protein showed better thermal stability and increased hydrophobic functional groups, contributing towards improved adhesion. In the second step of the study, canola protein-nanomaterial hybrid wood adhesive (CMCP-NM) was developed by exfoliating optimized addition level of NCC and GO based on our previous study. At 1% (w/w) addition level, dry wet and soaked adhesion significantly increased ($p < 0.05$) up to 12.50 ± 0.71 MPa, 4.79 ± 0.40 MPa, and 10.92 ± 0.75 MPa for NCC and up to 11.82 ± 1.15 MPa, 4.99 ± 0.28 MPa, and 10.74 ± 0.72 MPa for with GO (for dry, wet and soaked adhesion respectively). These improvement in adhesion and specifically water resistance is significantly higher than any other study reported to date (Hale, 2013; Li et al., 2011, 2012; Wang et al., 2014) on canola protein based adhesive. Improved cohesive interactions as observed in wood failure study, increased hydrophobic interactions, and synergistic effect of APS induced crosslinked protein network might be responsible for the improvement in adhesion and water resistance observed in CMCP-NM adhesive. Due to its excellent performance, CMCP-NM adhesive can be used as a green alternative for developing engineered wood products such as oriented strand boards (OSB).

In chapter 4, nanoengineered canola protein adhesive (CPA) prepared according to the method developed in chapter 3 by chemical modification followed by exfoliating GO was applied to replace commercial LPF resin used in ROSB production. The adhesive preparation method was slightly modified to accommodate technical specifications of pilot scale panel

processing while the major change was to increase its solid content to 30% (in 100% CPA) by adding inactive filler $CaCO_3$. Canola protein extraction, adhesive preparation and panel processing was conducted in a pilot scale processing facility to evaluate the suitability of our adhesive and technology at commercial level. Replacing commercial LPF content in adhesive formulation up to 40% (w/w) with CPA adhesive was able to produce ROSB panels with similar performance to 100% LPF adhesives; however, further increasing of CPA content reduced the panel performance. All six adhesive formulation used in the study showed MOE, MOR and IB strength values above the minimum requirement for OSB/ROSB panels as specified in CSA O437.0-93 (Canadian Standards Association, 1993) while bond durability (MOR in 2 h boil test) met the minimum requirement of CSA O437.0-93 up to 60% CPA replacement. Thickness swelling and water absorption did not change up to 40% CPA replacement in bond durability study, but increased beyond 60% CPA addition. Increasing CPA content increased the amount of inactive filler ($CaCO_3$) in adhesive formulation that leads to reduction in water resistance properties. Based on the panel performance, ROSB panels prepared with CPA adhesive can be used to replace commercial LPF adhesive up to 100% for panels used in internal applications, while up to 40% CPA replacement can be achieved without compromising mechanical or water resistance properties for exterior and structural applications based on the minimum requirement specified by CSA O437.0-93 standard method (Canadian Standards Association, 1993). The CPA adhesive prepared through a systematic modifications to canola protein was successful in improving both adhesion and water resistance, thereby proving our first hypothesis; exfoliating nanomaterials in protein matrix, and preparing hybrid wood adhesives with chemically modified canola protein will improve the adhesion and water resistance of canola protein based adhesive.

In the fifth study of this thesis, a mussel inspired soy protein derived adhesive with significantly improved ($p < 0.05$) adhesion and water resistance was developed by biomimetic modifications. Mussel adhesion mechanism is considered to be based on the oxidation and polymerization of 3,4-dihyroxyphenlalanine (DOPA) functional group; however, natural plant proteins do not have DOPA in its structure. Therefore, Tyr amino acid present in soy protein was modified into DOPA using a simple tyrosinase enzyme mediated reaction. The fluorescence study showed that ~48% conversion of Tyr residues into DOPA following tyrosinase modification. Fe^{3+} ions were identified to play a key role in mussel adhesion at higher pH, therefore Fe^{3+} was added to adhesive at optimized condition. Tyrosinase modification followed by addition of NaOH and Fe^{3+} (TSPI-NaOH/Fe^{3+} adhesive) has significantly ($p < 0.05$) increased the adhesion strength of soy protein from 4.97 ± 0.94 MPa, 1.79 ± 0.52 MPa, and 5.62 ± 0.65 MPa, up to 13.21 ± 1.58 MPa, 3.93 ± 0.21 MPa, and 12.10 ± 0.46 MPa for dry, wet and soaked strength respectively. Another interesting observation of TSPI-NaOH/Fe^{3+} adhesive was the adhesion into different surfaces such as mica (570.04 ± 70.87 KPa), glass (388.22 ± 34.50 KPa) and polystyrene (385.75 ± 89.15 KPa) which was not observed in unmodified soy proteins. The improvement in adhesion and water resistance is due to a combine effect of increased amount of DOPA in soy protein structure, DOPA mediated crosslinking of soy protein that increase cohesive interactions, and DOPA polymerization with functional groups present in the wood surface and the unique ability of DOPA in creating hydrophobic and electrostatic interactions. In addition, presence of NaOH and Fe^{3+} will accelerate DOPA polymerization and crosslinking. The biomimetic adhesive prepared by tyrosinase modification of soy protein shows promising potential in using as an alternative for petrochemical based adhesives which proves our second

hypothesis; biomimetic modification of soy protein to impart DOPA functional groups will improve adhesion and water resistance of soy protein based adhesives.

8.2 Recommendation for Future Studies

Protein based adhesives prepared by nanotechnological and biomimetic approaches showed great potential in adhesive applications with significantly improved adhesion and water resistance. ROSB panel production study showed that chemically modified canola protein-graphite oxide adhesive have the potential to replace commercial adhesive up to 40% without losing any of the panel performance properties at pilot scale processing conditions for exterior grade OSB panels while 100% replacement can be achieved for interior grade OSB panels (Canadian Standards Association, 1993). However, further research is expected in the following areas.

1. Increasing solid content of the adhesive without compromising adhesive performance remains as the major area of research required in the future for commercialization of this technology. In commercial OSB panel production, a minimum solid content above ~30% (w/w) is required for achieving optimum panel processing conditions. In this study, we had used $CaCO_3$ as an inorganic inactive filler to increase the solid content; however, as observed in our ROSB panel processing study, the presence of inactive filler in excess amount can reduce the mechanical performance of the panel. Therefore, an alternate method should be developed to either increase protein content of the adhesive without increasing viscosity, or to add an active filler with adhesive properties.

2. Another major obstacle in commercializing protein based adhesive is the cost of protein based adhesive compared to traditional synthetic adhesives. Low cost of traditional

adhesive was one of the major reason that protein based adhesives have replaced in the past. It is costly to extract protein from meal; therefore, modification of developed methods in order to use canola meal and soymeal instead of extracted proteins will be another area of interest for future studies.

3. CPA adhesive prepared in this study showed promising potential in applications of ROSB panel preparation. It would be interesting to explore the potential of this adhesive in other applications of engineered wood products such as wood lamination, particle boards, plywood's and medium density fiber boards.

4. Understanding the exact mechanism of nanomaterial, especially on GO in improving adhesion and water resistance will provide invaluable insight on protein-nanomaterial interaction and their effect on adhesion improvement. Therefore, a adhesion mechanism study using a model systems would provide better understanding on the nanomaterial induced adhesion improvement.

8.3 References

Bandara, N., Esparza, Y., & Wu, J. (**2017**). Exfoliating nanomaterials in canola protein derived adhesive improves strength and water resistance. *RSC Advances*, ***7(11)***, 6743-6752.

Bar-Cohen, Y. (**2012**). Introduction: nature as a source of inspiring innovation. In Y. Bar-Cohen (Eds.), *Biomimetics : nature-based innovation* (pp 2-34). Boca Raton : CRC Press.

Canadian Standards Association. (**1993**). Canadian standard association protocol for strand board. *CSA O437-93*, 1–88.

Canola Council of Canada. (**2016**). Canadian canola production 2016. Available at: http://www.canolacouncil.org/markets-stats/statistics/tonnes/ [2016/12/28]

COPA-Canadian Oilseed Processors Association. (**2016**). Canadian oilseed processing industry. Available at: http://copacanada.com/crush-oil-meal-production/ [2016/12/25]

Damodaran, S., & Zhu, D. (**2016**). A formaldehyde-free water-resistant soy flour-based adhesive for plywood. *Journal of the American Oil Chemists' Society*, ***93***(***9***), 1311–1318.

Frihart, C. (**2016**). Potential for biobased adhesives in wood bonding. In *International Convention of Society of Wood Science and Technology* (pp. 84–91). Curitiba, Brazil: Society of Wood Science and Technology.

Hale, K. (**2013**). *The potential of canola protein for bio-based wood adhesives*. (Master's dissertation). Kansas State University.

Hettiarachchy, N. S., Kalapathy, U., & Myers, D. J. (**1995**). Alkali-modified soy protein with improved adhesive and hydrophobic properties. *Journal of the American Oil Chemists' Society*, ***72***(***12***), 1461–1464.

Jeong, H. K., Jin, M. H., So, K. P., Lim, S. C., & Lee, Y. H. (**2009**). Tailoring the characteristics of graphite oxides by different oxidation times. *Journal of Physics D: Applied Physics*, ***42***(***65418***), 1–6.

Kaboorani, A., & Riedl, B. (**2011**). Effects of adding nano-clay on performance of polyvinyl acetate (PVA) as a wood adhesive. *Composites Part A: Applied Science and Manufacturing*, ***42***(***8***), 1031–1039.

Kaboorani, A., Riedl, B., Blanchet, P., Fellin, M., Hosseinaei, O., & Wang, S. (**2012**). Nanocrystalline cellulose (NCC): A renewable nano-material for polyvinyl acetate (PVA) adhesive. *European Polymer Journal*, ***48***(***11***), 1829–1837.

Kalapathy, U., Hettiarachchy, N. S., Myers, D., & Rhee, K. C. (**1996**). Alkali-modified soy proteins: effect of salts and disulfide bond cleavage on adhesion and viscosity. *Journal of the American Oil Chemists' Society*, ***73***(***8***), 1063–1066.

Khosravi, S., Khabbaz, F., Nordqvist, P., & Johansson, M. (**2014**). Wheat gluten based adhesives for particle boards: effect of crosslinking agents. *Macromolecular Materials and Engineering*, ***299***(***1***), 116–124.

Li, N., Qi, G., Sun, X. S., Stamm, M. J., & Wang, D. (**2011**). Physicochemical properties and adhesion performance of canola protein modified with sodium bisulfite. *Journal of the American Oil Chemists' Society*, ***89***(***5***), 897–908.

Li, N., Qi, G., Sun, X. S., & Wang, D. (**2012**). Effects of sodium bisulfite on the physicochemical and adhesion properties of canola protein fractions. *Journal of Polymers and the Environment*, ***20***(***4***), 905–915.

Liu, D., Chen, H., Chang, P. R., Wu, Q., Li, K., & Guan, L. (**2010**). Biomimetic soy protein nanocomposites with calcium carbonate crystalline arrays for use as wood adhesive. *Bioresource technology*, ***101***(***15***), 6235–6241.

Liu, Y., & Li, K. (**2004**). Modification of soy protein for wood adhesives using mussel protein as a model: The influence of a mercapto group. *Macromolecular Rapid Communications*, ***25***(***21***), 1835–1838.

Newkirk, R. (**2015**). Canola meal - Feed industry guide. Available at : http://www.canolacouncil.org/media/516716/2015_canola_meal_feed_industry_guide.pdf [2016/12/27]

Norde, W. (**2011**). Intermolecular interactions. In L. Frewer, A. Fischer, W. Norde, & F. Kampers (Eds.), *Nanotechnology in the Agri-Food Sector* (pp 5–22). Weinheim, Germany: Wiley-VCH.

Nordqvist, P., Lawther, M., Malmström, E., & Khabbaz, F. (**2012**). Adhesive properties of wheat gluten after enzymatic hydrolysis or heat treatment – A comparative study. *Industrial Crops and Products*, ***38***, 139–145.

OECD, & FAO. (**2016a**). OECD-FAO Agricultural outlook 2016-2025. Available at: http://www.oecd-ilibrary.org/agriculture-and-food/oecd-fao-agricultural-outlook-2016_agr_outlook-2016-en [2016/12/25].

Pizzi, A. (**2013**). Bioadhesives for wood and fibres. *Reviews of Adhesion and Adhesives*, ***1***(***1***), 88–113.

Pizzi, A. (**2016**). Wood products and green chemistry. *Annals of Forest Science*, ***73***(***1***), 185–203.

Qi, G., Li, N., Wang, D., & Sun, X. S. (**2016**). Development of high-strength soy protein adhesives modified with sodium montmorillonite clay. *Journal of the American Oil Chemists' Society*, ***93***(***11***), 1509–1517.

Santulli, C. (**2016**). Nanoclay based natural fibre reinforced polymer composites: mechanical and thermal properties. In M. Jawaid, A. K. Qaiss, & R. Bouhfid (Eds.), *Nanoclay Reinforced Polymer Composites* (pp 81–101). Singapore: Springer Singapore.

Silva, C. J. S. M., Sousa, F., Gubitz, G., & Cavaco-Paulo, A. (**2004**). Chemical modifications on proteins using glutaraldehyde. *Food Technology and Biotechnology*, ***42***(***1***), 51–56.

Wang, C., Wu, J., & Bernard, G. M. (**2014**). Preparation and characterization of canola protein isolate–poly(glycidyl methacrylate) conjugates: A bio-based adhesive. *Industrial Crops and Products*, ***57***, 124–131.

Zhu, D., & Damodaran, S. (**2014**). Chemical phosphorylation improves the moisture resistance of soy flour-based wood adhesive. *Journal of Applied Polymer Science*, ***131***(***13***), 40451–40457.

BIBLIOGRAPHY

Aachary, A., Thiyam-Hollander, U., & Eskin, M. (**2015**). Canola/rapeseed proteins and peptides. In Z. Ustunol (Eds.), *Applied Food Protein Chemistry* (pp 194–218). Chichester, UK: John Wiley & Sons, Ltd.

Abaee, A., Madadlou, A., & Saboury, A. (**2017**). The formation of non-heat-treated whey protein cold-set hydrogels via non-toxic chemical cross-linking. *Food Hydrocolloids*. ***63***, 43-49.

Aguilar-Bolados, H., & Lopez-Manchado, M. (**2015**). Effect of the morphology of thermally reduced graphite oxide on the mechanical and electrical properties of natural rubber nanocomposites. *Composites Part B:*, ***87***, 350–356.

Aider, M., & Barbana, C. (**2011**). Canola proteins: composition, extraction, functional properties, bioactivity, applications as a food ingredient and allergenicity – A practical and critical review. *Trends in Food Science & Technology*, ***22*(*1*)**, 21–39.

AlBIO-Alberta Innovates Biosolutions. (**2013**). Recommendations to build Alberta's bioeconomy. Available at: http://bio.albertainnovates.ca/media/57924/ bioe_final_report_web_may2013.pdf [2016/12/30]

Alexandre, M., & Dubois, P. (**2000**). Polymer-layered silicate nanocomposites: preparation, properties and uses of a new class of materials. *Materials Science and Engineering: R: Reports*, ***28*(*1–2*)**, 1–63.

Alizadeh-Pasdar, N., & Li-Chan, E. (**2000**). Comparison of protein surface hydrophobicity measured at various pH values using three different fluorescent probes. *Journal of Agricultural and Food Chemistry*, ***48*****(*****2*****)**, 328–334.

Aluko, R., & McIntosh, T. (**2001**). Polypeptide profile and functional properties of defatted meals and protein isolates of canola seeds. *Journal of the Science of Food and Agriculture,* ***81*****(*****4*****)**, 391–396.

Anderson, T. J., & Lamsal, B. P. (**2011**). Zein extraction from corn, corn products, and coproducts and modifications for various applications: a review. *Cereal Chemistry*, ***88*****(*****2*****)**, 159–173.

André, N., Cho, H.W., Baek, S. H., & Jeong, M.K. (**2008**). Prediction of internal bond strength in a medium density fiberboard process using multivariate statistical methods and variable selection. *Wood Science and Technology*, ***42*****(*****7*****)**, 521–534.

Antos, J., & Francis, M. (**2006**). Transition metal catalyzed methods for site-selective protein modification. *Current Opinion in Chemical Biology*, ***10***, 253–262.

Arshad, M., Kaur, M., & Ullah, A. (**2016**). Green biocomposites from nanoengineered hybrid natural fiber and biopolymer. *ACS Sustainable Chemistry & Engineering*, ***4*****(*****3*****)**, 1785–1793.

ASA-American Soybean Association. (**2015**). World soybean production - 2015. Available at : http://soystats.com/international-world-soybean-production/ [2016/12/16]

BIBLIOGRAPHY

ASTM. (**2011**). D2339-98(2011) Standard test method for strength properties of adhesives in two-ply wood construction in shear by tension loading. *Annual Book of ASTM Standards.* Available at: http://compass.astm.org/EDIT/html_annot.cgi?D2339+98%5C [2012/12/04]

ASTM. (**2013**). *ASTM D1037-13* Standard test methods for evaluating properties of wood-base fiber and particle. *Annual Book of ASTM Standards*. Available at: https://doi.org/10.1520/D1037-06A.1.2 [2013/03/12]

ASTM. (**2013**). D1151-00(2013) Standard practice for effect of moisture and temperature on adhesive bonds. *Annual Book of ASTM Standards.* Available at: http://compass.astm.org/EDIT/html_annot.cgi?D1151 +00%5C [2013/02/03]

Baier, R., Shafrin, E., & Zisman, W. (**1968**). Adhesion: mechanisms that assist or impede it. *Science*, ***162***, 1360–1368.

Baldan, A. (**2012**). Adhesion phenomena in bonded joints. *International Journal of Adhesion and Adhesives*, ***38***, 95–116.

Bandara, N., & Wu, J. (**2017**). Chemically modified canola Protein-Nanomaterial Hybrid Wood Adhesive Shows Improved Adhesion and Water Resistance. (Unpublished data)

Bandara, N., Chen, L., & Wu, J. (**2011**). Protein extraction from triticale distillers grains. *Cereal Chemistry*, ***88*****(*****6*****)**, 553–559.

Bandara, N., Chen, L., & Wu, J. (**2013**). Adhesive properties of modified triticale distillers grain proteins. *International Journal of Adhesion and Adhesives*, ***44***, 122–129.

Bandara, N., Esparza, Y., & Wu, J. (**2017**). Exfoliating nanomaterials in canola protein derived adhesive improves strength and water resistance. *RSC Advances*, ***7(11)***, 6743-6752.

Bandara, N., Esparza, Y., & Wu, J. (**2017**b). Graphite oxide improves adhesion and water resistance of protein–graphite oxide hybrid wood adhesive (Unpublished data).

Bandara, N., Zeng, H., & Wu, J. (**2013**). Marine mussel adhesion: biochemistry, mechanisms, and biomimetics. *Journal of Adhesion Science and Technology*, ***27*(*18–19*)**, 2139–2162.

Bar-Cohen, Y. (**2012**). Introduction: nature as a source of inspiring innovation. In Y. Bar-Cohen (Eds.), *Biomimetics : Nature-based Innovation* (pp 2-34). Boca Raton : CRC Press.

Barth, A. (**2007**). Infrared spectroscopy of proteins. *Biochimica et Biophysica Acta*, ***1767*(*9*)**, 1073–1101.

Bilgiç, C., Topaloğlu Yazıcı, D., Karakehya, N., Çetinkaya, H., Singh, A., & Chehimi, M. M. (**2014**). Surface and interface physicochemical aspects of intercalated organo-bentonite. *International Journal of Adhesion and Adhesives*, ***50***, 204–210.

Böhm, R., Hauptmann, M., Pizzi, A., Friedrich, C., & Laborie, M. P. (**2016**). The chemical, kinetic and mechanical characterization of tannin-based adhesives with different crosslinking systems. *International Journal of Adhesion and Adhesives*, ***68***, 1–8.

Bonnardeaux, J. (**2007**). Uses for canola meal. Available at: https://www.agric.wa.gov.au/canola/Western-Australian-canola-industry [2016/12/20]

Bragg, W., & Bragg, W. (**1913**). The reflection of X-rays by crystals. *Proceedings of the Royal Society of London - Series A*, ***88*(*605*)**, 428–438.

Brinchi, L., Cotana, F., Fortunati, E., & Kenny, J. M. (**2013**). Production of nanocrystalline cellulose from lignocellulosic biomass: Technology and applications. *Carbohydrate Polymers*, ***94*(*1*)**, 154–169.

Brody, A., Bugusu, B., Han, J., & Sand, C. (**2008**). Innovative food packaging solutions - scientific status summary. *Journal of Food Science*, ***73*(*8*)**, R107–R116.

Brown, C. H. (**1952**). Some structural proteins of Mytilus edulis. *Microscale Science*, ***93***, 487–489.

Burzio, L. A., & Waite, J. H. (**2000**). Cross-linking in adhesive quinoproteins: studies with model decapeptides. *Biochemistry*, ***39*(*36*)**, 11147–11153.

Canadian Standards Association. (**1993**). Canadian standard association protocol for strand board. *CSA O437-93*, 1–88.

Canola Council of Canada. (**2016**). Canadian canola production 2016. Available at: http://www.canolacouncil.org/markets-stats/statistics/tonnes/ [2016/12/28]

Cha, H. J., Hwang, D. S., & Lim, S. (**2008**). Development of bioadhesives from marine mussels. *Biotechnology Journal*, ***3*(*5*)**, 631–638.

Chen, W., Yan, L., & Bangal, P. (**2010**). Preparation of graphene by the rapid and mild thermal reduction of graphene oxide induced by microwaves. *Carbon*, ***48*(*4*)**, 1146–1152.

Chen, X., Deng, X., Shen, W., & Jiang, L. (**2012**). Controlled enzymolysis preparation of nanocrystalline cellulose from pretreated cotton fibers. *BioResources*, *7*(***3***), 4237–4248.

Cheng, H. N., Dowd, M. K., & He, Z. (**2013**). Investigation of modified cottonseed protein adhesives for wood composites. *Industrial Crops and Products*, ***46***, 399–403.

Chupin, L., Motillon, C., Charrier-El Bouhtoury, F., Pizzi, A., & Charrier, B. (**2013**). Characterization of maritime pine (*Pinus pinaster*) bark tannins extracted under different conditions by spectroscopic methods, FTIR and HPLC. *Industrial Crops and Products*, ***49***, 897–903.

COPA-Canadian Oilseed Processors Association. (**2016**). Canadian oilseed processing industry. Available at: http://copacanada.com/crush-oil-meal-production/ [2016/12/25]

Coyne, K. J., Qin, X.X., & Waite, J. H. (**1997**). Extensible collagen in mussel byssus: a natural block copolymer. *Science*, ***277*****(*****5333*****)**, 1830–1832.

Cranston, E. D., & Gray, D. G. (**2006**). Morphological and optical characterization of polyelectrolyte multilayers incorporating nanocrystalline cellulose. *Biomacromolecules*, ***7*****(*****9*****)**, 2522–2530.

Cui, J., Lu, X., Zhou, X., Chrusciel, L., Deng, Y., Zhou, H., Brosse, N. (**2015**). Enhancement of mechanical strength of particleboard using environmentally friendly pine (*Pinus pinaster L.*) tannin adhesives with cellulose nanofibers. *Annals of Forest Science*, ***72*****(*****1*****)**, 27–32.

Cushen, M., Kerry, J., Morris, M., Cruz-Romero, M., & Cummins, E. (**2012**). Nanotechnologies in the food industry – Recent developments, risks and regulation. *Trends in Food Science & Technology*, ***24*****(*****1*****)**, 30–46.

D'Amico, S., Müller, U., & Berghofer, E. (**2013**). Effect of hydrolysis and denaturation of wheat gluten on adhesive bond strength of wood joints. *Journal of Applied Polymer Science*, ***129*(*5*)**, 2429–2434.

Dalsin, J. L., Hu, B. H., Lee, B. P., & Messersmith, P. B. (**2003**). Mussel adhesive protein mimetic polymers for the preparation of nonfouling surfaces. *Journal of the American Chemical Society*, ***125*(*14*)**, 4253–4258.

Damodaran, S., & Zhu, D. (**2016**). A formaldehyde-free water-resistant soy flour-based adhesive for plywood. *Journal of the American Oil Chemists' Society*, ***93*(*9*)**, 1311–1318.

Deak, N. A., Murphy, P. A., & Johnson, L. A. (**2006**). Fractionating soybean storage proteins using Ca^{2+} and $NaHSO_3$. *Journal of Food Science*, ***71*(*7*)**, C413–C424.

Denbow, D. M., Ravindran, V., Kornegay, E. T., Yi, Z., & Hulet, R. M. (**1995**). Improving phosphorus availability in soybean meal for broilers by supplemental phytase. *Poultry Science*, ***74*(*11*)**, 1831–42.

Desai, S., Patel, J., & Sinha, V. (**2003**). Polyurethane adhesive system from biomaterial-based polyol for bonding wood. *International Journal of Adhesion and Adhesives*, ***23*(*5*)**, 393–399.

Deshmukh, M. V. (**2004**). *Synthesis and Characterization of Mussel Adhesive Peptides*. (Doctoral dissertation) Department of chemistry, Universität Regensburg, Phillips Universität, Germany.

Detlefsen, W. (**2002**). Phenolic resins: some chemistry technology and history. In D. Dillard & Pocius AV (Eds.), *Adhesive Science and Engineering–2: Surfaces, Chemistry and Applications* (pp 869-946). Amsterdam: Elsevier.

Dhimiter, B., Herrick, C. A., Smith, T. J., Woskie, S. R., Streicher, R. P., Cullen, M. R., Redlich, C. A. (**2007**). Skin exposure to isocyanates: reasons for concern. *Environmental Health Perspective*, ***115*****(*****3*****)**, 328–335.

Ebnesajjad, S. (**2008**). Introduction and adhesion theories. In S. Ebnesajjad (Eds.), *Adhesives Technology Handbook* (pp 1–26). Norwich, NY: William Andrew Inc.

Efhamisisi, D., Thevenon, M. F., Hamzeh, Y., Karimi, A. N., Pizzi, A., & Pourtahmasi, K. (**2016**). Induced tannin adhesive by boric acid addition and its effect on bonding quality and biological performance of poplar plywood. *ACS Sustainable Chemistry & Engineering*, ***4*****(*****5*****)**, 2734–2740.

El-Thaher, N., Mussone, P., Bressler, D., & Choi, P. (**2014**). Kinetics study of curing epoxy resins with hydrolyzed proteins and the effect of denaturants urea and sodium dodecyl sulfate. *ACS Sustainable Chemistry & Engineering*, ***2*****(*****2*****)**, 282–287.

Even, M. A., Wang, J., & Chen, Z. (**2008**). Structural information of mussel adhesive protein mefp-3 acquired at various polymer/mefp-3 solution interfaces. *Langmuir*, ***24*****(*****11*****)**, 5795–5801.

Fancy, D. A., & Kodadek, T. (**1999**). Chemistry for the analysis of protein-protein interactions: rapid and efficient cross-linking triggered by long wavelength light. *Proceedings of the National Academy of Sciences*, ***96*****(*****11*****)**, 6020–6024.

FAO - Food and Agriculture Organization. (**2016**). Food Outlook - 2016. Available at : http://www.fao.org/3/a-I5703E.pdf [2016/12/26]

FAOSTAT. (**2010**). Agricultural data. *Food and Agricultural Organization, United Nations,* Available at: http://faostat.fao.org [2016/12/18]

Feipeng Liu, & Joel Barker. (**2007**). Multi-step preheating processes for manufacturing wood based composites. US 7258761 B2. USPTO.

Filpula, D. R., Lee, S. M., Link, R. P., Strausberg, S. L., & Strausberg, R. L. (**1990**). Structural and functional repetition in a marine mussel adhesive protein. *Biotechnology progress*, ***6*(*3*)**, 171–177.

Freedonia Group. (**2016**). *World adhesives and sealants - Industry study with forecast for 2019 & 2024*. Available at: http://www.freedoniagroup.com/industry-study/world-adhesives-sealants-3377.htm [2016/12/20].

Frihart, C. (**2013**). Wood Adhesion and Adhesives. In R. M. Rowell (Eds.), *Handbook of Wood Chemistry and Wood Composites* (pp 255–319). Boca Raton, FL: CRC.

Frihart, C. (**2016**). Potential for biobased adhesives in wood bonding. In *International Convention of Society of Wood Science and Technology* (pp. 84–91). Curitiba, Brazil: Society of Wood Science and Technology.

Frihart, C. R., & Hunt, C. G. (**2010**). Adhesives with wood materials: bond formation and performance. *US Department of Agriculture Forest Service, general technical report*: 508.

Frihart, C. R., Birkeland, M. J., Frihart, C. R., & Birkeland, M. J. (**2014**). Soy properties and soy wood adhesives. In R. Brentin (Eds.), *Soy-Based Chemicals and Materials* (pp 167–192). Washington, DC. American Chemical Society .

Gandini, A. (**2008**). Polymers from renewable resources: a challenge for the future of macromolecular materials. *Macromolecules*, ***41*(*24*)**, 9491–9504.

Gardner, D. (**2006**). Adhesion mechanisms of durable wood adhesive bonds. In D. Stokke & L. Groom (Eds.), *Characterization of the cellulosic cell wall* (pp 254–265). Ames, Iowa: Wiley-Blackwell.

Gatoo, M., Naseem, S., Arfat, M., Dar, A., Qasim, K., & Zubair, S. (**2014**). Physicochemical properties of nanomaterials: implication in associated toxic manifestations. *BioMed Research International*, ***2014*(*498420*)**, 1–9.

Gerrard, J. A. (**2002**). Protein–protein crosslinking in food: methods, consequences, applications. *Trends in Food Science & Technology*, ***13*(*12*)**, 391–399.

González, Z., Botas, C., Álvarez, P., Roldán, S., Blanco, C., Santamaría, R., Menéndez, R. (**2012**). Thermally reduced graphite oxide as positive electrode in vanadium redox flow batteries. *Carbon*, ***50*(*3*)**, 828–834.

Grala, W., Verstegen, M. W., Jansman, A. J., Huisman, J., & van Leeusen, P. (**1998**). Ileal apparent protein and amino acid digestibilities and endogenous nitrogen losses in pigs fed soybean and rapeseed products. *Journal of Animal Science*, ***76*(*2*)**, 557.

Grdadolnik, J. (**2002**). A FTIR investigation of protein conformation. *Bulletin of the Chemists and Technologists of Macedonia*, ***21***, 23–34.

Grundmeier, G., & Stratmann, M. (**2005**). Adhesion and de-adhesion mechanism polymer/metal interfaces: Mechanistic understanding based on in situ studies of buried interfaces. *Annual Review of Materials Research*, ***35*(*1*)**, 571–615.

Guo, M., & Wang, G. (**2016**). Whey protein polymerization and its applications in environmentally safe adhesives. *International Journal of Dairy Technology*. ***69(4)***, 481-488.

Guvendiren, M., Messersmith, P., & Shull, K. (**2007**). Self-assembly and adhesion of DOPA-modified methacrylic triblock hydrogels. *Biomacromolecules*, ***9*(*1*)**, 122–128.

Habibi, Y., Lucia, L. A., & Rojas, O. J. (**2010**). Cellulose nanocrystals: chemistry, self-assembly, and applications. *Chemical Reviews*, ***110*(*6*)**, 3479–3500.

Haemers, S., Koper, G. J. M., & Frens, G. (**2003**). Effect of oxidation rate on cross-linking of mussel adhesive proteins. *Biomacromolecules*, ***4*(*3*)**, 632–640.

Hale, K. (**2013**). *The potential of canola protein for bio-based wood adhesives*. (Master's dissertation). Kansas State University.

Hamarneh, A. I., Heeres, H. J., Broekhuis, A. A., & Picchioni, F. (**2010**). Extraction of *Jatropha curcas* proteins and application in polyketone-based wood adhesives. *International Journal of Adhesion and Adhesives*, ***30*(*7*)**, 615–625.

Han, C., Zhang, N., & Xu, Y.-J. (**2016**). Structural diversity of graphene materials and their multifarious roles in heterogeneous photocatalysis. *Nano Today*, ***11*(*3*)**, 351–372.

Haris, P. I., & Severcan, F. (**1999**). FTIR spectroscopic characterization of protein structure in aqueous and non-aqueous media. *Journal of Molecular Catalysis B: Enzymatic*, ***7*****(*****1–4*****)**, 207–221.

Hasegawa, Y., Shikinaka, K., Katayama, Y., Kajita, S., Masai, E., Nakamura, M., Shigehara, K. (**2009**). Tenacious epoxy adhesives prepared from lignin-derived stable metabolic intermediate. *Sen'i Gakkaishi*, ***65*****(*****12*****)**, 359–362.

He, Z., Chapital, D. C., Cheng, H. N., & Dowd, M. K. (**2014**). Comparison of adhesive properties of water- and phosphate buffer-washed cottonseed meals with cottonseed protein isolate on maple and poplar veneers. *International Journal of Adhesion and Adhesives*, ***50***, 102–106.

Heendeniya, R. G., Christensen, D. A., Maenz, D. D., McKinnon, J. J., & Yu, P. (**2012**). Protein fractionation byproduct from canola meal for dairy cattle. *Journal of Dairy Science*, ***95*****(*****8*****)**, 4488–4500.

Herrero, A. M., Carmona, P., Cofrades, S., & Jiménez-Colmenero, F. (**2008**). Raman spectroscopic determination of structural changes in meat batters upon soy protein addition and heat treatment. *Food Research International*, ***41*****(*****7*****)**, 765–772.

Hettiarachchy, N. S., Kalapathy, U., & Myers, D. J. (**1995**). Alkali-modified soy protein with improved adhesive and hydrophobic properties. *Journal of the American Oil Chemists' Society*, ***72*****(*****12*****)**, 1461–1464.

Hight, L. M., & Wilker, J. J. (**2007**). Synergistic effects of metals and oxidants in the curing of marine mussel adhesive. *Journal of Materials Science*, ***42*****(*****21*****)**, 8934–8942.

Hoet, P., Bruske-Hohlfeld, I., & Salata, O. (**2004**). Nanoparticles – known and unknown health risks. *Journal of Nanobiotechnology*, ***2*****(*****1*****)**, 1–12.

Hontoria-Lucas, C., López-Peinado, A. J., López-González, J. d. D., Rojas-Cervantes, M. L., & Martín-Aranda, R. M. (**1995**). Study of oxygen-containing groups in a series of graphite oxides: Physical and chemical characterization. *Carbon*, ***33*****(*****11*****)**, 1585–1592.

Huang, W., & Sun, X. (**2000**a). Adhesive properties of soy proteins modified by sodium dodecyl sulfate and sodium dodecylbenzene sulfonate. *Journal of the American Oil Chemists' Society*, ***77*****(*****7*****)**, 705–708.

Huang, W., & Sun, X. (**2000**b). Adhesive properties of soy proteins modified by urea and guanidine hydrochloride. *Journal of the American Oil Chemists' Society*, ***77*****(*****1*****)**, 101–104.

Hummers, W. S., & Offeman, R. E. (**1958**). Preparation of graphitic oxide. *Journal of the American Chemical Society*, ***80*****(*****6*****)**, 1339–1339.

Hüttermann, A., Mai, C., & Kharazipour, A. (**2001**). Modification of lignin for the production of new compounded materials. *Applied Microbiology and Biotechnology*, ***55*****(*****4*****)**, 387–384.

Hwang, D. S., Zeng, H., Masic, A., Harrington, M. J., Israelachvili, J. N., & Waite, J. H. (**2010**). Protein- and metal-dependent interactions of a prominent protein in mussel adhesive plaques. *The Journal of biological chemistry*, ***285*****(*****33*****)**, 25850–25858.

Imam, S. H., Bilbao-Sainz, C., Chiou, B.-S., Glenn, G. M., & Orts, W. J. (**2013**). Biobased adhesives, gums, emulsions, and binders: current trends and future prospects. *Journal of Adhesion Science and Technology*, ***27*****(*****18–19*****)**, 1972–1997.

Ito, S., Kato, T., Shinpo, K., & Fujita, K. (**1984**). Oxidation of tyrosine residues in proteins by tyrosinase. Formation of protein-bonded 3, 4-dihydroxyphenylalanine and 5-S-cysteinyl-3, 4-dihydroxyphenylalanine. *Biochemical Journal*, ***222*(*2*)**, 407–411.

Jackson, S., & Nuzzo, R. G. (**1995**). Determining hybridization differences for amorphous carbon from the XPS C 1s envelope. *Applied Surface Science*, ***90*(*2*)**, 195–203.

Jang, Y., Huang, J., & Li, K. (**2011**). A new formaldehyde-free wood adhesive from renewable materials. *International Journal of Adhesion and Adhesives*, ***31*(*7*)**, 754–759.

Jeong, H. K., Jin, M. H., So, K. P., Lim, S. C., & Lee, Y. H. (**2009**). Tailoring the characteristics of graphite oxides by different oxidation times. *Journal of Physics D: Applied Physics*, ***42*(*65418*)**, 1–6.

Jiang, J., Xiong, Y., & Chen, J. (**2010**). PH shifting alters solubility characteristics and thermal stability of soy protein isolate and its globulin fractions in different pH, salt concentration, and temperature. *Journal of Agricultural and Food Chemistry*, ***58*(*13*)**, 8035–8042.

Johns, W. (**1982**). Isocyanates as Wood Binders—A Review. *The Journal of Adhesion*, ***15*(*1*)**, 59–67.

Jus, S., Kokol, V., & Guebitz, G. (**2008**). Tyrosinase-catalysed coupling of functional molecules onto protein fibres. *Enzyme and Microbial Technology*, ***42*(*7*)**, 535–542.

Kaboorani, A., & Riedl, B. (**2011**). Effects of adding nano-clay on performance of polyvinyl acetate (PVA) as a wood adhesive. *Composites Part A: Applied Science and Manufacturing*, ***42*(*8*)**, 1031–1039.

Kaboorani, A., & Riedl, B. (**2012**). Nano-aluminum oxide as a reinforcing material for thermoplastic adhesives. *Journal of Industrial and Engineering Chemistry*, ***18*****(*****3*****)**, 1076–1081.

Kaboorani, A., Riedl, B., Blanchet, P., Fellin, M., Hosseinaei, O., & Wang, S. (**2012**). Nanocrystalline cellulose (NCC): A renewable nano-material for polyvinyl acetate (PVA) adhesive. *European Polymer Journal*, ***48*****(*****11*****)**, 1829–1837.

Kadota, J., Fukuoka, T., Uyama, H., Hasegawa, K., & Kobayashi, S. (**2004**). New positive-type photoresists based on enzymatically synthesized polyphenols. *Macromolecular Rapid Communications*, ***25*****(*****2*****)**, 441–444.

Kalapathy, U., Hettiarachchy, N. S., & Rhee, K. C. (**1997**). Effect of drying methods on molecular properties and functionalities of disulfide bond-cleaved soy proteins. *Journal of the American Oil Chemists' Society*, ***74*****(*****3*****)**, 195–199.

Kalapathy, U., Hettiarachchy, N. S., Myers, D., & Hanna, M. A. (**1995**). Modification of soy proteins and their adhesive properties on woods. *Journal of the American Oil Chemists' Society*, ***72*****(*****5*****)**, 507–510.

Kalapathy, U., Hettiarachchy, N. S., Myers, D., & Rhee, K. C. (**1996**). Alkali-modified soy proteins: effect of salts and disulfide bond cleavage on adhesion and viscosity. *Journal of the American Oil Chemists' Society*, ***73*****(*****8*****)**, 1063–1066.

Kamke, F. A., & Lee, J. N. (**2007**). Adhesive penetration in wood—a review. *Wood and Fiber Science*, ***39*****(*****2*****)**, 205–220.

Kasran, M., Cui, S. W., & Goff, H. D. (**2013**). Emulsifying properties of soy whey protein isolate–fenugreek gum conjugates in oil-in-water emulsion model system. *Food Hydrocolloids*, ***30*(*2*)**, 691–697.

Kei, S., Shibusawa, T., Ohashi, K., Castellanos, J. R. S., & Hatano, Y. (**2008**). Effects of density profile of MDF on stiffness and strength of nailed joints. *Journal of Wood Science*, ***54*(*1*)**, 45–53.

Keimel, F. (**2003**). Historical development of adhesive and adhesive bonding. In A. Pizzi & K. Mittal (Eds.), *Handbook of Adhesive Technology* (pp 1–12). Boca Raton, FL: CRC Press.

Khajali, F., & Slominski, B. A. (**2012**). Factors that affect the nutritive value of canola meal for poultry. *Poultry science*, ***91*(*10*)**, 2564–2575.

Khan, U., May, P., Porwal, H., Nawaz, K., & Coleman, J. N. (**2013**). Improved adhesive strength and toughness of polyvinyl acetate glue on addition of small quantities of graphene. *ACS Applied Materials & Interfaces*, ***5*(*4*)**, 1423–1428.

Khosravi, S., Khabbaz, F., Nordqvist, P., & Johansson, M. (**2010**). Protein-based adhesives for particleboards. *Industrial Crops and Products*, ***32*(*3*)**, 275–283.

Khosravi, S., Khabbaz, F., Nordqvist, P., & Johansson, M. (**2014**). Wheat gluten based adhesives for particle boards: effect of crosslinking agents. *Macromolecular Materials and Engineering*, ***299*(*1*)**, 116–124.

Khosravi, S., Nordqvist, P., Khabbaz, F., & Johansson, M. (**2011**). Protein-based adhesives for particleboards-Effect of application process. *Industrial Crops and Products*. ***32(3)***, 275-283.

Kim, H., Abdala, A., & Macosko, C. (**2010**). Graphene/polymer nanocomposites. *Macromolecules*, ***43*****(*****16*****)**, 6515–6530.

Kinloch, A. J. (**1980**). The science of adhesion - Part 1: Surface and interfacial aspects. *Journal of Materials Science*, ***15*****(*****9*****)**, 2141–2166.

Kinloch, A. J. (**1982**). The science of adhesion - Part 2: Mechanics and mechanisms of failure. *Journal of Materials Science*, ***17*****(*****3*****)**, 617–651.

Kinsella, J. E. (**1979**). Functional properties of soy proteins. *Journal of the American Oil Chemists' Society*, ***56*****(*****3*****)**, 242–258.

Kishi, H., Fujita, A., Miyazaki, H., Matsuda, S., & Murakami, A. (**2006**). Synthesis of wood-based epoxy resins and their mechanical and adhesive properties. *Journal of Applied Polymer Science*, ***102*****(*****3*****)**, 2285–2292.

Klockeman, D., Toledo, R., & Sims, K. (**1997**). Isolation and characterization of defatted canola meal protein. *Journal of Agricultural and Food Chemistry*, ***45*****(*****10*****)**, 3867–3870.

Kodadek, T., Duroux-Richard, I., & Bonnafous, J.-C. (**2005**). Techniques: Oxidative cross-linking as an emergent tool for the analysis of receptor-mediated signalling events. *Trends in Pharmacological Sciences*, ***26*****(*****4*****)**, 210–217.

Koichi, M., & Tomida, M. (**2004**). Heat-induced secondary structure and conformation change of bovine serum albumin investigated by fourier transform infrared spectroscopy. *Bochemistry*, ***43*****(*****36*****)**, 11526–11532.

Kolster, P., de Graaf, L. A., & Vereijken, J. M. (**1997**). Application of cereal proteins in technical applications. *Cereals: Novel uses and processes*, 107–116.

Kong, J., & Yu, S. (**2007**). Fourier transform infrared spectroscopic analysis of protein secondary structures. *Acta Biochimica et Biophysica Sinica*, ***39*****(*****8*****)**, 549–559.

Kong, X., Liu, G., & Curtis, J. M. (**2011**). Characterization of canola oil based polyurethane wood adhesives. *International Journal of Adhesion and Adhesives*, ***31*****(*****6*****)**, 559–564.

Krishnamoorthy, K., Veerapandian, M., Yun, K., & Kim, S. J. (**2013**). The chemical and structural analysis of graphene oxide with different degrees of oxidation. *Carbon*, ***53***, 38–49.

Krishnan, H. (**2001**). Biochemistry and molecular biology of soybean seed storage proteins. *Journal of New Seeds*, ***2*****(*****3*****)**, 1–25.

Krzyzaniak, A., Burova, T., & Haertle, T. (**1998**). The structure and properties of Napin-seed storage protein from rape (*Brassica napus* L.). *Food/Nahrung*, ***42*****(*****3–4*****)**, 201–204.

Kuboe, Y., Tonegawa, H., & Ohkawa, K. (**2004**). Quinone cross-linked polysaccharide hybrid fiber. *Biomacromolecules*, ***5*****(*****2*****)**, 348–357.

Kumar, A., Depan, D., Singh Tomer, N., & Singh, R. (**2009**). Nanoscale particles for polymer degradation and stabilization—Trends and future perspectives. *Progress in Polymer Science*, ***34*****(*****6*****)**, 479–515.

Kumar, R., Choudhary, V., Mishra, S., Varma, I. K., & Mattiason, B. (**2002**). Adhesives and plastics based on soy protein products. *Industrial Crops and Products*, ***16*****(*****3*****)**, 155–172.

Lagrain, B., Goderis, B., Brijs, K., & Delcour, J. A. (**2010**). Molecular basis of processing wheat gluten toward biobased materials. *Biomacromolecules*, ***11*****(*****3*****)**, 533–541.

Lambuth, A. L. (**1994**). Protein adhesives for wood. In A. Pizzi & K.L. Mittal (Eds.), *Handbook of Adhesive Technology*, (pp 457–478). New York: NY. Marcel Dekker Inc.

Lambuth, A. L. (**2001**). Blood and casein glues. In D. Satas & A. A. Tracton (Eds.), *Coatings Technology Handbook* (pp 519–530). New York: NY. Marcel Dekker Inc.

Lee, B., Dalsin, J., & Messersmith, P. (**2006**). Biomimetic adhesive polymers based on mussel adhesive proteins. In A. Smith & J. Callow (Eds.), *Biological Adhesives* (pp 257–278). Berlin, Heidelberg: Springer.

Lee, C., Wei, X., Kysar, J. W., & Hone, J. (**2008**). Measurement of the elastic properties and intrinsic strength of monolayer graphene. *Science*, ***321*****(*****5887*****)**, 385–388.

Lee, H., Scherer, N. F., & Messersmith, P. B. (**2006**). Single-molecule mechanics of mussel adhesion. *Proceedings of the National Academy of Sciences of the United States of America*, ***103*****(*****35*****)**, 12999–13003.

Lee, S., & Park, S. (**2014**). Isothermal exfoliation of graphene oxide by a new carbon dioxide pressure swing method. *Carbon*, ***68***, 112–117.

Lei, H., Du, G., Wu, Z., Xi, X., & Dong, Z. (**2014**). Cross-linked soy-based wood adhesives for plywood. *International Journal of Adhesion and Adhesives*, ***50***, 199–203.

Lei, H., Pizzi, A., Navarrete, P., Rigolet, S., Redl, A., & Wagner, A. (**2010**). Gluten protein adhesives for wood panels. *Journal of Adhesion Science and Technology*, ***24*****(*****8–10*****)**, 1583–1596.

Li, D., Müller, M. B., Gilje, S., Kaner, R. B., & Wallace, G. G. (**2008**). Processable aqueous dispersions of graphene nanosheets. *Nature Nanotechnology*, ***3*****(*****2*****)**, 101–105.

Li, J. Y., Yeh, A. I., & Fan, K. L. (**2007**). Gelation characteristics and morphology of corn starch/soy protein concentrate composites during heating. *Journal of Food Engineering*, ***78*****(*****4*****)**, 1240–1247.

Li, K. (**2007**). Formaldehyde-free lignocellulosic adhesives and composites made from the adhesives. US 7722712 B2. USPTO.

Li, N., Qi, G., Sun, X. S., & Wang, D. (**2012**). Effects of sodium bisulfite on the physicochemical and adhesion properties of canola protein fractions. *Journal of Polymers and the Environment*, ***20*****(*****4*****)**, 905–915.

Li, N., Qi, G., Sun, X. S., & Wang, D. (**2012**). Effects of sodium bisulfite on the physicochemical and adhesion properties of canola protein fractions. *Journal of Polymers and the Environment*, ***20*****(*****4*****)**, 905–915.

Li, N., Qi, G., Sun, X. S., Stamm, M. J., & Wang, D. (**2011**). Physicochemical properties and adhesion performance of canola protein modified with sodium bisulfite. *Journal of the American Oil Chemists' Society*, ***89*****(*****5*****)**, 897–908.

Li, X., Luo, J., Gao, Q., & Li, J. (**2016**). A sepiolite-based united cross-linked network in a

soybean meal-based wood adhesive and its performance. *RSC Advances*, ***6*****(*51*)**, 45158–45165.

Li, Z., Zhang, W., Luo, Y., & Yang, J. (**2009**). How graphene is cut upon oxidation? *Journal of the American Chemical Society*, ***131*****(*18*)**, 6320–6321.

Liang, J., Huang, Y., Zhang, L., & Wang, Y. (**2009**). Molecular level dispersion of graphene into poly (vinyl alcohol) and effective reinforcement of their nanocomposites. *Advanced Functional Materials*, ***19*****(*14*)**, 2297–2302.

Lin, Q., Gourdon, D., Sun, C., Holten-Andersen, N., Anderson, T. H., Waite, J. H., & Israelachvili, J. N. (**2007**). Adhesion mechanisms of the mussel foot proteins mfp-1 and mfp-3. *Proceedings of the National Academy of Sciences of the United States of America*, ***104*****(*10*)**, 3782–3786.

Linse, S., Cabaleiro-Lago, C., Xue, W.-F., Lynch, I., Lindman, S., Thulin, E., Dawson, K. A. (**2007**). Nucleation of protein fibrillation by nanoparticles. *Proceedings of the National Academy of Sciences of the United States of America*, ***104*****(*21*)**, 8691–8696.

Liu, D., Bian, Q., Li, Y., Wang, Y., Xiang, A., & Tian, H. (**2016**). Effect of oxidation degrees of graphene oxide on the structure and properties of poly (vinyl alcohol) composite films. *Composites Science and Technology*, ***129***, 146–152.

Liu, D., Chen, H., Chang, P. R., Wu, Q., Li, K., & Guan, L. (**2010**). Biomimetic soy protein nanocomposites with calcium carbonate crystalline arrays for use as wood adhesive. *Bioresource technology*, ***101*****(*15*)**, 6235–6241.

Liu, D., Chen, X., Yue, Y., Chen, M., & Wu, Q. (**2011**). Structure and rheology of nanocrystalline cellulose. *Carbohydrate Polymers*, ***84*****(*****1*****)**, 316–322.

Liu, H., Li, C., & Sun, X. S. (**2015**). Improved water resistance in undecylenic acid (UA)-modified soy protein isolate (SPI)-based adhesives. *Industrial Crops and Products*, ***74***, 577–584.

Liu, J., Fu, S., Yuan, B., Li, Y., & Deng, Z. (**2010**). Toward a universal adhesive nanosheet for the assembly of multiple nanoparticles based on a protein-induced reduction/decoration of graphene oxide. *Journal of the American Chemical Society*, ***132*****(*****21*****)**, 7279–7281.

Liu, K. (**2012**). *Soybeans: chemistry, technology, and utilization*. Liu, K. (Eds). New York, USA: Chapman an Hall.

Liu, Y., & Li, K. (**2002**). Chemical modification of soy protein for wood adhesives. *Macromolecular Rapid Communications*, ***23*****(*****13*****)**, 739–742.

Liu, Y., & Li, K. (**2004**). Modification of soy protein for wood adhesives using mussel protein as a model: The influence of a mercapto group. *Macromolecular Rapid Communications*, ***25*****(*****21*****)**, 1835–1838.

Lu, Q., Danner, E., & Waite, J. (**2013**). Adhesion of mussel foot proteins to different substrate surfaces. *Journal of The Royal Society Interface*, ***10*****(*****70*****)**, 2012–759.

Luo, J., Li, C., Li, X., Luo, J., Gao, Q., & Li, J. (**2015**). A new soybean meal-based bioadhesive enhanced with 5,5-dimethyl hydantoin polyepoxide for the improved water resistance of plywood. *RSC Advances*, ***5*****(*****77*****)**, 62957–62965.

Luo, J., Luo, J., Bai, Y., Gao, Q., & Li, J. (**2016**). A high performance soy protein-based bio-adhesive enhanced with a melamine/epichlorohydrin prepolymer and its application on plywood. *RSC Advances*, ***6*****(*72*)**, 67669–67676.

Luo, J., Luo, J., Yuan, C., Zhang, W., Li, J., Gao, Q., & Chen, H. (**2015**). An eco-friendly wood adhesive from soy protein and lignin: performance properties. *RSC Advances*, ***5*****(*122*)**, 100849–100855.

Maeva, E., Severina, I., Bondarenko, S., Chapman, G., O'Neill, B., Severin, F., & Maev, R. G. (**2004**). Acoustical methods for the investigation of adhesively bonded structures: A review. *Canadian Journal of Physics*, ***82*****(*12*)**, 981–1025.

Malik, M., & Kaur, R. (**2016**). Mechanical and thermal properties of castor oil-based polyurethane adhesive: effect of TiO_2 filler. *Advances in Polymer Technology*, ***35*****(*4*)**, 21637–21644.

Manamperi, W. A. R., Chang, S. K. C., Ulven, C. A., & Pryor, S. W. (**2010**). Plastics from an improved canola protein isolate: preparation and properties. *Journal of the American Oil Chemists' Society*, ***87*****(*8*)**, 909–915.

Mansouri, N., Pizzi, A., & Salvado, J. (**2007**). Lignin-based polycondensation resins for wood adhesives. *Journal of Applied Polymer Science*, ***103*****(*3*)**, 1690–1699.

Marquis, D., Chivas-Joly, C., & Guillaume, É. (**2011**). *Properties of nanofillers in polymer*. INTECH Open Access Publisher.

Marra, A. (**1992**). *Technology of wood bonding: Principles in practice*. New York: Van Nostrand Reinhold.

Mathias, J., Grédiac, M., & Michaud, P. (**2016**). Bio-based adhesives. In Pacheco-Torgal F, V. Ivanov, N. Karak, & H. Jonkers (Eds.), *Biopolymers and Biotech Admixtures for Eco-Efficient Construction Materials* (pp 369–385). Waltham, MA: Elsevier Ltd.

Mcallister, M. J., Li, J.-L., Adamson, D. H., Schniepp, H. C., Abdala, A. A., Liu, J., Aksay, I. A. (**2007**). Single sheet functionalized graphene by oxidation and thermal expansion of graphite. *Chemistry of Materials*, ***19*****(*****18*****)**, 4396–4404.

McBain, J. W., & Hopkins, D. G. (**1924**). On adhesives and adhesive action. *The Journal of Physical Chemistry*, ***29*****(*****2*****)**, 188–204.

Mekonnen, T. H., Mussone, P. G., Choi, P., & Bressler, D. C. (**2014**). Adhesives from waste protein biomass for oriented strand board composites: development and performance. *Macromolecular Materials and Engineering*, ***299*****(*****8*****)**, 1003–1012.

Mo, X., Sun, X. S., & Wang, Y. (**1999**). Effects of molding temperature and pressure on properties of soy protein polymers. *Journal of Applied Polymer Science*, ***73*****(*****13*****)**, 2595–2602.

Mo, X., Sun, X., & Wang, D. (**2004**). Thermal properties and adhesion strength of modified soybean storage proteins. *Journal of the American Oil Chemists' Society*, ***81*****(*****4*****)**, 395–400.

Mojica, L., Dia, V., & Mejia, E. (**2015**). Soy proteins. In Z. Ustunol (Eds.), *Applied Food Protein Chemistry* (pp 141–191). Chichester, UK: John Wiley & Sons, Ltd.

Monahan, J., & Wilker, J. J. (**2003**). Specificity of metal ion cross-linking in marine mussel adhesives. *Chemical Communications*, ***2003*****(*****14*****)**, 1672–1673.

Monahan, J., & Wilker, J. J. (**2004**). Cross-linking the protein precursor of marine mussel adhesives: Bulk measurements and reagents for curing. *Langmuir*, ***20*****(*****9*****)**, 3724–3729.

Moon, R. J., Frihart, C. R., Wegner, T., Moon, R. J., Frihart, C. R., & Wegner, T. (**2006**). Nanotechnology applications in the forest products industry. *Forest products journal*, ***56*****(*****5*****)**, 4–10.

Moubarik, A., Mansouri, H. R., Pizzi, A., Charrier, F., Allal, A., & Charrier, B. (**2013**). Corn flour-mimosa tannin-based adhesives without formaldehyde for interior particleboard production. *Wood Science and Technology*, ***47*****(*****4*****)**, 675–683.

Nagano, T., Hirotsuka, M., Mori, H., Kohyama, K., & Nishinari, K. (**1992**). Dynamic viscoelastic study on the gelation of 7 S globulin from soybeans. *Journal of Agricultural and Food Chemistry*, ***40*****(*****6*****)**, 941–944.

Newkirk, R. (**2015**). Canola meal - Feed industry guide. Available at : http://www.canolacouncil.org/media/516716/2015_canola_meal_feed_industry_guide.pdf [2016/12/27]

Nicholson, C., Abercrombie, J., Botterill, W., & Brocato, R. (**1991**). History of adhesives. *ESC Reports*.

Nietzel, T., Dudkina, N. V, Haase, C., Denolf, P., Semchonok, D. A., Boekema, E. J., Sunderhaus, S. (**2013**). The native structure and composition of the cruciferin complex in *Brassica napus*. *The Journal of Biological Chemistry*, ***288*****(*****4*****)**, 2238–2245.

Norde, W. (**2011**). Intermolecular interactions. In L. Frewer, A. Fischer, W. Norde, & F. Kampers (Eds.), *Nanotechnology in the Agri-Food Sector* (pp 5–22). Weinheim, Germany: Wiley-VCH.

Nordqvist, P., Khabbaz, F., & Malmstroem, E. (**2010**). Comparing bond strength and water resistance of alkali-modified soy protein isolate and wheat gluten adhesives. *International Journal of Adhesion and Adhesives*, ***30*****(*****2*****)**, 72–79.

Nordqvist, P., Lawther, M., Malmström, E., & Khabbaz, F. (**2012**). Adhesive properties of wheat gluten after enzymatic hydrolysis or heat treatment – A comparative study. *Industrial Crops and Products*, ***38***, 139–145.

Nordqvist, P., Thedjil, D., Khosravi, S., Lawther, M., Malmström, E., & Khabbaz, F. (**2012**). Wheat gluten fractions as wood adhesives-glutenins versus gliadins. *Journal of Applied Polymer Science*, ***123*****(*****3*****)**, 1530–1538.

O'Brien, N., & Cummins, E. (**2008**). Recent developments in nanotechnology and risk assessment strategies for addressing public and environmental health concerns. *Human and Ecological Risk Assessment: An International Journal*, ***14*****(*****3*****)**, 568–592.

OECD, & FAO. (**2016a**). OECD-FAO Agricultural outlook 2016-2025. Available at: http://www.oecd-ilibrary.org/agriculture-and-food/oecd-fao-agricultural-outlook-2016_agr_outlook-2016-en [2016/12/25].

OECD, & FAO. (**2016b**). OECD-FAO Agricultural Outlook 2016-2025. Oilseed industry. Availabe at: http://www.oecd-ilibrary.org/agriculture-and-food/oecd-fao-agricultural-outlook-2016_agr_outlook-2016-en [2016/12/25].

Ohkawa, K., Nishida, A., Ichimiya, K., Matsui, Y., & Nagaya, K. (**1999**). Purification and characterization of a DOPA-containing protein from the foot of the Asian freshwater mussel, *Limnoperna fortunei*. *Biofouling*, ***14*****(*****3*****)**, 181–188.

Pandey, J., Lee, J., Chu, W., Kim, C., Ahn, S., & Lee, C. (**2008**). Cellulose nano whiskers from grass of Korea. *Macromolecular Research*, ***16*****(*****5*****)**, 396–398.

Papov, V. V, Diamond, T. V, Biemann, K., & Waite, J. H. (**1995**). Hydroxyarginine-containing polyphenolic proteins in the adhesive plaques of the marine mussel *Mytilus edulis*. *Journal of Biological Chemistry*, ***270*****(*****34*****)**, 20183–20192.

Paredes, J., Villar-Rodil, S., & Martínez-Alonso, A. (**2008**). Graphene oxide dispersions in organic solvents. *Langmuir*, ***24*****(*****19*****),** 10560–10564.

Park, S., & Ruoff, R. S. (**2009**). Chemical methods for the production of graphenes. *Nature Nanotechnology*, ***4*****(*****4*****)**, 217–224.

Peng, B. L., Dhar, N., Liu, H. L., & Tam, K. C. (**2011**). Chemistry and applications of nanocrystalline cellulose and its derivatives: A nanotechnology perspective. *The Canadian Journal of Chemical Engineering*, ***89*****(*****5*****)**, 1191–1206.

Pizzi, A. (**1994**a). *Advanced Wood Adhesives Technology*. New York, NY. CRC Press.

Pizzi, A. (**1994**b). Urea-formaldehyde adhesives. In *Pizzi A.* (Eds.) *Advanced wood adhesives technology.* (pp 19-66). New York: NY. Marcel Dekker.

Pizzi, A. (**2003**a). Melamine-formaldehyde adhesives. In A. Pizzi & K. Mittal (Eds.), *Handbook of Adhesive Technology* (pp 653-680). New York: NY. Marcel Dekker.

Pizzi, A. (**2003**b). Natural phenolic adhesives I: Tannin. In A. Pizzi & K. Mittal (Eds.), *Handbook of adhesive technology* (pp 573-588). New York: NY. Marcel Dekker.

Pizzi, A. (**2003**c). Resorcinol Adhesives. In A. Pizzi & K. Mittal (Eds.), *Handbook of Adhesive Technology* (pp 599-614). New York: NY. Marcel Dekker.

Pizzi, A. (**2006**). Recent developments in eco-efficient bio-based adhesives for wood bonding: opportunities and issues. *Journal of Adhesion Science and Technology*, ***20*****(*****8*****)**, 829–846.

Pizzi, A. (**2013**). Bioadhesives for wood and fibres. *Reviews of Adhesion and Adhesives*, ***1*****(*****1*****)**, 88–113.

Pizzi, A. (**2016**). Wood products and green chemistry. *Annals of Forest Science*, ***73*****(*****1*****)**, 185–203.

Popa, V., Ungureanu, E., & Todorciuc, T. (**2007**). On the interaction of lignins, furan resins and furfuryl alcohol in adhesive systems. *Cellulose Chemistry and Technology*, ***41***, 119–123.

Posudievsky, O., & Khazieieva, O. (**2012**). Preparation of graphene oxide by solvent-free mechanochemical oxidation of graphite. *Journal of Materials Chemistry*, ***22*****(*****25*****)**, 12465–12467.

Qi, G., Li, N., Wang, D., & Sun, X. S. (**2013**). Physicochemical properties of soy protein adhesives modified by 2-octen-1-ylsuccinic anhydride. *Industrial Crops and Products*, ***46***, 165–172.

Qi, G., Li, N., Wang, D., & Sun, X. S. (**2016**). Development of high-strength soy protein adhesives modified with sodium montmorillonite clay. *Journal of the American Oil Chemists' Society*, ***93(11)***, 1509–1517.

Qi, H. (**2013**). Growing Bioeconomy-Alberta Activities and Capacities. In M. Bruins & T. Boxtel (Eds.), *Biorefinery for Food, Fuel and Materials* (pp 103). Wageningen, The Netherlands: Proceedings of Symposium Biorefinery for food fuel and materials.

Qiao, W., Li, S., Guo, G., Han, S., Ren, S., & Ma, Y. (**2015**). Synthesis and characterization of phenol-formaldehyde resin using enzymatic hydrolysis lignin. *Journal of Industrial and Engineering Chemistry*, ***21***, 1417–1422.

Raftery, G., Harte, A., & Rodd, P. D. (**2009**). Bonding of FRP materials to wood using thin epoxy gluelines. *International Journal of Adhesion and Adhesives*, ***29(5)***, 580–588.

Rajasekar, R., Moganapriya, C., Sathish Kumar, P., & Navaneethakrishnan, P. (**2016**). Binders such as adhesives, gums, wallpaper paste, resins or any subclass in polymer division. In Inamuddin Y (Eds.), *Green Polymer Composites Technology: Properties and Applications* (pp 49–62). Boca Raton, FL: CRC Press.

Raquez, J. M., Deleglise, M., Lacrampe, M. F., & Krawczak, P. (**2010**). Thermosetting (bio) materials derived from renewable resources: a critical review. *Progress in Polymer Science*, ***35(4)***, 487–509.

Rebollar, M., Pérez, R., & Vidal, R. (**2007**). Comparison between oriented strand boards and other wood-based panels for the manufacture of furniture. *Materials & Design*, ***28*****(*****3*****)**, 882–888.

Rowell, R. M. (**2005**). *Handbook of wood chemistry and wood composites*. Boca Raton, Florida: CRC Press.

Salari, A., Tabarsa, T., Khazaeian, A., & Saraeian, A. (**2013**). Improving some of applied properties of oriented strand board (OSB) made from underutilized low quality paulownia (*Paulownia fortunie*) wood employing nano-SiO_2. *Industrial Crops and Products*, ***42***, 1–9.

Santulli, C. (**2016**). Nanoclay based natural fibre reinforced polymer composites: mechanical and thermal properties. In M. Jawaid, A. K. Qaiss, & R. Bouhfid (Eds.), *Nanoclay Reinforced Polymer Composites* (pp 81–101). Singapore: Springer Singapore.

Sarikaya, M. (**1994**). An introduction to biomimetics: A structural viewpoint. *Microscopy Research and Technique*, ***27*****(*****5*****)**, 360–375.

Sato, S., & Nakamura, H. (**2013**). Ligand-directed selective protein modification based on local single-electron-transfer catalysis. *Angewandte Chemie International*, ***52***, 8681–8684.

Schniepp, H. C., Li, J.-L., McAllister, M. J., Sai, H., Herrera-Alonso, M., Adamson, D. H., Aksay, I. A. (**2006**). Functionalized single graphene sheets derived from splitting graphite oxide. *The Journal of Physical Chemistry B*, ***110*****(*****17*****)**, 8535–8539.

Schultz, J., & Nardin, M. (**2003**). Theories and mechanisms of adhesion. In A. Pizzi & K. Mittal (Eds.), *Handbook of Adhesive Technology* (pp 53–68). Boca Raton, FL: CRC Press.

Schwarzkopf, M., Huang, J., & Li, K. (**2009**). Effects of adhesive application methods on performance of a soy-based adhesive in oriented strandboard. *Journal of the American Oil Chemists' Society*, ***86*****(*****10*****)**, 1001–1007.

Schwarzkopf, M., Huang, J., & Li, K. (**2010**). A Formaldehyde-free soy-based adhesive for making oriented strandboard. *The Journal of Adhesion*, ***86*****(*****3*****)**, 352–364.

Sen, S., Patil, S., & Argyropoulos, D. S. (**2015**). Thermal properties of lignin in copolymers, blends, and composites: a review. *Green Chemistry*, ***17*****(*****11*****)**, 4862–4887.

Sever, M. J., Weisser, J. T., Monahan, J., Srinivasan, S., & Wilker, J. J. (**2004**). Metal-mediated cross-linking in the generation of a marine-mussel adhesive. *Angewandte Chemie, International Edition*, ***43*****(*****23*****)**, 2986.

Shao, G., Lu, Y., Wu, F., Yang, C., Zeng, F., & Wu, Q. (**2012**). Graphene oxide: the mechanisms of oxidation and exfoliation. *Journal of Materials Science*, ***47*****(*****10*****)**, 4400–4409.

Sharpe, L., & Schonhorn, H. (**1964**). Surface energetics, adhesion and adhesive joints. *Advances in Chemistry Series*, ***43***, 189–201.

Shin, H., Kim, K., Benayad, A., & Yoon, S. (**2009**). Efficient reduction of graphite oxide by sodium borohydride and its effect on electrical conductance. *Advanced Functional Materials*, ***19*****(*****12*****)**, 1987–1992.

Shtein, M., Nadiv, R., Buzaglo, M., Kahil, K., & Regev, O. (**2015**). Thermally conductive graphene-polymer composites: size, percolation, and synergy effects. *Chemistry of Materials*, ***27*****(*****6*****)**, 2100–2106.

Silva, C. J. S. M., Sousa, F., Gubitz, G., & Cavaco-Paulo, A. (**2004**). Chemical modifications on proteins using glutaraldehyde. *Food Technology and Biotechnology*, ***42*****(*1*)**, 51–56.

Silverman, H. G., & Roberto, F. F. (**2007**). Understanding marine mussel adhesion. *Marine Biotechnology*, ***9*****(*6*)**, 661–681.

Sobral, P., Palazolo, G., & Wagner, J. (**2010**). Thermal behavior of soy protein fractions depending on their preparation methods, individual interactions, and storage conditions. *Journal of Agricultural and Food Chemistry*, ***58*****(*18*)**, 10092–10100.

Somani, K. P., Kansara, S. S., Patel, N. K., & Rakshit, A. K. (**2003**). Castor oil based polyurethane adhesives for wood-to-wood bonding. *International Journal of Adhesion and Adhesives*, ***23*****(*4*)**, 269–275.

Song, Y., Seo, J., Choi, Y., Kim, D., & Choi, B. (**2016**). Mussel adhesive protein as an environmentally-friendly harmless wood furniture adhesive. *International Journal of Adhesion and Adhesives*, ***70***, 260–264.

SoyCanada. (**2016**). Canada's growing soybean industry. Available at : http://soycanada.ca/ industry/industry-overview/ [2016/12/22]

Staffas, L., Gustavsson, M., & McCormick, K. (**2013**). Strategies and policies for the bioeconomy and bio-based economy: an analysis of official national approaches. *Sustainability*, ***5*****(*6*)**, 2751–2769.

Stankovich, S., Piner, R. D., Nguyen, S. T., & Ruoff, R. S. (**2006**). Synthesis and exfoliation of isocyanate-treated graphene oxide nanoplatelets. *Carbon*, ***44*****(*15*)**, 3342–3347.

Staswick, P. E., Hermodson, M. A., & Nielsen, N. C. (**1981**). Identification of the acidic and basic subunit complexes of glycinin. *The Journal of biological chemistry*, ***256*****(*****16*****)**, 8752–8755.

Staswick, P. E., Hermodson, M. A., & Nielsen, N. C. (**1984**a). Identification of the cystines which link the acidic and basic components of the glycinin subunits. *The Journal of biological chemistry*, ***259*****(*****21*****)**, 13431–1345.

Staswick, P. E., Hermodson, M. A., & Nielsen, N. C. (**1984**b). The amino acid sequence of the A2B1a subunit of glycinin. *The Journal of biological chemistry*, ***259*****(*****21*****)**, 13424–13430.

Stoeckel, F., Konnerth, J., & Gindl-Altmutter, W. (**2013**). Mechanical properties of adhesives for bonding wood-A review. *International Journal of Adhesion and Adhesives*, ***45***, 32–41.

Sun, X., & Bian, K. (**1999**). Shear strength and water resistance of modified soy protein adhesives. *Journal of the American Oil Chemists' Society*, ***76*****(*****8*****)**, 977–980.

Suppavorasatit, I., De Mejia, E. G., & Cadwallader, K. R. (**2011**). Optimization of the enzymatic deamidation of soy protein by protein-glutaminase and its effect on the functional properties of the protein. *Journal of Agricultural and Food Chemistry*, ***59*****(*****21*****)**, 11621–11628.

Tan, H., Zhang, Y., & Weng, X. (**2011**). Preparation of the plywood using starch-based adhesives modified with blocked isocyanates. *Procedia Engineering*, ***15***, 1171–1175.

Tan, S., Mailer, R., Blanchard, C., & Agboola, S. (**2011**). Canola proteins for human consumption: extraction, profile, and functional properties. *Journal of food science*, ***76*****(*****1*****)**, R16-28.

Tanaka, Y., & Kakiuchi, H. (**1964**). Study of epoxy compounds. Part VI. Curing reactions of epoxy resin and acid anhydride with amine, acid, alcohol, and phenol as catalysts. *Journal of Polymer Science Part A: General Papers*, ***2*****(*8*)**, 3405–3430.

Tandang-Silvas, M. R. G., Fukuda, T., Fukuda, C., Prak, K., Cabanos, C., Kimura, A., Maruyama, N. (**2010**). Conservation and divergence on plant seed 11S globulins based on crystal structures. *Biochimica et Biophysica Acta*, ***1804*****(*7*)**, 1432–1442.

Taylor, S. W., Chase, D. B., Emptage, M. H., Nelson, M. J., & Waite, J. H. (**1996**). Ferric ion complexes of a DOPA-containing adhesive protein from *Mytilus edulis*. *Inorganic chemistry*, ***35*****(*26*)**, 7572–7577.

Taylor, S. W., Luther III, G. W., & Waite, J. H. (**1994**). Polarographic and spectrophotometric investigation of iron (III) complexation to 3, 4-dihydroxyphenylalanine-containing peptides and proteins from *Mytilus edulis*. *Inorganic chemistry*, ***33*****(*25*)**, 5819–5824.

Thanh, V., & Shibasaki, K. (**1976**). Major proteins of soybean seeds. A straightforward fractionation and their characterization. *Journal of Agricultural and Food Chemistry*, ***24*****(*6*)**, 1117–1121.

Thanh, V., & Shibasaki, K. (**1977**). Beta-conglycinin from soybean proteins. Isolation and immunological and physicochemical properties of the monomeric forms. *Biochimica et Biophysica Acta (BBA) - Protein Structure*, ***490*****(*2*)**, 370–384.

Thanh, V., & Shibasaki, K. (**1979**). Major proteins of soybean seeds. Reversible and irreversible dissociation of β-conglycinin. *Journal of Agricultural and Food Chemistry*, ***27*****(*4*)**, 805–809.

Tien, H., Huang, Y., Yang, S., Wang, J., & Ma, C. (**2011**). The production of graphene nanosheets decorated with silver nanoparticles for use in transparent, conductive films. *Carbon*, ***49*****(*****5*****)**, 1550–1560.

Tzeng, Y., Diosady, L., & Rubin, L. (**1990**). Production of Canola Protein Materials by Alkaline Extraction, Precipitation, and Membrane Processing. *Journal of Food Science*, ***55*****(*****4*****)**, 1147–1151.

Ullah, A., Vasanthan, T., Bressler, D., Elias, A. L., & Wu, J. (**2011**). Bioplastics from feather quill. *Biomacromolecules*, ***12*****(*****10*****)**, 3826–3832.

Updegraff, I. (**1990**). Amino resin adhesives. In I. Skeist (Eds.), *Handbook of Adhesives* (pp 341–346). Boston, MA: Springer US.

Ustunol, Z. (**2015**). Amino acids, peptides and proteins. In Z. Ustunol (Eds.), *Applied Food Protein Chemistry* (pp 12–15). Singapore: John Wiley & Sons.

Van Doosselaere, P. (**2013**). Production of Oils. In G. Calliauw, R. Hamilton, & W. Hamm (Eds.), *Edible Oil Processing* (pp 55–96). Chichester, UK: John Wiley & Sons.

Van Nhiem, D., Berg, J., Kjos, N. P., Trach, N. X., & Tuan, B. Q. (**2013**). Effects of replacing fish meal with soy cake in a diet based on urea-treated rice straw on performance of growing Laisind beef cattle. *Tropical Animal Health and Production*, ***45*****(*****4*****)**, 901–909.

Veigel, S., Rathke, J., Weigl, M., & Gindl-Altmutter, W. (**2012**). Particle board and oriented strand board prepared with nanocellulose-reinforced adhesive. *Journal of Nanomaterials*, ***2012***, 1–8.

Veraverbeke, W. S., & Delcour, J. A. (**2002**). Wheat protein composition and properties of wheat glutenin in relation to bread making functionality. *Critical Reviews in Food Science and Nutrition*, ***42*****(*****3*****)**, 179–208.

Verdejo, R., Bernal, M. M., Romasanta, L. J., & Lopez-Manchado, M. A. (**2011**). Graphene filled polymer nanocomposites. *Journal of Material Chemistry*, ***21*****(*****10*****)**, 3301–3310.

Waite, J. H. (**1983**). Evidence for a repeating 3,4-dihydroxyphenylalanine- and hydroxyproline-containing decapeptide in the adhesive protein of the mussel, *Mytilus edulis* L. *Journal of Biological Chemistry*, ***258*****(*****5*****)**, 2911–2915.

Waite, J. H. (**2002**). Adhesion a la moule. *Integrative and Comparative Biology*, ***42*****(*****6*****)**, 1172–1180.

Waite, J. H., & Qin, X. (**2001**). Polyphosphoprotein from the adhesive pads of *Mytilus edulis*. *Biochemistry*, ***40*****(*****9*****)**, 2887–2893.

Waite, J. H., Qin, X. X., & Coyne, K. J. (**1998**). The peculiar collagens of mussel byssus. *Matrix Biology*, ***17*****(*****2*****)**, 93–106.

Waite, J., Andersen, N., Jewhurst, S., & Sun, C. (**2005**). Mussel adhesion: finding the tricks worth mimicking. *Journal of Adhesion*, ***81*****(*****3–4*****)**, 297–317.

Wanasundara, J. P. D. (**2011**). Proteins of *Brassicaceae* oilseeds and their potential as a plant protein source. *Critical Reviews in Food Science and Nutrition*, ***51*****(*****7*****)**, 635–677.

Wang, C., & Wu, J. (**2012**). Preparation and characterization of adhesive from spent hen proteins. *International Journal of Adhesion and Adhesives*, ***36***, 8–14.

Wang, C., Wu, J., & Bernard, G. M. (**2014**). Preparation and characterization of canola protein isolate–poly(glycidyl methacrylate) conjugates: a bio-based adhesive. *Industrial Crops and Products*, ***57***, 124–131.

Wang, P., Cheng, L., Gu, Z., Li, Z., & Hong, Y. (**2015**). Assessment of starch-based wood adhesive quality by confocal Raman microscopic detection of reaction homogeneity. *Carbohydrate Polymers*, ***131***, 75–79.

Wang, S., Winistorfer, P. M., & Young, T. M. (**2007**). Fundamentals of vertical density profile formation in wood composites. Part III - MDF density formation during hot-pressing. *Wood and Fiber Science*, ***36*****(*****1*****)**, 17–25.

Wang, W., Bringe, N. A., Berhow, M. A., & Gonzalez de Mejia, E. (**2008**). B-Conglycinins among sources of bioactives in hydrolysates of different soybean varieties that inhibit leukemia cells in vitro. *Journal of Agricultural and Food Chemistry*, ***56*****(*****11*****)**, 4012–4020.

Wang, Y., Mo, X., Sun, X. S., & Wang, D. (**2007**). Soy protein adhesion enhanced by glutaraldehyde crosslink. *Journal of Applied Polymer Science*, ***104*****(*****1*****)**, 130–136.

Wang, Y., Shi, Z., Yu, J., Chen, L., Zhu, J., & Hu, Z. (**2012**). Tailoring the characteristics of graphite oxide nanosheets for the production of high-performance poly (vinyl alcohol) composites. *Carbon*, ***50*****(*****15*****)**, 5525–5536.

Wang, Y., Sun, X. S., & Wang, D. (**2006**). Performance of soy protein adhesive enhanced by esterification. *Transactions of the ASAE-American Society of Agricultural Engineers*, ***49*****(*****3*****)**, 713-719.

Wang, Z., Gu, Z., Hong, Y., Cheng, L., & Li, Z. (**2011**). Bonding strength and water resistance of starch-based wood adhesive improved by silica nanoparticles. *Carbohydrate Polymers*, ***86*(*1*)**, 72–76.

Wang, Z., Gu, Z., Li, Z., Hong, Y., & Cheng, L. (**2013**). Effects of urea on freeze–thaw stability of starch-based wood adhesive. *Carbohydrate Polymers*, ***95*(*1*)**, 397–403.

Wang, Z., Li, Z., Gu, Z., Hong, Y., & Cheng, L. (**2012**). Preparation, characterization and properties of starch-based wood adhesive. *Carbohydrate Polymers*, ***88*(*2*)**, 699–706.

Widsten, P., & Kandelbauer, A. (**2008**). Adhesion improvement of lignocellulosic products by enzymatic pre-treatment. *Biotechnology Advances*, ***26*(*4*)**, 379–386.

Woerfel, J. (**1995**). Extraction. In D. Erickson (Eds.), *Practical Handbook of Soybean Processing and Utilization* (pp 65–92). Champaign, Illinois: AOCS Press.

Wool, R. P. (**2015**). Nanoclay biocomposites. In R. P. Wool & X. S. Sun (Eds.), *Bio-based polymers and composites* (pp 523–550). Cambridge, Massachusetts: Academic Press.

Wu, J., & Muir, A. D. (**2008**). Comparative structural, emulsifying, and biological properties of two major canola proteins, cruciferin and napin. *Journal of Food Science*, ***73*(*3*)**, C210–C216.

Wu, S., Murphy, P., Johnson, L., & Fratzke, A. (**1999**). Pilot-plant fractionation of soybean glycinin and β-conglycinin. *Journal of the American Oil Chemists Society*, ***76*(*3*)**, 285–293.

Xia, Y., & Larock, R. C. (**2010**). Vegetable oil-based polymeric materials: synthesis, properties, and applications. *Green Chemistry*, ***12*(*11*)**, 1893–1909.

Xu, H., Ma, S., Lv, W., & Wang, Z. (**2011**). Soy protein adhesives improved by SiO_2 nanoparticles for plywoods. *Pigment & Resin Technology*, ***40*****(*****3*****)**, 191–195.

Xu, Y., Bai, H., Lu, G., Li, C., & Shi, G. (**2008**). Flexible graphene films via the filtration of water-soluble noncovalent functionalized graphene sheets. *Journal of the American Chemical Society*, ***130*****(*****18*****)**, 5856–5857.

Xu, Z., & Gao, C. (**2011**a). Aqueous liquid crystals of graphene oxide. *ACS nano*, ***5*****(*****4*****)**, 2908–2915.

Xu, Z., & Gao, C. (**2011**b). Graphene chiral liquid crystals and macroscopic assembled fibres. *Nature Communications*, ***2*****(*****571*****)**, 1–9.

Yang, I., Kuo, M., Myers, D. J., & Pu, A. (**2006**). Comparison of protein-based adhesive resins for wood composites. *Journal of Wood Science*, ***52*****(*****6*****)**, 503–508.

Yang, X., Tu, Y., Li, L., Shang, S., & Tao, X. (**2010**). Well-dispersed chitosan/graphene oxide nanocomposites. *ACS Applied Materials & Interfaces*, ***2*****(*****6*****)**, 1707–1713.

Yoon, G., Seo, D.-H., Ku, K., Kim, J., Jeon, S., & Kang, K. (**2015**). Factors affecting the exfoliation of graphite intercalation compounds for graphene synthesis. *Chemistry of Materials*, ***27*****(*****6*****)**, 2067–2073.

Yu, M., Hwang, J., & Deming, T. J. (**1999**). Role of L-3,4-Dihydroxyphenylalanine in Mussel Adhesive Proteins. *Journal of the American Chemical Society*, ***121*****(*****24*****)**, 5825–5826.

Yuan, C., Luo, J., Luo, J., Gao, Q., & Li, J. (**2016**). A soybean meal-based wood adhesive improved by a diethylene glycol diglycidyl ether: properties and performance. *RSC Advances*, ***6*****(*78*)**, 74186–74194.

Yuge, R., Zhang, M., Tomonari, M., Yoshitake, T., Iijima, S., & Yudasaka, M. (**2008**). Site identification of carboxyl groups on graphene edges with Pt derivatives. *ACS Nano*, ***2*****(*9*)**, 1865–1870.

Zeng, H., Hwang, D. S., Israelachvili, J. N., & Waite, H. (**2010**). Strong reversible Fe^{3+}-mediated bridging between DOPA-containing protein films in water. *Proceedings of the National Academy of Sciences of the United States of America, **107(29)***, 12850-12853.

Zhang, X., Monroe, M., Chen, B., Chin, M., Heibeck, T., Schepmoes, A., & Jacobs, J. (**2010**). Endogenous 3,4 dihydroxyphenylalanine and dopaquinone modification on protein. *Molecular & Cellular Proteomics*, ***9*****(*6*)**, 1199–1208.

Zhang, Y., Ding, L., Gu, J., Tan, H., & Zhu, L. (**2015**). Preparation and properties of a starch-based wood adhesive with high bonding strength and water resistance. *Carbohydrate Polymers*, ***115***, 32–37.

Zhang, Y., Zhu, W., Lu, Y., Gao, Z., & Gu, J. (**2014**). Nano-scale blocking mechanism of MMT and its effects on the properties of polyisocyanate-modified soybean protein adhesive. *Industrial Crops and Products*, ***57***, 35–42.

Zhao, L., Liu, Y., Xu, Z., Zhang, Y., Zhao, F., & Zhang, S. (**2011**). State of research and trends in development of wood adhesives. *Forestry Studies in China*, ***13*****(*4*)**, 321–326.

Zhao, X., Chen, F., Xue, W., & Lee, L. (**2008**). FTIR spectra studies on the secondary structures of 7S and 11S globulins from soybean proteins using AOT reverse micellar extraction. *Food Hydrocolloids*, ***22*****(*****4*****)**, 568–575.

Zhao, X., Zhang, Q., Chen, D., & Lu, P. (**2010**). Enhanced mechanical properties of graphene-based poly(vinyl alcohol) composites. *Macromolecules*, ***43*****(*****5*****)**, 2357–2363.

Zhao, Y., Yan, N., & Feng, M. W. (**2013**a). Bark extractives-based phenol–formaldehyde resins from beetle-infested lodgepole pine. *Journal of Adhesion Science and Technology*, ***27*****(*****18–19*****)**, 2112–2126.

Zhao, Y., Yan, N., & Feng, M. W. (**2013**b). Biobased phenol formaldehyde resins derived from beetle-infested pine barks—structure and composition. *ACS Sustainable Chemistry & Engineering*, ***1*****(*****1*****)**, 91–101.

Zhong, Y. L., Tian, Z., Simon, G. P., & Li, D. (**2015**). Scalable production of graphene via wet chemistry: progress and challenges. *Materials Today*, ***18*****(*****2*****)**, 73–78.

Zhou, X., Zhang, J., Wu, H., Yang, H., Zhang, J., & Guo, S. (**2011**). Reducing graphene oxide via hydroxylamine: a simple and efficient route to graphene. *The Journal of Physical Chemistry C*, ***115*****(*****24*****)**, 11957–11961.

Zhu, D., & Damodaran, S. (**2014**). Chemical phosphorylation improves the moisture resistance of soy flour-based wood adhesive. *Journal of Applied Polymer Science*, ***131*****(*****13*****)**, 40451–40457.

APPENDICES

Appendix 1 (Supplementary information - Chapter 3)

Name	Position	FWHM	Area	At%	C/O ratio
O 1s	530.9	3.222	38501.54	30.62	
C 1s	284.5	4.606	28710.16	66.91	2.18
S 2p	167.31	3.181	1778.23	2.47	

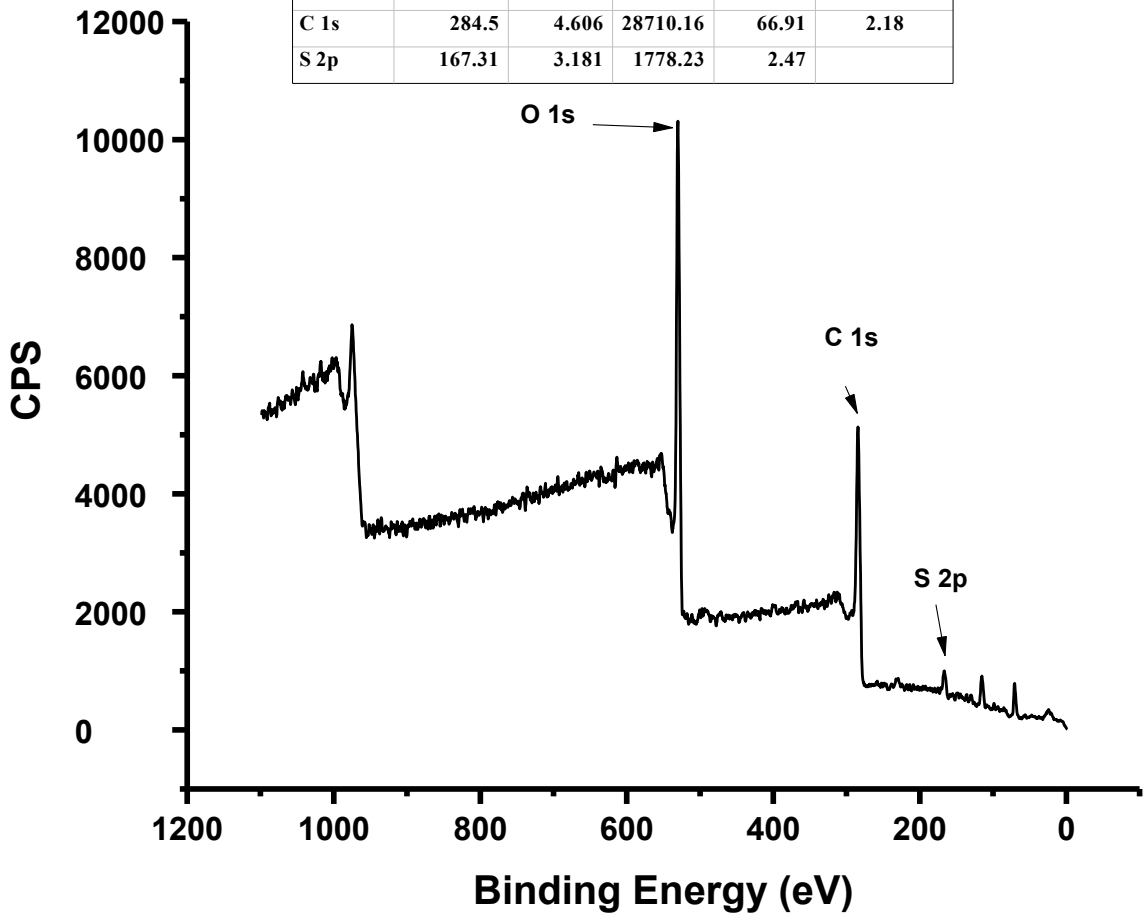

Supplementary Figure 3.1 – X-ray photoelectron spectra showing elemental composition and C/O ratio in graphite oxide used for the study

Supplementary Table 3.1 - Adhesion strength of SM-MMT and NCC dispersed Canola protein adhesive (SM-MMT/NCC addition was carried out according the protocol of Zhang et al (2014) to compare the method develop in our lab)

Sample	**Method developed by Zhang et al (2014)**		**Method developed in our lab**	
	Dry Strength (MPa)	***Wet Strength (MPa)***	***Dry Strength (MPa)***	***Wet Strength (MPa)***
(-) Control	3.41 ± 0.38	1.23 ± 0.07	3.41 ± 0.38	1.23 ± 0.07
pH Control	6.38 ± 0.84	1.98 ± 0.22	6.38 ± 0.84	1.98 ± 0.22
1% SM-MMT	6.20 ± 0.53	1.81 ± 0.53	9.29 ± 1.53	3.19 ± 0.57
3% SM-MMT	5.76 ± 0.34	1.57 ± 0.14	7.51 ± 1.11	2.81 ± 0.38
5% SM-MMT	5.16 ± 0.62	1.43 ± 0.18	6.71 ± 1.04	2.35 ± 0.47
7% SM-MMT	3.94 ± 0.49	1.36 ± 0.22	4.85 ± 0.64	1.85 ± 0.43
1% NCC	6.57 ± 0.38	1.95 ± 0.14	10.37 ± 1.63	3.57 ± 0.57
3% NCC	6.26 ± 0.27	1.78 ± 0.10	9.86 ± 1.87	3.03 ± 0.42
5% NCC	5.90 ± 0.21	1.63 ± 0.08	9.58 ± 1.14	2.99 ± 0.68
7% NCC	5.78 ± 0.35	1.61 ± 0.14	8.46 ± 1.31	2.84 ± 0.53

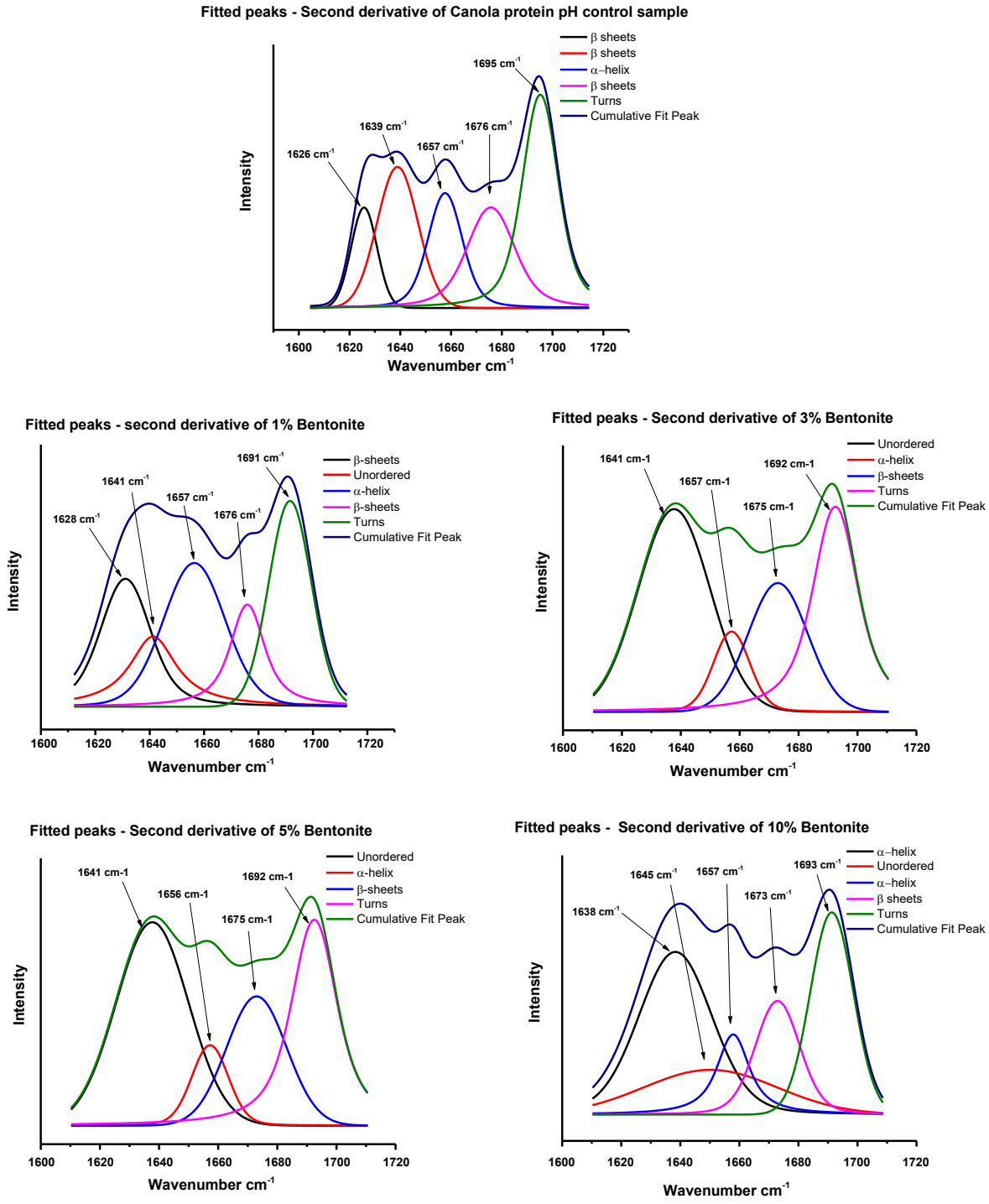

Supplementary Figure 3.2 – Peak fitting of FTIR second derivative spectra showing bentonite induced changes in protein secondary structure

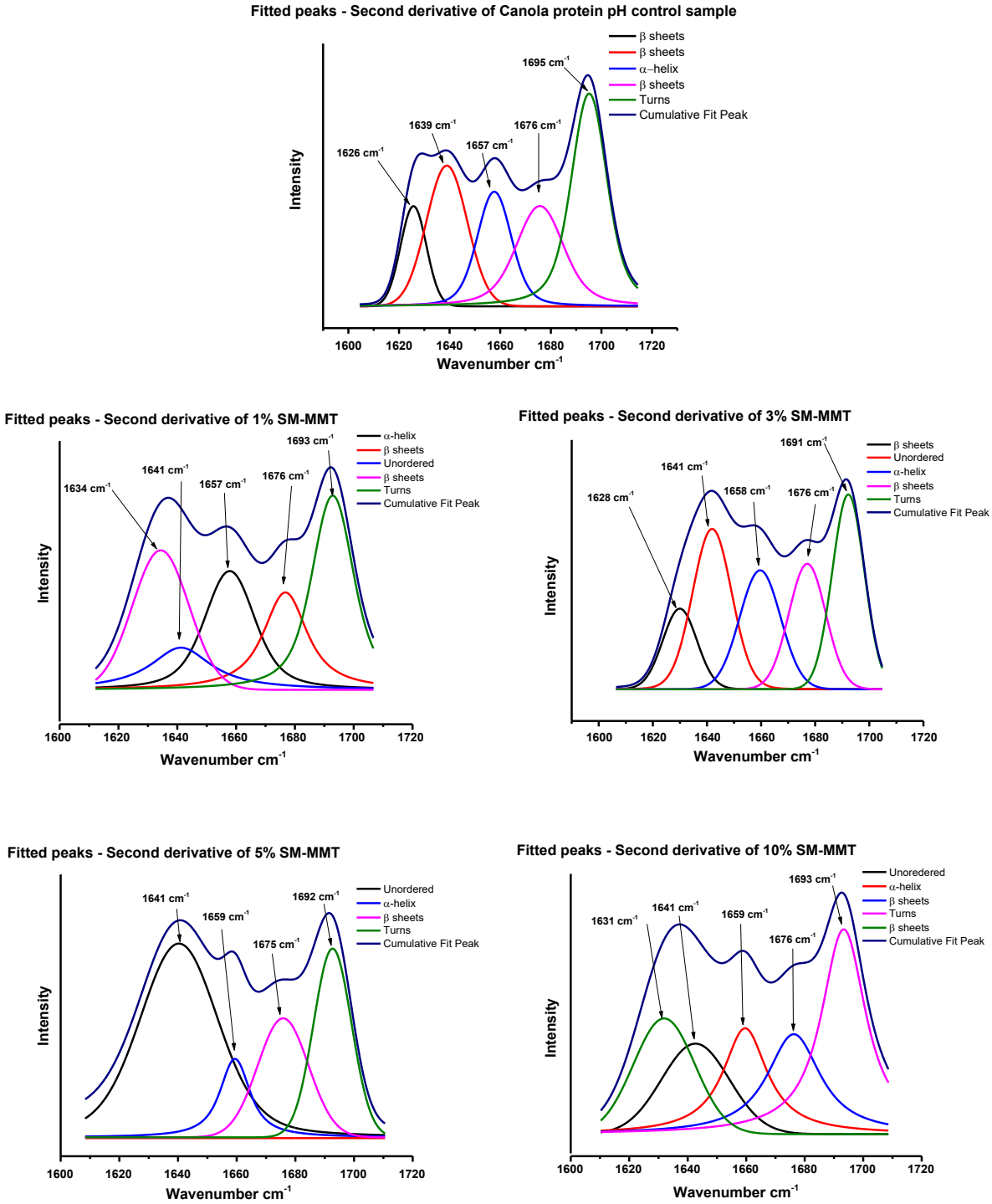

Supplementary Figure S3 – Peak fitting of FTIR second derivative spectra showing SM-MMT induced changes in protein secondary structure

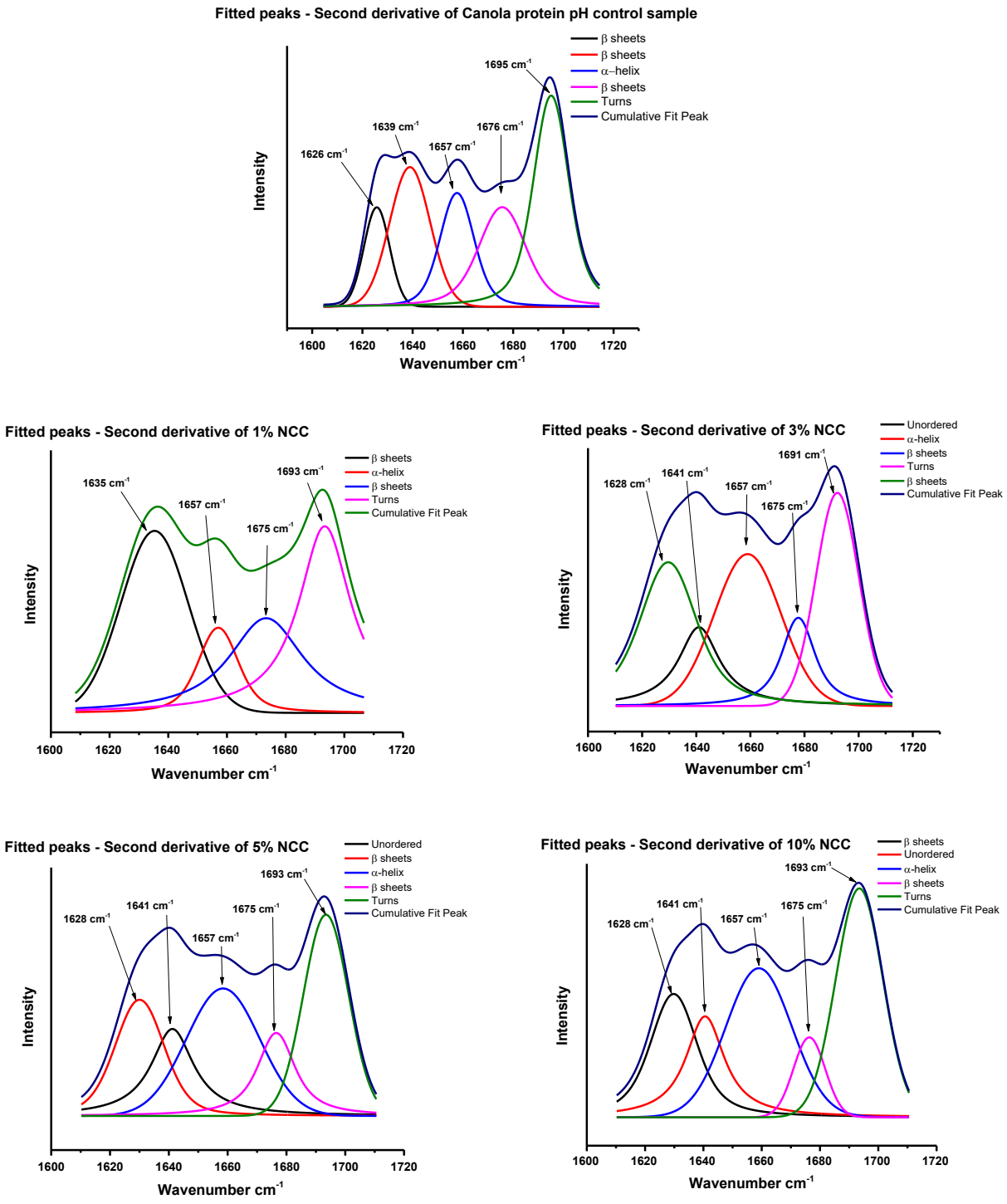

Supplementary Figure 3.4 – Peak fitting of FTIR second derivative spectra showing NCC induced changes in protein secondary structure

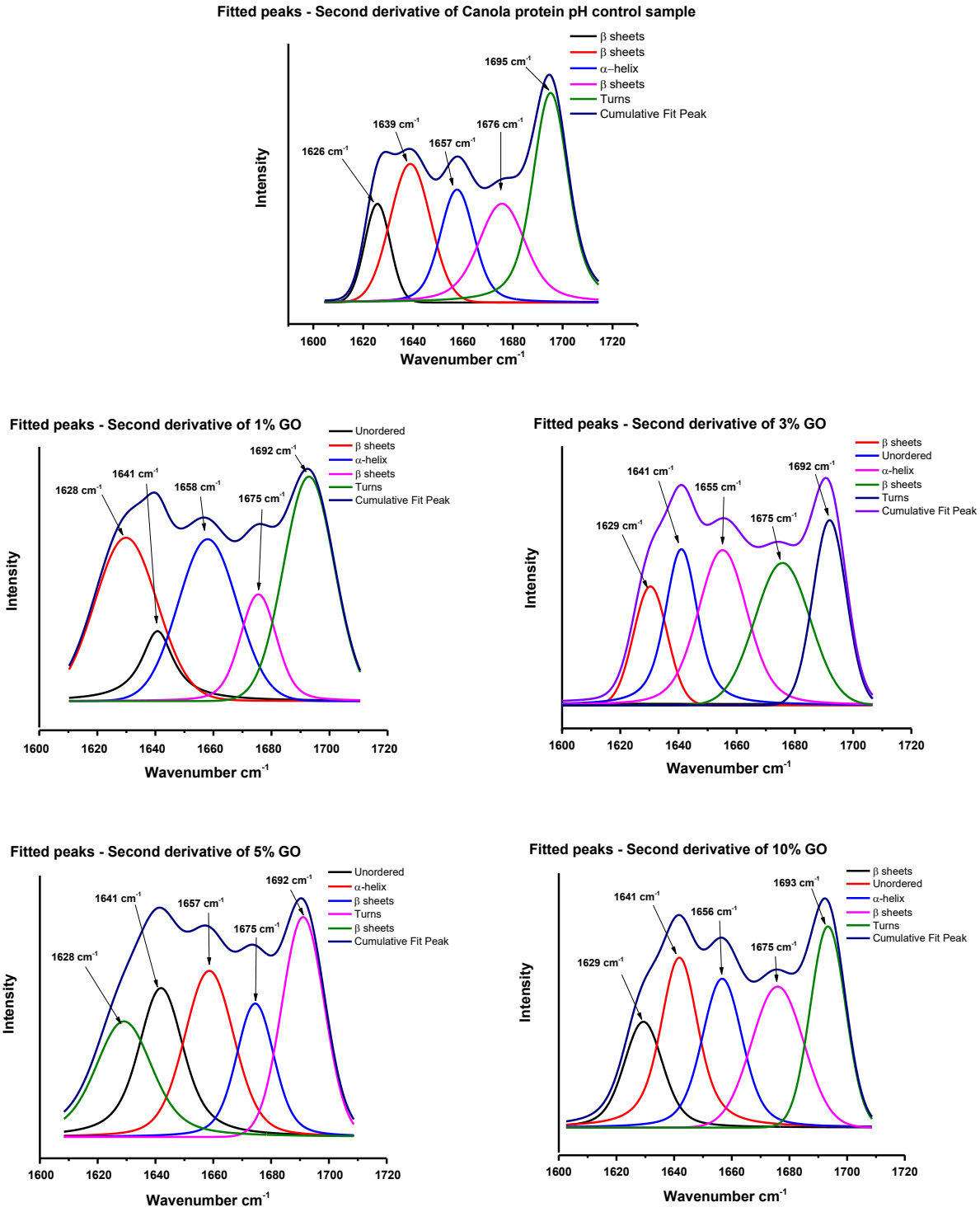

Supplementary Figure 3.5 – Peak fitting of FTIR second derivative spectra showing GO induced changes in protein secondary structure

Appendix 2 (Supplementary information - Chapter 4)

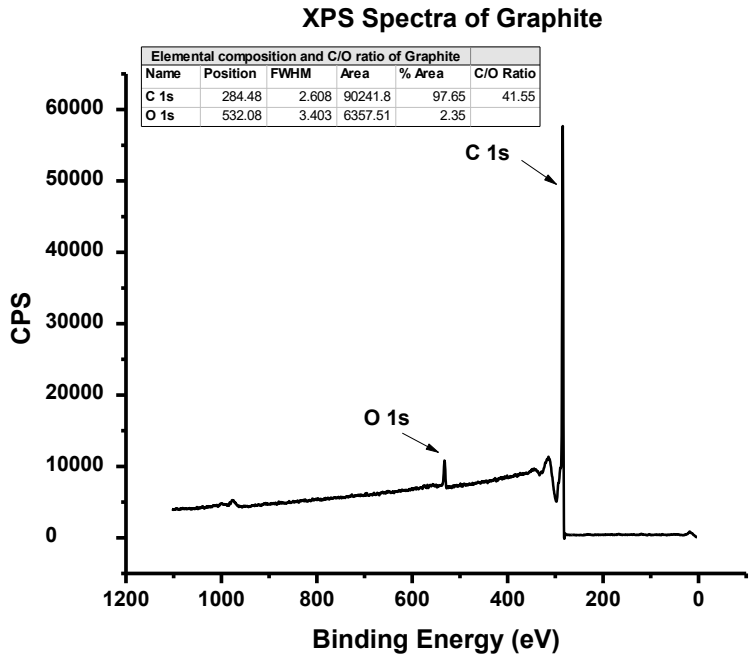

Supplementary Figure 4.1: a – X-ray photoelectron spectra showing elemental composition and C/O ratio in un-oxidized graphite

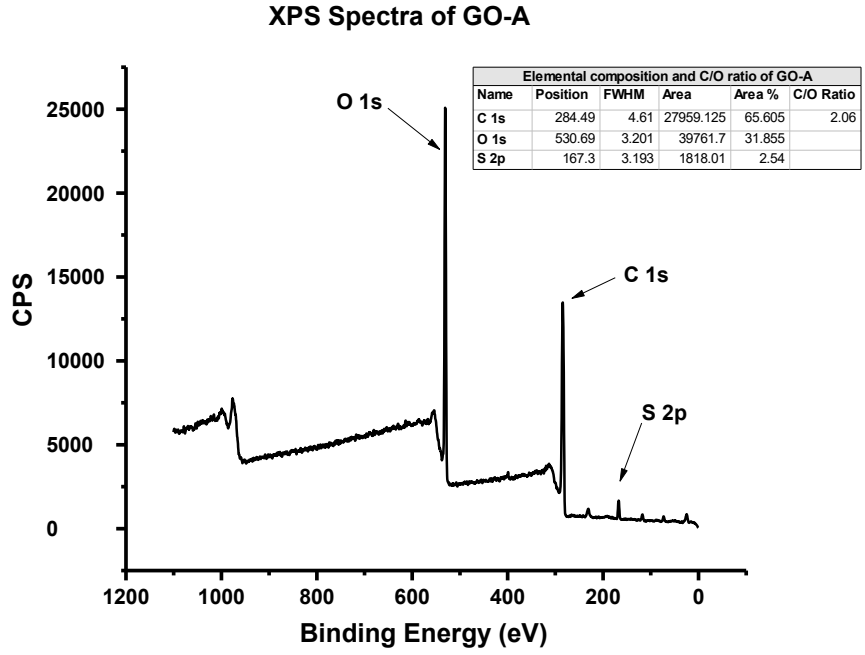

Supplementary Figure 4.1: b – X-ray photoelectron spectra showing elemental composition and C/O ratio in graphite oxide prepared with 0.5 hrs oxidation time (GO-A sample)

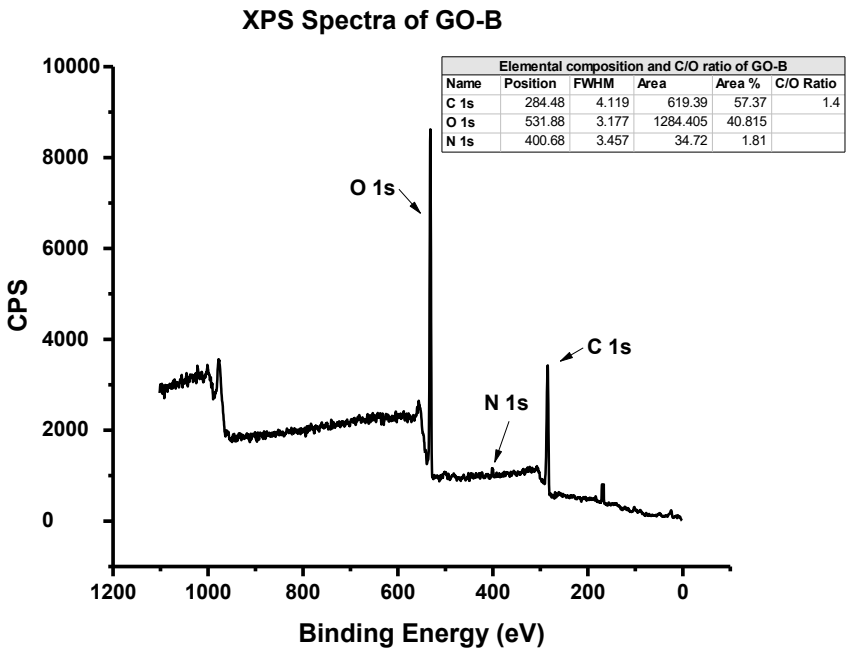

Supplementary 4.1: c – X-ray photoelectron spectra showing elemental composition and C/O ratio in graphite oxide prepared with 2 hrs oxidation time (GO-B sample)

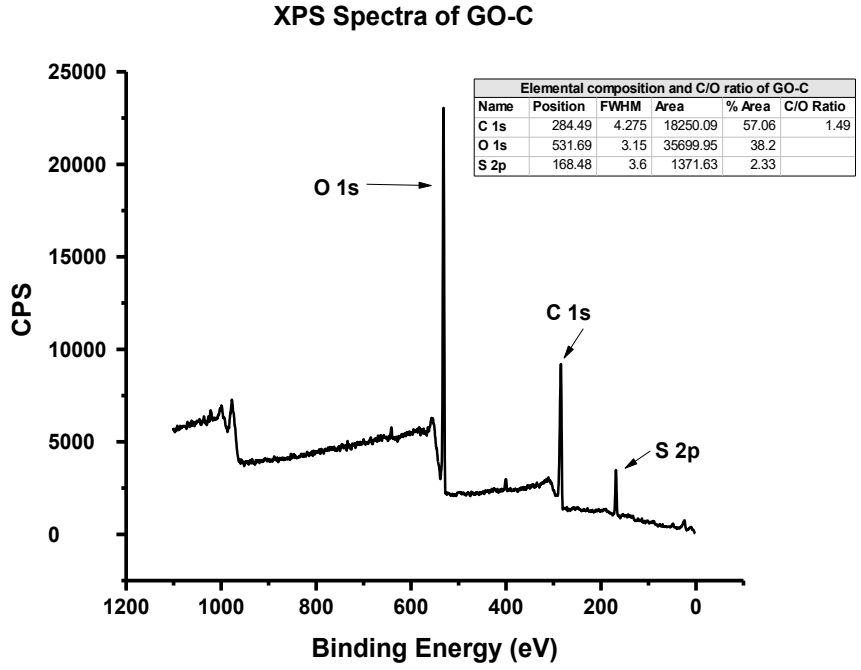

Supplementary Figure 4.1: d – X-ray photoelectron spectra showing elemental composition and C/O ratio in graphite oxide prepared with 4 hrs oxidation time (GO-C sample)

Figure S2: Secondary structural changes in pH Control sample

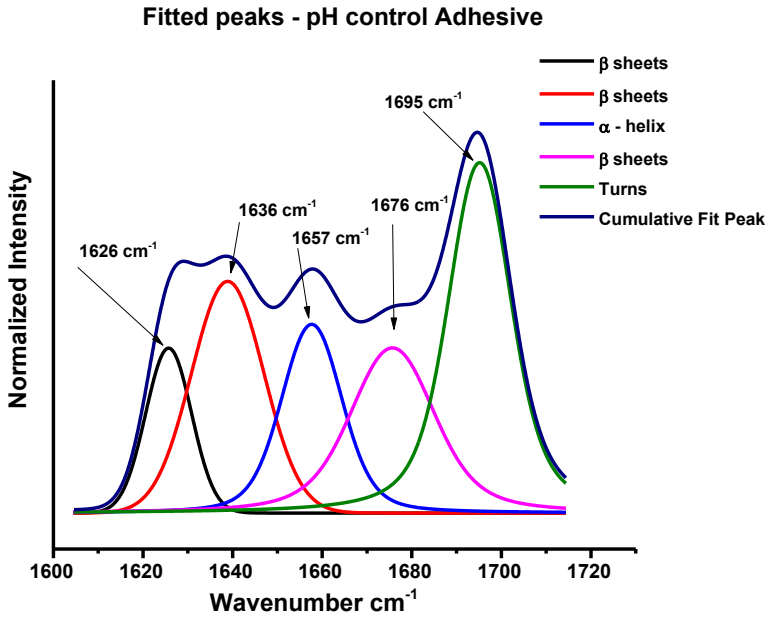

Supplementary Figure 4.2:a – Peak fitting of FTIR second derivative spectra showing changes in protein secondary structure in pH Control adhesive sample

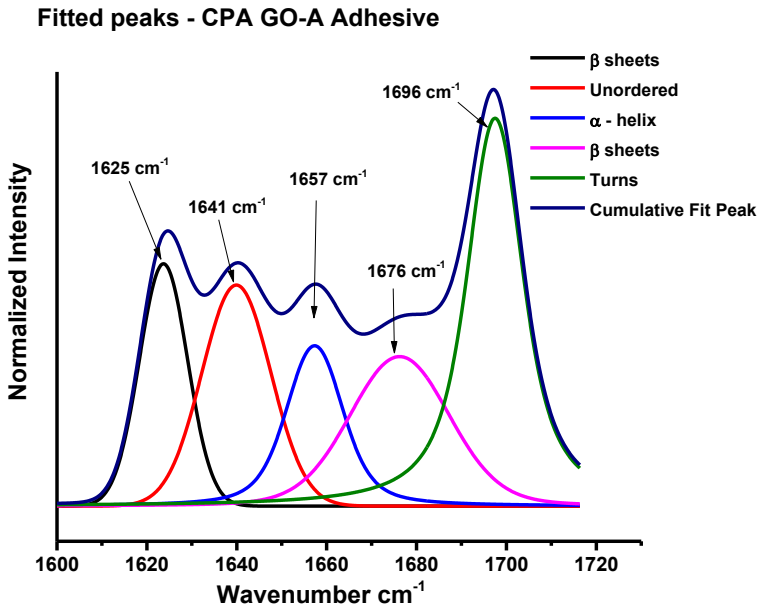

Supplementary Figure 4.2:b – Peak fitting of FTIR second derivative spectra showing changes in protein secondary structure in CPA GO-A Control adhesive sample

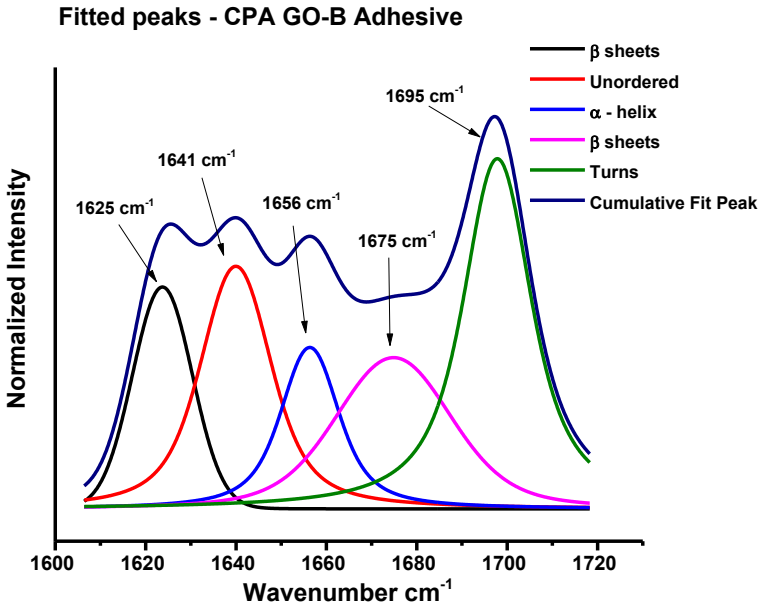

Supplementary Figure 4.2: c – Peak fitting of FTIR second derivative spectra showing changes in protein secondary structure in CPA GO-B Control adhesive sample

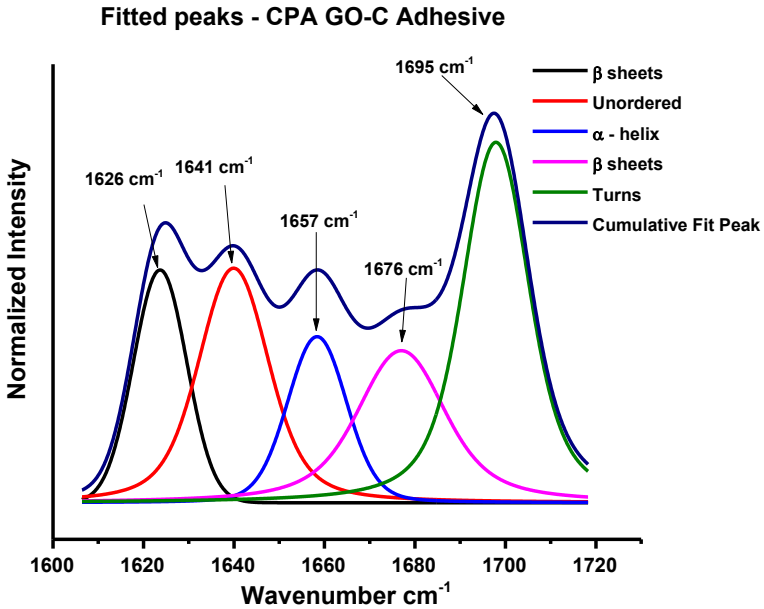

Supplementary Figure 4.2: d – Peak fitting of FTIR second derivative spectra showing changes in protein secondary structure in CPA GO-C Control adhesive sample